

Contents

CONTENTS	I
LIST OF FIGURES	VIII
LIST OF TABLES	XI
LIST OF EQUATIONS	XIII
LIST OF APPENDICES	XIV
ACKNOWLEDGEMENTS.....	XV
ABSTRACT	XVI
1 GENERAL INTRODUCTION	1
1.1 Scrap tyre management	1
1.2 Rationale for the project	5
1.3 Research aims	5
1.4 Thesis outline	6
2 LITERATURE REVIEW	7
2.1 Introduction	7
2.2 Tyre manufacture	7
2.3 Rubber reclamation.....	9
2.4 The recovery of tyre components	10
2.4.1 Tyre pyrolysis	11
2.4.1.1 Laboratory scale pyrolysis.....	12

2.4.1.2	Typical properties and markets for Carbon Blacks	13
2.4.1.3	Characteristics and potential uses of CB _p	14
2.4.1.4	Commercial scale pyrolysis plants	16
2.4.1.5	The Coalite [®] smokeless fuels process	18
2.4.2	Alternative methods of carbon black recovery	19
2.4.2.1	Rubber dissolution.....	19
2.4.2.2	Microwave treatment.....	20
2.4.3	Cement kilns	20
2.4.4	Tyre incineration with energy recovery	21
2.5	Summary	21
3	SITA TYRE RECYCLING	23
3.1	Introduction	23
3.2	General facility description	23
3.3	Process description	25
3.4	Current treatment of waste residues	28
3.4.1	Quantities of combustion residue disposed to landfill.....	28
3.4.2	Properties of STR solid waste residue	29
3.5	Summary	30
4	MAIN ANALYTICAL METHODS	31
4.1	Introduction	31
4.2	Analysis of total carbon.....	32
4.2.1	Sample preparation	34
4.2.2	Carbon analysis procedure.....	37
4.3	Analysis of total sulphur	38
4.3.1	Method description	39
4.3.1.1	Preparation of reagents	39
4.3.2	Adaptation of method for STR material	40

4.3.3	Sulphur analysis procedure	43
4.4	Total element digestion	44
4.4.1	Total digestion procedure	46
4.5	Aqua-Regia digestion	47
4.5.1	Aqua-Regia digestion procedure	48
4.6	ICP-AES analysis of digestion leachates	50
4.6.1	ICP-AES parameters for total digestion leachates.....	52
4.6.2	ICP-AES parameters for Aqua-Regia leachates	54
4.7	Summary	54
5	SAMPLING AND CHARACTERISATION	56
5.1	Introduction	56
5.2	Sampling procedure	58
5.3	Material characterisation	59
5.3.1	Characterisation of bushy wire	61
5.3.1.1	Bushy wire characterisation method.....	62
5.3.1.2	Sample preparation	62
5.3.1.3	Sample treatment	63
5.3.1.4	Sulphur analysis of wire specimens	64
5.3.1.5	Interpretation of wire characterisation.....	68
5.3.2	Physical characterisation of carbon ash	69
5.3.2.1	Particle size analysis.....	70
5.3.2.2	Magnetic distribution.....	71
5.3.2.3	Scanning Electron Microscope investigation	72
5.3.2.4	Mineral phase identification with X-Ray diffraction	77
5.3.3	Chemical characterisation of carbon ash	81
5.3.3.1	Concentration and distribution of carbon and sulphur	81
5.3.3.2	Concentration and distribution of major and minor elements	84
5.3.3.3	Interpretation of carbon ash characterisation	88

5.4	Interim summary and conclusions.....	91
6	SEPARATION STUDIES.....	93
6.1	Processing of carbon ash.....	93
6.1.1	Dry magnetic separation.....	93
6.1.1.1	Method.....	94
6.1.1.2	Results & discussion.....	95
6.1.1.3	Summary.....	97
6.1.2	Froth flotation.....	98
6.1.2.1	Method.....	99
6.1.2.2	Results & discussion.....	101
6.1.3	Acid demineralisation.....	104
6.1.3.1	Method.....	105
6.1.3.2	Results and discussion.....	107
6.2	Processing of bushy wire.....	114
6.2.1	Attrition scrubbing.....	114
6.2.1.1	Method.....	114
6.2.1.2	Results & discussion.....	117
6.2.1.3	Summary.....	121
6.3	Separation studies summary.....	122
7	PRODUCT USES AND ASSESSMENT.....	124
7.1	Introduction.....	124
7.2	Products derived from carbon ash.....	124
7.2.1	Britannia Zinc Ltd.....	125
7.3	Products derived from bushy wire.....	127
7.3.1	British Steel.....	127
7.3.2	Ervin Amasteel.....	128
7.3.3	Metabrasive.....	128
7.4	Summary.....	129

8	PILOT SCALE TEST WORK.....	131
8.1	Introduction	131
8.2	Dry magnetic separation of ash/wire	131
8.2.1	Initial pilot scale dry magnetic separation trial.....	133
8.2.1.1	Interim discussion.....	134
8.2.2	Assessment of shredding technology.....	135
8.2.2.1	Shredding tests.....	136
8.2.2.2	Alternative shredder technology.....	136
8.2.3	Dry magnetic separation of shredded ash/wire.....	138
8.2.3.1	Chemical analysis of non-magnetic product	141
8.2.4	Dry magnetic separation discussion and conclusions.....	141
8.3	Alternative method for ash/wire separation	143
8.3.1	Spiral classifier	143
8.3.1.1	Results	145
8.4	Scale-up and optimisation of wire attrition process.....	146
8.4.1	Attrition optimisation method.....	146
8.4.2	Results & discussion.....	147
8.4.3	Scale-up of attrition process	150
8.5	Summary	151
9	FLOAT AND SINK TEST WORK	153
9.1	Introduction	153
9.2	Review of float-sink practice	153
9.3	Development of float-sink testing method.....	156
9.3.1	Selection of separation technique	156
9.3.2	Selection of appropriate separation medium.....	159
9.3.2.1	Dense liquid preparation.....	160
9.3.3	Sample preparation	161
9.3.3.1	Comminution.....	161

9.3.3.2	Special treatment of 38-0 μm fraction.....	163
9.3.4	Experimental procedure.....	164
9.3.5	Centrifugal separation.....	165
9.3.5.1	Recovery of floats and sinks fractions.....	166
9.3.6	Chemical analysis of test samples.....	168
9.3.6.1	Elemental analysis.....	169
9.3.6.2	Mineral phase identification.....	169
9.4	Float-sink test results.....	170
9.4.1	Size characterisation of feed and grind material.....	170
9.4.2	Precision of float-sink test work.....	170
9.4.3	Mass distribution.....	173
9.4.4	Characterisation of feed and ground material.....	174
9.4.4.1	Bulk chemistry of feed sample.....	174
9.4.4.2	Distribution of elements before and after grinding.....	175
9.4.5	Characterisation of float-sink samples.....	178
9.4.6	Characterisation of 2.2rd samples.....	181
9.4.6.1	Major elements in float-sink fractions.....	181
9.4.6.2	Distribution of trace elements in float-sink fractions.....	192
9.4.6.3	Mineral phase identification in float-sink fractions.....	194
9.5	Interpretation of float-sink test.....	195
9.5.1	SEM investigation of float-sink feed samples.....	197
9.5.1.1	Non-ashed sample.....	197
9.5.1.2	Ashed sample.....	200
9.5.2	Elemental relationships in float-sink samples.....	202
9.6	Interim summary and conclusions.....	205
9.6.1	Sulphur phases in float-sink samples.....	206
9.6.2	Origins of elements in float-sink samples.....	209
10	CHARACTERISATION OF A TYRE PYROLYSIS CHAR.....	210
10.1	Introduction.....	210
10.2	Sample description.....	210

10.3	Characterisation	210
10.3.1	Particle size analysis	211
10.3.2	SEM analysis	213
10.3.3	Chemical characterisation	215
10.3.3.1	Carbon and sulphur concentration in size fractions	216
10.3.3.2	Concentration of major and minor elements in size fractions.....	217
10.3.3.3	Characterisation of bulk sample	218
10.4	Discussion	219
10.5	Summary	221
11	CONCLUSION.....	222
11.1	Discussion	222
11.2	Contributions to knowledge.....	225
11.3	Recommendations for future work.....	227
	PUBLICATIONS	228
	REFERENCES	229

List of Figures

Figure 1.1 Management of scrapped tyres in the UK, 1996 (Scrap Tyre Working Group, 1997)	3
Figure 2.1 Cross section of a modern car tyre (Kovac and Rodgers, 1994).....	9
Figure 2.2 Tertiary recycling process (Allred et al. 2000).....	16
Figure 2.3 Coalite tyre pyrolysis process (Anon, 2000)	18
Figure 3.1 STR plant viewed from front gates	24
Figure 3.2 Rear yard of STR plant showing combustion residue handling area	24
Figure 3.3 Whole tyres being loaded into feed hopper (CADDET, 1994).....	25
Figure 3.4 Schematic diagram of single combustion unit (in profile).....	26
Figure 4.1 Carbon combustion tube arrangement.....	33
Figure 4.2 Carbon analysis procedure for STR material	38
Figure 4.3 Effect of sample mass on sulphur analysis of carbon ash.....	41
Figure 4.4 Effect of oxidiser addition on sulphur analysis of carbon ash.....	42
Figure 4.5 Sulphur analysis procedure	43
Figure 4.6 Total element digestion procedure	46
Figure 4.7 Aqua-Regia digestion procedure	48
Figure 5.1 Combusted tyre material in storage bund.....	57
Figure 5.2 Summary of ash/wire characterisation method.....	60
Figure 5.3 Typical sample of hand separated bushy wire.....	61
Figure 5.4 Single core wire – no treatment (0.2% sulphur).....	65
Figure 5.5 Multiple core wire – no treatment (0.7% sulphur)	66
Figure 5.6 Multiple core wire - sanded (0.19% sulphur).....	67
Figure 5.7 Single core wire - sanded (0.017% sulphur).....	68
Figure 5.8 Carbon ash - fractional size distribution.....	71
Figure 5.9 Carbon ash - distribution of magnetic phases.....	72
Figure 5.10 SEM image of mixed particles in carbon ash	74
Figure 5.11 SEM image of mixed phase particle in carbon ash.....	74
Figure 5.12 SEM image of close up of carbon phase surface.....	75
Figure 5.13 SEM image of polished section.....	76
Figure 5.14 Summary of EDX analysis.....	76
Figure 5.15 XRD trace of fresh carbon ash	79
Figure 5.16 XRD trace of aged carbon ash.....	80
Figure 5.17 Carbon ash - fractional size versus % carbon.....	82
Figure 5.18 Carbon ash - fractional size versus % sulphur.....	82
Figure 5.19 Carbon ash - fractional size (magnetic) versus % carbon.....	83
Figure 5.20 Carbon ash - fractional size (magnetic) versus % sulphur.....	84
Figure 5.21 Concentration of major elements in non-magnetic fractions.....	86
Figure 5.22 Concentration of minor elements in non-magnetic fractions.....	86
Figure 5.23 Concentration of major elements in magnetic size fractions	87
Figure 5.24 Concentration of minor elements in magnetic size fractions.....	88
Figure 6.1 Polished section of froth flotation product (backscatter).....	101
Figure 6.2 Flotation feed sample (secondary electron image)	103

Figure 6.3 Flotation feed sample (backscattered electron image).....	103
Figure 6.4 Acid treatment of carbon ash	106
Figure 6.5 Carbon concentration of samples during HCl acid leach experiment.....	108
Figure 6.6 Sulphur concentration of samples during HCl acid leach experiment.....	108
Figure 6.7 Element extraction from carbon ash during HCl acid leaches.....	110
Figure 6.8 Wemco [®] laboratory scale attrition cell.....	115
Figure 6.9 Attrition scrubbing trial - sulphur content of steel wire during process	119
Figure 6.10 Wire - cut and screened (0.066% sulphur)	120
Figure 6.11 Wire - post attrition (0.027% sulphur)	120
Figure 6.12 Attrition of bushy wire - process summary	122
Figure 8.1 Laboratory and pilot scale generation of products	132
Figure 8.2 Dry magnetic separator with product collection bins	133
Figure 8.3 Columbus McKinnon [®] tyre shredder shown with discharge conveyor and feed hopper.....	135
Figure 8.4 Parke Rotashear [®] shredder.....	137
Figure 8.5 Parke Rotashear [®] cutting blades.....	137
Figure 8.6 Shredder product in roll-on-roll-off trailer	138
Figure 8.7 Cross conveyor product.....	140
Figure 8.8 Drum magnet separated phase.....	140
Figure 8.9 Separated carbon product	140
Figure 8.10 Closed grinding circuit.....	144
Figure 8.11 Spiral classifier separation of shredded ash/wire.....	144
Figure 8.12 Effect of attrition time on sulphur concentration of steel	148
Figure 8.13 Effect of solids loading on sulphur concentration of attrited steel	149
Figure 9.1 Flow chart of float-sink separation procedure.....	158
Figure 9.2 Re-agglomerated particle in 38-0 µm size fraction	163
Figure 9.3 Dispersed particles in 38-0 µm size fraction	163
Figure 9.4 Carbon Ash - size classification before and after grinding.....	170
Figure 9.5 Mass recovery at three separation densities	171
Figure 9.6 Coefficient of variation in mass of floats fraction at three separation densities	172
Figure 9.7 Percentage of material reporting to floats fraction at three separation densities.....	173
Figure 9.8 Distribution of major elements before and after grinding	176
Figure 9.9 Distribution of minor elements before and after grinding	177
Figure 9.10 Carbon concentration in floats at three separation densities.....	178
Figure 9.11 Carbon concentration in sinks at three separation densities	178
Figure 9.12 Distribution of carbon in floats fractions.....	180
Figure 9.13 Distribution of carbon in sinks fractions	180
Figure 9.14 Carbon concentration in 2.2rd float-sink fractions	182
Figure 9.15 Carbon distribution in 2.2rd float-sink fractions	182
Figure 9.16 Sulphur concentration in 2.2rd float-sink fractions	183
Figure 9.17 Sulphur distribution in 2.2rd float-sink fractions	183
Figure 9.18 Iron concentration in 2.2rd float-sink fractions	184
Figure 9.19 Iron distribution in 2.2rd float-sink fractions	184
Figure 9.20 Zinc concentration in 2.2rd float-sink fractions	186
Figure 9.21 Zinc distribution in 2.2rd float-sink fractions.....	186
Figure 9.22 Calcium concentration in 2.2rd float-sink fractions	187

Figure 9.23 Calcium distribution in 2.2rd float-sink fractions.....	187
Figure 9.24 Aluminium concentration in 2.2rd float-sink fractions	188
Figure 9.25 Aluminium distribution in 2.2rd float-sink fractions.....	188
Figure 9.26 Manganese concentration in 2.2rd float-sink fractions.....	189
Figure 9.27 Manganese distribution in 2.2rd float-sink fractions	189
Figure 9.28 Magnesium concentrations in float-sinks fractions at 2.2rd	190
Figure 9.29 Magnesium distribution in 2.2rd float-sink fractions	190
Figure 9.30 Copper concentration in 2.2rd float-sink fractions	191
Figure 9.31 Copper distribution in 2.2rd float-sink fractions	191
Figure 9.32 Trace element distribution in 2.2rd floats fractions.....	193
Figure 9.33 Trace element distribution in 2.2rd sinks fractions.....	193
Figure 9.34 SEM micrograph of ground 53-38 μm fraction.....	198
Figure 9.35 High magnification SEM image of ground 53-38 μm fraction - Image 1	198
Figure 9.36 High magnification SEM micrograph of ground 53-38 μm fraction - Image 2	199
Figure 9.37 SEM image of ashed 53-38 μm fraction.....	201
Figure 9.38 High magnification SEM image of ashed 53-38 μm fraction.....	201
Figure 9.39 Relationship between carbon and sulphur concentrations in float-sink samples	203
Figure 9.40 Relationship between zinc and sulphur concentrations in float-sink samples	203
Figure 9.41 Relationship between copper and iron concentrations in float-sink samples.....	204
Figure 9.42 Relationship between manganese and iron concentrations in float-sink samples.....	205
Figure 10.1 Coalite [®] pyrolysis char after magnetic separation.....	211
Figure 10.2 Pyrolysis char - fractional size distribution	212
Figure 10.3 Low magnification SEM image of Coalite [®] pyrolysis char.....	214
Figure 10.4 High magnification SEM image of Coalite [®] pyrolysis char - Image 1.....	214
Figure 10.5 High magnification SEM image of Coalite [®] pyrolysis char - Image 2.....	215
Figure 10.6 Pyrolysis char - fractional size versus % carbon	216
Figure 10.7 Pyrolysis char - fractional size versus % sulphur	216
Figure 10.8 Concentration of major elements in pyrolysis char fractions	217
Figure 10.9 Concentration of minor elements in pyrolysis char fractions	218

List of Tables

Table 2.1 Typical constituents of rubber compound (Rapra Technology Limited, 1995)	7
Table 2.2 Main constituents of car and truck tyres by weight (Rapra Technology Limited, 1995)	8
Table 2.3 Advantages and disadvantages of thermal treatment processes (Sharma et al. 2000)	11
Table 2.4 Chemical composition of carbon blacks (Othmer, 1992)	13
Table 2.5 Composition of carbon black produced by the Tertiary process (Allred et al. 2000).....	17
Table 3.1 Landfill disposal cost of annual STR output by material phase	29
Table 4.1 Comparison of carbon analysis of samples by two laboratories	35
Table 4.2 Precision and detection limit of carbon analysis method.....	36
Table 4.3 Reagents used in sulphur analysis	39
Table 4.4 CV and detection limit of sulphur analysis.....	43
Table 4.5 Comparison between total and Aqua-Regia digestions [n.d. - not determined].....	49
Table 4.6 Parameters used in the analysis of total digestion leachates by ICP-AES	52
Table 4.7 Parameters used in the analysis of Aqua-Regia leachates by ICP-AES.....	54
Table 5.1 Sulphur concentration of bushy wire samples	65
Table 5.2 Mineral phases identified in carbon ash samples.....	80
Table 5.3 Concentration of carbon and sulphur in bulk sample of carbon ash	81
Table 5.4 Concentration of elements in bulk carbon ash sample [<LOD - below limit of detection].....	85
Table 5.5 Combined analysis results of carbon ash bulk sample.....	90
Table 6.1 Dry magnetic separation of carbon ash fractions.....	95
Table 6.2 Dry magnetic separation of 'aged' carbon ash.....	97
Table 6.3 Ball mill conditions for carbon ash grinding prior to froth flotation.....	100
Table 6.4 Froth flotation results	101
Table 6.5 Element concentration in feed material by total digestion.....	110
Table 6.6 Bulk composition of recycled and commercial carbon blacks.....	112
Table 6.7 Attrition cell conditions.....	116
Table 6.8 Sulphur content of steel wire throughout attrition process	118
Table 7.1 Approximate market values of selected carbon based products *(Walters, 2002), **(Bruce, 1999).....	125
Table 7.2 Performance of carbon ash product against the BZL secondary fuel specification (n.a. - not analysed)	126
Table 7.3 Revenue generated from the sale of ash/wire derived products.....	130
Table 8.1 Analysis of magnetic separation trial carbon product.....	141
Table 8.2 Screw classifier product analysis.....	145
Table 8.3 Optimisation process conditions.....	147
Table 8.4 Precision in attrition optimisation test work	150
Table 8.5: Results of pilot scale attrition testing.....	151
Table 9.1 Calculated settling times in centrifuge and static float-sink tests	159
Table 9.2 Specific gravity of selected minerals present in carbon ash (adapted from (Carmichael, 1984))	160
Table 9.3 Ball milling conditions of carbon ash sample.....	162
Table 9.4 Mass of control samples before and after furnace drying	168
Table 9.5 Chemical analysis of bulk feed sample [LOD - limit of detection]	174
Table 9.6 Mineral phases identified in 53-38 µm and 106-75 µm float-sink fractions.....	194
Table 10.1 Combined analysis results of pyrolysis char bulk sample	219

Table 10.2 Comparison between carbon STR and Coalite bulk carbon phases [LOD - limit of detection].....220

List of Equations

Equation 4.1 Chemical reactions in total carbon apparatus	34
Equation 4.2 Detection limit of elements by ICP-AES	51
Equation 4.3 The determination of concentration in sample from concentration in solution	51
Equation 6.1 General reaction of metals with hydrochloric acid.....	105
Equation 9.1 Reaction of zinc oxide with sulphur during pyrolysis/incineration process	207
Equation 9.2 Calculation of excess sulphur in zinc oxide reaction.....	207

List of Appendices

Appendix 1	Results of Carbon Ash Characterisation	I
Appendix 2	Separation Studies Results	III
Appendix 3	Float-sink Test Results	VII
Appendix 4	Analytical Methods Development Results	XII
Appendix 5	Results of Pyrolysis Char Characterisation	XIV

Acknowledgements

I would like to thank Professor Nick Miles and Dr Brian Atkin for their supervision and advice.

The initial part of this work was funded from the Cleveland Waste Management Landfill Tax Credit Fund which is managed by the Industry Nature Conservation Association.

SITA Tyre Recycling Ltd are thanked for access to the site and samples.

Phil Hall, former manager of SITA Tyre Recycling Ltd, is thanked for providing encouragement, information and opportunities during this research.

Acknowledgement and thanks goes to Chris Somerfield for his valuable advice and suggestions on analytical and experimental matters. Thanks also goes to Dave Clift for the training provided for X-Ray Diffraction and Scanning Electron Microscope analysis.

Samuel Pollard is thanked for his assistance with the analysis of the pyrolysis samples which were supplied by Coalite[®] Smokeless Fuels Ltd.

Finally, I would like to thank KJB, my family, friends, little George and Bristol City FC. All of them helped in their own way.

Abstract

In excess of 1,000 million tyres are manufactured worldwide every year. The average tyre lasts for approximately 50,000 kilometres before it must be replaced. Each year in the UK approximately 37 million tyres reach the end of their useful life. The used tyre, which is almost identical to the replacement, then requires disposal. As the volume of road traffic increases alternative disposal routes are required to take up the resulting shortfall in capacity.

SITA Tyre Recycling operate an incinerator in the West Midlands which solely burns scrap tyres. The plant receives a significant proportion of UK scrap tyre waste stream as well as reject tyres from manufacturers. The main waste stream generated is disposed to landfill. The objective of this research was to determine if the waste had potential for recycling which would reduce the burden on landfill and possibly generate revenue through the sale of products.

By developing methods to sample and characterise the waste stream it was found to consist of multiple phases that could be individually treated to generate valuable products. Products based on carbon and steel were derived from the combusted rubber and bead wire respectively. Detailed examination of the carbon phase using a range of techniques revealed that many compounds used in the manufacture of the tyre rubber were highly dispersed in a carbon dominated matrix. The success of physical separation processes was limited by the difficulties associated with liberation of the valuable carbon from contaminating elements. The post-combustion steel was found to have an unacceptable sulphur concentration, which was mainly associated with surface coatings of the carbon phase. Through the application of traditional attrition scrubbing the surface coatings were removed and a reduced sulphur content steel product generated.

Pilot scale trials were used to generate large samples for industrial assessment and process optimisation purposes.

1 General Introduction

Robert Thompson invented the pneumatic tyre in the middle of the 19th Century, initially for use on horse drawn coaches. The discovery of vulcanisation in 1839, by Charles Goodyear, enabled the tyre to evolve from a rubberised canvas covering a tube into a complex fabric, steel and elastomer composite (Kovac and Rodgers, 1994). In 1888 André Michelin, together with his younger brother Edouard, formed the Michelin Company and pneumatic tyres began to be used on motor vehicles. In the present day more than 1,000 million tyres are manufactured world-wide each year. The average car tyre lasts for approximately 50,000 kilometres, before it is likely to require replacement. This figure is dependent to a large extent on driving style and the standard of maintenance (The Environment Agency, 1999). In the United Kingdom road traffic is forecast to grow at a rate of between 17% and 39% in the period from 1997 to 2011 (Department of the Environment, 1997). Assuming that there are no major increases in tyre longevity, the number of worn tyres requiring disposal would be expected to increase accordingly.

As the numbers of tyres in use increases the treatment of those that have reached the end of their useful life is becoming an increasingly important issue. When tyres are disposed of they have lost only a few grams of their original mass (Adhikari and S Maiti, 2000), indicating that a used tyre is essentially identical in its physical and chemical properties to that of a new tyre. In 1996 it was estimated that 37 million car and truck tyres, weighing approximately 380,000 tonnes, reached the end of their life in the UK (The Environment Agency, 1999).

1.1 Scrap tyre management

In the UK, garages or specialist tyre retailers are generally used to replace worn car tyres, the used tyres then become known within the industry as ‘casings’. At present the cost of the handling and disposal of the casing is recovered from the customer through the inclusion of a small ‘casings disposal’ charge in the final bill. The casings are then stored on-site until a sufficient quantity has accumulated before being

collected by re-treading companies or dealers. They are then inspected and sorted into three main categories:

1. Those of sufficient quality for re-treading.
2. Those meeting the standard required for resale as part worn tyres.
3. Those only suitable for material recycling, energy recovery or disposal.

Where large volumes of tyres are disposed of in landfill sites, or stockpiled, they represent a significant fire and health hazard. Discarded tyres are a breeding ground for mosquitoes as their shape traps water and can hold it for a long period of time, allowing larvae to develop (Ji-Won Yang et al. 1998). The uncontrolled burning of tyres can lead to the production of harmful substances which can effect air and water quality and contaminate soil. In 1989 a suspected arson attack started a fire in a Welsh landfill. The site contained approximately 10 million scrap tyres and was still burning in 1998 (The Environment Agency, 1999). Tyre fires affect the long-term settlement of sites and may subsequently cause problems with the future re-use and reclamation of the land. The European Council Directive on the landfill of waste contains legislation that will prohibit the disposal of whole tyres to landfill by the year 2003 and shredded tyres (whole tyres chipped into smaller pieces) by 2006 (European Council, 1999). The European Council End of Life Vehicles (ELV) Directive, due to be implemented by April 2002, will also have an impact on scrap tyre management. Tyres will have to be recovered from all scrapped vehicles either prior to vehicle shredding or segregated afterwards in such a way as they can be recycled (European Council, 2000).

The Government/Industry Scrap Tyre Working Group (STWG) compiles the annual UK tyre usage and disposal statistics. The statistics are based on estimates of replacement tyre sales, tyres on scrapped vehicles and the import of used casings for retreading. In 1996 approximately 37 million car and truck tyres reached the end of their useable life in the United Kingdom. The treatment of these scrap tyres is summarised in Figure 1.1.

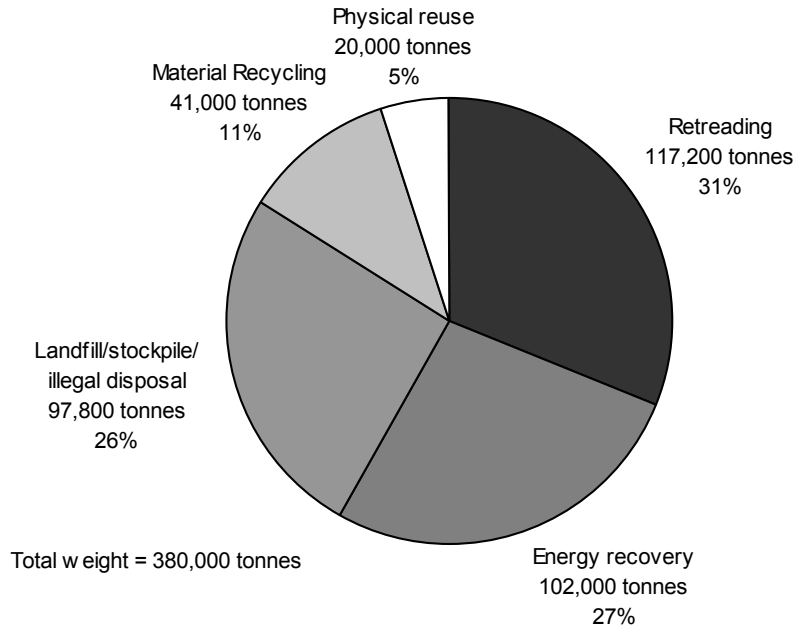


Figure 1.1 Management of scrapped tyres in the UK, 1996 (Scrap Tyre Working Group, 1997)

From Figure 1.1 it can be seen that 26% (97,800 tonnes) of the scrap tyre arisings were disposed of to landfill, this proportion will require an alternative treatment route as the EU Landfill Directive is incorporated into UK law. Retreading is the only treatment method where the tyre is reused for its original purpose. Lorry tyres are routinely retreaded, or re-grooved, a number of times before finally being discarded. The ability to retread a tyre is dependant on the casing being in relatively good condition, only 25% to 30% of car tyres and 60% to 65% of lorry tyres are suitable. In a tyre retreading process the old tread pattern is removed and a new tread bonded to the carcass, replacement sidewalls may also be added. In comparison with new tyres, retreaded tyres are generally cheaper to purchase; however, the public perceives them to be of a lower quality and potentially dangerous. This image problem limits the growth of the market for the use of retreaded tyres in the private sector (Ferrer, 1997).

The physical reuse of tyres is popular due to their abundance, durability and low cost. Uses for whole tyres include artificial reefs/breakwater formation, landfill engineering, silage clamps and gardening applications (The Environment Agency, 1999). The reuse of whole tyres is not a final treatment option since, in general, the casing will eventually require final disposal.

The 41,000 tonnes of tyres that were recycled for materials were mainly granulated. The granulated material has a variety of applications including sports surfaces, rubber boots and road building. Granulate is produced either by the mechanical grinding of whole tyres or alternatively cryogenic grinding. In cryogenic grinding the tyres are cooled in liquid nitrogen prior to grinding which causes the rubber to become brittle and hence reduces the energy required for the process (Adhikari and S Maiti, 2000). After grinding the steel and rubber phases are separated by dry magnetic separation.

The majority of the 102,000 tonnes of tyres that were treated by energy recovery in 1996 were processed at a single tyre incineration plant (SITA Tyre Recycling, described in Chapter 3) (The Environment Agency, 1999). The process uses tyres as the sole fuel source from which electricity is generated. Scrap tyres represent an attractive material for energy recovery processes due to their high calorific content in comparison with other fuels. They contain an average of 32 GJ per tonne, which is slightly higher than coal at 26 GJ per tonne (Department of Trade and Industry, 1997). Lower volume processors of tyres for energy recovery include use as a fuel in cement kilns and also in pyrolysis processes. In pyrolysis the energy is recovered from the tyres in the form of reusable fuel products. These processes are described in more detail later.

In the United States of America huge stockpiles of scrap tyres have built up, it is estimated that 2 billion tyres are stored at various locations around the country (Ji-Won Yang et al. 1998). Provision was made in the Intermodal Surface Transportation Efficiency Act of 1991 for U.S. states to begin incorporating crumb rubber (6300-400 μm approx.) into asphalt paving materials. However this was suspended due to technical problems concerning the use of crumb rubber in asphalt mixtures. In countries such as Japan and Korea where the automobile has not been in use for a significant time then scrap tyre management is not such an issue. Japan reuses the majority of scrap tyre arisings as a fuel in cement kilns and boilers (Ji-Won Yang et al. 1998).

The recovery of energy and/or materials from scrapped tyres could potentially provide a treatment route for the increasing volume of casings requiring disposal.

1.2 Rationale for the project

This research was initiated in 1998 after SITA Tyre Recycling Ltd approached the University of Nottingham with a view to commencing a study of their waste stream produced by the incineration of scrap tyres. The disposal of the residue to landfill represented a significant cost in the running of the plant, and was likely to rise, in part due to Landfill Tax. Clearly if a market could be identified for a part of, or the entire residue, then not only would disposal costs be reduced but revenue may also be generated. This would be a function of the market the residue was sold in to and its specification.

1.3 Research aims

This project investigates the potential for the recycling of a waste residue produced by the incineration of scrap tyres. This thesis presents the progression of research in the order in which it was undertaken. Samples collected during an initial characterisation study were used to develop suitable analytical methods for the quantitative determination of material properties. The separation of potential products from the waste residue was then investigated. The requirement to begin recycling the material as soon as possible necessitated the production of larger samples for industrial assessment. This was attempted through the scale-up of processes developed during the separation studies to pilot scale. Finally, a more detailed examination of a particular phase of the material was undertaken in an attempt to assess the possibility of generating higher value products.

1.4 Thesis outline

Chapter 2 - A literature review is presented discussing tyre manufacture and the range of methods that are employed to recover value and components from scrapped tyres.

Chapter 3 - The SITA Tyre Recycling plant is described in detail and the waste stream identified.

Chapter 4 - The main analytical techniques used for this research are selected and their development for the particular application is described.

Chapter 5 - The methods adopted for the collection and treatment of samples is described. The data from the characterisation of the samples is presented and potential products identified.

Chapter 6 - The production of separated product phases using a range of processing techniques is described.

Chapter 7 - The knowledge and samples obtained during Chapters 5 and 6 are supplied to potential end users of the products and the results discussed.

Chapter 8 - A pilot scale trial is described and the results presented.

Chapter 9 - A more detailed characterisation of a part of the waste stream is described following a review of similar practices.

Chapter 10 - The characterisation of a tyre pyrolysis char is described and the results compared to the SITA Tyre Recycling material.

Chapter 11 - The thesis is concluded.

2 Literature Review

2.1 Introduction

The recycling of the residues resulting from energy recovery processes as applied to scrap tyres has received increased interest in recent years mainly due to the potential of pyrolysis processes. Tyres represent a low cost, high availability, fuel source that is initially manufactured from high cost raw materials. The recovery of these materials from the scrapped tyre could offset the cost of the process and hence make it economically viable.

2.2 Tyre manufacture

The materials used during the manufacture of tyres are likely to determine the main properties of residues produced during energy recovery processes. The main mass of a tyre is composed of rubber hydrocarbon, which is generally a mixture of natural and synthetic rubbers. Other ingredients are then added to the rubber compound to enhance the properties of the tyre. Carbon black, a high purity (high cost) carbon product derived from crude oil or gas, is used as a reinforcing agent. The rubber is vulcanised by the addition of sulphur and the application of heat. Other chemicals, including zinc oxide are used to enhance and control the chemical reactions and quality of the final product (The Environment Agency, 1999). The relative weight of each constituent in the rubber compound is presented in Table 2.1.

Constituent	Weight (%)
Rubber hydrocarbon	51
Carbon black	26
Oil	13
Zinc oxide	2
Sulphur	1
Other chemicals	7

Table 2.1 Typical constituents of rubber compound (Rapra Technology Limited, 1995)

The other main ingredients of the tyre are steel and textile. Steel wire, usually coated in brass, is used to form the tyre beads, which hold the tyre onto the wheel. The brass coating (25-40 wt. % zinc) is electrodeposited onto the steel before the cable is drawn and results in a final coating thickness of approximately 0.2 μm (Orjela, 1994). The coating ensures adhesion between the bead and the rubber through the formation of a copper-sulphur film during vulcanisation (Chanel and Pebere, 2001). A fine woven steel mesh may also be used to reinforce the rubber, forming a steel belt. Textiles including rayon, nylon, fibreglass and polyester are also used for reinforcement. The proportions of rubber, steel and textile vary depending on tyre construction and end use and are summarised in Table 2.2.

Vehicle	Tyre type	Rubber compound (%)	Steel (%)	Textile (%)
Car	Steel braced radial	86	10	4
	Textile braced radial	90	3	7
	Cross ply	76	3	21
Truck	All steel radial	85	15	<0.5
	Cross ply	88	3	9

Table 2.2 Main constituents of car and truck tyres by weight (Rapra Technology Limited, 1995)

Modern tyres are almost entirely made of a radial construction where reinforcement layers run perpendicular to the direction of travel. The three main elements of the tyre (sidewalls, tread and bead) are placed in a former, which contains a mould of the required tread pattern. A rubber bladder is inflated inside the tyre and heat and pressure is applied. The heat causes the rubber to vulcanise whilst the pressure causes the tread impression to be moulded into the tyre (The Environment Agency, 1999). During vulcanisation chemical crosslinks are formed between polymer chains increasing the elasticity and decreasing the plasticity of the rubber product (Coran, 1994). The finished tyre (see Figure 2.1) is then subject to a number of safety and quality inspections prior to use.

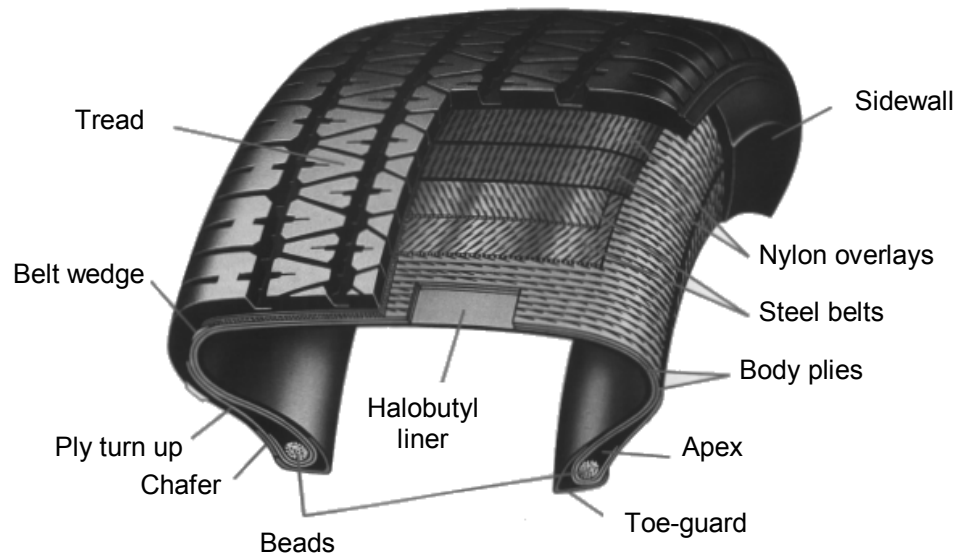


Figure 2.1 Cross section of a modern car tyre (Kovac and Rodgers, 1994)

2.3 Rubber reclamation

The reclamation and recycling of waste rubber has been reviewed extensively in Adhikari and S Maiti (2000). In reclamation of scrap rubber the three dimensionally inter-linked thermoset polymers must be transformed into a soft, plastic, reprocessible and vulcanisable material which would have similar properties to virgin rubbers. Three main techniques were found to exist that were broadly categorised as physical, chemical and biological. Physical processes used mechanical shear, often combined with external energy to break down the rubber into a powdered material, which could then be recombined into a rubber compound. Cryogenic grinding has also been used and with the advantage of lower equipment (reduced wear) and energy costs. The addition of microwave and ultrasonic energy can also be applied to rubber to selectively cleave the carbon-sulphur and sulphur-sulphur bonds formed during vulcanisation. In chemical processes solutions such as organic disulphides and mercaptans (organosulphur thios) and some inorganic elements have been used to selectively cleave the cross-links in the rubber. More recent advances have seen the application of biotechnology to separately recover sulphur and rubber from vulcanised rubber with micro-organisms. It was concluded that generally the reclaimed material was found to be inferior in comparison with virgin rubber, although microwave technology produced the highest quality product (Adhikari and S Maiti, 2000). It has

also been suggested that as rubber recipes have become increasingly sophisticated, reclaiming has greatly diminished as a rubber reusing technique (Piskorz et al. 1999).

The recovery of valuable tyre components in their original form, such as carbon black, can only be attempted when the bonds between them and the tyre material are broken so that the material is liberated. This generally involves the input of energy and can result in the liberation of a range of chemicals as well as the formation of other products. These processes are now summarised.

2.4 The recovery of tyre components

The majority of research in to the recovery and reuse of components from scrapped tyres has involved some form of energy recovery process. The main methods for converting tyres to energy with the reuse or recycling of tyre components are listed below:

- incineration
- direct use as a fuel in cement kiln
- pyrolysis

Processes also exist that utilise solvents to dissolve the tyre constituents in order to recover individual chemicals. The perceived advantages and associated problems of thermal treatment processes applied to scrap tyres have been summarised in Table 2.3.

Advantages	Associated problems
<ul style="list-style-type: none"> • Volume of waste can be reduced by more than 90% • Net energy producer with possible material recovery • Non-polluting and capable of destroying most of the organic substances, which are harmful to human health 	<ul style="list-style-type: none"> • Lead and cadmium salts remain as ash causing disposal problems • Production of toxic gases such as SO₂, H₂S etc. when tyres are burnt • Production of soot through the imperfect burning of waste • Shortage of appropriate incineration technology

Table 2.3 Advantages and disadvantages of thermal treatment processes (Sharma et al. 2000)

The potential for volume reduction and energy recovery available from thermal treatment processes is the main driving force for development. The main focus of research has concerned pyrolysis as the process is thought to have the added benefit of recovering valuable chemicals alongside fuel products.

2.4.1 Tyre pyrolysis

The pyrolysis of scrap tyres has been the subject of numerous studies. The pyrolysis process, when applied to tyres, is described as the degradation of the rubber, using heat, in the absence of oxygen. The organic volatile matter of tyres (mainly the rubber) is decomposed into lower molecular weight products (oils and gases), inorganic components (mainly steel and non-volatile carbon black) remain in the residue and may potentially be recycled (Rodriguez et al. 2001). The product compositions are dependent on the pyrolysis conditions as well as the composition of the feed tyres. The process is usually conducted under oxygen insufficiency or in an inert gas at either atmospheric or reduced pressures and in temperatures ranging from 300°-1000°C. The rubber feed can be in the form of granulate or sometimes whole tyres. The process is highly endothermic with a typical energy consumption of 4.0-5.7 MJ/kg of rubber (Piskorz et al. 1999).

2.4.1.1 Laboratory scale pyrolysis

Commercial tyre pyrolysis processes have had limited application world-wide, although many pilot scale processes have reported considerable success (Sharma et al. 2000). The majority of the published research on scrap tyre pyrolysis has been conducted at either laboratory or pilot scale. Significant yields of hydrocarbon liquid, char and gas have been reported from the pyrolysis of shredded tyres (Williams et al. 1990). During the process the tyre was converted to 55% oil, 10% gas and 35% solid char. Surface area determination of the char indicated that by increasing the temperature and heating rate of the process the surface area of the char product was improved. Similar product yields were reported in another study where a vacuum pyrolysis process generated 55% oil, 25% carbon black, 9% steel and 6% gas at both laboratory and pilot scale (Roy et al. 1990). The gross heating value of the oil was found to be 43MJ/kg with an associated sulphur content of less than 1% indicating a potential reuse as heating oil. A carbon black type material (char) generated during the pilot scale trial was supplied to two rubber product manufacturers for assessment. It was concluded that the carbon could partially replace commercial blacks for the preparation of low-grade rubber parts. The separated steel was also considered marketable and saleable.

The market value of the material produced by scrap tyre pyrolysis has been found to be insufficient to make the process economically feasible, this has necessitated the generation of higher value products to avoid significant subsidisation (Piskorz et al. 1999). Subsequently a great deal of research has been conducted in to the recovery of the potentially high value carbon black from the tyre, which is usually present in the char fraction of the pyrolysis products.

The main difference between the properties of commercially produced carbon blacks (CB) and those recovered from scrap tyre pyrolysis (CB_p) is the increased quantity of ash in the CB_p (Chaalal et al. 1996) (Darmstadt et al. 1994) (Williams et al. 1995) (Helleur et al. 2001) (Rodriguez et al. 2001). In commercial processes CB is manufactured by the incomplete combustion of a range of organic substances. The term CB refers to a group of industrial products consisting of furnace blacks, channel blacks, thermal blacks and lamp-blacks. CB is composed essentially of elemental

carbon in the form of near spherical particles coalesced into aggregates (Donnet and Voet, 1993). The most widely used technique for the production of CB is the furnace process where feedstocks such as heavy petroleum fractions are passed through a flame to produce the desired black. The quality and yield of product are controlled by the flame temperature and residence time. The carbon stream is then quenched in water prior to collection (Donnet and Voet, 1993). The sources of ash in the virgin carbon blacks are the feedstock and the quenching water, whereas in the CB_p the ash content is derived mainly from the inorganic compounds added to the rubber during the vulcanisation process (Darmstadt et al. 1994).

2.4.1.2 Typical properties and markets for Carbon Blacks

The majority of world-wide CB production is used in rubber compounding (90%), 70% of which is used in tyres. Commercially produced CB is in the form of fluffy powder, which consists almost entirely of elemental carbon (Othmer, 1992). The size and shape of the CB aggregates are the principal features that determine the performance of the material as a reinforcing agent. Some of the properties of the CB that are used to characterise and grade the material are particle size, surface area, aggregate size and aggregate morphology (Donnet and Voet, 1993). Chemically the blacks used in the rubber industry contain over 97% elemental carbon whilst specialist application blacks may contain over 99% carbon. The other main elements present in the CB are hydrogen, oxygen and sulphur, see Table 2.4. Blacks used for pigmentation purposes contain larger quantities of oxygen than normal blacks to improve the dispersion and flow characteristics.

Grade	Carbon (%)	Hydrogen (%)	Oxygen (%)	Sulphur (%)	Ash (%)	Volatile (%)
Rubber	97.3-99.3	0.20-0.40	0.20-1.20	0.20-1.20	0.10-1.00	0.60-1.50
Medium	99.4	0.30-0.50	0.00-0.12	0.00-0.25	0.20-0.38	
Acetylene	99.8	0.05-0.10	0.10-0.15	0.02-0.05	0.00	<0.4

Table 2.4 Chemical composition of carbon blacks (Othmer, 1992)

The sulphur present in the CB does not contribute to the sulphur cross-linking during the vulcanisation of the rubber compounds, the ash content of a furnace black may be

as high as 1% and consist principally of salts and oxides of calcium, magnesium and sodium (Othmer, 1992). The highest grades of carbon black are used in the tyre tread whilst lower grades are utilised in the sidewall and liner. Since the tread part of the tyre is the only portion that is significantly worn after disposal, the scrap tyre will contain a lower proportion of the highest grade CB (Piskorz et al. 1999).

The small volume of CB not used within the rubber industry are designated 'special blacks'. Most are manufactured to meet the specific requirement of the end user and therefore command a higher market price. Approximately 42% are used in plastics, 35% in printing inks, 7% in paper and 16% in miscellaneous applications. Medium and high colour grades are used in enamels, lacquers and plastics for their extreme jet-black colouration (Othmer, 1992).

2.4.1.3 Characteristics and potential uses of CB_p

The solid material (char) produced by the pyrolysis of tyres originates from the reinforcing carbon black used as a filler in tyre production. Char also contains almost all of the inorganic compounds present in tyres and a significant amount of the condensed by-products formed during pyrolysis (Helleur et al. 2001). In comparison with CB the sulphur content of CB_p is high, 2-3% compared to <1%. It has been calculated that more than 50% of the original sulphur in the tyre remains in the solid char residue after pyrolysis (Rodriguez et al. 2001).

The distribution of the non-carbon elements differs between the commercial CB and CB_p. In commercial CB it has been found that the inorganic components are concentrated on the particle surface as opposed to CB_p where only zinc sulphide, formed by the reaction of zinc oxide with sulphur derived from the decomposition of organic compounds, was concentrated on the surface (Darmstadt et al. 1994). At certain pyrolysis temperatures individual zinc sulphide particles were observed in the char, however, the particle size was similar to that of the carbon so a size separation was not effective in removing the mineral phase. X-Ray Diffraction showed that the CB_p contained both zinc oxide and zinc sulphide (as wurtzite and sphalerite). Sulphur has also been detected on the surface of some CB_p materials in the form of CS₂ (Lee et al. 1999).

When the surface areas of an acid de-mineralised CB_p and a commercial CB were measured the values were found to be comparable (Roy et al. 1999). This was thought to indicate that the CB structure changed only slightly during pyrolysis. The surface chemistry and activity were also found to be similar indicating a potential to replace commercial CB in certain applications

In order to increase the market value of CB_p an attempt was made to reduce the ash content with an acid-base demineralisation technique (Chaala et al. 1996). The initial ash content of a CB_p sample was found to be 14.6%. Treating the char with a sulphuric acid solution followed by a sodium hydroxide solution reduced the ash content to 3%. The carbon concentration of the material was subsequently increased from 80.4% to 93% by weight. The reduction of the ash content of the material directly influenced the specific area of the carbon by partially cleaning the surfaces of the carbon. The acid-base method was found to remove all of the zinc oxide and most of the zinc sulphide.

An alternative approach to the upgrading of the CB_p material has been attempted through activation to enhance the pore system and increase the internal surface area (Helleur et al. 2001). Activating CB_p, using steam, was found to produce a carbon product with a good surface area with excellent absorption properties for phenol and methylene blue

The suitability of the pyrolysis process in the application to the treatment of scrap tyres and the proper assessment of the recovered material requires that the process be scaled-up. In recent years a full-scale process in the United Kingdom known as 'Tyrolysis' failed to operate successfully mainly due to mechanical and material handling difficulties (Robinson, 1989). Two operational full-scale tyre pyrolysis processes, one of which has recently begun operation in the United Kingdom, are now described.

2.4.1.4 Commercial scale pyrolysis plants

A 100 tonnes per day tyre pyrolysis plant, located in Taiwan, has been described in detail by Allred et al. (2000). The process, known as 'Tertiary Recycling', is defined as the 'processing of plastics back to valuable chemicals or fuels for reuse'. The product streams generated by the process are liquid hydrocarbons, gaseous products, carbon black and steel. Tyres are fed into the system as 50 mm chips, formed by the shredding of whole tyres. A schematic diagram of the process has been presented in Figure 2.2.

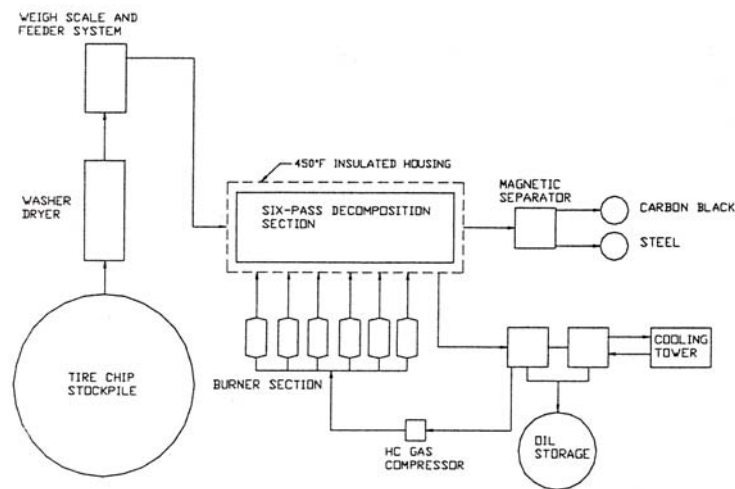


Figure 2.2 Tertiary recycling process (Allred et al. 2000)

A screw conveyor agitates and transports the tyre chips through the six stages of the heating zone. Oil seals at either end of the conveyor stop oxygen entering the system. As the material passes through the heated zone the gases are collected and filtered to remove any carbon black carried over before being cooled. Non-condensable gases are collected and recycled as fuel for the burners. A further screw conveyor is mounted at the discharge end of the reactor unit to remove the carbon black and steel, the conveyor has a water cooled jacket to lower the material temperature prior to separation. The product then enters a drum magnet, which separates the steel from the carbon black and are then moved to the pick up points for the materials.

The ash content of the recovered carbon black (8.12% by weight) is high in comparison with commercially produced carbon blacks. The bulk chemical composition has been presented in Table 2.5.

Element	(ppm)	Element	(ppm)
Aluminium	205	Molybdenum	6
Antimony	<1.0	Nickel	56
Arsenic	<1.0	Phosphorus	210
Barium	16	Potassium	301
Beryllium	<1.0	Selenium	<1.0
Bismuth	<1.0	Silicon	1960
Boron	16	Silver	<1.0
Cadmium	<1.0	Sodium	330
Calcium	9333	Strontium	<1.0
Chromium	40	Thallium	<1.0
Cobalt	<1.0	Tin	2
Copper	44	Titanium	962
Iron	1600	Vanadium	26
Lead	69	Zinc	45,866
Magnesium	533	Ash content (wt %)	8.12

Table 2.5 Composition of carbon black produced by the Tertiary process (Allred et al. 2000)

The surface area of the carbon black product was measured and found to be $25.31 \text{ m}^2\text{g}^{-1}$, which was comparable to that of a semi-reinforcing black used in tyre carcasses (Allred et al. 2000). The recovered carbon black was thought to be ready for sale into markets such as reinforcing rubbers and plastics or as an active ingredient in inks, toners and paints. The liquid fraction from the process was analysed for fuel value by distilling to determine the composition. The liquid was found to comprise of kerosene, naphtha and gasoline with a small proportion of solid residue. It was thought that the liquid fraction could either be used immediately as a valuable fuel source for ships and heating systems or upgraded into higher quality fuels based on the component fractions. The reclaimed steel is readily recycled and is desirable to steel mills due to its high bulk density. In general the process was claimed to be economically feasible with the key factors required for cost-effective operation defined as obtaining value for all of the components in the scrap and using a high volume continuous process (Allred et al. 2000).

2.4.1.5 The Coalite[®] smokeless fuels process

The adaptation of an existing process to the pyrolysis of scrap tyres has been attempted by Coalite[®]. Equipment that is usually used to generate smokeless fuel from a bituminous coal feedstock was adapted to accept baled whole tyres as part of a pilot trial (Anon, 2000). The tyres are heated for eight hours during which time oil and gas generated by the process are driven off. The solid product, consisting of char residue and scrap metal bands, is then allowed to cool for 16 hours (Anon, 2000). Existing Coalite[®] retorts (see Figure 2.3) have been adapted to accept 50 baled tyres each meaning that each battery could eventually be capable of processing 7,500 tonnes of tyres annually. After initially attempting to pyrolyse whole tyres the process was altered to process shredded tyres (Bell, 2002). This was primarily for reasons of improved material handleability.

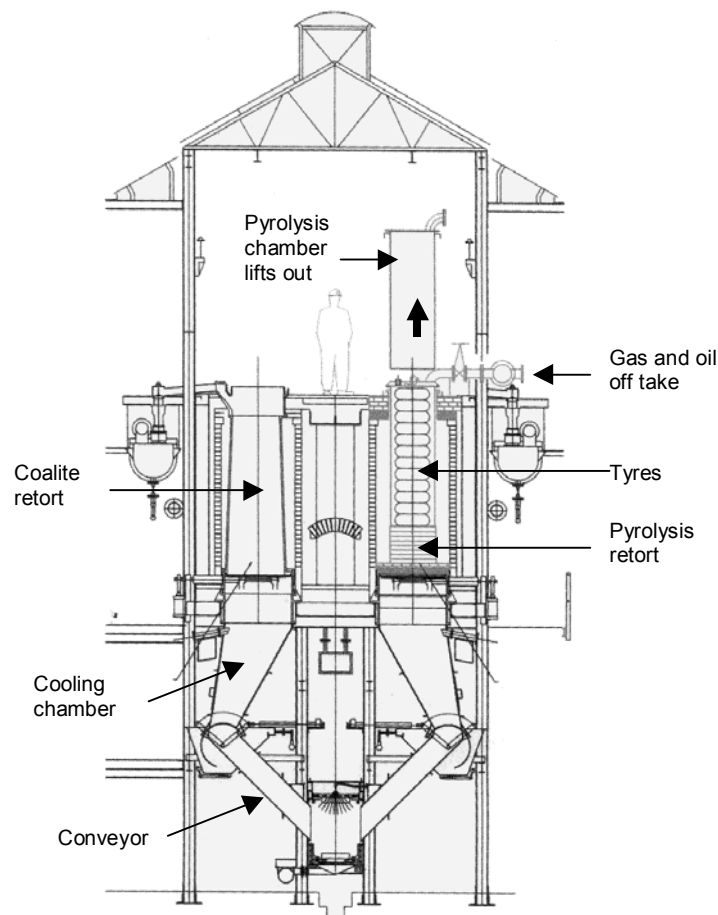


Figure 2.3 Coalite tyre pyrolysis process (Anon, 2000)

Markets for all of the products generated by the pyrolysis process have been identified. The oil produced during the process is similar to Brent Crude and would either be blended or sold as fuel oil. The gas would be recycled within the system to provide the heat for the process. The solid char could then either be blended back into the Coalite blend in as a coal substitute or possibly as a low-grade carbon black. The steel phase of the solid char would be baled and sold as scrap (Anon, 2000).

The adaptation of existing technology has the significant advantage of removing technical barriers associated with pyrolysis processes, making the start up costs lower. However, the success of the process is still reliant on identifying profitable markets for the materials produced. The process is currently undergoing further trials. The properties of the solid char are investigated in Chapter 10.

2.4.2 Alternative methods of carbon black recovery

2.4.2.1 Rubber dissolution

An alternative approach to the recovery of carbon black from scrap tyres was investigated in Piskorz et al. (1999). A hydrogenation process was developed to recover CB from rubber crumbs prepared from scrap tyres. In the process the rubber is dissolved in paraffinic lubricating oil through which hydrogen is bubbled allowing the CB to be freed from the polymer matrix. At optimal conditions the yield of the process was approximately 36% CB and inorganic additives, 1-2% gas, 8% naphtha and the remainder was oil. The most important and valuable product of the process was considered to be the CB. The process yielded 'primary' carbon black, which is the original component of the rubber, and a 'secondary' carbon black, which was produced by the decomposition of liquid organic molecules. The primary carbon contains ash and the sulphur derived from the inorganic materials added during compounding, these components are not present in the secondary carbon.

The ash content of the carbon as recovered from the process by filtering and drying was 17.6% (by weight) consisting of silicon, zinc, aluminium, sulphur and traces of iron and titanium. This was reduced to 9.7% using a wash with dilute hydrochloric acid. After acid washing the product had a carbon concentration of 86.8% the balance

of the material was mainly silica and titanium dioxide. It was suggested that it might not actually be necessary to remove the inorganic components since they are made up of useful compounding additives (Piskorz et al. 1999). A rubber compounding company assessed the recycled carbon black product for use within the industry. It was found that the product had properties similar to that of a low-grade commercial black. It was thought that the process could be adapted to accept whole tyre pieces since the steel wire would be freed from the polymer matrix and easily separated (Piskorz et al. 1999).

2.4.2.2 Microwave treatment

The application of microwave technology to the processing of scrap tyres has previously been investigated (Robinson, 1989). The process developed was essentially a pyrolysis process where the heat supplied to the shredded feed material was generated with a number of microwave generators. The advantage of the use of microwaves is claimed to be that the material heats very quickly from the inside out-ward which may then lead to a more efficient use of energy. The remainder of the process is then similar to pyrolysis operations with oil, carbon black, steel and gas being recovered and recycled. The system was found to be successful when operated as a small batch scale unit although significant investment was required to develop the process into a continuous commercial scale process.

2.4.3 Cement kilns

The use of scrap tyres as a fuel for cement kilns is beginning to increase with several trial projects being conducted in the United Kingdom by Castle[®], Blue Circle[®] and Rugby[®] Cement. (ERJ, 1999) (ENDS Report, 2000). European cement plants have been burning scrap tyres since the 1970s and plants also exist in North America, France and Japan (Ferrer, 1997).

The use of scrap tyres in cement kilns has the advantage that no waste is generated beyond what is normally created by the cement production process. The energy content of the rubber provides the heat required for the process whilst the steel constituent of the tyre contributes to the iron ore requirement, other combustion

residues are incorporated in to the cement without compromising the product quality (Ferrer, 1997). Cement kilns have traditionally used fossil fuels such as coal to provide the energy content however, where as manufacturers need to pay for coal they may charge a fee to accept tyres. Tyres are fed into the systems as either chipped (shredded whole tyres) or whole tyres depending on the type of kiln in use (The Environment Agency, 1999).

The distribution of cement kilns throughout the UK keeps transportation costs low although the high cost of fuel conversion together with associated environmental monitoring charges will mean that not all kilns start to accept tyres (ERJ, 1999).

2.4.4 Tyre incineration with energy recovery

Incineration has been widely used in the waste treatment industry, mainly due to the reduction in volume of the feed material that can be achieved. Many incinerators are also equipped with technology to generate electricity from the process of waste combustion. Incineration is, however, not a final disposal option since by-products of combustion (residues) remain and these ultimately require final disposal or reuse.

The incineration of waste tyres is defined as the reduction of the combustible fraction to an inert residue by controlled high temperature combustion (Sharma et al. 2000). The combustion process is spontaneous above 400°C, highly exothermic and once initiated becomes self-supporting (Sharma et al. 2000). The heat generated during the combustion of scrap tyres can then be converted to electricity using proven waste to energy technology from the municipal waste industry. The only waste to energy plant, solely burning scrap tyres, in the United Kingdom is based in Wolverhampton, West Midlands. The process is described in detail in Chapter 3.

2.5 Summary

The main focus of research concerning the recovery of materials and energy from scrap tyres is with the relatively unproven technology of pyrolysis. Although this process is routinely investigated at laboratory and pilot scale batch trials some commercial scale plants have failed to operate successfully. This has meant that the

technique is not yet widely used as a treatment method for scrap tyres around the world.

The recovery of energy from tyres is attractive due to their high calorific value and this is exploited through the application of processes such as cement kilns, pyrolysis and incineration. In pyrolysis the energy is recovered indirectly through the generation of fuel materials for subsequent reuse. The cost effectiveness of pyrolysis processes relies heavily on the recovery of carbon black from the feed tyres. Most of the research in the field has concentrated on the recovery and upgrading of the recovered carbon black which, in general, has been found to be inferior, and hence has a lower value, compared to commercially produced blacks.

The incineration of scrap tyres has the significant advantage over other treatment methods as a plant already operates at full-scale in the United Kingdom and is a significant part of the scrap tyre management strategy. The combustion residues may contain potentially valuable and recoverable materials as have been identified in pyrolysis processes although it has not previously been investigated to any great extent. By adopting a fresh approach to the recovery of any products from the material as opposed to individual components, such as the carbon black, it might be possible to make the incineration of scrap tyres a more environmentally attractive and cost effective treatment method.

3 SITA Tyre Recycling

3.1 Introduction

The scrap tyre incinerator located in Wolverhampton, United Kingdom became operational in 1993 and was originally operated by Elm Energy & Recycling (UK) Ltd. Since its construction the plant has been plagued by operational difficulties, which has meant that it has consistently operated below its original design capacity for scrap tyre processing and power production. In 1998 the UK division of the French SITA group, purchased and took over operation of the plant, which subsequently became known as SITA Tyre Recycling (STR). In 1998 STR commissioned the University of Nottingham to investigate the potential for the recovery of materials from the main waste stream generated from the facility.

The plant was originally designed to process 80,000 tonnes of scrap tyres per year, although the unreliability of certain aspects of the plant meant that, in the 18 month period to June 2000, the plant handled approximately 66,000 tonnes (SITA, 2000). The majority of the tyres handled at STR are supplied under the terms of a contract with Waste Tyre Solutions Ltd., a tyre collection and sorting company. Other sources of supply include UK based tyre manufacturers, including Goodyear and Michelin. Reject, faulty and development tyres are sent to STR for disposal since the incineration process represents a complete destruction of the casing ensuring that they never appear in the marketplace.

The charges made for the treatment of the tyres together with the revenue generated by the export of electricity are the main sources of income for the plant.

3.2 General facility description

The STR Waste to Energy Plant is designed to accept whole scrap tyres and use this material as a fuel to generate electricity. The facility consists of five individual combustion units with separate heat recovery systems supplying steam to a turbine generator. At full load the facility should generate approximately 25 MW of electricity for use on the plant with the remainder exported to the National Grid.

The plant (see Figure 3.1) is arranged in three main areas, all housed within a single building. The first area contains the administrative offices, storage and maintenance areas, on two floors. The boiler area is the largest area of the plant, this houses the five combustion units, five heat recovery steam generators, five air quality control systems and all other auxiliary equipment necessary for these components.



Figure 3.1 STR plant viewed from front gates

The equipment is arranged so that fuel enters the plant at the front wall, is fed into the combustion units and the resulting residues exit at the rear of the building (see Figure 3.2). The final area of the building incorporates the turbine hall and control room.



Figure 3.2 Rear yard of STR plant showing combustion residue handling area

A single stack is provided for the flues of all five units. Each combustion unit has an individual relief stack, which can open in the case of emergency to relieve pressure build up or used in cases of emergency shutdown. During normal plant operation three of the five combustion units are in use, one is on standby and the remaining unit is undergoing routine servicing.

3.3 Process description

Scrap tyres are transported onto the site in covered trailers. After passing over a weighbridge the trailers are parked in a holding area at the front of the site until they are moved into one of the ten raised loading bays where the tyres are removed and loaded directly into the combustion units. Tyres are unloaded from the trailers with small skid steer loaders, as pictured in Figure 3.3, and placed into feed hoppers. Under normal operating conditions tyres are loaded into each incineration unit at a rate of approximately 72 tyres per hour.



Figure 3.3 Whole tyres being loaded into feed hopper (CADDET, 1994)

A schematic of a single combustion unit, showing the progress of material through the incineration process, is presented in Figure 3.4. When the feed hopper contains the requisite quantity of tyres the lid closes and the control system checks various parameters including temperature and pressure before loading the tyres into the incinerator. When all criteria for feeding are met the tyres would be pushed into the incinerator and on to the drying hearth. The drying hearth consists of a set of refractory covered steel fingers which allow heat to circulate around the tyres, driving

off excess moisture prior to the hydraulic loading ram pushing the tyres onto the first pulse hearth. A design shortcoming of the original drying hearth was corrected during the refurbishment of Line 3 when the gaps between the fingers were reduced to stop tyres dropping straight through the grate and directly onto the pulse hearths. This often resulted in tyres rolling straight through the unit and appearing in the combustion residue in virtually the same state as they entered.

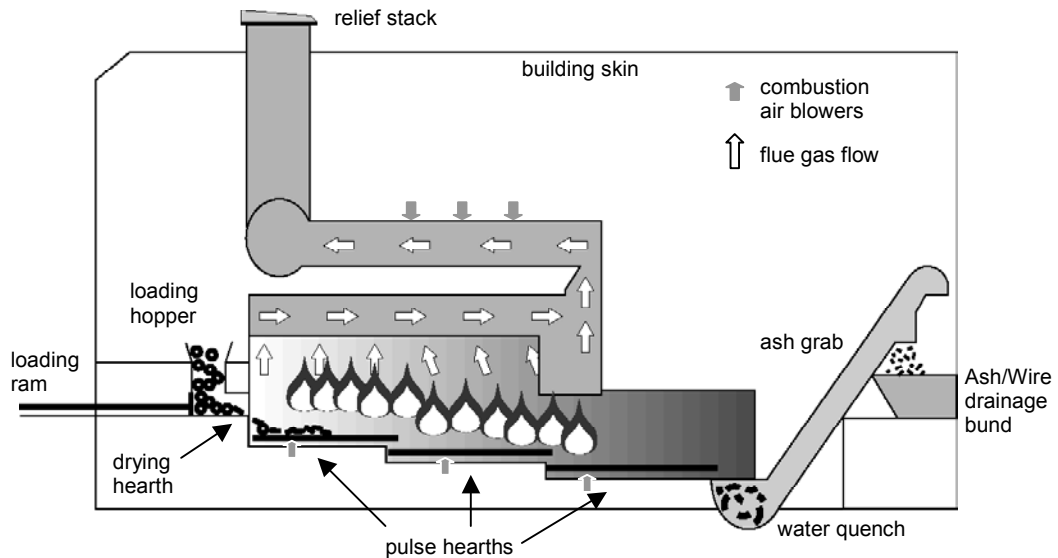


Figure 3.4 Schematic diagram of single combustion unit (in profile)

Each combustion unit consists of a series of three pulse hearths, over which the material moves as each hearth is regularly pulsed. Combustion of the tyres commences on the first hearth and progresses as the material is moved through the unit. The operating temperature of the units is in the region of 1050°C with a residence time of 2-3 hours. In theory the feed tyres should have been completely combusted before the final pulse hearth, however, combustion is still occurring on the final hearth. The main reason for this is that insufficient air is supplied to the hearths during the process to combust the carbon black from within the tyres. Attempts to increase the pressure of air injected through the injection nozzles resulted in the creation of localised heating zones at the nozzle heads which in turn caused increased slag production as melting and fusing of the tyre material occurred.

Gases produced during the combustion process are removed and pass through to the reburn tunnel. The gases are cooled to 780°C before passing through the boiler after which cool zinc oxide condenses and is recovered as a powder in a bag house filter. After zinc oxide removal the gases are treated in a flue gas desulphurisation (FGD) unit. The system used at STR involved the gases mixing in a reactor tower with lime and water. The lime is recycled through the system with a constant bleed off, fresh lime is introduced as required through an automated system of level controls. The treated gas stream is then discharged through the main stack.

As a consequence of the incomplete combustion, and carry over in the incinerator unit, the recovered zinc oxide also contains a carbon-based dust lifted from the hearths. The material recovered by the bag house filter consists of an approximate 50/50 mixture of zinc oxide and carbon dust. During the refurbishment of Line 3 the air injection nozzles in the reburn tunnel were moved nearer to the furnace so that the air was added whilst the gases were hot enough for secondary combustion to occur. This had the affect of increasing the burnout of the entrained carbon dust and resulted in a purer zinc oxide product.

After dropping from the end of the final pulse hearth the combusted tyre material enters a water quench. The quench acts as the seal on the end of the unit and also serves to cease combustion prior to subsequent handling operations. Quenched material is then pulled from the sump with the ash grab, which raises the material to the external ground level and deposits it into a drained storage bund located within the main building skin.

The combusted tyre material has previously been handled in a number of ways. The most recent method allows the material to drop into a three-sided bund which drains back into the water quench. Previous handling operations have included the direct depositing of the material into low-sided roll-on-roll-off trailers prior to being transported off site. However, failure to replace the full trailers with empty containers within sufficient time often resulted in spillage and previously necessitated units to be shut down as material backed up in the ash grab system.

The poor handleability characteristics of the combusted tyre material causes unusually high-stresses on the plant equipment employed in subsequent handling operations, mainly through the wrapping of wire around moving parts and the erosive effect of the wire rubbing the metal chute . This requires that maintenance must be carried out almost continuously to ensure that the handling operation does not interrupt the running of the incinerator.

3.4 Current treatment of waste residues

The combusted tyre residue is allowed to drain in the storage bunds from where four wheeled loaders, equipped with telescopic buckets, transport the material to high sided roll-on-roll-off trailers located in the yard at the rear of the facility. The material continues to drain in the trailers through taps prior to transportation off site. When they are full (approximately 15 tonnes of material) the trailers are transported to the nearby landfill facility at Poplars where they are emptied and later returned. The combusted tyre material is classed as an 'Industrial/Difficult' waste and costs approximately £12.70 per tonne to dispose of which £5 represents transport, £6.50 landfill charges and £1.20 landfill tax. The landfill tax contains a reduction as a result of the high water content of the waste.

The zinc oxide by-product is reused within a zinc smelting process operated by Britannia Zinc Ltd. The carbon dust associated with the zinc oxide provides a useful source of energy for the process whilst the zinc is recovered in the smelting process.

3.4.1 Quantities of combustion residue disposed to landfill

Under normal operating conditions approximately 80-90% of the original feed tyre mass is recovered from the system as ash, wire and water. In an operational year where 66,000 tonnes of scrap tyres are treated the incineration process results in approximately 52-60,000 tonnes of waste residue requiring disposal. Based on a 40% burnout of the feed tyres the approximate mass split of the main phases within the combusted tyre material, as present in the drainage bunds, is 20% steel, 35% ash and 45% water (Hall, 2000). The cost of landfill disposal of each of these phases can then be calculated and is presented in Table 3.1.

Phase	tonnes/year	Cost to landfill
Steel	13,000 (20%)	£165,000
Ash	23,000 (35%)	£292,000
Water	30,000 (45%)	£381,000
Total	66,000 (100%)	£838,000

Table 3.1 Landfill disposal cost of annual STR output by material phase

From Table 3.1 it can be seen that a significant part of the disposal cost is associated with the quantity of the water in the waste stream. By reprocessing some, or all of, the waste stream into products considerable savings could be made in disposal costs. Any revenue generated through the sale of the products would enhance the cost effectiveness of the treatment process.

3.4.2 Properties of STR solid waste residue

Routine analysis of the combusted tyre material by Elm Energy and STR revealed that the ash phase of the waste residue contains relatively high levels of carbon, this carbon percentage relates directly to the quantity of carbon black found in tyres. These levels were usually in the range of 40% to 70%; however it should be noted that the results of any chemical analysis on the ash material are a reflection of how much steel wire was hand removed from the sample prior to the sample being packaged for analysis.

The steel wire present in the combustion residue has previously been thought to be suitable for recycling. However, initial experiments conducted by STR revealed that samples of post combustion steel contained sulphur levels in excess of specifications supplied by potential purchasers. Previous attempts to produce a clean, separated, steel product from the combustion residue have included high-pressure jet water washing, dunking of steel into water tanks and wet and dry trommelling. The most successful method in terms of separating the steel from the ash phase was achieved by drying the material and then passing through a trommel. However, the sulphur content of the steel was still in excess of the target and the drying stage resulted in rusting of

the steel product. The use of a trommel on the dried material also released huge amounts of dust, which made it environmentally unacceptable.

3.5 Summary

It has been recognised that the main combustion residue generated by the tyre incineration residue might have some potential for recycling, although initial investigations have suggested that the recovery of products from the material is not straightforward. Recycling all, or a part of, the combustion residue could potentially generate a further revenue stream for the plant, not only through the sale of products but also as a result of savings made due to the diversion of the waste stream from landfill.

The first step in assessing the potential for the recovery of material from the waste stream was a detailed sampling and characterisation study to accurately determine the properties of the combustion residue beginning with the development of suitable analytical methods. Once the properties of the waste stream were known the potential for recycling could be determined.

4 Main analytical methods

4.1 Introduction

A number of quantitative and qualitative analytical techniques were used in this study. The application of standard physical characterisation techniques, such as wet-sieve particle size analysis, was relatively straightforward and has been described in context within the experiments. The quantitative chemical analysis of the material was more difficult. The difficulties were mainly associated with the application of analytical techniques to a previously unanalysed sample matrix. The non-existence of a directly applicable sample standard meant that a high degree of uncertainty in the accuracy of results might be encountered unless precautions were taken. Analytical techniques were chosen that were thought to be the most suitable for the material after consideration was given to analysis speed, instrument availability, data quality and cost. The selected techniques were then adapted to enhance the accuracy and precision of analysis of the material as far as possible. The development of the standard procedures is discussed in detail in this chapter.

The analysis of the material was not conducted completely blind since the components of the original tyre were known, and some previous results were available that had been carried out at external laboratories on behalf of STR. The results of the previous analysis were used to provide an indication of the range of elements that may be present in the samples, although without corresponding details on the sample collection and preparation it was only a guide. The analytical techniques chosen for the study were all available at the University of Nottingham and procedures had previously been developed for the analysis of coals or other geological samples. Carbon and sulphur in samples was determined using coulometric titration techniques whilst the concentration of all other elements was measured using an acid dissolution and quantitative analysis of the resulting solutions. Two different acid dissolution techniques were used within this research; a total element microwave assisted digestion was used to provide an initial complete assay of the material whilst an Aqua-Regia digest was used to provide a more rapid, less hazardous, analysis of samples generated by other experiments.

The procedures described are for the analysis of the portion of the combustion residue derived from the rubber, the analysis of the steel phase was conducted externally and is described in the next chapter

4.2 Analysis of total carbon

The carbon content of samples was measured using a UIC[®] Coulometrics Inc. CO₂ coulometer. The instrument measures the carbon dioxide released during combustion of the samples, in an oxygen stream. The sample to be analysed is weighed into a ceramic boat and placed in the oxygen stream in a furnace heated to 950°C. The resultant gas stream passes through a series of scrubbers (see Figure 4.1) to remove interfering gases such as sulphur and nitrogen oxides before passing to a titration cell. The cell contains ethanolamine and an indicator with which the carbon dioxide reacts to form a strong titratable organic acid (see Equation 4.1). The change in pH causes a colour change in the cell reagents, which is detected automatically through the measurement of the absorbance of a beam of light transmitted through the cell. Due to the colour change current is applied to the system, which results in the oxidation of the silver electrode causing the generation of base in the cathode compartment and the neutralisation of the acid. This process continues until the production of carbon dioxide by the sample has ceased and the indicator permanently returned to the original colour. The current applied in the regeneration process is counted, in terms of number of electron transfers, and together with the knowledge of the reaction stoichiometry is used to calculate the quantitative amount of carbon dioxide. This can then be used to determine the total carbon concentration in the sample.

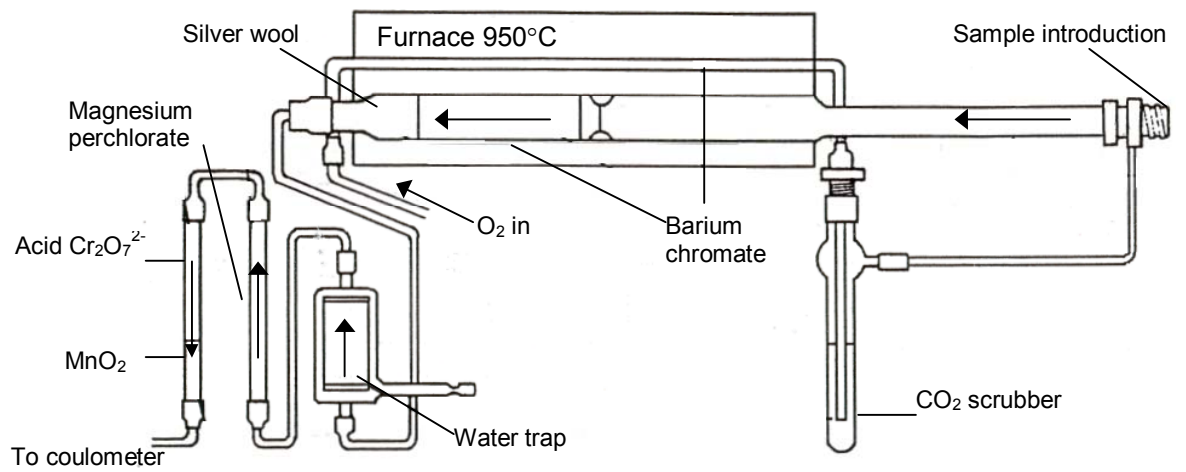
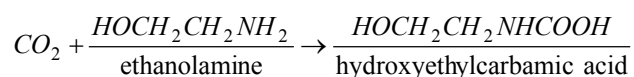
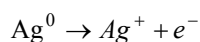


Figure 4.1 Carbon combustion tube arrangement

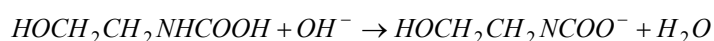
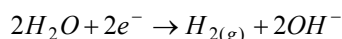
Reaction of carbon dioxide with ethanolamine forming titrateable acid



Anode



Cathode



Equation 4.1 Chemical reactions in total carbon apparatus

4.2.1 Sample preparation

All samples were analysed after oven drying at 85°C and then powdered. The samples were powdered in a Tema[®] mill until the maximum particle size was <75 µm. This operation typically required approximately 30 grams of material to be milled for a period of 5 minutes, although a certain amount of judgement was used in the mass of the charge since larger particle sizes occupied more volume in the mill. The 30 grams of sample for powdering was split from the main sample mass using a riffle to ensure that it was representative. After powdering the maximum particle size of the sample was checked by passing it through a 75 µm wire mesh screen, oversized material was re-milled. The sample was then placed in a clean glass jar and labelled. A second stage of drying (105°C, overnight) was carried out immediately prior to analysis to remove any moisture from the sample that might have been adsorbed during storage. This ensured that the dry mass of the sample was measured prior to any analysis.

Powdering the sample enhanced rapid and complete combustion of the sample in the furnace by increasing the available surface area of sample. It also serves to improve the homogenisation of the sample prior to analysis through mixing.

As mentioned previously the accuracy of the method, when applied to the STR material, could not be determined due to the unavailability of a suitable standard. However, a high purity calcium carbonate (CaCO₃) was used within analytical runs to

check for the correct operation of the instrument. By assuming the calcium carbonate to be 100% pure the measured carbon concentration should be 119994 ppm since carbon represents 11.9994% by mass of the compound. In reality the measured carbon will usually be slightly lower than this is figure as the material is not 100% pure and complete recovery of carbon is unlikely due to losses in the system. After a number of initial unknown samples were analysed it was clear that the carbon concentration of the material was very high (>60%). An important role of the standard was, therefore, to check that the cell reagents were not being exhausted. In general, the calcium carbonate standard was run at least once an hour (or every 5 samples) although where samples contained abnormally high, or low, levels of carbon the standard was run more frequently to check for instrument error.

Carbon concentrations of the levels detected in the samples had not previously been determined on the particular instrument being used. To check that the particular instrument was capable of the determination of high carbon concentrations a pair of samples were analysed using an Exeter Analytical[®] *CE440* Elemental CHN analyser, located in the department of chemistry at the University of Nottingham. The results are presented in Table 4.1 and represent an average of two separate analyses in each sample by each instrument.

Sample	Carbon (%)	
	UIC [®] Coulometer	Exeter Analytical <i>CE440</i>
Carbon Ash (a)	61.0%	66.0%
Carbon Ash (b)	80.0%	79.8%

Table 4.1 Comparison of carbon analysis of samples by two laboratories

The results suggest that the UIC[®] instrument is capable of measuring carbon present in samples at elevated concentrations as the results are good agreement, particularly for the higher the concentration sample. The sample with a carbon concentration in the range of 60-70% was not measured as precisely between the instruments. This might be explained by a number of factors, including non-homogeneity of the sample. The majority of the carbon analysis conducted during this study was expected to be in the >70% concentration range so the lack of agreement in the lower range did not

warrant further investigation. All subsequent analysis was carried out using the UIC[®] instrument.

The detection limit of the technique can be determined by measuring the level of carbon produced when an empty sample carrier is analysed in accordance with the standard procedure. The ceramic sample carriers are reused so determining the detection limit within the analytical run was used to detect potential cross contamination occurring during the analysis. The detection limit from two separate determinations conducted at random points within a run are presented in Table 4.2. If a significant proportion of the analysis was to be conducted at carbon levels near the detection limit it would have been important to determine the detection limit from a larger number of samples. Since the sample has zero mass it cannot be converted to a concentration. The coefficient of variation (CV) was also calculated through the repetitive analysis (52 determinations) of the calcium carbonate standard to provide a measure of the precision

Detection limit ($\mu\text{g C}$)	CV (%)
8	2.5

Table 4.2 Precision and detection limit of carbon analysis method

The coefficient of variation calculated takes the whole method in to account from weighing through to analysis. The low CV indicated that the method was capable of producing precise (i.e. reproducible) data. The detection limit of the technique was found to be insignificant (in comparison with 3000-4000 μg carbon recovered from 0.0050 g of sample) since the level of carbon in the samples was very high. For this reason the results were not adjusted to take the background level in to account. The sample mass used in the analysis was selected on the basis of initial tests after considering a sensible analysis time and the practicality of weighing the sample on a four decimal place balance. When $0.005 \text{ g} \pm 0.0005 \text{ g}$ of the sample was analysed the

analysis was usually complete within 10 minutes and the post analysis content of the boat contained no visible unburned carbon. The high level of carbon in the samples meant that the fifth decimal place ($1/100000^{\text{th}}$ of a gram) of the sample mass was significant so a more sensitive balance was used when one became available, this instrument was capable of recording to a further decimal place. The final procedure used for the carbon analysis of the samples is presented in Figure 4.2.

4.2.2 Carbon analysis procedure

After each analysis the contents of the boat was emptied onto a white tile and the contents inspected. Incomplete combustion was easily detected by the presence of black carbon within the normally pale grey residue. If any unburned carbon was detected then the result was discarded and the sample reanalysed, this only occurred on a single occasion in all the analytical runs.

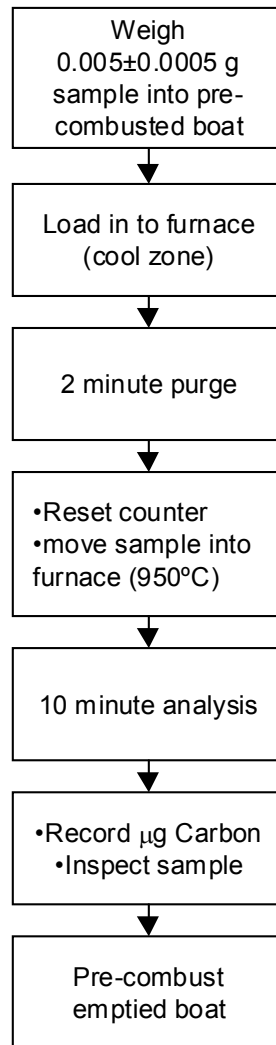


Figure 4.2 Carbon analysis procedure for STR material

4.3 Analysis of total sulphur

The total sulphur content of samples was determined with a similar technique to carbon using a UIC[®] Model 3200 Sulphur coulometer. Previous work had found the technique to be precise and in good agreement with published data for a range of geochemical reference standards (Atkin and Somerfield, 1994). The authors also surmised that the main advantages of the technique over alternative analysis methods for sulphur (e.g. XRF) was that a reference standard was not required and that sulphur could be measured rapidly in a solid sample. A method for the analysis of sulphur in the STR material was adapted from an in-house method developed previously for the total sulphur analysis of coals (Somerfield, 1998). The development of the method is now described.

4.3.1 Method description

In the analysis of total sulphur in coal method developed by Somerfield, (1998) the dry, powdered, sample to be analysed is weighed into a 'single-use' ceramic boat. The boat is then placed in a glass combustion tube, which sits in a dual stage furnace. The first stage of the furnace is heated to 1000°C and the second stage to 850°C, the sample is combusted in stage 1. A stream of pure oxygen passes through the tube to combust the sample resulting in the production of gases, including sulphur dioxide, which is then carried through a packing of glass wool to remove particulate matter and into a titration vessel. The sulphur dioxide is oxidised in the anode compartment of the titration vessel by free iodine, which is then regenerated automatically with a proportional current. The amount of sulphur in the sample is then determined automatically within the instrument through the integration of the current input to the system and displayed as μg sulphur, which can be related to the sample mass to provide a concentration.

4.3.1.1 Preparation of reagents

The reagents that form the solutions used in the titration cell are shown in Table 4.3. The solutions were made fresh on each day of the analysis since it was found that the anode solution discoloured during short-term storage, indicating solution instability. When older reagents were used it was also found that the instrument was difficult to get working in a reliable manner, typically the sulphur measured in standards were consistently low.

Anode solution	Cathode solution
8.3 g L ⁻¹ potassium iodide	15.81 g L ⁻¹ sodium thiosulphate
13.94 g L ⁻¹ potassium sulphate	
0.05 ml L ⁻¹ sulphuric acid (conc.)	

Table 4.3 Reagents used in sulphur analysis

When the reagents were placed in the relevant cells of the titration vessel approximately 1 ml of propan-2-ol was added to the anode compartment, the role of

which is to reduce the viscosity of the solution, which in turn decreased the bubble size of the gas introduced through the diffuser.

4.3.2 Adaptation of method for STR material

Using the previous method for the analysis of sulphur in coal as a base a new method was developed to produce reliable data for the STR material. The main body of the method was retained whilst the sample mass, analysis time and oxidiser addition were altered. To compensate for the lack of an appropriate sulphur standard an in-house coal standard, Point-of-Ayr (POA) was repeatedly analysed at the start of each run until the results were satisfactory. This process was usually found to take up to five POA samples and it was thought that this was due to the reagents warming to room temperature before accurate analysis was possible. The analysis of unknown samples was then conducted with the standard run at regular intervals to monitor data quality.

A typical sample of carbon ash was used to develop the method. A dried, powdered sub-sample was accurately weighed (0.1 ± 0.02 g) into a ceramic boat. The boat was then loaded into the apparatus and apparent sulphur content monitored for a period of time. It was noticed that after an initial ten-minute analysis period the sulphur content of the sample was still increasing so it was left in the furnace for a further ten minutes. After withdrawing the sample from the furnace it was noticed that the residue remaining in the boat contained black specs indicating the presence of non-combusted material. This would potentially lower the sulphur recovery from the sample and cause bias in the results. In an attempt to achieve more complete combustion in the same time period the sample mass was halved and then the analysis was repeated. The results are summarised in Figure 4.3.

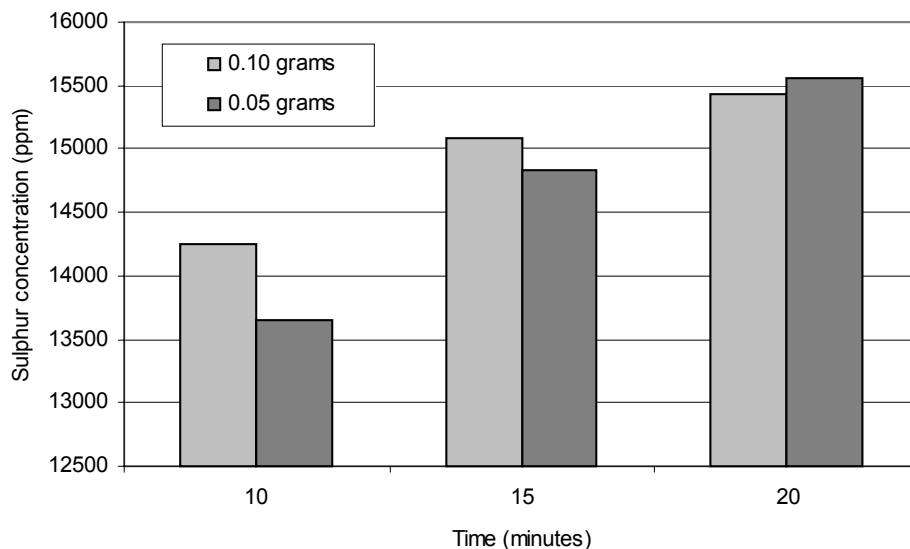


Figure 4.3 Effect of sample mass on sulphur analysis of carbon ash

From Figure 4.3 it can be seen that the apparent sulphur concentration of the samples increases with analysis time indicating slow combustion of the sample. The higher sample mass appears to produce more sulphur initially although the lower mass sample appears to combust more completely resulting in a higher sulphur concentration after twenty minutes analysis. However, the presence of unburned material was still detected in the post analysis samples. It was thought that the sample was developing a surface crust in the ceramic boat during combustion therefore limiting the combustion of the sub-surface sample. Improved combustion of the carbon ash was attempted by the addition of an oxidising agent with the sample. When mixed with the samples it was thought that the oxidiser would provide extra oxygen throughout the entire sample, improving the recovery of sulphur. The oxidiser used in the analysis was tungsten oxide (WO_3) although vanadium pentoxide (V_2O_5) has previously been used (Atkin and Somerfield, 1994). The effect of the oxidiser addition on the sulphur analysis was determined by mixing 0.05 g of sample with 1 g of oxidiser and the sulphur recovery over time measured. The results are summarised in Figure 4.4, the full results are presented in Appendix 4.

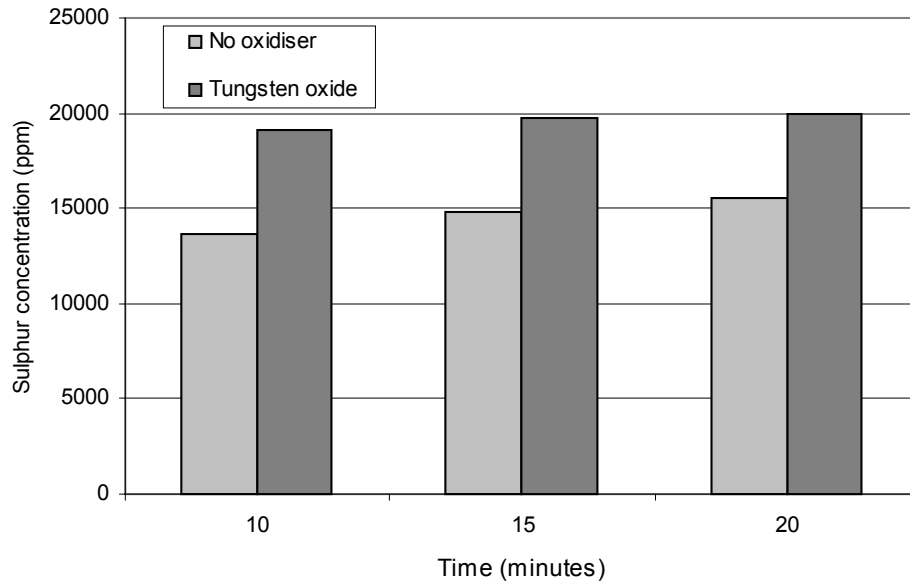


Figure 4.4 Effect of oxidiser addition on sulphur analysis of carbon ash

No visible unburned material was detected in the post analysis sample (after twenty minutes) indicating improved combustion of the sample in comparison with the non-oxidised samples. From Figure 4.4 it is seen that the addition of oxidising agent to the sample improved the recovery of sulphur and also reduced the time required by the sample to fully combust. After twenty minutes no further sulphur was measured in the sample (beyond normal background levels). The contribution of the oxidiser to the amount of sulphur measured in the sample was determined by analysing the oxidiser only, the results have been presented in Table 4.4, this figure also represented the lower limit of detection of the method for sulphur. Although the results indicated that the sulphur recovery was essentially complete after fifteen minutes the analysis period was set at twenty minutes as this allowed sulphur and carbon analysis to be conducted simultaneously. From this information a standard method was developed for use on all further analysis of sulphur in the carbon ash material. As with the carbon method the CV was determined for sulphur analysis and is presented in Table 4.4.

Detection limit	CV (%)
$\mu\text{g S}$	
51	7.2

Table 4.4 CV and detection limit of sulphur analysis

The CV of 7.2% (calculated from 30 determinations of the coal standard) is higher than that experienced with carbon analysis but was still acceptable. A typical sample of the STR material was found to yield 750-850 μg of sulphur from 0.05 g of sample. The results were not adjusted to take account of the background sulphur measured in the oxidiser only sample as it represented <10% of the total sulphur in the samples.

4.3.3 Sulphur analysis procedure

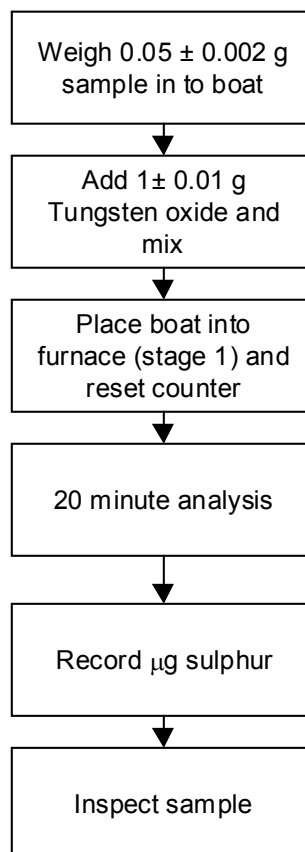


Figure 4.5 Sulphur analysis procedure

The POA coal standard was run at least once every five samples within the analytical run.

4.4 Total element digestion

The concentration of all other elements in the STR samples was determined using a total element digestion technique developed previously for the analysis of coal samples (Laban and Atkin, 1999). The principle of the technique was to dissolve the sample completely using a combination of acids in a sealed Teflon[®] digestion vessel, the contents of which was heated in a microwave. A CEM[®] MDS-81D 650W microwave digestion system was used for the experiment, which could be programmed to operate at specific power intensities and duration. The microwave was capable of holding up to 12 digestion vessels on a turntable at one time. Each vessel consisted of a base, screw cap and relief valve. The screw caps were tightened with a CEM[®] motorised capping station to ensure the same torque was applied to each vessel, which then controls the relief pressure. The technique assumes the complete dissolution of the sample and so the concentration of an element in the sample was determined by measuring it in the leachate solution. Two acid stages are used to dissolve the sample, first nitric and then a combined hydrochloric/hydrofluoric stage. A final boric acid stage is also included in the method. When applied to the STR samples the nitric acid stage would attack the organic phases and, due to its oxidising properties, dissolve many elements whilst breaking down the carbon matrix, improving the liberation of any entrapped phases. After the addition of hydrochloric acid the leachant is similar to Aqua-Regia which draws less soluble elements into solution. The hydrofluoric acid dissolves the silica phases. The addition of boric acid in the final stage had a dual purpose. The acid complexes the excess fluoride ions making the final leachate less hazardous to handle and it also prevents the precipitation of relatively insoluble fluorides such as CaF_2 (Laban and Atkin, 1999).

The digestion was carried out on the dry, powdered, samples as prepared previously for sulphur and carbon analysis. The procedure used to digest the samples is outlined in Figure 4.6. Initially a 0.2 g sample mass was used in the digestion although this was abandoned when a considerable amount of undissolved residue was observed in the post digestion leachates. When the sample mass was adjusted to 0.1 g very little

solid residue remained after digestion indicating that most of the sample was in solution. After the total digest the vessel contents were allowed to cool and were then made up to a 100 ml volume in a flask prior to quantitative analysis with Inductively Coupled Plasma-Atomic Emission Spectrometry (ICP-AES). This part of the analysis could not tolerate any solid particles in the solutions as this might lead to blockages in the sample nebuliser, therefore any remaining residue had to be removed from the solutions. This was carried out by centrifuging the samples with the addition of a non-ionic surfactant (500 μ l of 1% Brij-35[®]) to aid the separation. Approximately one half of each residue-laden solution was decanted into a clean 50 ml polypropylene centrifuge and the lid sealed. The tube was then centrifuged at 3000 rpm for 5 minutes, or longer if the solids were still in suspension. After centrifuging, the solids formed a plug at the base of the tube allowing the clear solution to be decanted into a clean sample bottle. The second half of each sample was then centrifuged in the same tube as the first half and the solution added to the relevant bottle. The samples were then ready for ICP-AES analysis.

4.4.1 Total digestion procedure

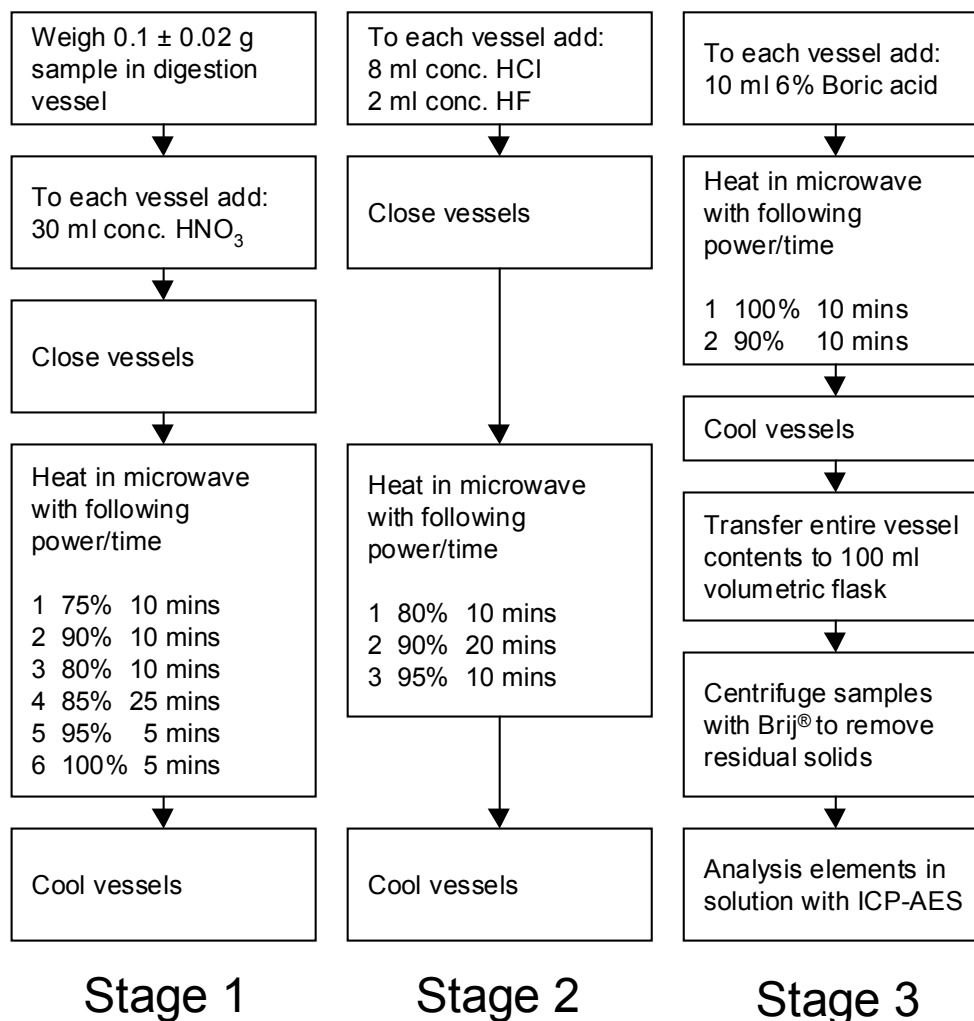


Figure 4.6 Total element digestion procedure

After the samples were retrieved from the microwave moisture was observed in the vent pipes indicating that the vessels had, at some stage, vented to release pressure. This introduces a potential source for a reduction in accuracy and precision that might be biased towards the loss of more volatile elements such as cadmium. However, venting of the vessels was unavoidable for safety reasons. Digestion vessels that contained the reagents only were run within batches to detect any cross contamination of the samples that may have occurred during the digestion and subsequent solution preparation stages. The solid residue that remained in the post digestion liquor meant that <100% of the sample was drawn into solution which would then lead to reduced accuracy. By adjusting method parameters such as power, time and sample mass it

might have been possible to ensure that all samples were completely digested therefore improving accuracy. This was not undertaken as it would have taken a considerable period of time and the data from the method in its current state was perfectly useable.

4.5 Aqua-Regia digestion

The time consuming, and potentially hazardous nature of the total digestion method necessitated the use of an alternative method for the analysis of the large numbers of samples generated by various experiments during this research. A slightly less aggressive leach method using Aqua-Regia was developed, the leachates were analysed with ICP-AES as with the total method. Aqua-Regia consists of a mixture of concentrated hydrochloric and concentrated nitric acid in a 3:1 ratio by volume. The limitations of this method, in comparison with the total digestion method, are that silica phases are not quantitatively dissolved and that it is an open top method, which can lead to the loss of volatile elements and an increased risk of cross contamination.

Samples were accurately weighed into a 200 ml conical flask which were then placed in a fume cupboard. The Aqua-Regia (30 ml) was then added to each vessel which were then placed on to a cold hotplate. Once the acid had been added to all of the samples the hotplate was switched on and slowly heated to 85-90°C. The samples were heated for a period of 12 hours, the acid was allowed to evaporate until the solid residue was nearly dry at which point 30 ml of 10% nitric acid (by volume) was added. The vessels continued to be heated for a further 30 minutes after which time the hotplate was switched off and the samples allowed to cool. The cooled samples were then individually transferred (sediment included) to 100 ml volumetric flasks and the volume made up with additional 10% nitric acid. The solutions were then prepared for analysis with ICP-AES by removing the solids using a centrifuge as described in the total digestion method.

Cross contamination was minimised by ensuring an adequate spacing between the digestion vessels and could be detected with the use of strategically placed blank samples. The less than total nature of this dissolution makes it unsuitable for accurate characterisation purposes however all samples analysed using the same method can be

compared to each other. The method used to conduct Aqua-Regia digestions is summarised in Figure 4.7.

4.5.1 Aqua-Regia digestion procedure

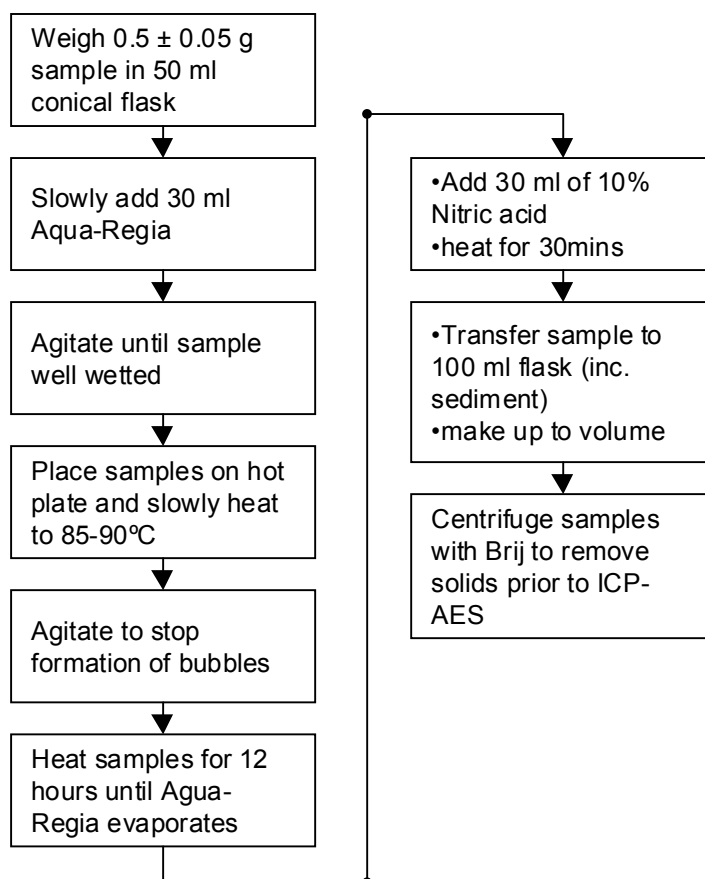


Figure 4.7 Aqua-Regia digestion procedure

It was found that using conical flasks, rather than beakers, reduced the cross contamination potential of the samples. After the acid was added to the beakers a short period of effervescing occurred which caused small drops of leachate to escape from the beaker and land either on the hotplate or in other samples. The effervescing reduced over time but was found to result in the corrosion of the hotplate leaving an imprint of the beaker positions after use, indicating potential cross contamination. This was greatly reduced with the use of conical flasks, which caused most of the escaping leachate to run back down the insides of the glass. It was important to closely monitor the samples for the first two hours so that effervescing and bubbling

samples could be temporarily removed from the hotplate to cool before being replaced. The number of samples digested at any one time was also limited to allow sufficient space between the vessels to reduce the potential for cross contamination.

By digesting the same sample using the two different digestion methods a comparison of the recovery of each element into solution could be made. The relative recovery of an element from the same sample digested using the total method compared to the Aqua-Regia method is presented in Table 4.5.

Element	Concentration in ash	Recovery
	Total method ($\times 10^4$ ppm)	Aqua-Regia (%)
Ba	0.002	111.5
Cd	<LOD	<LOD
Cr	<LOD	<LOD
Cu	0.020	87.4
Ni	<LOD	<LOD
Pb	0.008	81.8
Zn	3.7	82.4
Al	0.2	51.2
Ca	0.98	83.4
Fe	3.4	90.6
Mg	0.11	60.8
Mn	0.019	89.9
Si	0.6	n.d.
Ti	0.021	28.7

Table 4.5 Comparison between total and Aqua-Regia digestions [n.d. - not determined]

It can be seen that, with only a couple of exceptions, the Aqua-Regia digest compared well with the total digest in terms of element recovery. The recovery is generally in excess of 80% for the elements analysed although it is not so good for aluminium, magnesium and titanium. The relatively low concentration of titanium in the sample indicated that the low recovery of this element is not critical although it needs to be considered when interpreting data. This was also the case with aluminium and magnesium. Barium appeared to be recovered effectively with both methods.

4.6 ICP-AES analysis of digestion leachates

Once the elements to be analysed were in solution they can be quantitatively analysed using Inductively Coupled Plasma-Atomic Emission Spectrometry (ICP-AES). The basis of the technique is that when an atom is excited, and then returns to its ground state, it emits radiation of intensity that is directly proportional to the number of emitting atoms and hence concentration. In inductively coupled plasma the sample is atomised in a plasma formed in argon. The sample is introduced as an aerosol and temperatures of up to 10,000°C can be generated ensuring complete atomisation of the sample without any interference effects of chemical reactions (Tyson, 1994). The technique is capable of analysing a wide range of elements since each element has an exclusive set of wavelengths at which radiation is emitted as the atoms return to their ground state. Quantification is achieved by comparing the radiation intensity with a calibration curve formed with a standard containing a known concentration of the element and a blank sample. The standard and blank samples are prepared in the same acid matrix in which the sample is digested. The instrument analyses each element in solution individually through the use of a monochromator, which enables detection of the energy emitted at a single wavelength. The detection wavelength for each element was selected on the basis of signal intensity and potential interference. In this research interference problems were not encountered so each detection wavelength was selected based solely on the strongest available intensity. The wavelengths used for the quantitative analysis are presented in Table 4.6 (total digests) and Table 4.7 (Aqua-Regia).

The ICP-AES instrument used was a Perkin Elmer[®] Plasma 400 which was equipped with a Gilson[®] 180 position sample changer. This enabled a large number (up to 168 unknowns) of samples to be analysed automatically. The analytical run was controlled with software (QC Expert[®]) which enables parameters such as the number of repeats, wash time and quality control limits to be defined for the run. The concentration of each element in the sample solutions was measured twice and the average result quoted throughout this thesis. The minor and major elements in the same samples were analysed in separate analytical runs along with quality control and standard solutions for each group of elements. The instrument was programmed to recalibrate

every hour and to check the calibration against the quality control solution in the same period.

The detection limit of an element in solution is defined as three times the standard deviation measured when 10 analyses of the element in a blank sample are taken. This was generally carried out at the end of each analytical run when the instrument was behaving in a similar manner to that of the analysis period. The detection limit of each element in the sample is then calculated using Equation 4.2.

$$\text{Detection limit in sample (ppm)} = \text{detection limit in solution} \times \frac{\text{sample volume (ml)}}{\text{sample mass (g)}}$$

Equation 4.2 Detection limit of elements by ICP-AES

The concentration of elements in the sample is calculated with the knowledge of the original sample mass and dilution volume using Equation 4.3. At this point any further dilutions carried out to reduce element concentrations in the solutions in order to bring them in to range can be taken in to account. However, the requirement to do this is minimised by the correct selection of standard concentrations since further dilutions may introduce further systematic errors in the analysis.

$$\text{Element concentration in sample (ppm)} = \text{concentration in solution (ppm)} \times \frac{\text{sample volume (ml)}}{\text{sample mass (g)}}$$

Equation 4.3 The determination of concentration in sample from concentration in solution

4.6.1 ICP-AES parameters for total digestion leachates

Element	Wavelength nm	Standard ppm	QC ppm	Standard Deviation	Detection limit ppm	CV (%)
Al	397	500	100	0.0070	21	21.1
Ca	315	500	100	0.0200	60	1.7
Fe	273	750	200	0.0160	48	3.9
Mg	279	100	20	0.0200	60	3.3
Mn	257	200	40	0.0005	2	2.9
Si	251	50	10	0.0830	249	34.2
Ti	334	20	5	0.0008	2	2.6
Ba	233	4	1	0.0030	9	17.3
Cd	229	4	1	0.0012	4	244.4
Cr	267	4	1	0.0064	19	37.2
Cu	324	4	1	0.0013	4	2.2
Ni	231	4	1	0.0071	21	55.0
Pb	220	4	1	0.0184	55	23.1
Zn	213	4	1	0.0019	6	2.7

Table 4.6 Parameters used in the analysis of total digestion leachates by ICP-AES

The coefficient of variation (CV) has been calculated for each element by conducting multiple digestions (a total of 8 determinations over 2 batches) on the same sample and compiling the results of the ICP-AES analysis. The CV provides a measure of the precision for the whole analysis method when applied to the STR material. A 100% precise method would yield identical results from each replicate sample resulting in a zero CV. It can be seen that the CV varies widely depending on the element being analysed. For zinc, copper, titanium, manganese, magnesium, iron and calcium, the CV was below 5% indicating that the method is precise for the analysis of these elements. The precision of aluminium (21%) and silicon (34%) was not as good.

The difficulty in analysing silicon in coals with ICP-AES has previously been investigated (Laban and Atkin, 1999). It was found that the element was often detected in samples known to contain no silicon, this was thought to be due to storage of the digestion acids in glass containers. Silicon was also found to exhibit a high residence time in ICP-AES that was not satisfactorily resolved even with extended

purging between samples with hydrofluoric acid. This meant that silica built up in the system causing recorded levels to build up over the course of an analytical run.

The precision of barium (17%), chromium (37%), nickel (55%) and lead (23%) measured in the STR samples was poor. The precision determined for cadmium (244%) renders the data virtually unusable. The poor precision for the determination of certain elements in the STR samples would become a major issue if the outcome of experiments were judged by relatively small changes in concentration of these elements. Otherwise the method is suitable for application to the STR material.

The detection limit of the ICP-AES was determined by conducting ten repeat measurements of the elements in the dissolution matrix only. The detection limit for the total digestion is presented in Table 4.6. Where the result of the analysis of a sample was below the detection limit the result is quoted as 'less than limit of detection' (<LOD).

4.6.2 ICP-AES parameters for Aqua-Regia leachates

Element	Wavelength nm	Standard ppm	QC ppm	Standard deviation	Detection limit ppm	CV (%)
Al	397	500	100	0.0070	11	3.7
Ca	315	500	100	0.0040	6	0.7
Fe	273	1000	500	0.0100	15	2.3
Mg	279	100	20	0.0230	35	2.8
Mn	257	20	5	0.0001	<1	3.7
Si	-	-	-	-	-	-
Ti	334	50	10	0.0005	1	4.1
Ba	233	4	1	0.0014	2	28.5
Cd	229	4	1	0.0016	2	22.0
Cr	267	4	1	0.0014	2	53.1
Cu	324	8	2	0.0018	3	4.1
Ni	231	4	1	0.0032	5	77.2
Pb	220	4	1	0.0240	36	5.1
Zn	213	250	50	0.0020	3	1.6

Table 4.7 Parameters used in the analysis of Aqua-Regia leachates by ICP-AES

The precision of the method for each element follows the same general pattern as for the total digest, in many cases it is superior to those measured in the total digests. However, it is important to note that the Aqua-Regia digestion is not a total method so although it appears to be more precise it is likely to be less accurate. The inferior precision for certain elements in the total digest might be explained by increased interference caused by the higher quantities of elements in the solutions. Silicon was not analysed in the Aqua-Regia solutions, since it was not quantitatively dissolved in the digestion.

4.7 Summary

The methods described in this chapter have been applied to the chemical characterisation of the material generated by the STR process. The same methods have then been used to measure the performance of separation systems and the assessment the products generated. Two digestion procedures were defined for

different applications, one for detailed characterisation and the other for a more rapid analysis.

Although the true accuracy of the methods adopted for the analysis of carbon, sulphur and other elements could not be determined the precision was measured enabling a certain amount of confidence to be applied to the data. For certain elements the precision of the digestion methods was found to be poor. However, it should be noted that the low precision was generally associated with elements that were found to be present at low concentrations in the samples, so has little impact on the overall analysis.

The incomplete dissolution of samples during the total digestion procedure could have been improved by removing the carbon from the sample, leaving only the inorganic phases for digestion. This could have been achieved using a low-temperature-ashing process to remove the carbon without altering the sample. However during sample preparation for mineral phase identification experiments it was found that the generation of sufficient sample mass for analysis would have taken in excess of a day per sample, therefore it was not considered.

An important point to note at this stage is the importance of a representative and consistent sample collection and treatment procedure to the reliable analysis of any element in the material. For example, in the analysis of carbon 0.005 grams of sample is analysed and the result generated is then used to describe the output of a 66,000 tonnes per year waste stream.

5 Sampling and Characterisation

Characterisation of the solid waste residue resulting from tyre incineration was carried out by retrieving samples from STR and transporting them to the University of Nottingham where they would be worked upon. An initial sight seeing visit to the plant was carried out prior to the collection of any characterisation samples to allow a sampling strategy to be developed.

The objective of the sampling and characterisation was to:

- Develop a suitable sampling procedure to recover small, representative, samples for analysis
- Establish the nature of the waste residue resulting from tyre incineration at STR
- Characterise the material with a view to the eventual production of saleable products

5.1 Introduction

Observations of the incineration process, from tyre loading to waste handling and treatment, were made to understand the normal operating regime of the plant. The appearance of the waste material when observed in the storage bunds was a black, wet, steaming heap containing a number of visibly different phases. On closer inspection three discernible phases were identified in a heterogeneous mixture. These were steel wire, mainly in the form of intact beads, a black ash material and water. To ensure that the material sampled for use in this research consisted solely of the combusted tyre residue and not a mixture of various site residues it was decided that samples should be collected directly from the storage bunds. A typical heap of the combusted tyre material is pictured in Figure 5.1.

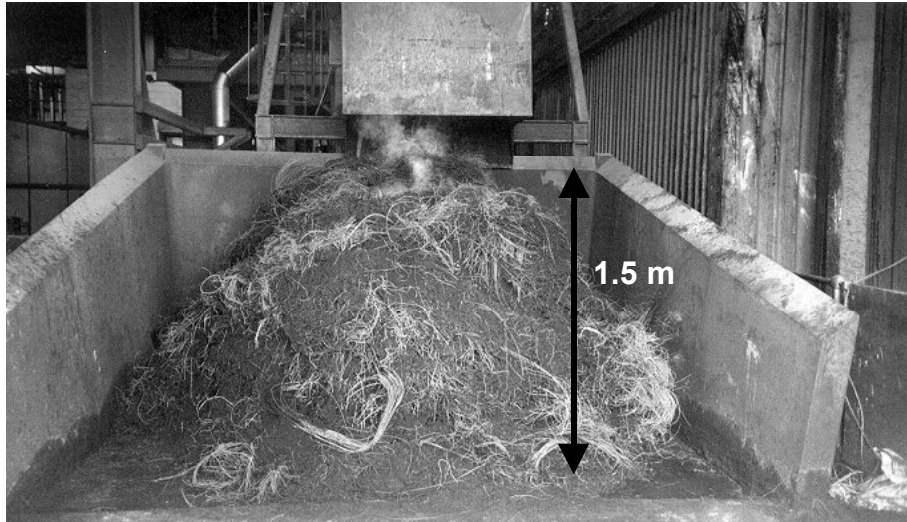


Figure 5.1 Combusted tyre material in storage bund

The combusted tyre material is dropped into the storage/drainage bund by an automated grab which pulls material from the water quench sump at basement level and raises it up to ground level. Once emptied the grab returns to the sump to collect more material, the cycle is continuous and was found to take approximately two minutes between discharges. Some grabfulls of material were observed to consist predominantly of wire whilst others consisted mostly of the black ash material, causing the distribution of phases within the heap to be highly heterogeneous. Freshly deposited material was still hot when present in the bund causing the water associated with the waste to steam, although it was not too hot to handle when rubber gloves were worn. Excess water pulled up with the grab quickly drains in the bund and returns to the sump, however a significant amount of water is retained in the material and does not drain as readily.

Older ash material that remained uncollected or had been set aside on the site was observed to dry completely and break down to form a fine black dust. It was also found that the combusted tyre material degraded after only a few hours of storage in the open air, in particular the steel wire rapidly corroded and broke down into the ash. For this reason it was decided that a number of smaller samples would be taken as and when they were required for characterisation experiments rather than larger bulk samples.

The combusted tyre material produced by STR is known colloquially as 'ash/wire', with the wire-free ash phase separately referred to as 'carbon ash'. Intact wire beads pulled from the ash/wire are generally referred to as 'bushy wire' due to the materials handling characteristics and low bulk density. The phases within the combusted tyre material will therefore be referred to as carbon ash, ash/wire and bushy wire throughout the remainder of this thesis.

5.2 Sampling procedure

The retrieval of representative sub samples for analysis from residues generated by industrial processes can be difficult due to heterogeneity, changes in process conditions and variations in the feed material. In the case of sampling of the ash/wire residue it was further complicated by the health and safety implications caused by working in a potentially hazardous environment and also by the requirement to avoid disrupting the normal operation of the plant. In situations where ideal sampling conditions cannot be achieved then a method should be developed that is 'fit for purpose' (Perry and Thompson, 1998). For this study the samples collected from STR were required to be representative of typical incinerator output. To minimise the hazards associated with sample retrieval a safe system of work was developed with the co-operation of the STR staff. To comply with the system the acquisition of a 'permit to work' was required prior to the collection of any samples, under supervision, as well as the wearing of appropriate personal protective equipment.

Samples of the ash/wire were always taken from the process line that, according to the operational staff, had been operating at closest to typical conditions and for the longest period of time. Samples were taken directly from the bunds and were collected when the grab was on the return-to-sump part of the cycle. If untypical materials (e.g. non-combusted or partially combusted tyre casings or refractory fragments) were observed in a bund no sample was taken from that process line at that time. It was found that during the start-up or shutdown procedures of a combustion unit partially burned tyres were often observed in the storage bund. Fragments of refractory were frequently observed in the ash/wire material, they were usually present as large, >10 cm, fragments but it was noted that smaller fragments would be difficult to identify due to the black colouration caused by the wet carbon ash phase.

The presence of intact beads in the ash/wire heap made taking representative samples extremely difficult due to the poor handleability of the material. The collection of entire grab loads was impractical for safety reasons so it was necessary to collect sub-samples of recently deposited grab loads from the heap. The cone and quartering technique that might normally be used to extract a representative sample from a heap was impractical due to the lack of time between fresh deposits and also the difficulty in splitting the sample due to the presence of intact beads. Samples of the wire and carbon ash phases were therefore collected separately due to the different handling characteristic of each material but always from the same ash/wire heap at a similar time.

Samples of bushy wire were pulled from the heap by hand, loosely attached carbon ash shaken off, and placed into plastic sample buckets and the lids sealed. Samples of the carbon ash phase were collected with a small trowel that was used to pick in-between the wire beads. Smaller wire pieces present in the heap were collected with this phase. The carbon ash was then placed in separate sample buckets for transportation to the University of Nottingham. Upon arrival at the University the samples were either dried by thinly spreading the material onto trays in a drying oven heated to 85°C, or used immediately, depending on the test work to be carried out. Overnight drying of bushy wire and carbon ash samples within 2-3 hours of collection was observed to stabilise the material with respect to the corrosion of the wire phase. No corrosion products developed in the dried samples during subsequent storage.

5.3 Material characterisation

The ash/wire material was characterised with a view to the separation and concentration of potentially valuable products from the current waste stream. As such the steel wire and carbon ash phases were characterised separately since it was likely that they would eventually be sold into separate markets. The materials would also require substantially different analytical techniques during characterisation. The overall balance of the three main phases in the ash/wire, based on the material as disposed to landfill during typical plant operation, has previously been estimated as 20% bushy wire, 35% carbon ash and 45% water by weight (Hall, 2000). After the

retrieval of samples the majority of the water was found to be associated with the carbon ash phase. After shaking deposits from the bushy wire little moisture was associated with the phase. By monitoring the weight of the samples during oven drying it was determined that individual samples often contained >50% water. The moisture content of samples was related to the position from which the sample was collected, samples from the base of the heap were usually wetter than those retrieved from nearer the top.

A summary of the characterisation study together with the location at which the work was conducted is presented in Figure 5.2.

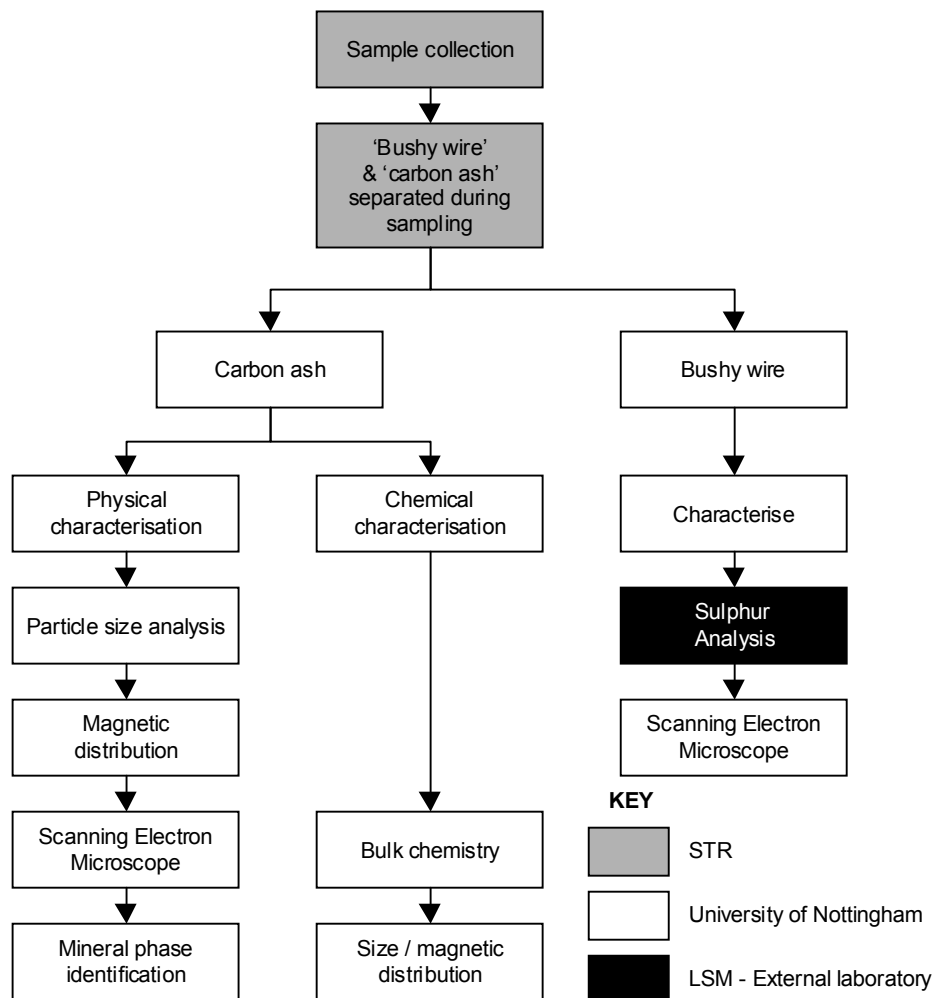


Figure 5.2 Summary of ash/wire characterisation method

As much of the work as possible was carried out at the University of Nottingham where conditions could be more easily controlled minimising the possibility of sample

contamination. Analysis of the bushy wire was a specialist task and was carried out at an external laboratory, London & Scandinavian Metallurgical (LSM) Co. Ltd. The analytical technique used is described later.

5.3.1 Characterisation of bushy wire

The wire present in the ash/wire is derived mainly from the steel wire used as beads in the construction of the original tyre. The beads are generally made from high quality tensile steel and are usually coated with brass, an alloy of copper and zinc. The low bulk density of this phase made the handling, storage and treatment of the material very difficult. A typical sample of bushy wire as retrieved from a bund is pictured in Figure 5.3.

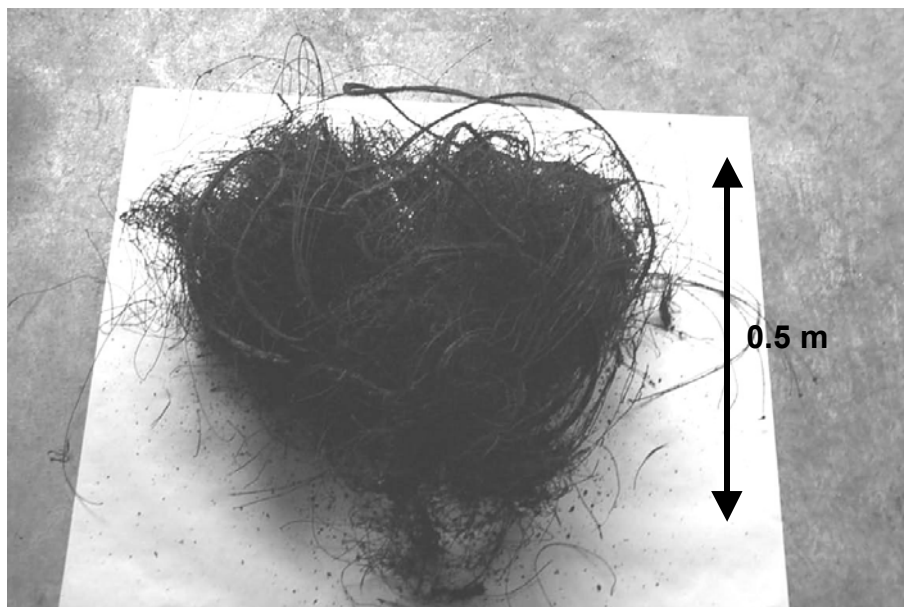


Figure 5.3 Typical sample of hand separated bushy wire

Discussions between STR and steel reprocessing companies had previously revealed that a high quality scrap steel product that would be acceptable for reprocessing would be required to be virtually free of carbon coatings and have a sulphur content of less than 0.04%. This level is similar to the sulphur content of the virgin steel used in tyre manufacture (0.03%) (Kovac and Rodgers, 1994). Previous test work conducted by STR had indicated that the sulphur content of the post combustion steel was far in excess of the 0.04% sulphur target (Hall, 2000).

5.3.1.1 Bushy wire characterisation method

To assess the possibility of achieving the product specification the concentration and association of sulphur and carbon ash with the steel was determined. A series of experiments were designed to ascertain the starting concentration and then to determine the association of the sulphur with the wire. The results of the experiment would be used to provide information on whether the sulphur was chemically bonded with the steel or more simply associated with surface coatings of carbon ash. This would then influence the choice of any separation system employed to treat the steel.

The wire was present in the bushy wire mainly as intact beads but also as finer, smaller lengths that would originally have been in the tyre as reinforcement bands or outer strands on the beads. Over the course of the sampling it was observed that the wire appeared in a number of forms but could be classified into two main groups. These were multiple core cables, formed by winding a number of single strands (helicoidal braid) and single core wire. Occasionally beads originating from heavy goods vehicle tyres were present in the bushy wire. These larger diameter beads were formed from a number of square section strands bound together with steel straps to form a larger rectangular cross section that was up to 20×10 mm.

5.3.1.2 Sample preparation

Specimen wire samples for characterisation were retrieved from the ash/wire by manually pulling a selection of different wire forms from the heap. The samples were then stored in sealed plastic sample buckets prior to transportation. To make the samples easier to handle the intact beads were cut, using side cutters, into lengths of approximately 20 cm. Individual samples were then stored in sealed sample bags prior to treatment which was carried out within hours of sample collection to ensure that experiments were carried out on representative, non-corroded specimens.

5.3.1.3 Sample treatment

The specimen wire samples were subjected to a series of surface cleaning tests. Samples of the 'cleaned' wire together with wire samples in the original form (as collected) were then analysed. All samples were analysed for sulphur concentration whilst selected samples were examined further with a Scanning Electron Microscope (SEM). The surface cleaning regimes applied to the samples started with a simple wiping and then increased in severity, as listed below:

- No treatment (to provide base line data)
- Wire surface wiped with dry cloth
- Wire rinsed with water, then surface wiped dry with cloth
- Wire surface sanded using a medium grade sandpaper

Specimen wire samples of the two main forms (single and multiple core) were cut into shorter sections (approximately 10 cm) to provide a similar starting material for each of the cleaning regimes. For each wire form sub-samples of the original specimens were then oven dried at 85°C and packaged for analysis to provide information on the starting properties of the material. Identical pieces of the each wire form were then subjected to surface wiping with a dry cloth. With one end of the specimen being held a cloth was wrapped around and pulled down the length of the wire. After wiping was completed the specimen was dried and packaged for analysis. Further wire samples were subject to rinsing in a large beaker of water prior to being wiped dry as with the previous sample. Finally samples were sanded with a sheet of medium grade sandpaper. With one end of the sample held the sandpaper was rubbed along the length of the wire ensuring that as much as possible of the wire surface made contact with the sandpaper. Many of the cleaning tests were repeated a number of times since the cleaning actions imparted on each specimen were difficult to replicate. The results of the analysis have been expressed as a range of sulphur concentrations in these cases. After the relevant treatment had been applied to the specimens all were dried overnight at 85°C. They were then individually packaged in sealed plastic bags for despatch to the external laboratory.

Portions of selected cleaned and original wire specimens were retained for SEM analysis to provide high magnification images of the wire surface allowing the extent of surface deposit removal to be assessed. Short (<1 cm) wire specimen samples were mounted onto a 30 mm diameter aluminium sample stub using a double sided sticky tab. The stub was then sputter coated in aluminium to enhance the conduction of charge through the sample. Since metal samples are good at conducting the charge created during analysis it would not normally be necessary to coat the samples however, the coating also served to stabilise loosely attached surface deposits onto the samples.

5.3.1.4 Sulphur analysis of wire specimens

An external laboratory (London & Scandinavian Metallurgical (LSM) Company Ltd.) that specialises in the analysis of steels was employed to analyse sulphur concentrations in specimen wire samples. Analysis at the laboratory was carried out using a LECO[®] *CS444* elemental analyser. The basis of the technique was similar to that used to measure total sulphur in the carbon ash phase except higher temperatures were used to vaporise the steel, releasing all of the sulphur. The instrument is typically accurate to $\pm 0.5\%$ of the sulphur present (relative percentage) (Hurditch, 1999). Samples of approximately 5-10 grams were sent to the laboratory, which used about 1 gram for each sulphur determination. As a result of discussions with the LSM laboratory staff it was found that the accurate analysis of sulphur in the wire samples was difficult due to alteration of the sample state during transportation. On arrival at the laboratory some samples had dissociated into separate phases of wire and carbon ash material. In all samples the carbon ash had originally been attached to the wire surface prior to despatch. For this reason the laboratory was instructed to analyse a representative sub-sample of the entire contents of a sample bag as opposed to the wire phase only.

The results of the sulphur analysis on the wire specimens are presented in Table 5.1. Specimen wire samples that had been prepared for SEM were photographed resulting in clear, high magnification, images of the wire and any associated surface deposits. A selection of the images produced by SEM analysis of the specimens generated during

the cleaning experiments are presented in Figure 5.4, through to Figure 5.7. The associated sulphur concentration of each sample is labelled in the image description.

	sulphur concentration (%)	
	Multiple core	Single core
No treatment (as collected)	0.360 – 0.700	0.150 – 0.200
Wiped (dry)	0.211	0.041 – 0.059
Wiped (wet)	0.053	0.041 – 0.053
Sanded	0.050 – 0.190	0.017 – 0.041

Table 5.1 Sulphur concentration of bushy wire samples

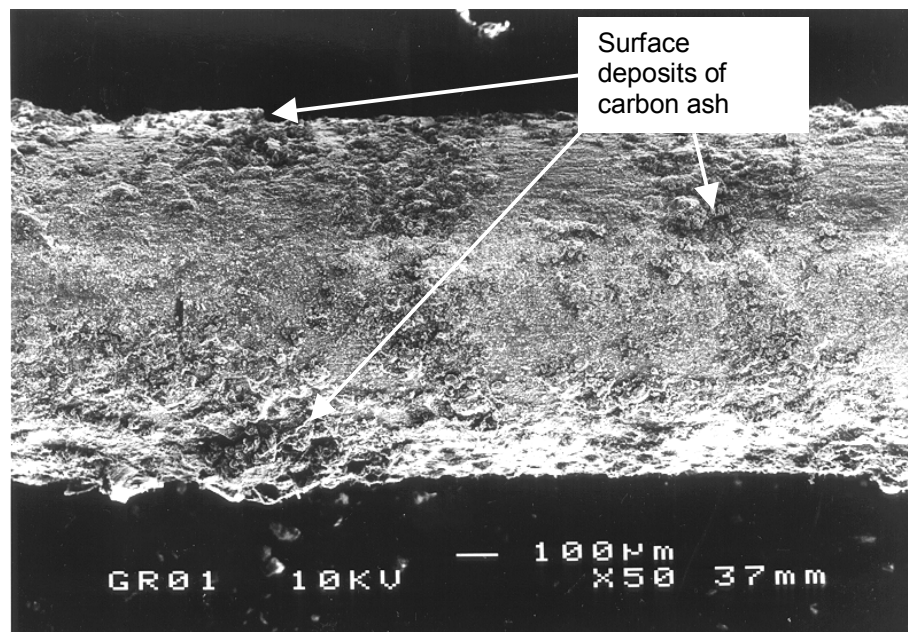


Figure 5.4 Single core wire – no treatment (0.2% sulphur)

Figure 5.4 is an image of single core wire specimen in the state collected from the ash/wire heap. Deposits of carbon ash (shown in Figure 5.4) are present on the wire surface in a layer that varies in thickness.

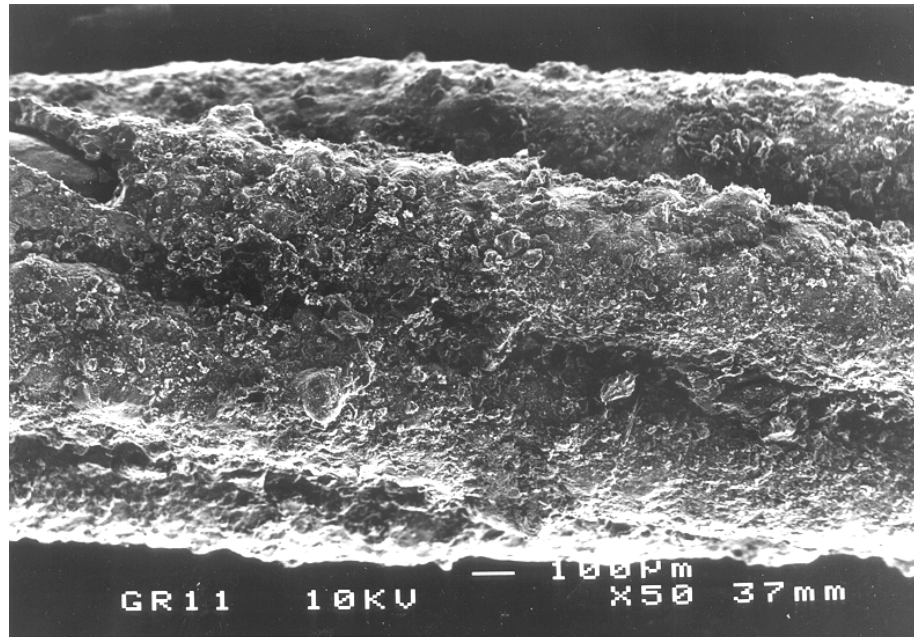


Figure 5.5 Multiple core wire – no treatment (0.7% sulphur)

Figure 5.5 shows a multiple stranded specimen of wire as collected from the heap. Carbon ash deposits are visible on the wire surface and also inside the strands of the cable. The sulphur concentration of the specimen (0.7%) is greater than the 0.04% specification and is also greater than the concentration associated with a single core sample of wire (0.2%). In one part of the sample (top left) a portion of the surface coating has been removed from the wire. At that point the coating thickness is in the order of 100 µm.

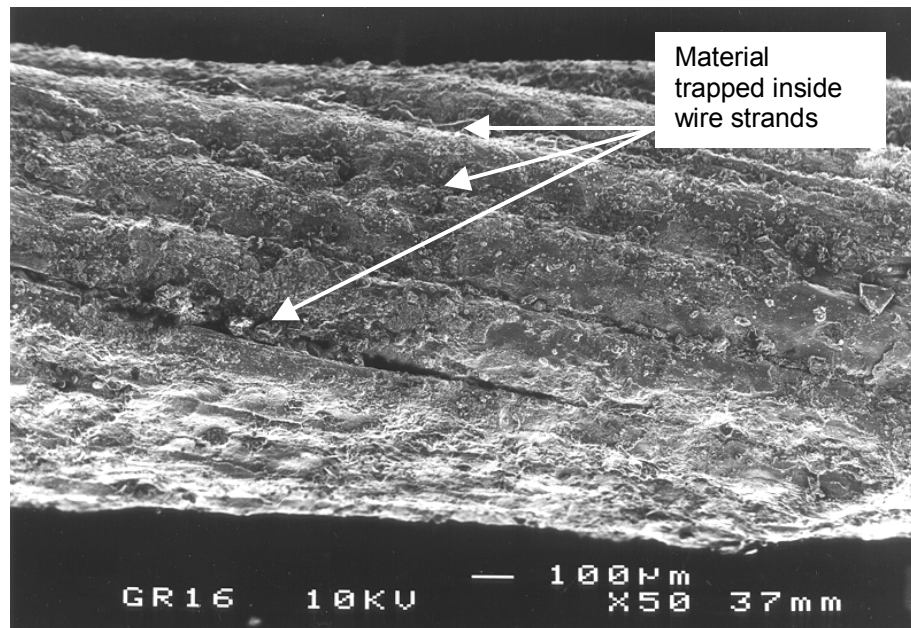


Figure 5.6 Multiple core wire - sanded (0.19% sulphur)

A multiple stranded specimen of wire that had been cleaned with sandpaper is presented in Figure 5.6. The amount of carbon ash attached to the wire surface is reduced although some material remains trapped inside the strands of the wire. The sulphur content of the specimen was reduced from 0.7% to 0.19% during sanding, although the level remains in excess of the 0.04% threshold. A similarly treated single core wire specimen is pictured in Figure 5.7.

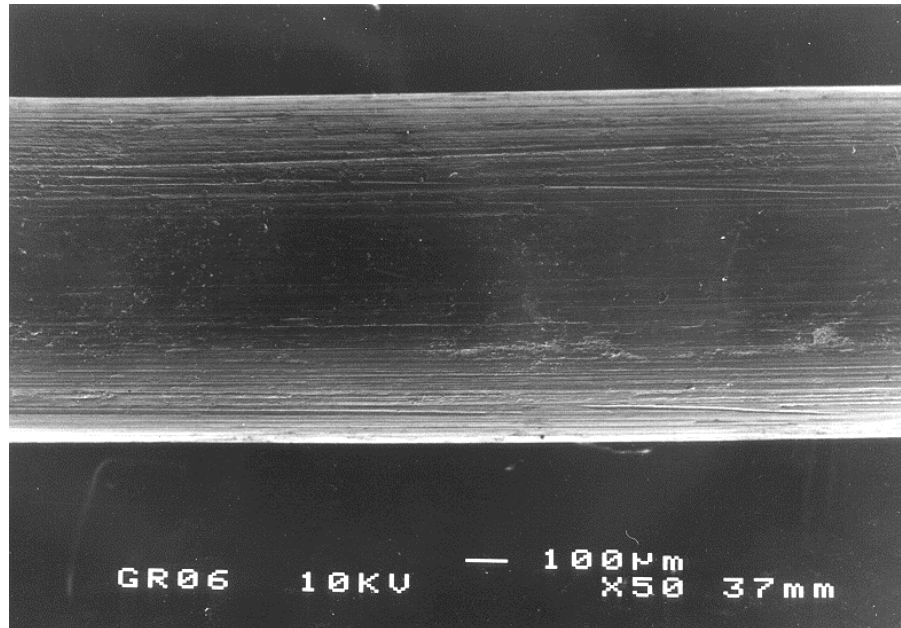


Figure 5.7 Single core wire - sanded (0.017% sulphur)

Figure 5.7 shows a single core piece of wire that was cleaned by surface sanding. Virtually the entire surface coating of carbon ash has been removed in comparison with the initial sample pictured in Figure 5.4. Scratches on the wire surface, caused by the sandpaper, are also visible. The sulphur concentration of the specimen was reduced to 0.017% which is significantly below the 0.04% reprocessing target.

5.3.1.5 Interpretation of wire characterisation

The starting sulphur concentration of the post combustion steel was found to be higher than the maximum level specified for reprocessing. Specimen wire samples were found to have sulphur concentrations of between 0.2% and 0.7%, with the higher sulphur concentration associated with the multiple core wound wire. Images generated by SEM investigation of the wire revealed significant quantities of carbon ash deposited on the wire surface of the untreated samples. In the multiple core wire the carbon ash was trapped inside the wound strands of wire.

The results of the cleaning experiments indicated that a significant proportion of the sulphur content of the post combustion steel wire was associated with surface deposits of carbon ash. Removing the surface deposits was effective in reducing the sulphur concentration of the wire samples with a direct relationship between the amount of

deposit removed and the sulphur concentration. Although wiping the wire (wet or dry) did reduce the sulphur concentration, only loosely associated surface deposits were removed and subsequently the sulphur content remained relatively high. The more aggressive sanding action removed sufficient carbon ash to achieve the 0.04% target. The results also indicated that the multiple core wire was not cleaned as effectively by the sanding action compared to the single core wire. This was due to much of the wire surface not being available to the sandpaper causing the carbon ash trapped inside the structure to remain, resulting in an elevated sulphur content when compared to the sanded single core wire.

5.3.2 Physical characterisation of carbon ash

Samples of the carbon ash phase collected from the ash/wire material were found to consist mainly of weakly formed agglomerated material that broke down easily and became progressively finer during routine handling. To determine the distribution and concentration of material properties the carbon ash was characterised both physically and chemically. The physical characterisation consisted of particle size analysis, the determination of the distribution of magnetic phases, SEM analysis and mineral phase identification with X-Ray Diffraction (XRD). Chemical characterisation was carried out to determine the concentrations and distribution of elements in the carbon ash. The main techniques used in the chemical characterisation have been described previously in Chapter 4. This information would then be used to identify potential products that could be generated from the material and the types of processes that might be employed to produce them.

Characterisation of this ‘bushy wire free’ portion of the waste material was found to be complicated by the presence of fine wire splinters that could also have formed a part of the bushy wire samples. Passing the dried samples through a laboratory scale dry magnetic separator removed most of the fine wire and also a portion of the ash, indicating the presence of an agglomerated ferrous/carbon phase. The magnetic phases were added back into the sample for characterisation purposes. A large sample, approximately 20 kg, of carbon ash was collected from STR and prepared for physical analysis. Sub-samples for individual tests were split from the bulk sample using a series of riffles (larger to smaller capacity) to split identical representative fractions

from the large initial sample. The sub-samples were dried immediately to stabilise the material with the exception of the fraction used as the charge for particle size analysis, which was conducted on the material as collected from the bunds (i.e., wet).

5.3.2.1 Particle size analysis

The particle size and size distribution of material in the approximate range present in the carbon ash was determined using a sieving technique. A number of techniques exist to impart motion to the sieve to promote the movement of particles to the appropriate sieve (e.g. vibrating sieve shakers) and the operation can be carried out on wet or dry material. The sample state has an influence on the technique selection and samples already in the form of a slurry can be analysed with a wet sieving method (Wills, 1997). Since the carbon ash was wet after collection then the analysis was carried out using a wet technique as drying the material might alter the measured distribution. In wet sieving the material is only dried after the analysis is completed to enable the dry mass of the each fraction to be determined.

A series of British Standard 200 mm diameter wire mesh sieves were selected to provide a distribution of mass across the particle size range (sieve sizes [μm]: 3350, 2000, 1000, 500 and 75). The maximum particle size in the carbon ash was observed to be approximately 30 mm in diameter, although many of the larger particles consisted of weakly formed agglomerates that quickly broke down during handling. The sieves were loaded into a vibrating cascade assembly with the largest aperture sieve at the top. A 1 kg (wet weight) sample of carbon ash, riffled from the large freshly collected sample, was placed into the top sieve. Material passing through each sieve then fell onto the next smallest sieve until the particle diameter was in excess of the nominal sieve aperture, at which point the particle was retained in the sieve. A very slow running hose delivering tap water was used to gradually move the sample onto the appropriate sieve. The operation was carried out until the water passing from each sieve was virtually free from particulate matter. A bucket placed at the end of the cascade collected the material passing through the 75 μm sieve.

After the test was complete the contents of each sieve was recovered and dried in an oven at 85°C overnight prior to weighing. The water associated with the sub sieve

(<75 μm) material was pressed out of the sample with a pressure filter and the solids collected on a 240 mm Schleicher & Schuel[®] 595 filter paper, the sample was then dried along with the other fractions. The masses of each fraction were then used to determine the particle size distribution for the carbon ash material. The distribution is presented in Figure 5.8.

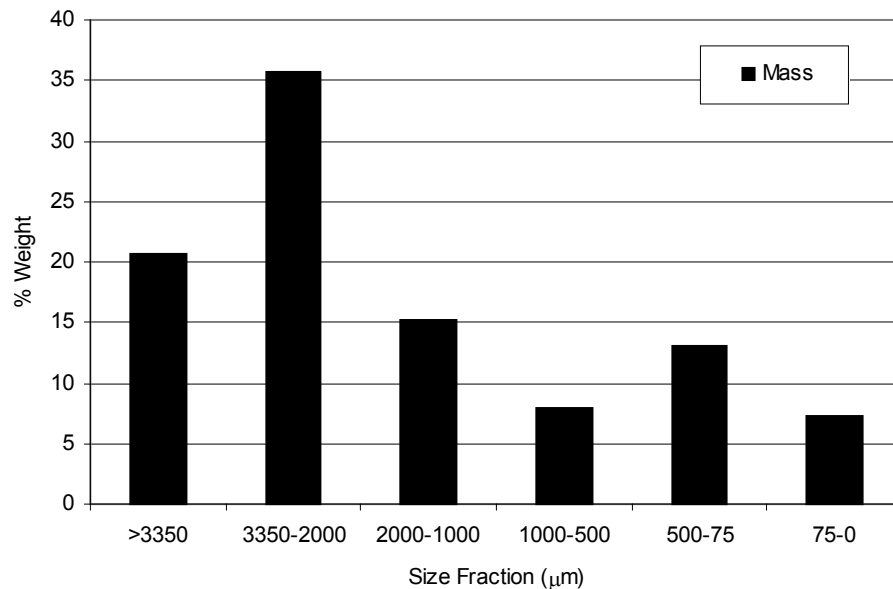


Figure 5.8 Carbon ash - fractional size distribution

The majority of the carbon ash material reported to the 3350-2000 μm although material is distributed across the entire particle size range. During wet sieving it was observed that the final size distribution of the material was significantly influenced by the measurement method. It was thought that the action of the vibrating sieve shaker combined with the running hose might cause increased breakage of particles causing the size distribution to appear finer than it actually was.

5.3.2.2 Magnetic distribution

To determine the distribution of magnetic phases in the carbon ash the dry size fractions were separated using a Boxmag-Rapid[®] laboratory scale dry magnetic separator. The method applied to the treatment of the carbon ash with the equipment is discussed in detail in the following chapter concerning separation studies. Each size

fraction was passed through the separator and the magnetic and non-magnetic portions collected and weighed. The results of the magnetic characterisation are presented in Figure 5.9.

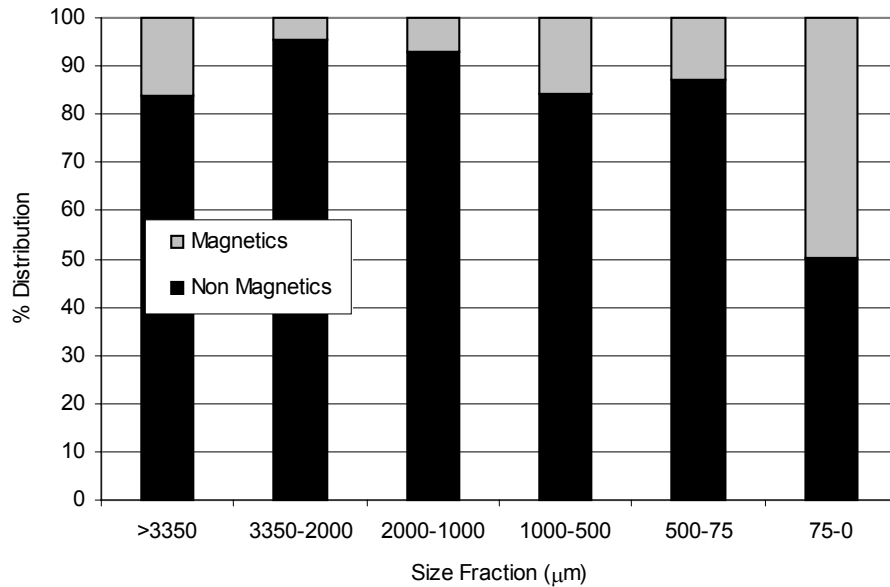


Figure 5.9 Carbon ash - distribution of magnetic phases

The 75-0 μm size fraction contained 50% magnetic material (by weight), which was composed entirely of a magnetic carbon ash phase. The magnetic material in the larger size fractions consisted of a combination of carbon ash and wire phases whilst the largest size fraction (>3350 μm) consisted solely of fine wire pieces. The magnetic and non-magnetic separated fractions were retained for chemical analysis.

5.3.2.3 Scanning Electron Microscope investigation

Scanning electron microscope (SEM) analysis was carried out to provide information on the association and distribution of elements within particles of carbon ash. Samples for analysis were prepared in one of two ways, polished or unpolished. Polished mounts can be used to provide information on phases present within particles and are prepared by setting a sample in a resin and then polishing the surface to reveal a cross section of the particles in the sample. Unpolished mounts should enable the particle size, shape and surface features to be investigated.

Polished mounts were prepared for analysis by setting carbon ash particles into Simplex Rapid[®] dental resin on a 30 mm diameter mount. The mount was then polished using a Struers Pedemat Rotapol-1[®] polisher. Silicon carbide paper was used to grind the surface of the mount followed by a final polish with a silica suspension and a soft cloth. Non-polished mounts were prepared by sparsely sprinkling a small mass (<0.5 g) of sample onto a double-sided sticky tab attached to a 30 mm diameter stub. After preparation all mounts were sputter coated in gold to improve conduction during analysis.

Analysis was carried out using a JEOL[®] J6400 SEM fitted with a NORAN[®] Series II EDX analyser system. The EDX system allowed the semi-quantitative determination of the elemental composition of specific points or small areas in the sample. Images were collected using a solid-state backscattered electron detector. The samples were introduced into the sample chamber on a rotating bezel, which enabled different areas of the mount to be viewed. The sample chamber was placed under vacuum prior to operation.

Size fractions generated during the particle size analysis were used for SEM analysis since the relatively small particle size range minimised the affect of larger particles masking smaller particles during analysis. Initial analysis was carried out on the 500-75 μm fraction. Images of the non-polished samples are presented in Figure 5.10 through to 5.12. The polished mount is pictured in Figure 5.13. The points in the samples at which EDX analysis was carried out are annotated on the images and the results summarised in Figure 5.14.

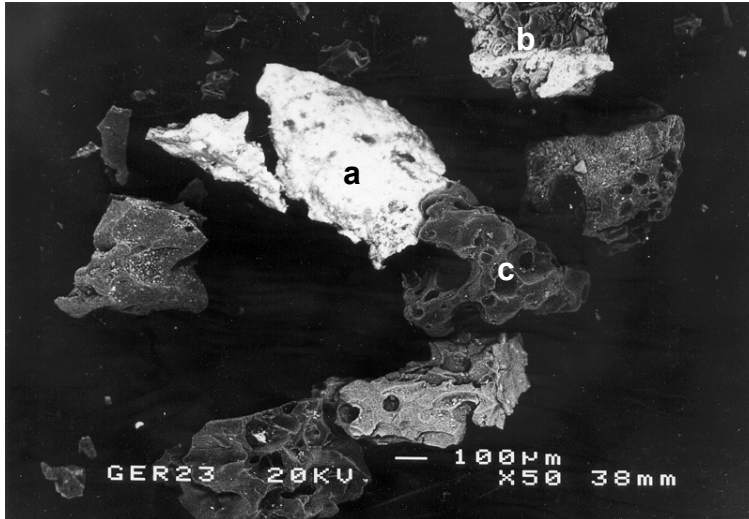


Figure 5.10 SEM image of mixed particles in carbon ash

Backscattered electron image of a mixed group of carbon ash particles that include:

- an iron based particle (a)
- a mixed iron/carbon particle (b)
- a carbon based particle with little visible contamination (c)

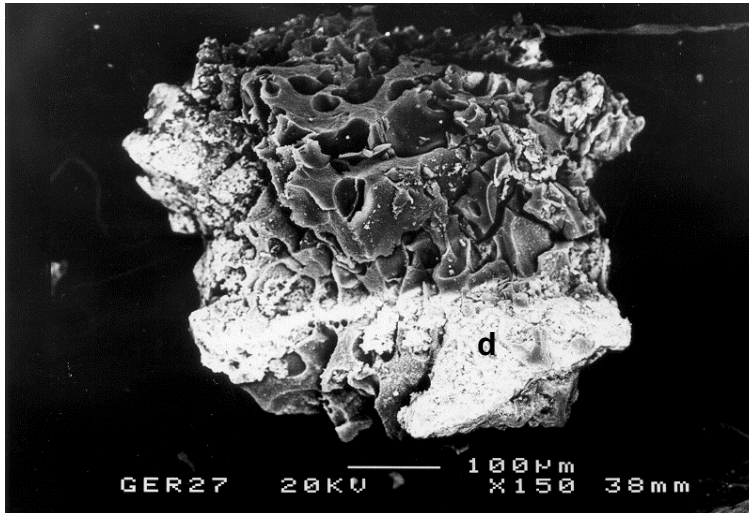
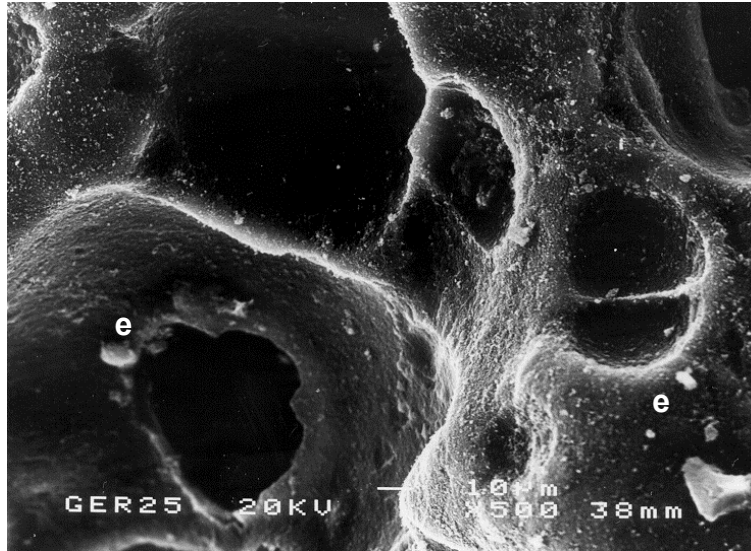


Figure 5.11 SEM image of mixed phase particle in carbon ash

Backscattered electron image of particle (b) in Figure 5.10. The mixed phase particle consists of an iron based coating (d) deposited on a part of a porous carbon based particle.

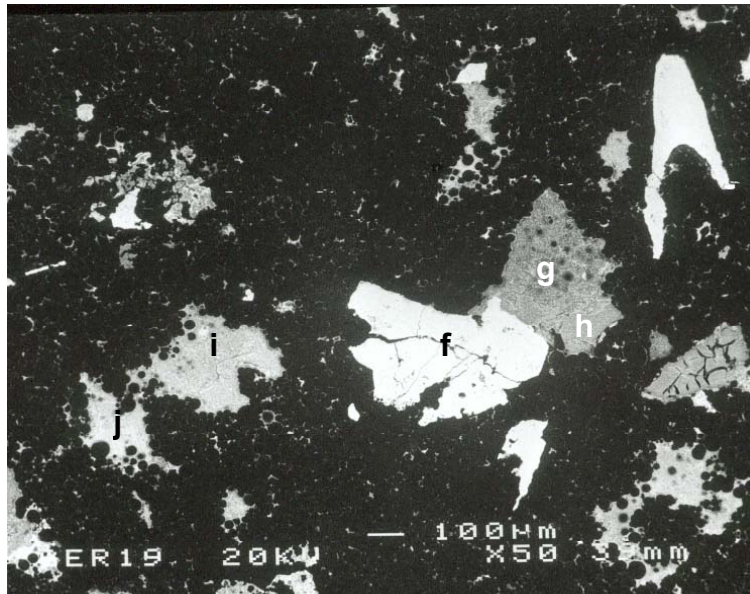


Close-up image of the surface of the carbon particle (c) in Figure 5.10.

Sub 10 μm particles (e) of metallic elements are visible on the surface.

Figure 5.12 SEM image of close up of carbon phase surface

During analysis of the polished mount it was found that the polishing process had not been successful in providing a cross section of the sample, probably due to the relative softness of the material in comparison with coals. Polishing the carbon ash sample caused the particles to smear over the sample surface making the analysis of the sample very difficult as the particle boundaries could not clearly be seen. A second attempt to prepare a polished mount was made by remounting the sample in resin and polishing at a slower rate. This provided a sample that could be analysed although much of the sample was still smeared. A single image of a relatively unaffected area of the sample is presented in Figure 5.13.



An iron based particle (f) silica/calcium/aluminium phase (g) incorporating a darker silicon/calcium/oxygen phase (h).

A separate particle consisting of sulphur and zinc (l) close to a mixed phase dominated by silicon and oxygen (j)

Figure 5.13 SEM image of polished section

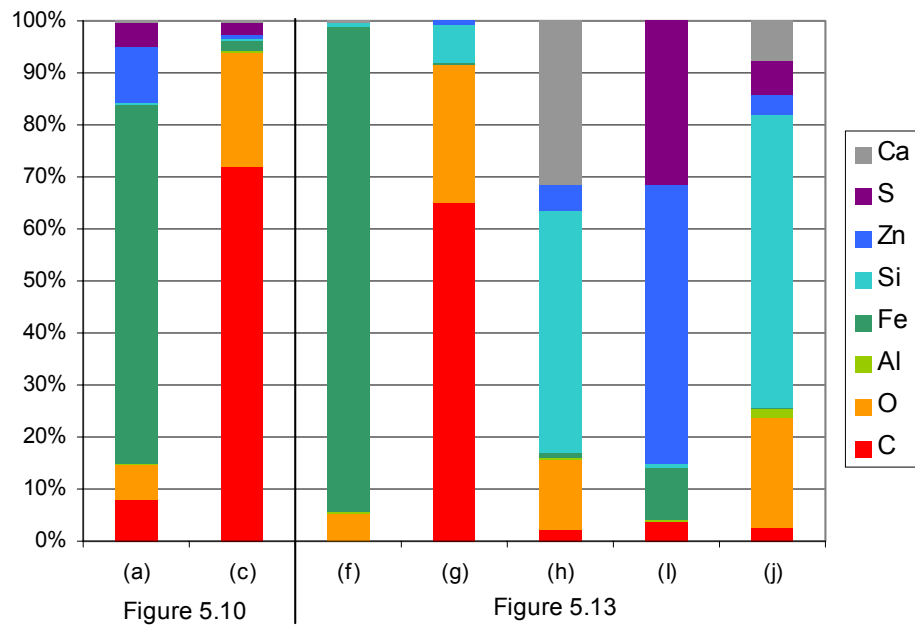


Figure 5.14 Summary of EDX analysis

The EDX analysis (see Figure 5.14) indicated that particles or areas in the sample contained mixed phases. The exception to this was point (f) which was dominated by iron. SEM-EDX analysis indicated the presence of three main particle types within the carbon ash:

- Carbon particles with little or no visible contamination
- Carbon particles with a metallic association (mainly iron but also zinc, sulphur and other trace elements). This was the dominant particle type
- Free metallic phases (mainly Fe)

EDX analysis determined that the dominant metallic phase was iron, present both as a single element and also as a mixed phase associated with other metallic elements such as zinc. The majority of carbon particles had a surface association of very fine metallic particulates and some had a larger iron based coating as pictured in Figure 5.11. The carbon particles were observed to have a porous structure and it was suspected that the fine metallic material on the particle surface was also present inside the pores. This would normally be confirmed with the analysis of the polished mount although this was not possible due to the difficulties encountered during sample preparation.

EDX analysis provided information for the chemical characterisation stage of this study by identifying some of the elements that should be included in the analysis.

5.3.2.4 Mineral phase identification with X-Ray diffraction

X-ray diffraction (XRD) analysis is a non-quantitative technique used to identify crystalline mineral phases directly in solid materials. The technique compares an X-ray trace generated by the feed sample to a library of standard responses generated by known minerals. After removal of the background signal the peaks in the sample trace are automatically compared to a database of minerals and a relative merit assigned to the possibility of a mineral being present in the sample. A certain amount of judgement is used in combination with the merit rating to determine the mineral phases present as some combinations of peaks might indicate the presence of a number of minerals. With some knowledge of the elements that might, or might not, be present in the sample certain mineral phases could be discounted.

Analysis was carried out using a Hiltonbrooks[®] X-Ray Generator with a Philips[®] copper tube goniometer, diffraction data was analysed by Sietronics[®] X-ray analytical software. Initial analysis of a single carbon ash sample found that the high level of

carbon present in the sample masked the majority of the peaks in the sample, preventing accurate analysis. To improve the analysis accuracy the majority of the carbon needed to be removed, leaving a concentrated volume of the mineral phases intact. Ashing the material at high temperatures (850-1000°C) may have resulted in the loss or alteration of minerals present in the sample along with the carbon so a low temperature ashing (LTA) technique was used. The technique, often used in the analysis of coals, exposes the sample to an oxygen stream that has been 'activated' with a radio frequency oscillator. The process serves to ash the sample freeing and concentrating the mineral matter making it available for analysis. Since the LTA process occurs at temperatures of approximately 150°C the mineral phases generally closely correspond to the starting species in the raw sample (Allen et al. 1986).

Low temperature ashing of the samples was carried out using an AVE[®] low temperature asher. Powdered carbon ash samples were placed into one of two glass petri dishes and evenly distributed. The dishes were placed inside the LTA chamber, which was then evacuated of air. Once the pressure in the chamber fell below 0.6 millibar and was stable the oxygen stream was activated by gradually increasing the forward radio frequency power to 80 W. At approximately 10 W the reflected power strikes back to zero and the plasma is set up. The instrument timer was set for a period of one hour after which time the plasma was automatically switched off. During ashing of the samples at 80 W the temperature in the chamber did not rise above 90°C, indicated on the instrument control panel. After each hour the chamber was slowly returned to atmospheric pressure by allowing air to leak back into the chamber through a valve. The usual method of re-pressurising the chamber by opening a vent was found to be too harsh, resulting in the loss of powdered material from the dishes. The sample was then inspected and any agglomerates broken up with a pin. During ashing only the top surface of the carbon ash was oxidised so the sample was stirred to present a new layer of carbon ash after each hour before returning to the chamber. A sample was defined as ready for XRD analysis when no visible carbon remained in the sample, this was simple to detect since the non-oxidised sample was black whilst the colouration changed to a light brown after ashing. Typically, complete ashing of a sample took between six and eight one-hour cycles. After treatment the contents of the two dishes were combined to form a single, larger, sample of sufficient quantity

for XRD analysis. The 'carbon free' samples were then mounted into a standard aluminium slide for mineral identification.

XRD analysis was initially carried out on two different samples of carbon ash. One sample was riffled from the bulk sample (all size fractions) and was been defined as 'fresh' carbon ash. The second sample was derived from the same sample but had been allowed to 'age' (sample not dried after collection), it contained visible corrosion by-products.

The XRD traces (after baseline removal) generated from the fresh samples of carbon ash phase are presented in Figure 5.15 and the aged sample in Figure 5.16. The two traces presented for the 'fresh' sample represent analysis of two different carbon ash samples collected on different days approximately 1 month apart. Both samples were prepared in an identical manner and have been included for completeness. The traces can be seen to be very similar.

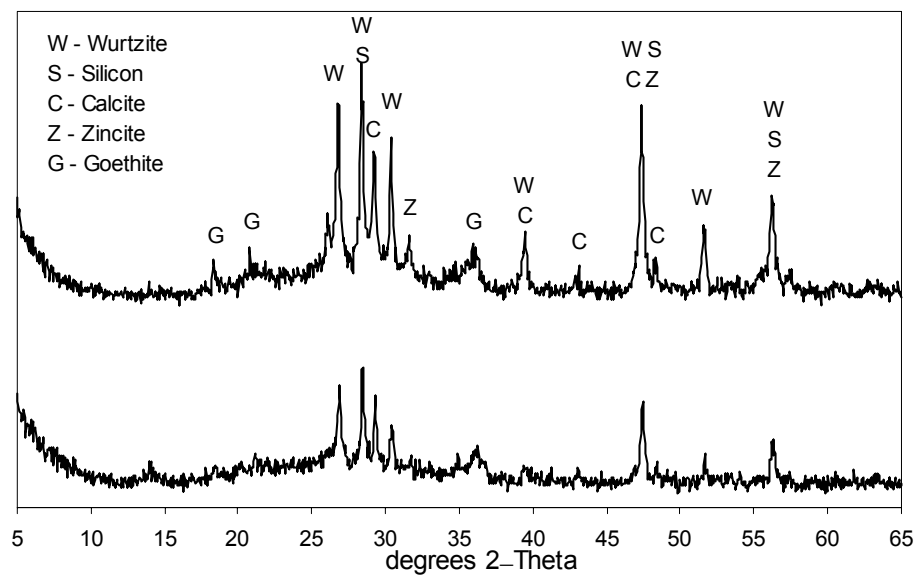


Figure 5.15 XRD trace of fresh carbon ash

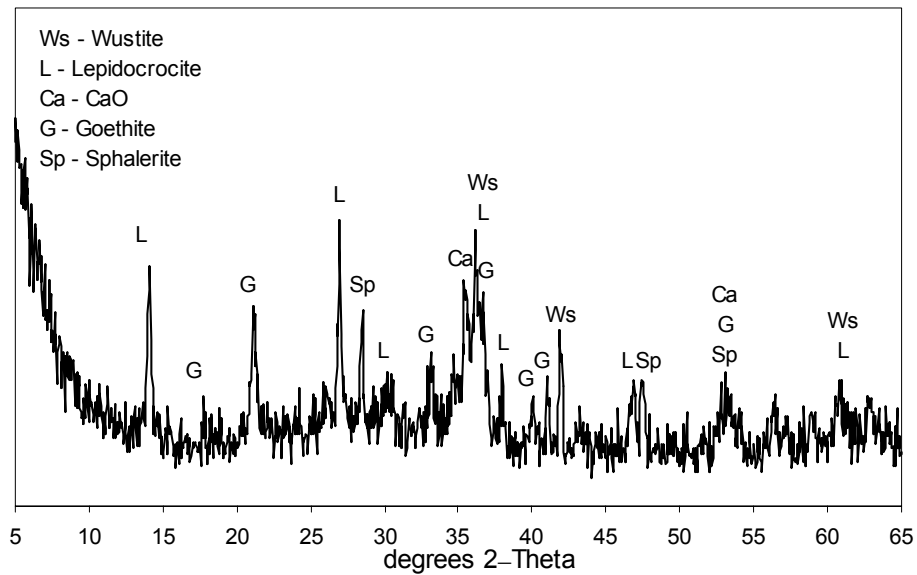


Figure 5.16 XRD trace of aged carbon ash

The mineral and inorganic phases identified in both sample preparations are summarised in Table 5.2.

'Fresh'	'Aged'
Calcite (CaCO_3)	Sphalerite (ZnS)
Zincite (ZnO)	Wustite (FeO)
Sphalerite (ZnS)	Goethite (FeO(OH))
Wurtzite (ZnS)	Lepidocrocite (Fe(OH)_3)
Silicon (Si)	CaO
Goethite (FeO(OH))	

Table 5.2 Mineral phases identified in carbon ash samples

XRD analysis detected a series of mineral phases in the carbon ash, which differed between the 'fresh' and 'aged' samples. Zinc bearing minerals were detected in three forms, as zinc sulphide (wurtzite and sphalerite) and also as zinc oxide (zincite). Calcite and silicon were detected in the only the fresh sample, goethite was detected in both the fresh and aged sample. The detection of silicon in the sample was not expected. The element would be derived from the silica (SiO_2) used as filler in the rubber component of the tyre and would be unlikely to undergo transformation to silicon in the incinerator due to insufficient temperatures. It was not clear why XRD detected the element as silicon. The aged sample contained minerals associated with

the oxidation of iron such as goethite, wustite and lepidocrocite. Calcite was not detected in the aged sample although calcium oxide was detected.

5.3.3 Chemical characterisation of carbon ash

Following the physical characterisation stage the carbon ash was characterised chemically to quantify and investigate the distribution of components within the material. The presence of elements including carbon, sulphur, calcium, zinc, iron, aluminium and silicon were detected during the XRD and SEM investigations. Further elements were included in the analysis on the basis that they formed component parts of the original tyres so would be likely to appear in the carbon ash.

The samples of carbon ash to be chemically characterised were the size fractions (magnetic and non-magnetic) together with the bulk sample (all size fractions). The bulk sample, as used in the XRD analysis, was prepared by drying and then passing through a magnetic separator to remove fine wire splinters.

5.3.3.1 Concentration and distribution of carbon and sulphur

Carbon and sulphur concentrations were determined using the methods described previously in Chapter 4. The average carbon and sulphur concentrations measured in the bulk sample are presented in Table 5.3.

	Carbon (%)	Sulphur (%)
bulk sample	81.0	1.8

Table 5.3 Concentration of carbon and sulphur in bulk sample of carbon ash

The results of the carbon and sulphur analysis in the non-magnetic carbon ash fractions are presented in Figure 5.17 and Figure 5.18. The full results are available in Appendix 1.

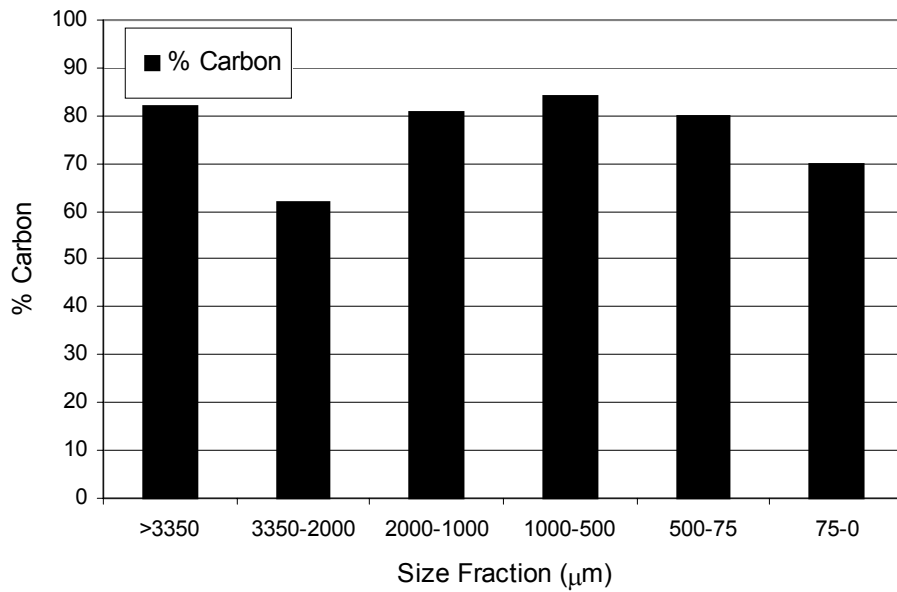


Figure 5.17 Carbon ash - fractional size versus % carbon

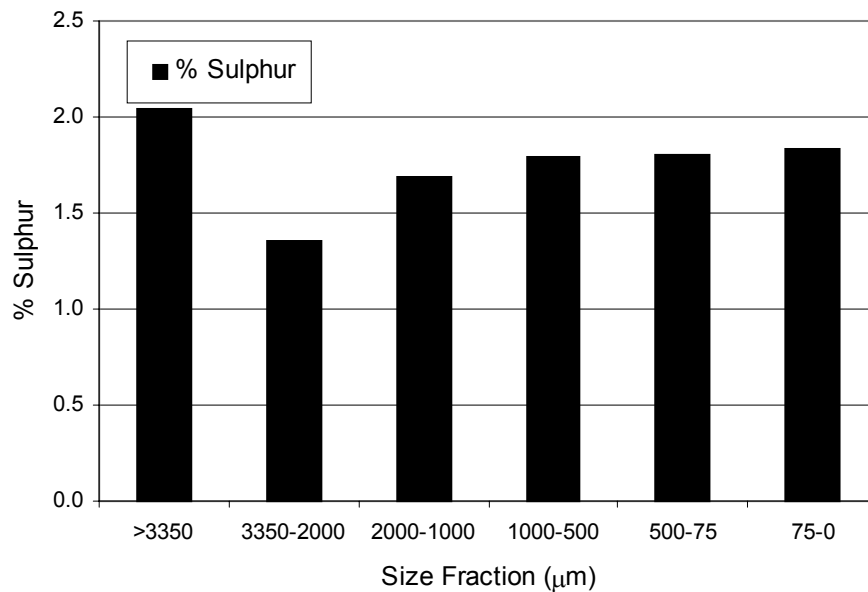


Figure 5.18 Carbon ash - fractional size versus % sulphur

Carbon and sulphur concentrations measured in the carbon ash size fractions were relatively uniform across the entire particle size range. The carbon and sulphur content of the 3350-2000 µm material was lower in comparison to the other fractions which might indicate the increased concentration of another component in the fraction. The results of the carbon and sulphur analysis conducted on the magnetic

carbon ash fractions are presented in Figure 5.19 and Figure 5.20. The domination of fine wire splinters in the largest size fraction ($>3350 \mu\text{m}$) meant that sulphur and carbon could not be determined as the sulphur content in wire could not be measured using the standard analytical method.

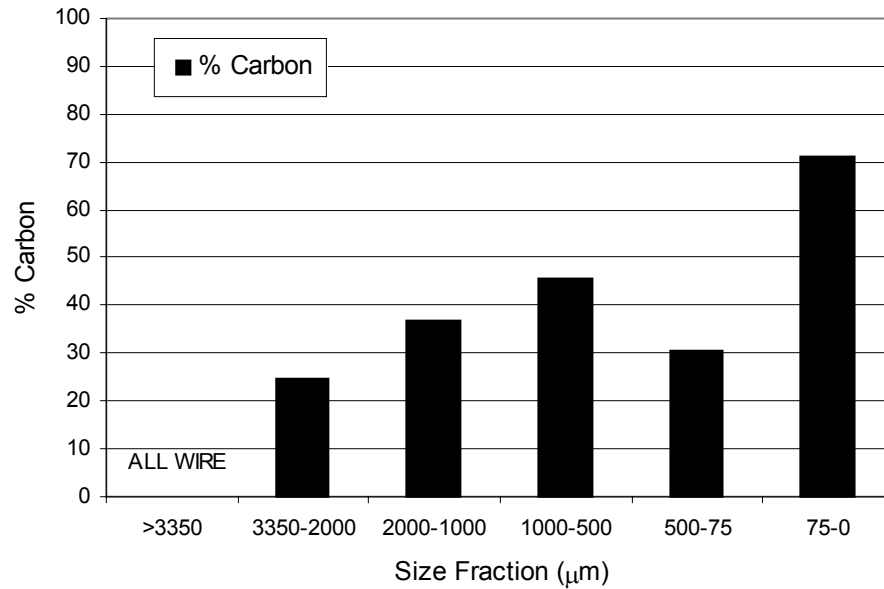


Figure 5.19 Carbon ash - fractional size (magnetic) versus % carbon

The highest carbon concentration was measured in the finest particle size fraction. The carbon content of the $75-0 \mu\text{m}$ magnetic fraction is similar to the same sized non-magnetic fraction. In the remaining size fractions the carbon content was significantly lower in comparison with the non-magnetic material.

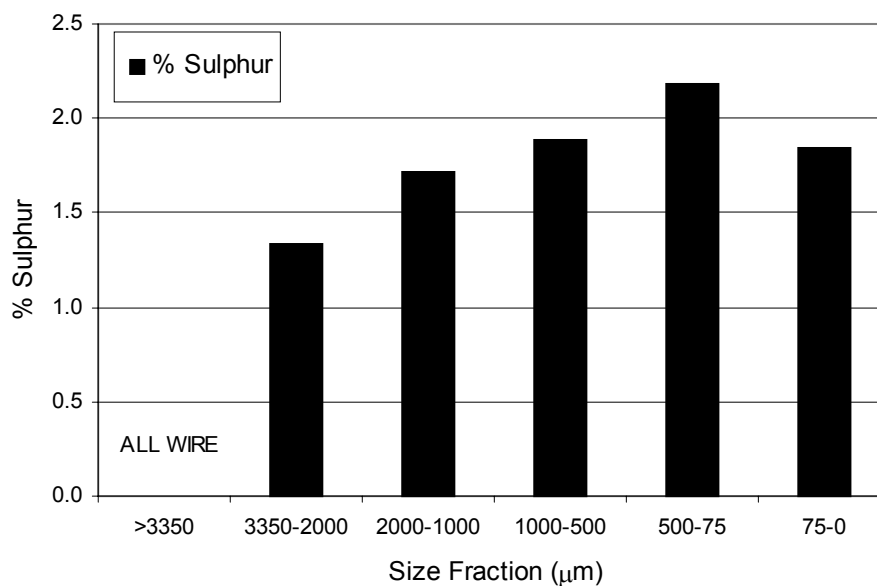


Figure 5.20 Carbon ash - fractional size (magnetic) versus % sulphur

From Figure 5.20 it can be seen that the sulphur content of the magnetic size fractions followed a similar trend to the carbon levels measured in the same samples. It should be noted that the presence of fine wire pieces in all of the magnetic fractions might have adversely effected the accuracy of the results obtained. Although the wire provided mass to the samples being analysed, carbon and sulphur was only measured in the carbon ash phase, the wire remained intact after analysis.

5.3.3.2 Concentration and distribution of major and minor elements

The quantitative determination of other elements in the carbon ash was carried out using the total digestion technique described in Chapter 4 and the concentrations determined using ICP-AES. The main bulk of the analysis was performed in one of two separate batches that were carried out concurrently. Each batch contained 12 separate samples, the maximum possible with the equipment being used. Batch one contained 6 replicate samples of the bulk sample and 6 of the size fractions. Batch two contained a further 2 bulk replicates, the remaining size fractions, 3 randomly selected repeats and a blank.

The results gained from the analysis of replicate samples were found to be in good agreement so, where relevant, the results represent an average of two or more determinations. The results of analysis of the bulk sample are presented in Table 5.4.

Element	($\times 10^4$ ppm)	Element	($\times 10^4$ ppm)
Ba	0.002	Al	0.2
Cd	<LOD	Ca	0.98
Cr	<LOD	Fe	3.4
Cu	0.020	Mg	0.11
Ni	<LOD	Mn	0.019
Pb	0.008	Si	0.6
Zn	3.7	Ti	0.021

Table 5.4 Concentration of elements in bulk carbon ash sample [<LOD - below limit of detection]

The dominant elements measured in the bulk sample were zinc (3.7%), iron (3.4%) and calcium (1.0%). The result for silicon is included in the data although it should be noted that it might not be reliable for the reasons discussed in Chapter 4.

The concentration of elements across the particle size range for the non-magnetic fractions are presented in Figure 5.21 and 5.22. The elements have been grouped into high (major) and low (minor) concentrations for ease of presentation. Elements present at concentrations below the detection limit have been omitted.

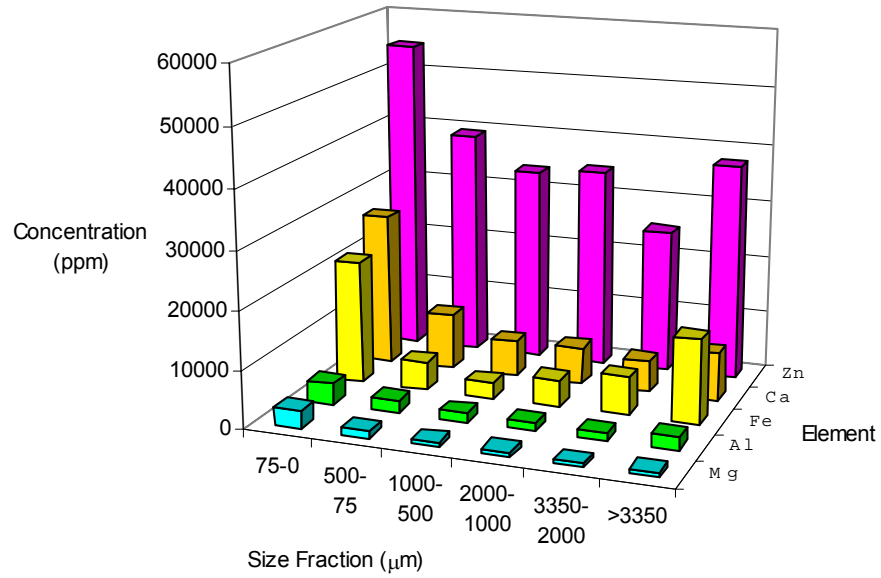


Figure 5.21 Concentration of major elements in non-magnetic fractions

Zinc and calcium and to a lesser extent iron, aluminium and magnesium, were more concentrated in the finest size fraction. The zinc concentration was slightly lower in the 3350-2000 μm fraction compared to the rest of the size range. Elements present in minor concentrations in the non-magnetic samples are presented in Figure 5.22.

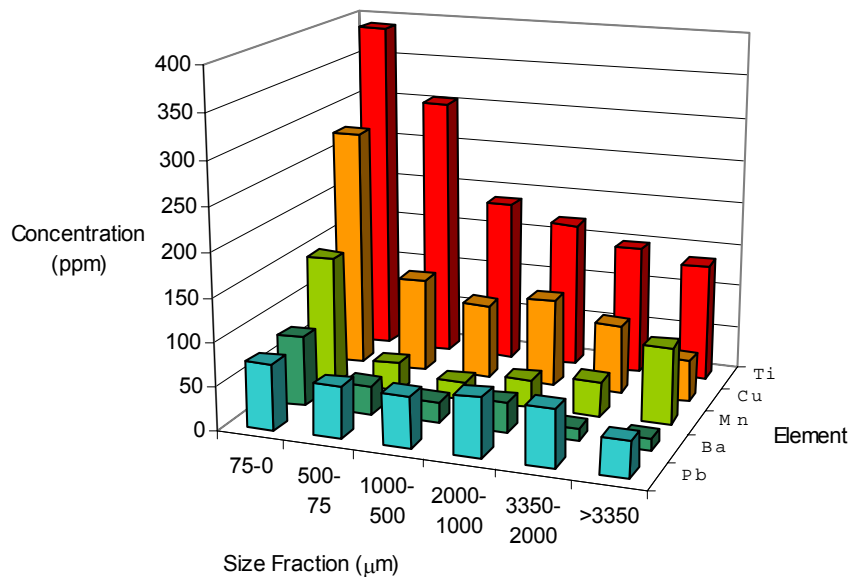


Figure 5.22 Concentration of minor elements in non-magnetic fractions

From Figure 5.22 it is seen that minor elements were generally most concentrated in the finest size fractions.

The concentration of major elements in the magnetic size fractions is presented in Figure 5.23.

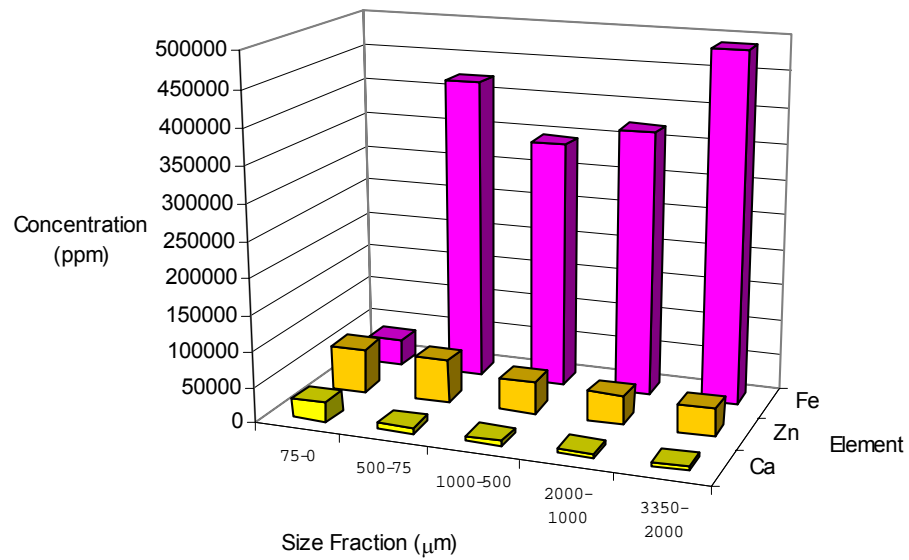


Figure 5.23 Concentration of major elements in magnetic size fractions

In the magnetic fractions it can be seen that the dominant element was iron which was measured at concentrations of 34% to 49% with the exception of the finest fraction where it was 3.6%. Calcium and zinc were slightly more concentrated in the finest fraction.

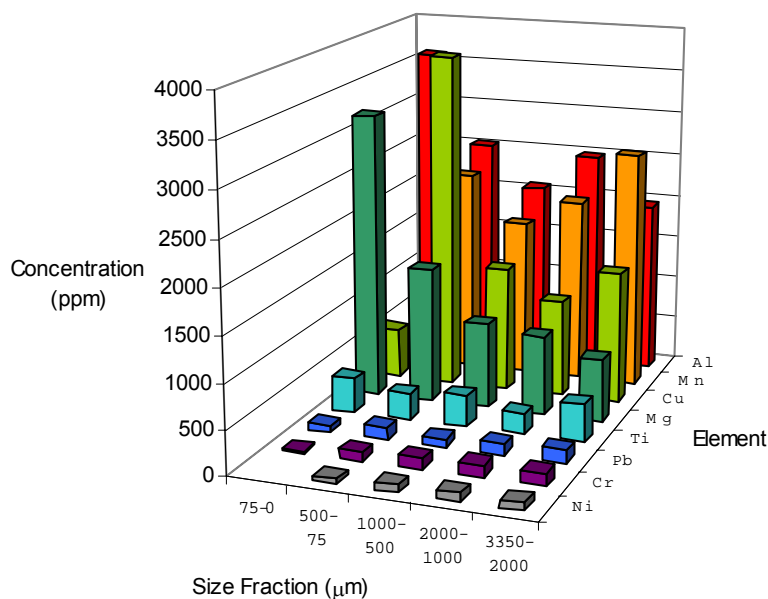


Figure 5.24 Concentration of minor elements in magnetic size fractions

From Figure 5.24 it can be seen that the concentration of minor elements in the magnetic fractions do not show a clear pattern as was found in the non-magnetic fractions. Although certain elements (e.g. magnesium) are slightly more concentrated in the finest fraction.

5.3.3.3 Interpretation of carbon ash characterisation

As shown in Figure 5.8 the majority of the carbon ash reported to the coarser size fractions (i.e. >2000 μm). However, it was found that the larger particles, consisting of weakly formed agglomerated material, quickly broke down during handling and continued to break down during the wet sieve analysis. The material therefore became progressively finer with time. Subsequent analysis carried out on individual size fractions should therefore only be used as an indication of element distribution and not a definitive result.

The experiment to determine the distribution of magnetic phases (see Figure 5.9) within the carbon ash fractions found that 50% (by weight) of the material in the finest fraction reported to the magnetic fraction. Considerably less of the material was magnetic in the coarser fractions although it should be noted that this could be

attributed to inferior liberation of magnetic phases. The magnetic material extracted from the finest fraction consisted mainly of a mixed carbon-magnetic phase. Similar concentrations of carbon and iron were measured in both the magnetic and non-magnetic fraction. In the larger size fractions the magnetic fractions were dominated by steel wire with a relatively small amount of the carbon ash. This was confirmed with the elevated iron concentrations measured in the samples and the relatively low carbon.

SEM-EDX analysis found that the carbon ash consisted of carbon, metallic and mixed carbon-metallic particles. On closer inspection the carbon particles had a surface association of very fine metallic particles indicating high dispersion of non-carbon phases throughout the carbon ash. The metallic phases were usually dominated by iron although many consisted of iron-zinc alloys and usually contained sulphur. Some carbon particles appeared to have been partially coated with an iron phase, possibly as a result of the corrosion of the bushy wire in the wet samples. Mineral phases identified in the mixed phase included a number of iron oxide minerals indicating that the degrading steel wire was re-distributed onto nearby surfaces of carbon particles.

Mineral phases identified in 'fresh' carbon ash included zinc sulphide, zinc oxide, calcite, silicon and goethite. Goethite is weakly magnetic in comparison with steel wire which might partly explain the iron content associated with the non-magnetic fractions. However, it might also indicate that a part of the iron phase is more highly dispersed in the carbon ash compared to the liberated steel wire. As well as iron other elements were more concentrated in the magnetic fractions including chromium, copper, nickel, and manganese. This might be due to their association with the steel wire used to produce the tyre beads. The magnetic separation of the carbon ash is discussed in more detail in Chapter 6.

The bulk sample, which represented the typical output of STR after removal of the bushy wire, contained a high concentration of carbon (80.9%) and a sulphur content of 1.8%. The high level of carbon remaining in the ash indicates that the burnout of tyres in the incinerator is low, this might be as a result of insufficient air supply, insufficient residence time or a combination of both. Carbon and sulphur concentrations measured in the size and magnetically separated fractions revealed that

the sulphur concentrations were relatively uniform varying between 1.4% and 2.2%. Carbon in the non-magnetic fractions varied between 62% and 84% whilst the levels varied more widely in the magnetic fractions due to the influence of steel wire. The lower carbon concentration measured in the 3350-2000 μm indicated the increased concentration of a different element in that fraction although no peaks in the other elements were observed. A relatively low concentration of zinc and sulphur was also recorded in this fraction. The result could be explained by the presence of a piece of refractory reporting to the sample. The presence of the silica based material would reduce the concentration of other elements in the sample whilst itself remaining undetected due to the difficulties encountered analysing silica with ICP-AES. If the accurate analysis of silicon became a major issue during this study then an alternative analytical technique would have to be developed for the element.

The results of the carbon, sulphur and total digestion have been combined in Table 5.5 to provide a more complete analysis of the bulk sample.

Element	Concentration ($\times 10^5$ ppm)
C	8.09
Zn	0.37
Fe	0.34
S	0.18
Ca	0.098
Si	0.06
Al	0.2
Mg	0.011
Ti	0.0021
Cu	0.0020
Mn	0.0019
Pb	0.0008
Ba	0.0002
Cd, Cr, Ni	<LOD

Table 5.5 Combined analysis results of carbon ash bulk sample

The principal components in the sample are carbon (81%), zinc (3.7%), iron (3.4%) and sulphur (1.8%). The concentrations of potentially toxic elements such as lead, cadmium, chromium and nickel were low and with the exception of lead were present at concentrations below the detection limit of the analysis method.

5.4 Interim summary and conclusions

The combustion residue generated by the tyre incineration process at STR was split into two separate phases, namely 'bushy wire' and 'carbon ash', for characterisation with a view to identifying potential products that might be generated.

The main issue associated with the generation of a steel product from the bushy wire phase had previously been identified as the sulphur content of the post-combustion steel. A series of tests determined that the sulphur content of the steel was associated with surface deposits of carbon ash. Removing virtually the entire surface coating on the steel wire reduced the sulphur content to an acceptable level for reprocessing. This cleaning mechanism could then be exploited and developed into a process to generate a product.

The components of the carbon ash reflected the component ingredients of the feed tyres, the dominant element being carbon. The bulk of the carbon is likely to be derived from the carbon black used in tyre production as also found by (Helleur et al. 2001) and (Chaala et al. 1996) in chars resulting from pyrolysis processes. Significant concentrations of zinc, sulphur and calcium derive from the additives included in the rubber compound, which control and enhance the vulcanisation process as well as defining some of the performance characteristics of the rubber.

This carbon ash generated by the STR process possesses similar properties to the material generated by the tertiary recycling process (Allred et al. 2000), summarised in Chapter 2. The zinc and calcium concentrations are similar although the iron concentration in the tertiary process was lower, probably as a result of the magnetic separation of the wire from the char phase after the process. The mineral phases identified in the carbon ash included those found by (Darmstadt et al. 1994) in pyrolysis chars which included zincite, wurtzite and sphalerite. These factors indicate a similarity between the STR incinerator residue and the chars produced by laboratory and pilot scale pyrolysis processes. Significantly, the carbon concentration is usually reported as being slightly higher in tyre pyrolysis chars. This might be due to the differing feedstock used by the processes since a 'wire-free' rubber is often prepared for laboratory scale pyrolysis whilst whole tyres are combusted at STR. This causes

more iron phases to be present in the carbon ash complicating the separation of wire from the char due to handleability difficulties.

The high concentration of carbon in the carbon ash suggests that the main potential product that could be generated from the phase would be based on the element. Markets for such a material might include fuels or possibly higher value uses after a reprocessing stage. Concentration of the carbon phase might lead to the generation of a product with increased value and a wider range of application. This would require the removal, or reduction, of the non-carbon phases in the carbon ash.

The initial characterisation study concentrated on the collection and analysis of a small number of samples over a relatively short time period. The analysis to date assumes that the samples collected during that time were representative of the plant output over the long-term. The assessment of the variation of ash/wire properties over a longer time period would have required a larger number of samples to be collected over an extended time period. However, it is likely that the data gathered by this sampling operation would be heavily biased by the effectiveness of the separation employed to split the wire phase from the ash/wire samples. For this reason a long term sampling operation was not undertaken although samples collected for further test work were compared to the original samples to check that the properties of the material had not altered significantly.

The separate treatment of the two phases (bushy wire and carbon ash) is essentially a primary separation process that might subsequently form a part of a full treatment process. The final products generated from the phases would require further reprocessing to form the saleable material, suitable process are now investigated.

Separation Studies

This section of work is predominantly concerned with the production of cleaned and separated phases of steel wire and carbon ash derived products. This was investigated through the novel application of established mineral processing techniques. The specific treatment of the materials was dependant on the product specifications demanded by potential purchasers, but the main aims were to produce a virtually sulphur free steel product and a high carbon concentrate. The treatment of the carbon ash and bushy wire have been investigated separately.

6.1 Processing of carbon ash

The type of material with the highest value that could be potentially extracted from the carbon ash would be a product with a similar specification to carbon black. The main characteristic of carbon blacks are very high carbon concentrations, usually >95%. Products with a lower carbon content could potentially be used as a fuel substitute but would command a lower market value. Characterisation of the carbon ash revealed a relatively high concentration of contaminants (approximately 20-40%) in comparison to carbon black. A number of routes were examined as potential methods to upgrade the material in terms of carbon concentration.

6.1.1 Dry magnetic separation

Throughout the characterisation phase of this research the carbon ash phase was separated from the ash/wire material in two stages. Firstly the bushy wire was hand picked from the ash/wire sample and the remaining material dried. The dried material was then passed through a magnetic separator to remove further wire and other magnetic phases. The suitability of the application of dry magnetic separation to produce a carbon concentrate, mainly through the removal of iron phases, was examined using a laboratory scale dry magnetic separator.

6.1.1.1 Method

The samples passed through the separator were generated from the size characterisation experiment conducted in Chapter 5 and a bulk sample (all size fractions). An aged sample as analysed previously with XRD was also examined. All samples had been dried overnight in an oven at 85°C before being used. A laboratory scale Boxmag-Rapid[®] electromagnetic ore separator was used to separate each sample individually.

The instrument was equipped with a vibrating feed hopper, which fed material onto the main conveyor. Material on the conveyor then passed under a permanent strip magnet, positioned 15 mm above the belt, and then under a single disc separator. The revolving disc, which could be adjusted vertically to alter the belt clearance, was magnetised by a stationary electromagnet. The disc was aligned so that a greater gap existed at the leading edge than on the trailing edge to allow the removal of magnetic products of different susceptibilities into the collectors on either side of the belt. Particles with a lower susceptibility would be removed at the trailing edge of the disc. Non-magnetic material passing both the permanent magnet and electromagnet drops from the end of the conveyor into a container and formed the product.

The equipment manufacturer recommends a maximum particle size of 1.4 mm and a minimum of 0.105 mm for effective separation, although the maximum disc clearance is 6 mm (Boxmag-Rapid Ltd, 2002). In each test the individual sample to be separated was fed onto the main belt using the vibratory feeder, most samples were subject to a single pass but multiple passes were also carried out on some samples. The vibration frequency and belt speed were adjusted until a monolayer, or as close as possible, of particles was achieved. This was to reduce the possibility of physical entrainment of magnetic material in the non-magnetic product. Increasing the belt speed reduced the concentration of material on the belt but also reduced throughput time. The disc clearance was adjusted so that the trailing edge of the disc was just sufficient to clear the largest particle in the sample without brushing material from the belt. This only occurred during separation of the largest fraction (>3350 µm). With the belt running and disc rotating the current supplied to the electromagnet was adjusted from zero to 1.4 amps, a figure recommended by the manufacturer, and maintained at that level

throughout the experiments to provide a consistent level of magnetism. After each pass the non-magnetic material was collected from the end of the conveyor and retained for analysis.

As a part of the characterisation study a complete analysis was carried out on the samples since they formed a part of the material characterisation. Details of the analytical techniques used can be found in Chapter 4. This section re-examines the same data and concentrates on the carbon content of the product with the associated iron concentration used as an indication of the quality of separation.

6.1.1.2 Results & discussion

The performance of the separation for each sample was observed during the experiment. For all samples the permanent strip magnet scalped larger magnetic phases from the feed material as well as fine wire splinters, no splinters reported to the product in any fraction. Magnetic phases were also removed by the rotating disc, this occurred almost entirely at the leading edge indicating that the magnetic phases present in the material were generally highly susceptible.

The carbon and iron concentrations of the product derived from each fraction are presented in Table 6.1.

Carbon ash fraction (μm)	Carbon (%)	Iron (%)
>3350	82.1	1.45
3350-2000	60.8	0.66
2000-1000	80.6	0.47
1000-500	84.0	0.28
500-75	80.0	0.50
75-0	69.8	2.14
Bulk (after 5 passes)	80.9	3.41

Table 6.1 Dry magnetic separation of carbon ash fractions

The carbon concentration of the magnetically separated fractions were generally found to be greater than 80% with the exception of the finest size fraction and also the

3350-2000 μm sample. The low carbon concentration in this fraction was thought to be due to the presence of refractory (non-magnetic) material in the sample since the associated iron concentration of the sample was low (0.66%). The carbon concentration of the $<75 \mu\text{m}$ size fraction was slightly lower at 69.8% with a higher associated iron content of 2.1%. The less effective removal of iron from the fine fraction could be explained by the difficulties encountered in forming a mono-layer of material on the conveyor belt which might have led to physical entrainment of magnetic phases. Re-passing the fraction through the separator improved the removal of magnetic phases by presenting the particles in a different orientation on each pass. It was found that repeated passing of the fractions caused slightly more material to report to the magnetic process stream however the majority was removed during the first pass. The exception to this was in the treatment of the bulk sample.

Separation of the bulk sample resulted in a product with a carbon concentration of 80.9% and an iron concentration of 3.41%. The magnetic separation of the bulk sample was not as affective in removing the iron content with a single pass since it was observed that magnetic material was often trapped under non-magnetic material on the conveyor. By increasing the speed of the conveyor and maintaining a constant feed from the hopper a thinner layer of material was presented to the magnets resulting in less physical entrainment of magnetic phases. However, the increased belt speed also meant that the throughput time was reduced which might result in a less effective separation. Increasing the number of passes compensated for the reduced throughput time. A total of five passes were conducted on the bulk sample, no further magnetic material was removed on the fifth pass.

The result of a magnetic separation conducted on the aged sample containing visible by-products of iron corrosion is shown in Table 6.2. This sample was also subject to five passes.

	Carbon (%)	Iron (%)
Older bulk sample	65.4	14.2

Table 6.2 Dry magnetic separation of 'aged' carbon ash

The carbon content of a freshly collected and separated bulk sample (80.9%) was significantly higher than that generated by separation of an aged sample (65.4%). There are two main mechanisms that might account for the increased concentration of iron in the product generated by the separation of the aged sample. As identified in Chapter 5 the steel wire in the carbon ash breaks down forming agglomerated iron-carbon particles during ageing. The conversion of highly magnetic, and well-liberated, steel wire pieces to less magnetically susceptible poorly liberated mineral phases combine to reduce the carbon concentration of the product. The formation of mixed carbon-magnetic phases is thought to be the main problem in the separation of the aged sample since phases such as goethite, although weakly magnetic, can still be recovered through magnetic separation (Svoboda, 1987). The lower overall magnetic susceptibility of mixed phase particles caused more iron to report to the product due to insufficient attraction to the magnets. The presence of mixed particles in the fresh samples also caused significant concentrations of carbon to report to the magnetic fractions, see Figure 5.19.

6.1.1.3 Summary

The dry magnetic separation of carbon ash demonstrated that a product with a carbon concentration of greater than 80% could be generated through the removal of magnetic material present in the samples. The age of the sample was found to be a major factor in the effectiveness of the separation. Samples that were dried within hours of collection generated a product with higher carbon concentration (and lower iron concentration) in comparison with a sample that had only been dried days after collection.

This trial was carried out on a completely dry sample using a dry magnetic separator. Since the ash/wire material is produced by the combustion units with a high moisture content a wet separation process might have been used. Wet systems, where the feed

material is presented in the form of a slurry, have several advantages over dry systems including reduced dust hazard and good separation of fine material through reduced physical entrainment (Svoboda, 1987). However, the final product stream is likely to require drying at some stage prior to re-use meaning either a wet and dry system could be used. The use of a pilot scale dry magnetic separator is investigated in Chapter 8.

6.1.2 Froth flotation

Flotation is a process for separating valuable solid raw material from waste based on the differences in the surface properties of raw materials (Lynch et al. 1981). The process is used in coal preparation to remove a large proportion of ash forming minerals. Coal is naturally hydrophobic (water repellent) whereas clay and many other minerals associated with coal are hydrophilic (readily wetted by water). When air is bubbled into a mixture of liberated hydrophilic and hydrophobic particles suspended in water, the hydrophobic particles will tend to adhere to the air bubbles. Provided the combined density of the particle plus the air bubble is less than the density of the water it will float to the surface forming a froth, which is then removed and becomes the product. Material that is not floated remains in the slurry and forms the tailings.

In order for a mineral to be floated an air bubble must be able to attach to a particle and lift it to the water surface. For this reason the flotation process is usually only applicable to relatively fine particles (<0.5 mm) as the adhesion between the bubble and larger particles may not be sufficient and the bubble may separate from the particle prior to reaching the surface. The successful flotation of fine coal particles has previously been achieved with a mechanical-type cell on particles as small as $12\ \mu\text{m}$ although the selectivity decreased with decreasing particle size (Tsai, 1985).

All minerals are classified into two main groups, polar and non-polar. Non-polar minerals are composed of weak covalent bonds or Van der Waals forces and the surfaces do not readily attach to water and hence are hydrophobic. Non-polar minerals include graphite, sulphur, diamond and coal (Wills, 1997). Polar type minerals exhibit strong covalent surface or ionic bonding which react strongly with water molecules making them naturally hydrophilic. The polar group of minerals is then sub-divided

into groups sorted by the magnitude of the polarity. Many non-polar minerals can be rendered hydrophobic, and hence floatable, through the addition of chemicals known as collectors. Other reagents termed 'frothers' may be dissolved in the slurry to impart the ability of the floated material to form a stable froth (Lynch et al. 1981).

A simple froth flotation experiment was designed to determine the potential of the technique in separating mineral matter from the carbon ash, hence upgrading the carbon concentration of the product. In theoretical operation froth flotation applied to a slurry of carbon ash would result in the carbon reporting to the product whilst other mineral phases (e.g. zincite, sphalerite and goethite) would not be floated and concentrate in the tailings. Prior to flotation the carbon ash was ground to enhance the liberation of mineral phases from carbon.

6.1.2.1 Method

The flotation trial was conducted using a Denver[®] Equipment Company laboratory scale flotation cell. A sample of carbon ash was collected from STR, dried in an oven (85°C, overnight) and then passed once through a Boxmag-Rapid[®] electromagnetic separator with the aim, primarily, to remove any steel wire. The non-magnetic carbon ash phase was then ground in a ball mill to enhance the liberation of contaminant phases from the carbon matrix. Sub-samples of the ground product were retained for SEM analysis and to provide information on the properties of the feed material. A 40% (by weight) slurry was prepared of carbon ash/water and placed into a ceramic ball mill with a steel charge for a period of 20 minutes under the conditions detailed in Table 6.3.

Mill internal dimensions	
length (mm)	300
diameter (mm)	190
grinding time (minutes)	20
Ball charge distribution	
large (25mm)	34
medium (19mm)	35
small (12mm)	75
total charge weight (kg)	2400
Feed material	
Weight (carbon ash g)	1333
Weight (water g)	2000
% solids w/w	40

Table 6.3 Ball mill conditions for carbon ash grinding prior to froth flotation

After the liberation stage the slurry was removed from the mill and placed into the flotation cell. The pulp sample was then agitated with a rotating impeller to retain the solids in suspension and Methyl-isobutyl-carbinol (MIBC) frothing agent added on a drop by drop basis using a pipette to aid the formation of a stable froth. Air was then introduced into the cell, which was sheared into a fine mist of bubbles by the impeller. The bubbles then rose to the pulp surface where particles attached to the bubbles were removed as the froth and scraped into a tray. Initially the froth formed at the slurry surface was unstable. It quickly broke down causing floated material to return to the slurry. A stable froth was formed through the addition of further MIBC, which was added with the airflow turned off to allow the reagent to mix with the slurry. Samples of the froth were scraped from the pulp surface into a container and dried in an oven at 85°C in preparation for analysis. Flotation continued until no further froth was produced at which point a sample of the tailings was taken by removing the water with a pressure filter and drying the filter cake along with the froth sample. Once dry a portion of each sample was riffled from the whole sample and powdered in a Tema[®] mill prior to chemical analysis. Samples of the feed, froth and tailings were analysed for carbon and sulphur concentration using the methods described in Chapter 4.

6.1.2.2 Results & discussion

The results of the carbon and sulphur analysis of the feed, froth and tailings are presented in Table 6.4.

	Carbon (%)	Sulphur (%)
Feed	78.2	1.6
Froth	78.6	1.7
Tailings	72.9	1.6

Table 6.4 Froth flotation results

The results show that the carbon concentration of the flotation product (78.6%) was similar to that of the feed material (78.2%). The tailings (72.9%) had a slightly lower carbon concentration than the feed. The sulphur concentration was uniform across all of the samples. This indicated that the contaminants were being carried over into the froth along with the carbon phase. The association of contaminants with the carbon product after grinding was investigated with the SEM. A polished sample of the flotation product was prepared using the method described in Section 5.2.3.2 and is presented in Figure 6.1.

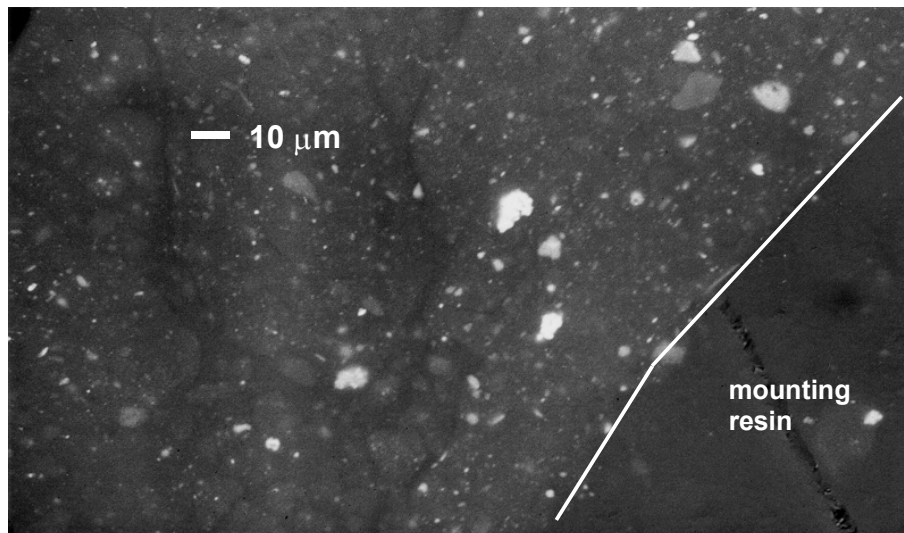


Figure 6.1 Polished section of froth flotation product (backscatter)

Interpretation of the SEM investigation of the sample was complicated due to smearing of the particle boundaries during polishing. However, the analysis showed

that small, <10 μm , metallic-based phases were locked inside the carbon matrix and hence reported to the flotation product. This indicated that the phases were not effectively liberated during ball milling, which might account for the carry over of contaminants in the froth. This was investigated by analysing a non-polished sample of the ground feed sample. Images of a typical area of the sample were collected with the secondary electron detector (see Figure 6.2), and the same sample region at a similar magnification using the backscattered electron detector in Figure 6.3. Contrast in the image collected with the secondary electron detector was as a result of sample topography whilst the contrast in the backscattered image was mainly due to the mean atomic number of particles, carbon appears quite dull whilst most metallic phases are bright. The point marked 'X' in each image denotes the same point in each image.

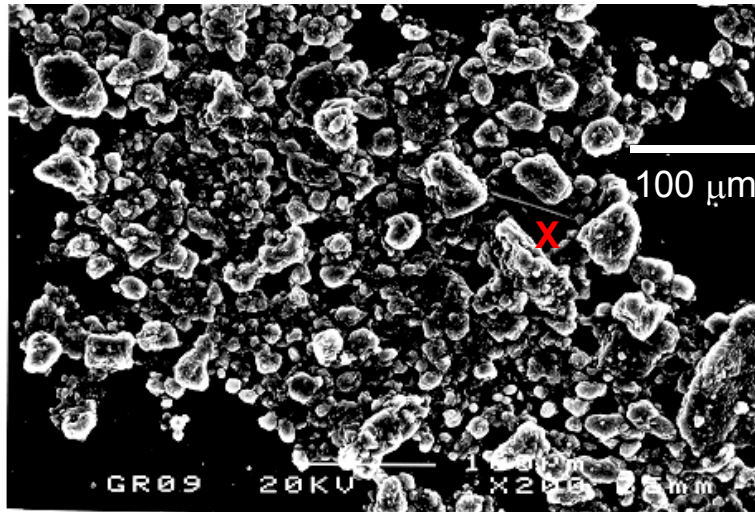


Figure 6.2 Flotation feed sample (secondary electron image)

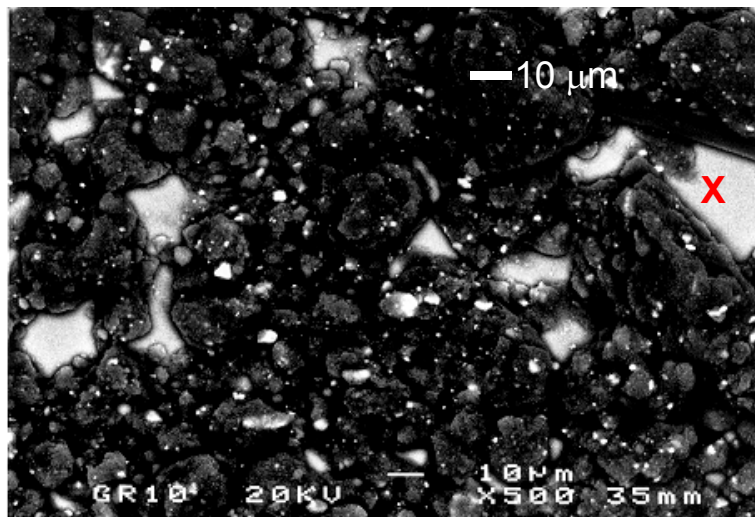


Figure 6.3 Flotation feed sample (backscattered electron image)

A general view of the flotation feed material shows that the maximum nominal particle size is approximately 100 μm , although the majority of the material was significantly finer. The particles appear to be discrete with no signs of re-agglomeration. With the same sample area viewed with the backscattered electron detector the distribution and association of metallic phases can be determined. Metallic phases are visible all over the particle surfaces, with most particles having a metallic association, very few discrete metallic phases were observed in the sample as many would have been removed during magnetic separation. From Figure 6.3 it can be seen that, if the region was assumed to be representative, all of the non-carbon

phases present in the feed sample were $<10\ \mu\text{m}$ and most were $<5\ \mu\text{m}$. Spot EDX analysis on a different region of the sample revealed the metallic associations consisted mainly of iron and zinc in both mixed phases and single phases (mainly iron) as seen previously in the characterisation chapter.

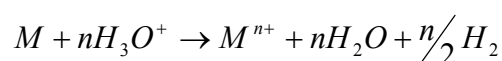
The dispersed metallic associations within the carbon phase may account for the carry over of contaminants into the flotation product. It also indicates that the grinding stage was not effective in liberating the phases and that the feed material might need to be significantly finer for effective separation using conventional flotation.

6.1.3 Acid demineralisation

Dry magnetic separation and froth flotation are essentially physical separation processes that rely on the physical liberation of contaminant and product phases. To test the performance of a chemically based separation system in reducing the non-carbon content of the carbon ash an acid leach test was carried out. In this process the non-desirable (ash) content of the carbon ash is drawn into solution resulting, theoretically, in a purer carbon product. This is essentially a partial digestion of the sample as opposed to the total analysis carried out previously utilising a microwave digestion technique. A leaching process has previously been applied to a carbon product derived from a tyre pyrolysis process and it was found to be efficient in reducing the ash content (Chaala et al. 1996). This involved a leach process consisting of both an acid and a base step resulting in a carbon product of 93.9% which was generated from an 80.4% starting material. This treatment process was thought to expand the range of utilisation of the product. Demineralisation processes have also been applied to coals, where the mineral matter has a detrimental environmental effect on the utilisation of the coal for combustion purposes (Mukherjee and Borthakur, 2001). Acid demineralisation is also employed in the production of ultra clean coals where the mineral matter is reduced to an extent ($<0.1\%$) that the material could be used to produce a wide range of fuels and chemicals (Steel and Patrick, 2001).

6.1.3.1 Method

An acid leach test was carried out on a sample of carbon ash to assess the ability of the process to remove undesirable ash phases from the carbon matrix. Hydrochloric acid (HCl) was selected as the leaching medium due to its low price and ability to leach most metallic elements. Similarly sulphuric acid (H₂SO₄) could have been used although the presence of sulphur compounds might have complicated subsequent sulphur analysis. An oxidising acid, such as nitric acid, could also have been used although it is possible that it may attack the carbon phase as well as the mineral phases. The general reaction of metals with aqueous hydrochloric acid is presented in Equation 6.1.



Equation 6.1 General reaction of metals with hydrochloric acid

Two acid concentrations were used in the test at two different experimental conditions. A 1M HCl leach was conducted at room temperature whilst a 5M HCl leach was conducted at 90-100°C on a hotplate. The acid concentrations and leaching conditions were chosen to provide information on the leaching process at two extreme conditions, in this initial study the role of acid temperature and concentration was not investigated separately. Heating the acid might improve the penetration of the acid into the carbon ash material. The physical availability of ash phases to leaching was determined by leaching the material in two states, in the original particle size distribution and in a powdered form.

A sample of ash/wire was collected from STR and the bushy wire removed by hand. The remaining material was then dried and passed through a magnetic separator using the method as described previously. The sample was then split into two; one half was powdered in a Tema[®] mill so that all of the material passed through a 75 µm wire mesh screen. The remaining material was retained in its original size distribution. Chemical analysis was then carried out on a sub-sample of the powdered material to provide information on the starting concentrations of the sample prior to the acid

leach. The treatment scheme for each sample subjected to the acid leach test is presented in Figure 6.4.

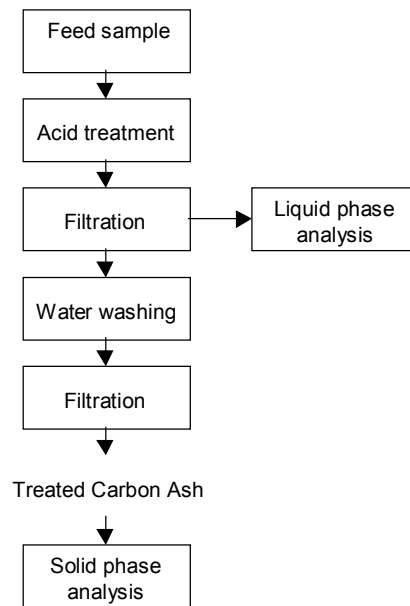


Figure 6.4 Acid treatment of carbon ash

The acid leach was carried out on a total of three samples, all of which were conducted in duplicate. The carbon ash sample was leached in the two preparation states. An analytical coal standard (used previously as a sulphur analytical standard) was leached alongside the carbon ash samples to detect any experimental error, particularly in the analysis conducted on the post leach samples.

Approximately 5 g of the each sample was weighed accurately into a 200 ml conical flask. A 100 ml volume of the relevant acid concentration was then added to each flask and the contents gently stirred to ensure the sample was completely wetted by the acid. The large volume of acid used in comparison with the low mass of solids ensured that the acid would be in excess so would not limit the leaching. The samples being leached at 90-100°C were placed onto a hotplate located in a fume cupboard. The room temperature samples were also placed in a fume cupboard. The samples were then leached for a period of 4 hours, a length of time that was considered to be long enough not to limit the leaching process.

After 4 hours the post leach samples were separated from the acid by filtration through a Whatman[®] 542 filter paper. It was necessary to allow the hot leaches to cool prior to filtration as the hot acid corroded the paper. The cooling procedure might have allowed some compounds to drop out of solution and form a precipitate, which would then be present in the solid phase after filtration. Although no precipitates were observed during the course of the experiment. The post-leach acid solution was retained and made up to a 200 ml volume with distilled water for liquid phase analysis (ICP-AES). The post leach solid samples were rinsed with large volumes of distilled water to remove as much of the residual acid as possible. This process was carried out by placing the solid sample into a centrifuge tube with water and repeatedly centrifuging with the water being replaced each time until the measured pH of the used wash water was similar to that of the feed water. The samples were then oven dried overnight at a temperature of 105°C in preparation for solid phase (carbon and sulphur) analysis.

Prior to carbon and sulphur analysis being carried out on the samples the non-powdered post leach samples had to be powdered. This was carried out using a pestle and mortar as the low sample mass meant that the Tema[®] mill could not be used. The solid samples were then analysed using the methods defined in Chapter 4.

6.1.3.2 Results and discussion

The results of the carbon and sulphur determinations on the pre and post leach material have been presented in Figure 6.5 and Figure 6.6. The full results can be found in Appendix 2.

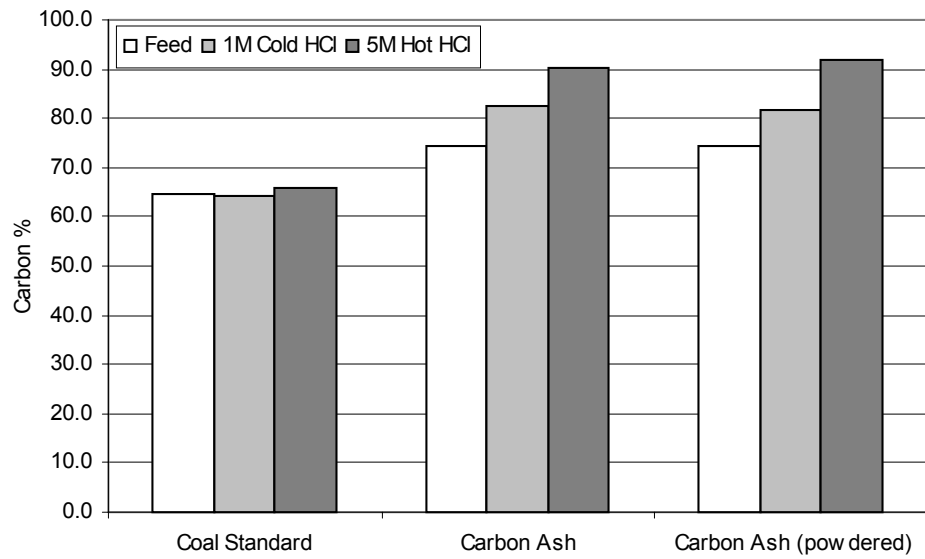


Figure 6.5 Carbon concentration of samples during HCl acid leach experiment

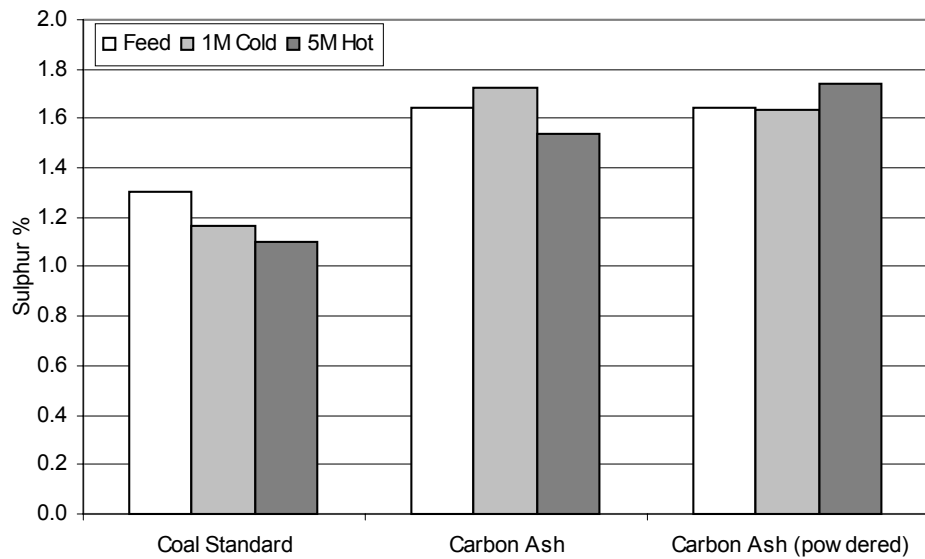


Figure 6.6 Sulphur concentration of samples during HCl acid leach experiment

In the leaching experiment the feed sample contained 74.5% carbon and 1.6% sulphur. After the application of the acid leach to the samples the carbon concentration of the remaining solids was significantly increased, indicating the removal of non-carbon phases by the leachant. The influence of sample preparation

appears to be minimal with similar carbon concentrations gained for the two sample types at both leaching conditions. The highest carbon concentration achieved during the experiment was 91.9%. This was obtained with a 5M hot HCl leach on a powdered carbon ash sample. The 1M, room temperature, leach on the same sample generated a carbon product of 81.9% carbon.

From Figure 6.6 it can be seen that the sulphur content in the post leach material was similar to the starting concentration in the carbon ash for each of the leach test conditions. The acid leach, at all conditions, appears to have had an unmeasurable effect on the removal of sulphur from the sample. During the mixing of the acid with the samples the odour of rotten eggs was detected, probably caused by the production of gaseous hydrogen sulphide. This is an indication that some sulphur was being removed from the samples.

The HCl leach on the coal was expected to have little impact on the carbon and sulphur content of the sample, as the mineral/metallic content is low in comparison with the carbon ash. The majority of the sulphur in the coal sample is bound in the organic phase and in the form of pyrite (iron sulphide), neither of which will be effected by the HCl leach. The small reduction in the sulphur content of the coal, and subsequent increase in carbon concentration, may have occurred as a result of the dissolution of a trace mineral phase such as zinc sulphide. The main purpose of the coal standard was to determine the effect of inadequate washing of the samples prior to analysis. The similar levels of carbon and sulphur measured in the post leach material when compared to the feed sample indicates that no interfering elements remain associated with the solid sample as a result of the leach and the analysis can be assumed to be accurate. If the carbon ash is assumed to behave similarly during the leach then the post leach analysis of the material should also be accurate.

ICP-AES analysis of the leachant was used to quantitatively measure the elements drawn into solution from the carbon ash. The concentrations of each element in the carbon ash was then compared to the analysis of the same feed sample, see Table 6.5, by the total digestion method described in Chapter 4.

Element	Concentration ($\times 10^4$ ppm)
Zn	3.7
Fe	3.4
Ca	0.98
Al	0.2
Mg	0.11
Ti	0.021
Cu	0.020
Mn	0.019
Pb	0.008
Ba	0.002
Cd	<LOD
Ni	<LOD
Cr	<LOD

Table 6.5 Element concentration in feed material by total digestion

The relative percentage of each element extracted from the carbon ash can then be calculated, this data is presented in Figure 6.7.

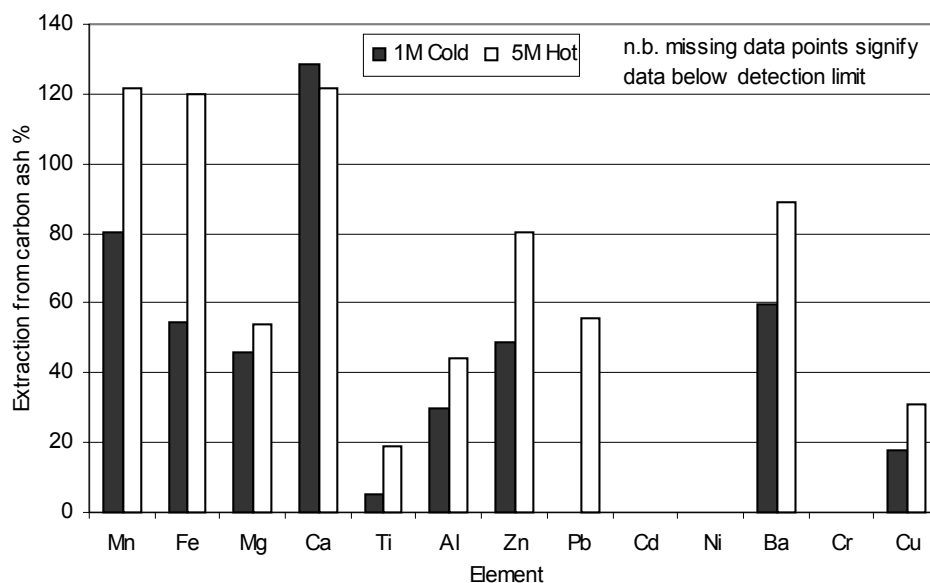


Figure 6.7 Element extraction from carbon ash during HCl acid leaches

It should be noted that expressing the leachability of elements as a quotient between two separate analytical methods can only be used as an approximation. Whilst each leaching technique (total digestion and hydrochloric acid) is capable of producing precise data within the same method, the true accuracy of either method for the

analysis of the carbon ash is not known. This might partly explain the extractions in excess of 100% presented in Figure 6.7 although they could also be attributed to non-homogeneity of the sample. In general it can be seen that the more aggressive leach extracted more of each element from the carbon ash. Elements such as manganese, iron and calcium appear to be completely removed from the sample. Zinc is partially removed from the carbon ash; approximately 80% was extracted with the hot HCl leach. During the characterisation of the carbon ash zinc was detected in three mineral phases, zinc oxide and two forms of zinc sulphide. Since no removal of sulphur from the carbon ash was measured it is possible that only the oxide mineral was leached from the material. However this is unlikely, as the zinc-sulphide minerals are soluble in acid and the reaction results in the production of hydrogen sulphide. This may indicate that the majority of the sulphur in the carbon ash is present as an alternative, acid-insoluble form.

Copper and titanium appear to be minimally extracted from the carbon ash although the elements only exist in the feed material in low concentrations so do not significantly contribute to the ash content. Cadmium, nickel and chrome were not measurable in the leachate solutions.

The results of the leaching test show that the process has potential for the production of a high carbon concentrate. However, a relatively aggressive leaching condition (5M Hot HCl) was required to generate a carbon concentrate in excess of 90% and this might limit the application of the process. This product is compared to a virgin black that is used in tyre production and also a tyre pyrolysis derived black treated with 1M H_2SO_4 and 5M NaOH in Table 6.6.

Carbon black	Element (wt. %)					
	C	H	O	S	N	Ash
CB _p - treated (Chaala et al. 1996)	93.0	0.5	0.3	2.3	0.8	3.1
N539 - commercial	98.2	0.4	0.4	0.8	0.0	0.2
Carbon Ash - treated (n.a. - not analysed)	91.9	n.a.	n.a.	1.7	n.a.	n.a.

Table 6.6 Bulk composition of recycled and commercial carbon blacks

It can be seen that although the properties of the acid leached carbon ash compares well with the treated pyrolysed material, the carbon concentration is significantly lower in comparison with the virgin black. The sulphur concentration in the carbon ash is also significantly higher than in the virgin carbon black.

Other than sulphur the major non-desirable phase remaining in the treated carbon ash is likely to be silicon based, this phase is essentially insoluble in the hydrochloric acid leach. The extent to which the silicon is removed from the carbon ash during the leaching could not be measured due to the difficulties associated with the analysis of silicon by ICP-AES. The removal of the silicon phase would probably require the use of a hydrofluoric acid and elevated temperatures. An attempt was made to detect the mineral phases that remained in the treated carbon ash using the X-ray diffraction technique described previously. However problems were encountered in the preparation of the sample for analysis. The extremely high carbon content of the treated sample meant that after low temperature ashing insufficient material remained for the analysis. During ashing the formation of a salt crust on the material surface was observed indicating incomplete washing of the sample. For these reasons XRD analysis was not conducted, as accurate results were unlikely to be obtained.

Optimisation of the leaching conditions through the adjustment of process variables such as time, temperature and acid concentration might improve the removal of ash phases from the carbon ash. A second processing stage utilising a base leach might improve the removal of amphoteric (soluble in acid and bases) phases, which are either unaffected or partially treated during the acid leach. For example, zinc oxide dissolves in acid, forming salts, and in bases, forming zincates (zinc hydroxides).

Aluminium behaves in a similar manner (Greenwood and Earnshaw, 1997). The results of the leach test indicate that not all of the zinc was removed from the sample. Some of the remaining zinc may be in the form of zinc oxide therefore a base leaching stage might have been beneficial. It would also be important to determine that the leaching process does not adversely affect the physical properties of the treated carbon ash since factors such as particle size, shape and porosity are important considerations in the final market for the product. This could be achieved through the use of standard techniques available for the measurement of such properties in carbon blacks.

The experiment demonstrated that a simple acid leach process was capable of producing a high carbon concentrate. With further refinement the process might possibly achieve a product specification with bulk properties similar to that of carbon black. This would require a hydrofluoric acid leach stage to remove the silica phase that, although expensive, might be economically viable if the product could be sold in the right market (i.e. as a carbon black). The removal of sulphur from the sample would require further investigation.

6.2 Processing of bushy wire

Characterisation of the wire phase in the ash/wire concluded that the sulphur contamination was due to surface deposits of carbon ash. Removing the surface coating was effective in reducing the sulphur concentration of the potential steel product to a level below the 0.04% required by re-processors. Through recreating the sanding action used to clean the wire samples in the form of a process a low sulphur concentration steel product should be created. The sanding action used abrasion between the sand particles on the sandpaper and surface deposits of carbon ash to dissociate the sulphur bearing ash from the steel wire. The development of the cleaning mechanism used in the characterisation study was attempted through the mineral processing technique of attrition scrubbing.

6.2.1 Attrition scrubbing

Attrition scrubbing has been previously been used in mineral processing operations to separate clay from the surface of a calcite gangue material and is described in Hassan and Abdel-Khalek (1998). In this application the cleaned clay was the product. The technique has also been used applied to the washing of contaminated soils. The removal of diesel contamination from the surface of sand particles has also been investigated through the use of attrition scrubbing (Feng et al. 2001). In each case the basis of the technique is to promote particle-particle contact, usually by stirring the material, as a slurry with water, which causes contaminants to be knocked from the surface of the gangue. The two phases can then be separated. A laboratory scale trial was conducted to determine the effectiveness of attrition scrubbing applied to the bushy wire material. In this particular application the surface of the steel required cleaning, by removing the carbon ash coating. Sand was used as the primary medium to abrade the wire surface but attrition would also occur due to wire on wire contact. Water was added to form a slurry and to assist the flow of material.

6.2.1.1 Method

Initial attrition scrubbing tests were carried using a Wemco[®] laboratory scale 1 litre attrition cell as pictured in Figure 6.8. When operating the impeller (steel covered in a

plastic coating) rotates inside the cell to provide the energy required to promote the attrition action.



Figure 6.8 Wemco[®] laboratory scale attrition cell

In order to be able to feed the bushy wire samples into the attrition cell the wire had to be reduced in size. A Retsch[®] cutting mill was used to reduce the intact beads to shorter lengths which were easier to handle. The reduction in length also reduced the risk of wire wrapping around the impeller during attrition. A 4 mm internal screen was fitted into the cutting mill which controlled the maximum wire length. Oversized lengths passing the screen were recycled through the mill.

Bushy wire for the attrition trial was collected from STR on the day of the test so that it could be operated on in the 'as produced' state. Wire was fed into the cutting mill, after shaking off the loosely associated carbon ash. Due to the arrangement of the feed chute of the cutting mill the intact beads had to be folded and in some cases pre-cut with wire cutters in order to feed them into the cutting chamber. It was noticed during the cutting operation that a considerable amount of carbon ash was dissociated from the bushy wire resulting in the creation of a fine black powder as well as the <4 mm (shredded) wire product. This was mainly due to the breaking up of the multiple core wire and subsequent liberation of previously trapped deposits of carbon ash. The carbon ash dust was not included in the feed sample for attrition scrubbing, it was

separated from the wire by passing the shredded material through a 500 µm wire mesh sieve. The large amount of energy imparted to the wire during cutting generated a significant amount of heat, driving off any moisture that may have been present in the freshly collected bushy wire samples. This meant that the shredded wire did not require further drying to stabilise the sample prior to attrition scrubbing. Approximately 3 kg of bushy wire was passed through the cutting mill to produce a feed material. Samples of the shredded wire were retained for analysis to provide a starting sulphur concentration for the attrition tests.

The bushy wire sample initially occupied most of the volume of a 20 litre sample bucket but this was reduced to approximately 1 litre after cutting to <4 mm. The size reduction of the bushy wire therefore had the added advantage of increasing the bulk density of the material making storage, transportation and handling easier. The attrition medium used in the tests was a widely available sharp sand, the size distribution of the sand can be found in Appendix 2.

Two simple initial attrition tests were carried out. For each test sub-samples of sand and shredded wire were riffled from the main stock and loaded into the attrition cell along with the water. Fresh sand was used for each test. The cell was then raised so that the impeller was able to stir the mixture, and the lid placed on top to retain any escaping material. The impeller was set to rotate at 1000 rpm and was then switched on for the period designated to each test as shown in Table 6.7.

	Test number	
	1	2
Water (ml)	278.5	278.5
Sand (g)	446	439
Wire (g)	204	211
Impeller speed (rpm)	1000	1000
Time (mins)	6	6 (total)

Table 6.7 Attrition cell conditions

For both tests the overall solids content of the slurry was set at 70% (by weight) with the wire/sand ratio set at approximately 1:2. The solids concentration of the slurry was

selected on the basis of observations made of a range of prepared slurries in the attrition cell. When the overall solids concentration was too low the number of particle-particle contacts was reduced, when the solids concentration was too high the slurry became difficult to stir which resulted in limited attrition scrubbing as the slurry moved around the cell as one solid mass. The weights of each of the individual feed components used in each test are also shown in Table 6.7.

In Test 1 the sample was treated for a period of 6 minutes. On completion of the test the wire was separated from the sand and water by passing the mixture over a 1000 μm wire mesh screen, the wire was collected on the screen whilst the sand passed through with the water. The wire was then gently rinsed with extra water to remove any associated sand in preparation for sulphur analysis.

The attrition conditions were almost identical for Test 2 but observations of the process were made at intervals during the test, after 2, 4 and 6 minutes. At each inspection the impeller was stopped and the cell lid removed to allow examination of the wire/water/sand mixture. After 6 minutes of treatment a sub-sample of the attrited wire was split by hand into separate fine wire and coarse wire samples for analysis. This would determine if the fine wire splinters were being cleaned as effectively as the coarser wire.

Wire samples from both tests were oven dried at 85°C overnight prior to despatch to LSM for sulphur analysis. Sub samples of wire were also retained for SEM analysis to examine the wire surface at high magnification.

6.2.1.2 Results & discussion

Test 1 observations

During screening of the sand and water from the attrited wire following Test 1 it was found that the slurry had a black colouration indicating the presence of carbon ash. The post attrition wire was visibly cleaner with respect to surface deposits of carbon ash when compared to the feed wire. Immediately after attrition the wire surface had a polished appearance although this quickly dulled.

Test 2 observations

After 2 minutes attrition the inspection revealed that some of the wire visible at the slurry surface was already being scrubbed to a similar extent to that found at the end of Test 2. After a total of 4 minutes attrition it was noticed that a large proportion of the fine wire splinters present in the feed sample had been displaced to the surface of the cell contents potentially lowering the scrubbing of the phase. By digging through the contents of the cell it was found that no wire had wrapped around the impeller blades indicating that the feed wire had been cut sufficiently short.

The sulphur content of the wire samples at each stage of the attrition process is presented in Table 6.8. Where duplicate analysis was carried out on the samples the results have been averaged and this figure is presented, the full results are presented in Appendix 2.

Wire samples	Sulphur (%)
As collected	0.15-0.70
Cutting to <4 mm	0.066
Cut and screened (feed to attrition tests)	0.058
Attrition test 1	0.038
Attrition test 2 - fine wire	0.048
Attrition test 2 - coarse wire	0.027

Table 6.8 Sulphur content of steel wire throughout attrition process

The liberation of carbon ash from the wire during the wire cutting stage can be seen to reduce the sulphur concentration of the material to 0.066%. By screening to remove loosely attached surface deposits from the <4 mm shredded product the sulphur content was reduced further to 0.058%. This was the material used as the feed in the attrition tests. The levels of sulphur in the steel before, during and after the attrition process have been summarised in Figure 6.9.

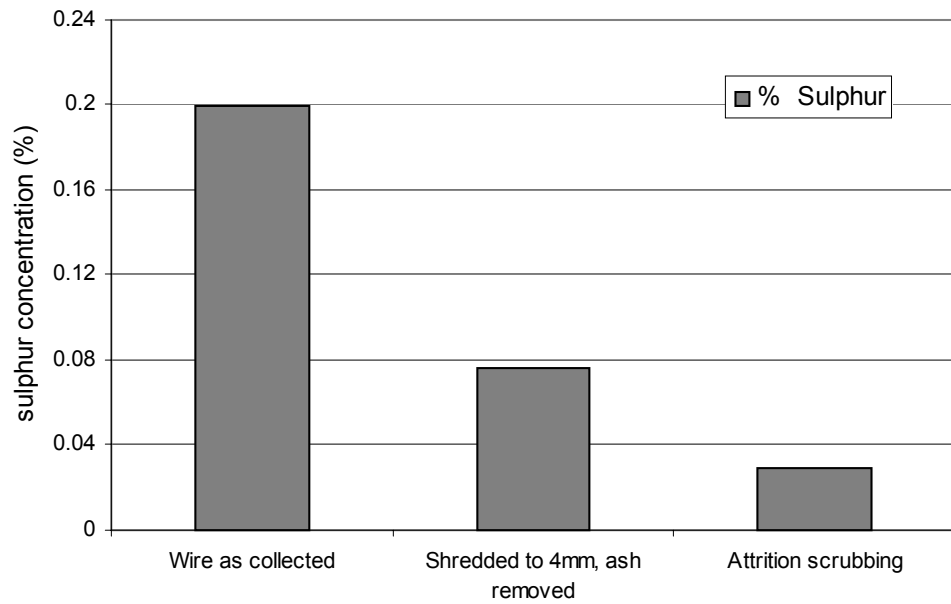


Figure 6.9 Attrition scrubbing trial - sulphur content of steel wire during process

From the results it can be seen that the attrition process was effective in lowering the sulphur content of the steel to below the 0.04% threshold. The results from attrition Test 2 confirmed that the fine wire splinters displaced to the surface of the sand/wire/water mixture were not cleaned as effectively as the remainder of the wire. The 'fine wire only' sample contained 0.048% sulphur whilst the 'coarse wire only' sample contained 0.027% sulphur. This indicated that the displacement of the fine wire to the top of the cell inhibited the cleaning of the fine wire. However the overall sulphur concentration of the wire from Test 1 (representative sample of coarse and fine wire) was below the 0.04% threshold.

The effectiveness of the attrition scrubbing process was further investigated with the SEM. An image of the steel wire cut to <4 mm is shown in Figure 6.10.



Figure 6.10 Wire - cut and screened (0.066% sulphur)

From Figure 6.10 it can be seen that after passing through the cutting mill, and removal of the carbon ash dust, surface deposits of carbon ash remain associated with the wire surface. These deposits account for a proportion of the sulphur content. A post attrition wire sample is presented in Figure 6.11.



Figure 6.11 Wire - post attrition (0.027% sulphur)

The wire surface can be seen to be almost entirely free from carbon ash deposits and subsequently has a reduced sulphur concentration (0.027%). Closer inspection of the wire surface reveals scouring marks produced by the sand abrading on the steel surface.

6.2.1.3 Summary

The sulphur analysis combined with the SEM images clearly show that the attrition process was effective in removing the surface coating of carbon ash thereby lowering the sulphur content of the steel product. The initial tests have shown the process to be capable of achieving the specified levels of 0.04% sulphur. Although the coarser wire pieces were cleaned more effectively than the fine wire the overall contribution of the two main wire forms to the material resulted in a product suitable for reprocessing. The original bushy wire had a very low bulk density and was difficult to handle. Reducing the wire length in a cutting mill had the added advantage of increasing the bulk density making it easier to handle, store and transport.

The process of the conversion of the high sulphur concentration bushy wire to a low sulphur concentration <4 mm product is summarised in Figure 6.12.

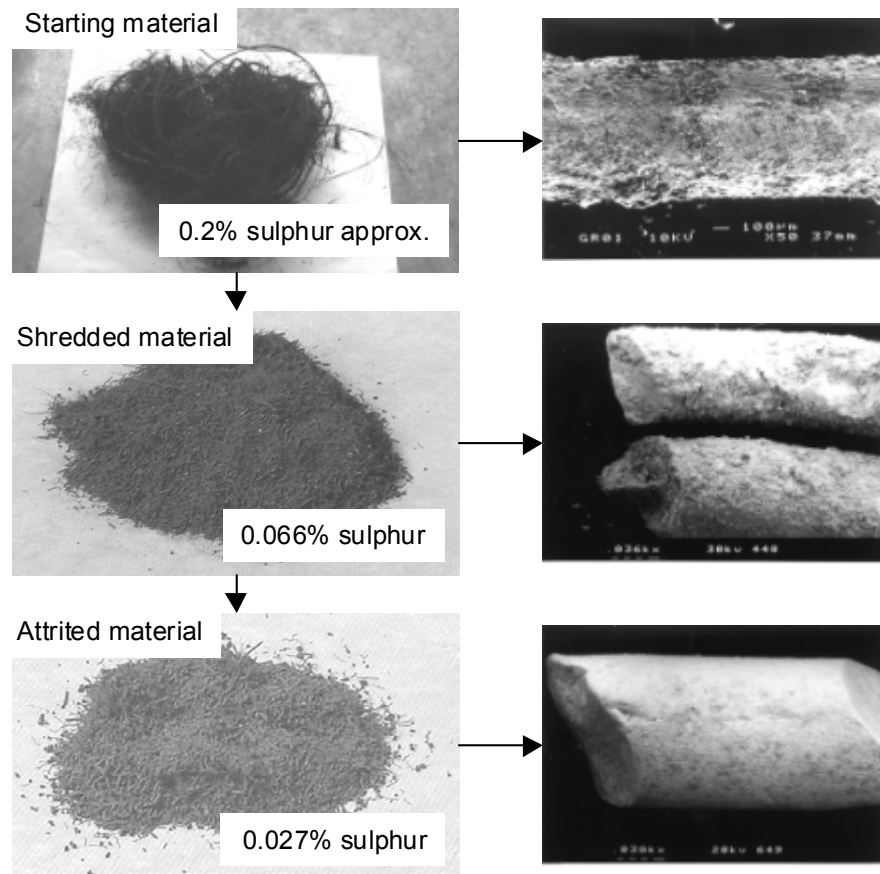


Figure 6.12 Attrition of bushy wire - process summary

The initial test work was carried out at a single solids loading rate and with a single wire/sand ratio. The process might be further improved by altering the process conditions, this is investigated during an attrition optimisation experiment described in Chapter 8.

6.3 Separation studies summary

The production of saleable products from the ash/wire phase was investigated through the application of a range of techniques. The carbon ash and bushy wire phases of the material were treated separately since it was likely to represent the highest value route for potential products. The carbon concentration of the carbon ash derived product was directly linked to value whilst the sulphur content of the steel controlled its market value.

Dry magnetic separation of the carbon ash resulted in a material with a carbon concentration of 80.9%, mainly through the removal of iron phases. A conventional flotation methodology was found to be unsuitable for processing the carbon ash mainly due to the high dispersion of the contaminant phases in the carbon matrix. An acid demineralisation process generated a 92% carbon product but would require further development to produce a material more closely related to the specification of high-value carbon blacks.

The application of an attrition scrubbing technique to the bushy wire was found to recreate the sanding action identified during the wire characterisation study. By scrubbing the carbon ash deposits from the wire surface the attrition process was able to generate a wire product with a sulphur content below that specified by steel reprocessors.

The products generated from the ash/wire material through laboratory scale attrition scrubbing and magnetic separation were supplied to potential purchasers for assessment.

Product Uses and Assessment

7.1 Introduction

Following the characterisation phase of this study potential products were identified in the STR waste stream. Processes were then developed to separate and concentrate these products from the ash/wire material during the separation studies. The approximate product specifications were already known, i.e. low sulphur concentration in steel and high carbon concentration in carbon ash. Details of the main characteristics of the products generated during the separation studies were then supplied to a wide range of potential purchasers who would be able to compare the material properties to their own requirements and determine suitability. Feedback from the purchasers could then be used to modify the separation processes to produce a more suitable material, although any modifications to the process would have to be offset against the cost of production. It was important to be able to produce materials where the cost of production was less than the final market price of the product.

Time was a factor in the developments of potential products, particularly in the case of the carbon ash. It was important for STR to begin diverting as much ash/wire as possible away from landfill and towards product generation. For this reason the carbon product generated by dry magnetic separation was chosen as the material to market to purchasers. Investigations into the generation of more highly concentrated carbon products were continued and are discussed in Chapter 9. The attrited steel wire was put forward as the other marketable product derived from the ash/wire.

7.2 Products derived from carbon ash

High value carbon based products, such as carbon blacks, generally require carbon concentration in excess of 95%. Through the application of mineral processing techniques the separation study found that a carbon product with a concentration of approximately 80% could be generated. Although this concentration of carbon would command a lower market value the cost of production such a material would be considerably lower than that of more concentrated carbon phase such as that

generated through the acid leach process. The approximate market value of some carbon products is summarised in Table 7.1.

Product	Carbon concentration	Market price (£/tonne)
Secondary fuel	70-80%	£25-30**
Tyre grade carbon blacks	>98.5%	£434-700*
Specialist carbon blacks (e.g. colourant)	>99.5%	£558-930*

Table 7.1 Approximate market values of selected carbon based products *(Walters, 2002), ** (Bruce, 1999)

It can be seen that, at present, the product derived from carbon ash is relatively low in value compared to carbon blacks. However, it should be considered that since the carbon ash is essentially a waste material, the cost of the raw material is zero (ignoring the plant running costs). The only production costs would therefore be associated with the separation and concentration processes employed meaning that a relatively low market price for the material might be acceptable.

7.2.1 Britannia Zinc Ltd

Britannia Zinc Ltd (BZL) is a part of the Australian based mining and minerals group MIM Holdings Ltd. The plant, located at Avonmouth near Bristol, is a major producer of zinc and lead with cadmium and sulphuric acid as co-products. The zinc smelter used at the site is the largest in the world with daily inputs of 1100 tonnes of sinter, 400 tonnes of coke and 8 tonnes of tuyere injected secondary material.

The plant has previously received the zinc oxide by-product recovered from the baghouse filters in the STR incinerator. It was the intention of BZL to inject the carbon ash derived product along with the secondary materials through tuyeres into the smelter. The secondary materials usually consisted of fine furnace drosses and other plant dusts. The high concentration of carbon in the carbon ash was expected to be beneficial to the process by potentially reducing the demand for coke in the

process. The zinc concentration in the material was also expected to provide a further zinc source in the process.

Two 10 kg specimen carbon ash samples were provided to BZL for assessment. Both samples were chemically similar, having been generated by laboratory scale magnetic separation, but varied in the physical preparation. The samples were split from the magnetic separation product using a riffle. One half was retained at the original particle size distribution whilst the other half was powdered in a Tema[®] mill. The original size distribution would have been similar to that determined in the characterisation study as shown in Figure 5.8. It was found that the mill could accept a maximum charge of approximately 300-500 g for effective operation therefore the sample was ground in several batches which were then mixed together to form the sample. The objectives of milling the sample were to homogenise the sample with respect to the chemical properties and also to enable tuyere injection. Particle size analysis was not carried out on the sample prior to despatch to BZL. Both samples were supplied dry in separate sealed containers.

At BZL each sample was then subjected to a series of test procedures to determine the chemical properties and suitability for tuyere injection. The results of tuyere injection suitability tests carried out by BZL together with the minimum specifications are presented in Table 7.2. The burnout tests were conducted in a drop tube furnace whilst the size analysis was determined with dry sieving using wire mesh screens. The particle size distribution of the non-powdered sample was not carried out as it did not pass the burnout test.

	Burnout (%)	Material <75 µm (%)
BZL minimum specification	>50	80
Non-powdered	30	n.a.
Powdered	55	88

Table 7.2 Performance of carbon ash product against the BZL secondary fuel specification (n.a. - not analysed)

The powdered carbon ash sample achieved both the >50% burnout and the size distribution (specification 88% <75 µm) required for physical suitability for tuyere injection. The sample was also chemically suitable for the process, the full characterisation of the sample is presented in Table 5.5. At this stage it was decided that a larger sample would be required to carry out a full-scale trial. This would require a 100-200 tonne sample of carbon ash with similar physical and chemical properties to the powdered specimen sample. The production of such a sample was investigated and described in Chapter 8.

Additional product specifications identified by BZL included the requirement of the supplied material to have relatively consistent chemical properties over time. The most important of which was to maintain the carbon concentration of the supply in a relatively narrow band of 70-80% carbon. This was a quality control issue and would require addressing after the pilot-scale production of the material had been investigated.

7.3 Products derived from bushy wire

After the attrition process had been developed that enabled the sulphur concentration of the post combustion steel to be reduced to below 0.04%, a range of potential users were approached. Some had previously rejected bushy wire on the basis of the elevated sulphur content. A range of industrial steel users were supplied with 10 kg assessment samples, the outcome of discussions between STR and the companies is summarised below. The basic specification of the material supplied was a steel product consisting of <0.04% sulphur with a particle size of less than 4 mm.

During this phase of the study a market was also identified that was able to tolerate the higher sulphur levels in the untreated bushy wire, although this would probably command a lower market price.

7.3.1 British Steel

A sample of cleaned wire was supplied to British Steel (now Corus) for assessment in their laboratories at the Teeside Technology Centre. Their intention was to use the

recycled steel as a ladle coolant, which is used to control the cooling rate and hence physical properties of new steels. The main specifications for a product to be used as a ladle coolant are sulphur content and handleability. It was important for the material to be able to flow in a controllable and predictable manner so that it can easily be moved around a system.

In the <4 mm form the attrited wire was found to have a suitable sulphur concentration although the material was found to be an unsuitable shape for good flow characteristics. It was suggested by British Steel that a further size reduction of the steel, to create a more spherical particle shape, would be required to make the product suitable. A further size reduction of the product would probably be carried out after attrition and would be technically feasible. However further shredding of the wire would introduce significant added production costs, in part due to increased energy consumption. This increased cost would then have to be passed on to the purchaser.

7.3.2 Ervin Amasteel

Ervin Amasteel, a steel reprocessor based in the West Midlands, had previously rejected the STR bushy wire on the basis of elevated sulphur and phosphorus levels in the material, which were beyond the constraints of their system. The attrited material was found to be suitable in both physical handling and chemical characteristics and the company was willing to accept the material on a longer term contract basis.

7.3.3 Metabrasive

Metabrasive assessed the use of both attrited and untreated bushy wire material for reprocessing. Samples of bushy wire were pulled manually from the ash/wire heaps and packaged for transportation to Metabrasives plant located only a few miles away from STR in Wolverhampton. During a trial melt of the bushy wire it was found that the sulphur associated with carbon ash deposits on the bushy wire was not an issue for the system. The company was then willing to assess a larger sample of the wire which would take the form of approximately 10 tonnes of separated bushy wire which would be baled to reduce the bulk density. The production of such a sample is discussed in Chapter 8.

The bushy wire product would command a lower market value but would require relatively little processing except a primary separation of wire and carbon ash. The close proximity of the purchaser to the STR plant would keep transportation costs to a minimum.

7.4 Summary

Potential markets were identified for products derived from both the carbon ash and the bushy wire. A market for the magnetically concentrated carbon product was identified as a secondary fuel for use in a zinc smelter. The approximate market value of a product was suggested to be £25-30 per tonne as indicated in Table 7.1. In the form of the attrited product the bushy wire was expected to command a value of £30 per tonne (Hall, 2000). A lower value market was also identified for the wire in the original 'bushy' form.

By using the ash/wire disposal and cost information for a typical operational year, as presented previously in Figure 3.1, the revenue that might be generated through the sale of wire and carbon products can be estimated. The calculations assume 100% availability of the product phases within the ash/wire. The costs and revenues are summarised in Table 7.3.

	Disposal cost	Revenue from products
	£	£
Steel	165,000	
Carbon ash	292,000	
Water	381,000	
Attrited wire		390,000
Magnetically separated carbon		575,000
Total disposal cost	838,000	
Total revenue from products		965,000

Table 7.3 Revenue generated from the sale of ash/wire derived products

The total benefit of the generation of the products from the ash/wire waste stream would be a combination of the revenue and also the savings made from the diversion of waste from landfill.

The production of larger samples of carbon and wire products through the application of pilot scale equipment was then investigated.

8 Pilot Scale Test Work

8.1 Introduction

Initial characterisation of the ash/wire residue had identified the potential for the generation of two main products from the process stream at STR. A reduced sulphur steel product was generated from the bushy wire phase of the ash/wire attrition scrubbing and a high carbon concentrate product was generated from the carbon ash phase using dry magnetic separation.

In order to produce larger samples of the products for assessment by potential purchasers scale-up of the treatment processes was required. Large samples of separated bushy wire were required for size reduction prior to the optimisation and scale-up of attrition scrubbing. During this separation a 'wire free' portion of the ash/wire would also be generated which would form the basis of a carbon product. Pilot scale plant, of a capacity that would be similar to that utilised in a full-scale process, was employed with the following aims:

- Investigate the suitability of a dry magnetic separator in separating magnetic phases (mainly wire) from the ash/wire process stream.
- Generate large samples of bushy wire for optimisation and scale-up of attrition scrubbing.

Pilot scale test work was carried out on site at STR between October 1999 and March 2000. Analysis of samples produced by the operations was carried out at the University of Nottingham.

8.2 Dry magnetic separation of ash/wire

The carbon ash derived product found to be suitable for use as secondary fuel was generated using dry magnetic separation at laboratory scale. The bushy wire was removed manually and the feed sample was dried prior to the separation. At pilot scale the separation of the bushy wire and carbon ash was attempted directly from the ash/wire using a dry magnetic separator. The sample was not pre-dried, the

differences between the laboratory and pilot scale methods is summarised in Figure 8.1.

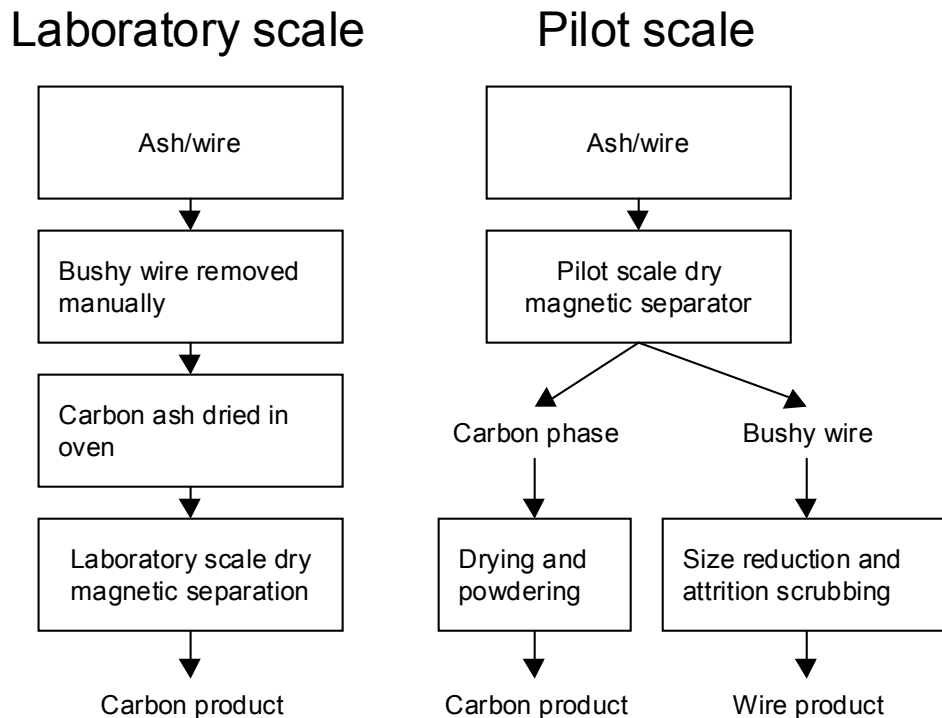


Figure 8.1 Laboratory and pilot scale generation of products

The separation of bushy wire from the ash/wire at pilot scale was attempted with a mobile magnetic separator brought on to the STR site. The separator consisted of a diesel driven variable speed (660 mm wide) v-profile conveyor fitted with a feed hopper, an overband magnet and a drum pulley magnet both supplied by Eriez[®] Magnets. In theoretical operation ash/wire material would be deposited into the feed hopper where a conveyor in the base would move the material onto the main conveyor belt where it first passes under an overband magnet. Magnetic material attracted to the overband magnet would be lifted from the main conveyor and ejected to one side. Material passing the overband magnet continues up the conveyor where it passes over a head drum pulley magnet. Material extracted by the drum magnet is deposited onto a chute, which diverts material into a container situated underneath the main conveyor. Material passing both magnets drops from the end of the conveyor into a receptacle. It was envisaged that the majority of the bushy wire would be separated by the overband magnet whilst the drum magnet would separate the finer

pieces of wire and other magnetic phases. The unit, together with material collection containers, is pictured on site at STR in Figure 8.2.



Figure 8.2 Dry magnetic separator with product collection bins

The speeds of the main, overband and feed hopper conveyors were adjustable from a control panel located near the overband magnet. The suitability of the separator was investigated with a series of trials, which developed as further information was gained.

8.2.1 Initial pilot scale dry magnetic separation trial

Handpicked 10-50 kg samples of ash/wire were manually loaded into the feed hopper to enable the feed, overband and main conveyor speeds to be adjusted. It was found that when the main conveyor speed was set too high bushy wire passed under the overband magnet without being picked up and ejected. The belt main belt speed was therefore set so that all the bushy wire in the test samples was recovered. Containers for the three separated fractions (overband, drum and non-magnetic products) were placed at the relevant points around the conveyor. With the conveyors running the separation of some larger samples of ash/wire was then attempted.

A single bucket (approximately 250 kg) of freshly deposited ash/wire material was collected from a drainage bund with a four wheeled loader and deposited into the feed hopper of the dry magnetic separator. Initially it was observed that the ash/wire material was moved from the feed hopper onto the main conveyor but after a short period of time material was held up in the feed hopper. Adjustment of the feed hopper

belt speed had no effect on the movement of the material. Observations made through access panels located in the side of the hopper revealed that the feed belt was sliding underneath the ash/wire material. After moving some material a void appeared between the belt and the remaining material in the hopper. This was due to the bushy wire supporting the weight of the material against the sides of the hopper. The material remaining in the hopper had to be removed manually.

In an attempt to aid the movement of material from the hopper a series of cleats were fitted to the feed conveyor. The rubber cleats were approximately 50 mm in height and were glued to the belt at 1 m intervals. The initial test run was then repeated with half a bucket (approximately 150 kg) of material deposited in the feed hopper. The cleats were found to significantly improve the movement of material onto the main belt. The speed of the feed conveyor was then adjusted to produce as thinner layer of material on the main belt as possible.

With the cleats fitted to the hopper conveyor a further material handling issue was then evident. Bushy wire on the main belt rapidly overloaded the overband magnet, it became trapped underneath the magnet and was not ejected. Ash/wire material then built up behind the blockage and periodically pushed the bushy wire onwards up the belt where it subsequently overloaded the drum magnet and ended up in the bin intended for the non-magnetic product. Altering the height of the overband magnet above the main conveyor had no effect on the ejection of bushy wire. At this stage it was decided that the dry magnetic separator was not suitable for separating the bushy wire directly from the ash/wire material.

8.2.1.1 Interim discussion

Problems associated with handling the ash/wire material made the separation of the magnetic and non-magnetic phases difficult. The large volume, low mass, bushy wire was not sufficiently attracted to the overband magnet for the discharge conveyor to pick it up and eject. After discussions with the magnet suppliers (Helmich, 2000) it was concluded that shredding the ash/wire would enhance the handleability and suitability for magnetic separation. This approach was also consistent with the treatment of the bushy wire phase since a size reduction was required as the first stage

of the attrition process. A new trial was then carried out which incorporated an ash/wire shredding stage prior to magnetic separation using the same equipment.

8.2.2 Assessment of shredding technology

Shredders are routinely used in the treatment of scrap tyres to reduce bulk density and also as a liberation stage prior to the generation of crumb rubber products. A relatively large capacity shredder was required that could cope with both high throughputs and also the large diameter steel beads present in the ash/wire. A number of units offered for the trial were rejected due to insufficient capacity before a suitable shredder became available. The Columbus McKinnon® 500 Hp shredder was originally designed to shred whole tyres into 50 mm (nominal) chips. The size reduction was achieved as tyres passed between two counter-rotating rolls with surface mounted, interlocking, cutting knives. The trailer mounted shredding unit on site at STR has been pictured in Figure 8.3.



Figure 8.3 Columbus McKinnon® tyre shredder shown with discharge conveyor and feed hopper

A number of adaptations were made to the shredding unit to make it suitable for treating the ash/wire material. The original tyre feed conveyor was not used since its flat profile would allow material to fall from the side. A feed hopper arrangement was manufactured so that the ash/wire could be dropped directly into the cutting box with existing plant machinery, see Figure 8.3. A size classification system, which re-circulated oversized material, was found to be ineffective for use with the ash/wire so was removed to avoid potential blockages. The discharge conveyor, which

normally discharges at right angles to the trailer, was adapted to discharge along the length of the trailer due to space restrictions. A roll-on-roll-off trailer was placed under the conveyor to receive the shredded material.

8.2.2.1 Shredding tests

With the shredder running an initial half-full bucket of freshly produced ash/wire was loaded into the shredder feed hopper. The material was then pulled through the cutters and dropped onto the discharge conveyor where the quality of the shredded product could be observed. A single pass of ash/wire through the shredder was found to generate a product containing wire pieces generally less than 300 mm in length. It was immediately noticed that the shredded material was much easier to sample, transport and store in comparison with the original ash/wire containing intact beads. However, large quantities of water were also released from the ash/wire during shredding that resulted in considerable amounts of carbon ash being washed away from the feed end of the discharge conveyor. This was thought to be due to the breaking up of agglomerated carbon ash material and the subsequent liberation of previously trapped moisture. In an attempt to alleviate this problem the ash/wire for shredding was allowed to drain overnight in a spare bund prior to shredding. Although this achieved an acceptable moisture level in the shredded product it had the disadvantage of enhancing the corrosion of the wire; some of the outer layers of wire were considerably degraded and broke down with manual handling. Shredding of the drained material again produced a wire product with pieces less than 300 mm in length but without the associated release of water. This suitability of the material for dry magnetic separation was then investigated. Approximately 2 tonnes of shredded, drained, material was produced for a new trial using the existing dry magnetic separation circuit.

8.2.2.2 Alternative shredder technology

A shredding trial was also carried out on an alternative shredder. The second shredder incorporated a self-sharpening blade system and an automated blade spreading system to allow large solid items to pass without damaging the equipment. The Parke Rotashear[®] shredder has been pictured in Figure 8.4, a close up of the cutting

blades is shown in Figure 8.5. The performance of the shredder in creating a suitable ash/wire material for dry magnetic separation was assessed by dropping samples of into the cutting box and observing the output.

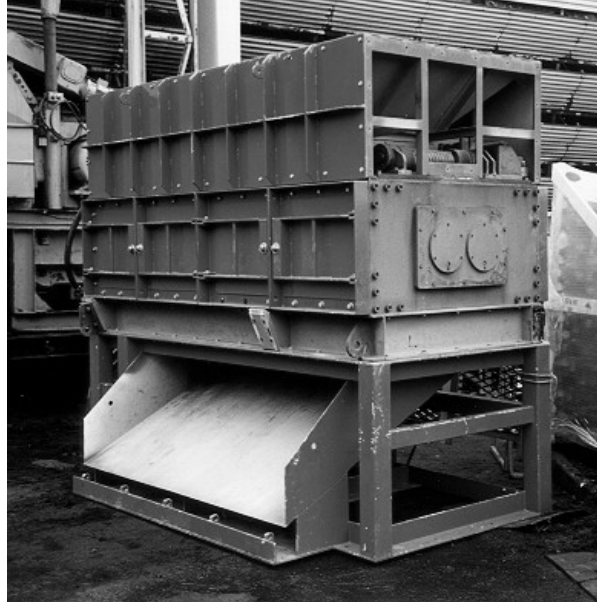


Figure 8.4 Parke Rotashear® shredder

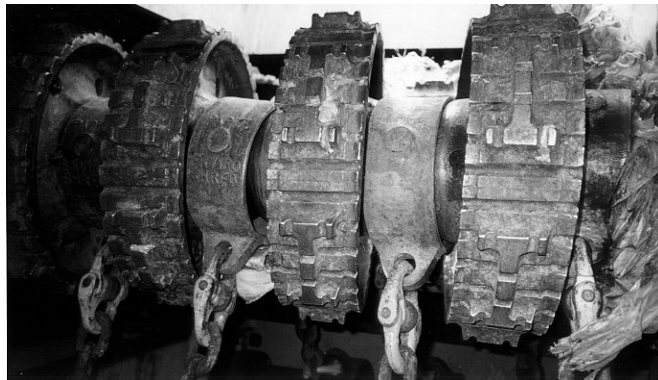


Figure 8.5 Parke Rotashear® cutting blades

The Rotashear® shredder was found to be affective in shredding the ash/wire material. However, in comparison with the product generated by the Colombus McKinnon® the wire pieces were considerably longer. Most intact beads in the feed material received only a single cut resulting in a product that was still difficult to handle and would cause similar problems during separation to those experienced with the original

ash/wire. For this reason the Columbus McKinnon[®] shredder was considered more suitable for the material.

8.2.3 Dry magnetic separation of shredded ash/wire

The drained ash/wire was shredded and deposited into a trailer (see Figure 8.6). In an ideal situation the shredded material would be fed directly into the feed hopper of magnetic separation equipment, however space restrictions ruled this out. The shredded material was taken from the trailer and deposited in the feed hopper of the magnetic separator using a four-wheeled loader.



Figure 8.6 Shredder product in roll-on-roll-off trailer

During the loading of the shredded ash/wire into the feed hopper there was a noticeable improvement in the handling characteristics. Material flowed easily onto the main conveyor at a rate that could be adjusted effectively with the speed control of the feed conveyor. The overband magnetic successfully pulled out the larger wire pieces from the shredded material although a portion of carbon ash was associated with this phase. Two mechanisms were responsible for this affect. Firstly, wire was

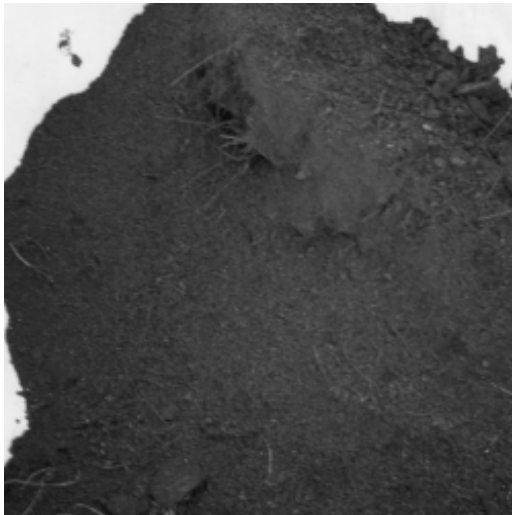
observed to drag carbon ash from the main belt as it was ejected into the collection bin and secondly due to carbon ash deposits associated with the surface of the wire. Through increasing the clearance of the overband magnet over the belt the amount of carbon ash dragged from the conveyor was reduced although it also reduced the recovery of wire from the ash/wire, which then passed onwards up the conveyor.

Finer wire pieces, which passed the overband magnet, were removed by the drum magnet. However, a small portion of wire also reported to the non-magnetic product whilst a considerable amount of the carbon ash (estimated at approximately 40% by weight of the carbon ash present in the shredded feed material) reported to the drum magnet product stream. The carry over of wire into the non-magnetic product was unusually high due to the entrapment of wire in agglomerated carbon ash material. The overall mass of the agglomerated particles mitigated any magnetic properties that were present. Images of each of the three phases separated during magnetic separation are shown in Figure 8.7 to 8.8.



Large wire pieces separated from the shredded ash/wire by the overband magnet. The fraction also contained some carbon ash dragged from the belt. This portion was retained and used in the attrition test work, which is described later.

Figure 8.7 Cross conveyor product



The separated fraction pulled from conveyor by the drum pulley magnet. Fine wire pieces are visible although the majority of the material (by weight) is a magnetic carbon ash phase.

Figure 8.8 Drum magnet separated phase



The non-magnetic separated fraction. The carry over of the finer wire pieces is visible together with the agglomerated carbon ash material.

Figure 8.9 Separated carbon product

8.2.3.1 Chemical analysis of non-magnetic product

A sub-sample (collected by temporarily diverting the product stream into a bucket) of the non-magnetic carbon product generated by the dry magnetic separation of the shredded ash/wire was analysed to determine the carbon concentration. The iron concentration was also measured. This would then provide an indication of the separation efficiency and allow a comparison to the laboratory scale test work. Carbon analysis was carried out using the procedure detailed Chapter 4. The iron concentration in the material was determined using an Aqua Regia digestion as described in Chapter 4 followed by ICP-AES analysis. The results are presented in Table 8.1.

	Carbon %	Iron %
Pilot-scale non-magnetic product	47.5	24.2
Lab-scale non-magnetic product	80.0	2.4

Table 8.1 Analysis of magnetic separation trial carbon product

The sample had a relatively low carbon concentration in comparison with the product generated using dry magnetic separation at laboratory scale. The associated iron content of the sample was significant and was due mainly to the visible carry over of physically entrapped wire in the phase. The material was also inferior to that generated by the laboratory scale separation of an 'aged' sample of carbon ash (65% carbon, 14% iron).

Recycling of the non-magnetic phase through the system, as had been carried out in the laboratory scale work, made very little difference to the quality of the separated product. The drum magnet extracted slightly more fine wire pieces after each additional pass but entrapped wire in the agglomerated carbon ash particles was still not removed.

8.2.4 Dry magnetic separation discussion and conclusions

The pilot scale separation trials clearly indicated that the application of a dry magnetic separator to the ash/wire as produced by the incinerator, and also after shredding, was

not appropriate to produce a high carbon concentrate. This was mainly due to the poor handleability characteristics of the material. Chemical analysis of the non-magnetic product confirmed that the carry over of fine wire into the carbon product was the main problem. The poor removal of iron from the non-magnetic carbon product could be attributed to two main reasons:

- Physical entrapment of fine wire pieces in carbon ash
- The formation of agglomerated particles with a lower overall magnetic susceptibility during the draining of the ash/wire material prior to shredding

Entrapment of the fine wire splinters was caused both by the handling of material after shredding and also by burial under carbon ash particles on the conveyor. The formation of a monolayer of particles on the conveyor would reduce the effect of the second problem however, in practice this would be difficult to achieve. The formation of iron corrosion products was difficult to avoid since the shredding of the non-drained material was not practical due to the release of water. Much of the water released during the shredding operation would originally have been locked in the pores of the carbon ash particles. The energy input by the cutting blades caused the larger and agglomerated particles to be broken up, liberating the trapped water.

The main difference between the laboratory scale dry magnetic separation and the pilot scale test was the moisture content of the feed material. In the laboratory test work the ash/wire material was completely dried prior to separation where as in the pilot scale separation the material retained a significant moisture level, even after drainage. A more appropriate route for the separation might have been to pulp the ash/wire with water and pump it through a fully wet magnetic separation system. This might allow better separation, as the magnetic and non-magnetic phases might exist as more liberated materials. Shredding of the material would still be employed since the increase in handleability is desirable and would be necessary in order to pump the slurry.

Due to the difficulties encountered in the pilot scale magnetic separation the production of the large carbon product test sample was abandoned whilst suitable

separation technology was investigated. The wire phase separated from the ash/wire was used in the attrition optimisation experiments discussed later.

8.3 Alternative method for ash/wire separation

8.3.1 Spiral classifier

The problems encountered during the pilot scale dry magnetic separation of the ash/wire led to the investigation of alternative techniques. Magnetic separation predominantly exploited the difference in magnetic susceptibility between the iron phases (strongly magnetic) and the carbon (non-magnetic). An alternative approach to the separation was attempted by exploiting the difference in size, and density, between the wire pieces and the carbon. Spiral classifiers use a continuously revolving spiral to move products up a slope from a settling pool containing a slurry of the product. Denser and coarser material settles in the pool and is removed by the spiral whilst the less dense and finer material overflows and is collected. The size and quality of the separation is determined by factors such as slurry feed rate, the speed of the spiral rotation and the height of the overflow weir (Wills, 1997). The separation of carbon ash and wire, from ash/wire generated during the shredding trial, was investigated using a spiral classifier. It was envisaged that wire pieces and relatively dense iron-carbon agglomerated material would be removed from the settling pool via the spiral whilst lower density carbon phase would overflow over the weir.

The spiral classifier used for the experiment usually formed a part of a closed grinding circuit as shown in Figure 8.10, the spiral, pool and overflow in use is shown in Figure 8.11. The normal spiral discharge route into the mill was blocked and the material collected from this point. With the spiral revolving, shredded material was fed at a point just above the settling pool. Water was continuously added from the top of the spiral to form the slurry in the pool. This had the affect of washing loosely attached carbon deposits from the wire whilst it was transported up the spiral.



Figure 8.10 Closed grinding circuit

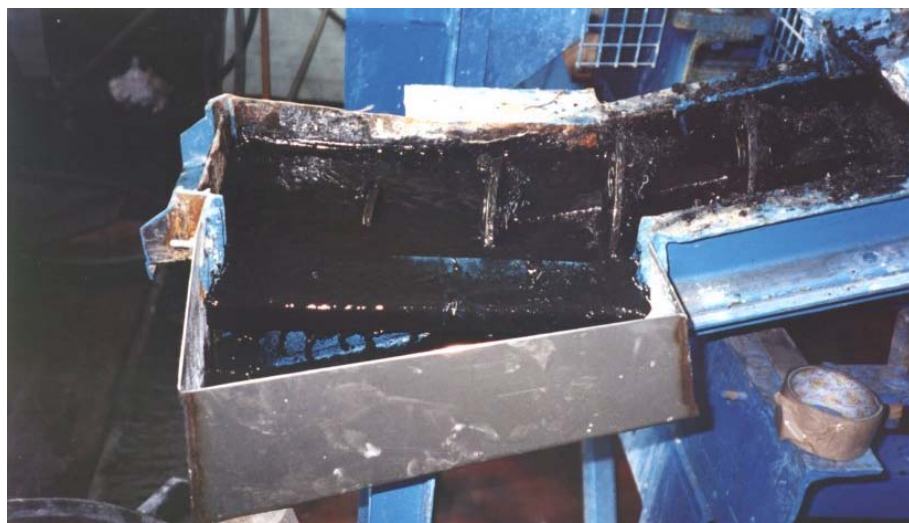


Figure 8.11 Spiral classifier separation of shredded ash/wire

The spiral was run until approximately 30 kg of shredded ash/wire had been separated. After a short period of feeding material into the classifier wire began to discharge from the top of the spiral. During the separation it was observed that only larger carbon-iron agglomerated particles were transported up the spiral due the gap between the spiral and the bed. Smaller particles were washed down into the pool. Occasionally wire pieces were observed to become tangled in the joints between the discs which formed the spiral, it was thought that the use of a classifier with a single continuous spiral would limit this handling problem. After draining the settling pool at the end of the test a deposit of fine wire pieces was found in the bottom. These were too small to be transported by the spiral but too dense to be carried over the weir. Samples of the weir overflow were taken by diverting the stream into a bucket. Water

was removed using a pressure filter and the solids were then dried in an oven overnight at 85°C prior to carbon analysis using the standard procedure described in Chapter 4.

8.3.1.1 Results

Together with the majority of the wire phase a mixed carbon phase was also discharged at the top of the spiral consisting mainly of coarse (>5 mm) mixed iron-carbon phases. This process stream would form the feed to the wire attrition process after a further size reduction. A sub-sample of the dried weir overflow product, which was found to be free of fine wire pieces, was subject to carbon analysis and the result, expressed as an average of two analyses, is presented in Table 8.2.

	Carbon (%)
Screw classifier carbon product	64.6

Table 8.2 Screw classifier product analysis

The carbon product stream had a relatively high carbon concentration (64.6%) in comparison with the non-magnetic product (47.5%) generated from a similar feed sample by pilot scale magnetic separation. This was thought to be due to the increased removal of fine wire by the spiral classifier.

The spiral classifier approach was more successful in the production of a carbon concentrate and also demonstrated potential for use in the primary separation of carbon ash and wire from shredded ash/wire. The high water content of the carbon product would necessitate a de-watering process although it is also possible that the carbon product could be further concentrated by passing the slurry through a wet magnetic separation system. The concentration of carbon in the carbon product resulting from the classifier might have been further improved by altering the process variables including increasing the weir height to increase the pool volume and hence increase the settling time.

8.4 Scale-up and optimisation of wire attrition process

In order for the attrition process to be developed into a full-scale process equipment suppliers would require information on optimum operating conditions. The initial attrition tests were conducted at a single solids loading rate and for an arbitrary period of time. An experiment was designed where the affect of the variation of process variables was measured in the sulphur content of the attrited wire product. The process variables investigated were the balance of water, sand and wire in the slurry and the length of time for which attrition was carried out. Wire for the tests was derived from a combination of the overband and drum magnet fractions of the pilot-scale dry magnetic separation trial.

8.4.1 Attrition optimisation method

Optimisation experiments were carried out using the same 1 litre attrition cell as used in the initial separation study. The wire sample generated by the dry magnetic separation trial was subject to further size reduction using the same Retsch[®] cutting mill fitted with a 4 mm internal screen. Since the wire had already been size reduced during the shredding operation the feeding of the material into the cutting mill was considerably easier than with the intact beads. When a large sample of <4 mm wire had been produced (approximately 60 kg) the sample was mixed to distribute the fine and coarse wire evenly throughout the sample. A sub-sample was riffled from the large sample to determine the starting concentration of sulphur in the wire for all the tests. The attrition media used in the experiment was the sharp sand as used in the initial experiment, fresh sand was used for each test.

In the optimisation experiments the overall pulp density, sand/wire ratio and attrition time were all varied. The pulp densities were set at 60% and 70% solids by mass since they were considered acceptable for slurry pumping. The ratio of sand to wire was then varied within the pulp density from levels of approximately 15% to 80% wire, the exact masses of sand and wire used are specified in Table 8.3. All of the material input conditions were conducted for an attrition time of 6 minutes. For the 1:1 wire to sand ratio at each pulp density the attrition time was varied from 2-10 minutes in 2 minute intervals. These conditions resulted in 18 separate attrition tests.

% solids by mass	mass (g)		
	Sand	Water (ml)	Wire
70	500	257	100
	400	257	200
	300	257	300
	200	257	400
	100	257	500
60	416	330	84
	333	330	167
	250	330	250
	167	330	333
	83	330	417

Table 8.3 Optimisation process conditions

The correct quantities of sand and wire were separated from the bulk sample using a riffle to ensure a similar feed material. For each test the correct mass of sand, wire and volume of water were added to the attrition cell. The impeller was then lowered into the cell, the lid closed and the impeller switched on at a speed of 1000 rpm. Attrition was then carried out for the necessary length of time for each test. After each run the sand and wire fractions were separated using a 1000 µm wire mesh screen. Sub-samples of the attrited wire, obtained by riffling the entire wire content recovered from the cell to approximately 5 g, were then prepared for sulphur analysis to assess the cleaning performance of each test. Each sample for analysis was gently rinsed with water to remove any loosely attached carbon ash deposits and then dried in an oven at 85°C, overnight. Duplicate runs of randomly selected tests were also conducted to check on the precision of the experiments. The results have been expressed as an average in these cases.

8.4.2 Results & discussion

The results of the sulphur analysis of each of the attrited wire products generated during the optimisation tests are presented in Figure 8.12 for the time variation and in Figure 8.13 for the solids loading variation. The sulphur concentration of the feed wire to each of the tests was 0.076%.

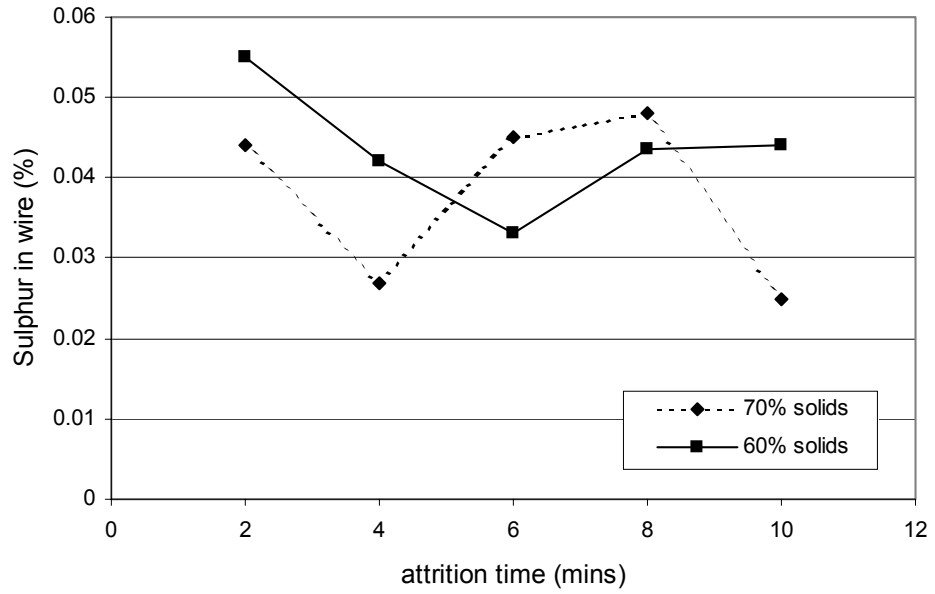


Figure 8.12 Effect of attrition time on sulphur concentration of steel

From Figure 8.12 it can be seen that any time dependence of the attrition performance was not clear, although this could be partly due to errors in the experiment, which is discussed later. In general it can be seen that the sulphur in the wire product was reduced with increasing attrition time, this is most obvious at the shorter attrition periods at both solids loading rates.

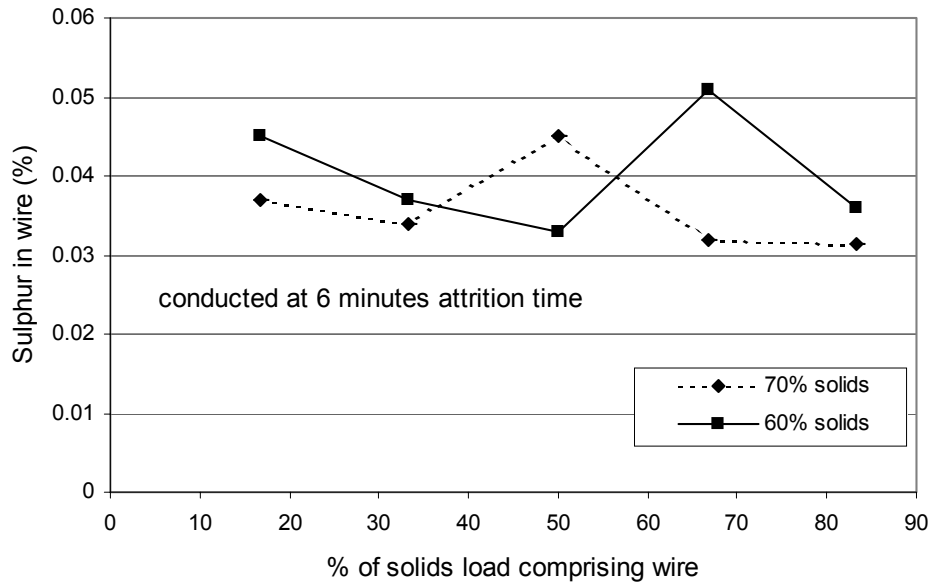


Figure 8.13 Effect of solids loading on sulphur concentration of attrited steel

The results presented in Figure 8.13 suggest that, in general, the performance of the 70% overall solids loading were superior with respect to sulphur removal from the wire. The variation of wire quantity within the solids load shows no clear differences although this may be due to the results being very close together, it might not actually be possible to remove any more sulphur using attrition scrubbing. This suggests that the type of attrition in the process, i.e. wire to wire or sand to wire, would have little effect on the final sulphur concentration of the wire. However, it should be noted that when the solids load was dominated by wire, the mixture was often difficult to get moving in the attrition cell. In some cases the slurry was observed to move around the cell as a single mass for a time before the stirring action mixed the slurry and started the attrition action.

The reproducibility of the sulphur concentrations of the products generated by the optimisation experiments were checked by repeating a selection of the test conditions. This allowed the precision of the method as a whole, from attrition to sampling and analysis, to be assessed. The individual test conditions replicated have been indicated in the results matrix in Appendix 2. For each of the duplicate tests two sulphur results were generated, see Table 8.4. For two of the three replicate tests the results can be seen to be in relatively good agreement, although the repeated Test 3 was not as good.

Test conditions (see results matrix in Appendix 2)	Sulphur (%)	
	Original test	Repeat test
1	0.031	0.037
2	0.033	0.030
3	0.032	0.055

Table 8.4 Precision in attrition optimisation test work

The poor precision measured for the optimisation experiment could be attributed to a number of factors including analytical error in sulphur measurement, sulphur variation in the feed material, contamination of the attrited wire during sample preparation or poor replication of attrition action. Since it was not known which figure was most appropriate for the Test 3, without conducting further experiments, an average of the two results was used. It was thought that the poor precision evident the test was most likely to be attributed to contamination of the attrited wire sub-samples prepared for analysis. This may have occurred due to insufficient rinsing of the carbon ash contaminated sand and water slurry from the wire samples. This might also explain the lack of clear relationships between sulphur concentration, time and solids loading evident in the optimisation data.

It can be seen that, in all cases, the sulphur content of the post attrition wire was lower than that of the feed wire, demonstrating that attrition scrubbing of the wire surface had occurred at each of the conditions tested. In general most of the tests generated a steel product below the target 0.04% sulphur concentration. The optimisation results therefore indicate that a range of process conditions were capable of achieving the target sulphur concentration of the steel product and this would allow full-scale equipment manufacturers to adjust the process variables to suit the equipment without adversely effecting the properties of the steel product.

8.4.3 Scale-up of attrition process

The results of the attrition optimisation experiment were supplied to mineral processing equipment manufacturer in Sweden (Svedala Ltd.) for a pilot scale test. A

large sample (20-30 kg) of the <4 mm (0.076% sulphur) wire was also supplied. A test was then carried out using a larger capacity attrition cell fed with an overall solids content in the slurry of 70% by mass. The solids mixture contained a sand to wire ratio of 2:1 and the attrition time was 6 minutes. The laboratory scale test run at these conditions yielded a product with 0.034% sulphur. After attrition the wire was separated from the slurry by passing the material over a drum magnet. A sub-sample of the wire product was then returned to the University of Nottingham for inspection and analysis. The sub-sample of the cleaned wire was then forwarded to LSM for sulphur analysis.

The result of the sulphur analysis on the pilot scale attrited wire product, from an average of two duplicate samples, is presented in Table 8.5.

	Sulphur concentration (%)
Feed sample to attrition	0.076
Pilot-scale test	0.047

Table 8.5 Results of pilot scale attrition testing

A steel product with a sulphur concentration of 0.047% was generated by the pilot scale attrition process. Although the sulphur content is slightly in excess of the 0.04% target it was thought that slight adjustment, such as increasing the attrition time, would have enabled the target concentration to be achieved.

8.5 Summary

The pilot scale test work revealed that the separation of the wire phase from the ash/wire material was not straightforward. Difficulties associated with handling the material made the dry magnetic separation of the wire directly from the ash/wire impossible. By shredding the ash/wire in a tyre shredder the handleability of the material was enhanced and the effectiveness of dry magnetic separation was improved. A wire phase was successfully recovered from the ash/wire and was subsequently used in the development of the attrition process. However, the pilot scale magnetic separation was not successful in producing a 'wire free' carbon product. The carbon content of the non-magnetic process stream was too low to be

suitable for application as a secondary fuel in a zinc smelter. An alternative approach to the primary separation of wire and carbon ash using a spiral classifier demonstrated that an approach based on exploiting density and size differences of the material phases might be more effective than dry magnetic separation.

At this stage of the project the production of large product assessment samples at STR was abandoned whilst more suitable separation techniques were identified. This also coincided with a total plant shut down to allow major renovations to be carried out following a period of poor reliability of the combustion units.

In all previous attempts to produce a concentrated carbon product through the application of physical and chemical techniques the success was limited due to the association of non carbon phases. The association, and level of dispersion, of these product contaminants was investigated to provide further information on the potential for separating them from the carbon product. An experiment was devised to identify and quantify the association of various contaminants and is described in the following chapter.

9 Float and Sink test work

9.1 Introduction

The separation studies carried out on the carbon ash phase of the ash/wire had determined that contaminants (i.e. non carbon) present in the potential products were not easily removed with standard physical processing techniques such as flotation and dry magnetic separation. This was due, in part, to the poor liberation of the desirable constituent from the undesirable phases. To provide more information on the liberation of contaminating phases a float-sink test, utilising a centrifuge, was adapted from similar procedures that had previously been carried out on fine coals by Palowitch and Nasiatka, (1961), Austin et al. (1994) and Killmeyer et al. (1992). The application of this type of test to the carbon ash would allow the association of contaminants with the carbon to be quantified and then the theoretical potential for physical separation to be determined.

A sample of carbon ash was first subject to a wet grinding operation to enhance the liberation of carbon from non-carbon phases prior to separation in the float-sink experiment. A suitable method for the float-sink characterisation of the carbon ash was developed following a review of the different techniques used throughout industry for the testing of fine coals. These are now reviewed and then the development of the test procedure is described.

9.2 Review of float-sink practice

The basis of float-sink testing is to place a sample into a solution/suspension of a known density (dense medium) and then to collect the fraction that is more dense than the medium (sinks) and the fraction that is less dense than the medium (floats). Static float-sink tests, where the sample is left in a container of the media for a period of time, are used to determine the theoretical beneficiation of coals (Bird and Messmore, 1924), (Killmeyer et al. 1992), (Franzidis and Harris, 1986). These type of tests are routinely carried out on coarse (>9.5 mm) and intermediate (9.5-0.5 mm) samples, however, they have been found to be unreliable when applied to finer (<0.5 mm) samples for a number of reasons. These include the susceptibility of fine particles to

thermal currents in the dense media (Killmeyer et al. 1992) and the excessive time required to conduct the tests (Franzidis and Harris, 1986). At present no standardised technique exists for determining the physical beneficiation potential of the fine material generated during the grinding of coals (Killmeyer et al. 1992). The unreliability of static float-sink tests on fine coal has driven the development of alternative methods (Franzidis and Harris, 1986; Killmeyer et al. 1992).

A procedure using a centrifuge to increase the gravimetric force for separating coal from impurities and also for reducing the time required for testing was assessed by the United States of America Bureau of Mines (Palowitch and Nasiatka, 1961). Using this procedure the float-sink testing of coals finer than 1.18 mm was found to significantly reduce the time required for separation. The particle size was not found to limit the centrifugal technique, a <75 µm coal sample was also separated successfully although repeated centrifuging of the float fraction was required to liberate all of the sinks material. The separations were conducted in organic liquids such as carbon tetrachloride where the density was altered through the addition of unleaded petrol. An aqueous zinc chloride solution was also tested as the separating medium in the procedure. Sample preparation was varied depending on the dense media type being used in the separation. Where organic liquids were used the sample was air dried to remove moisture from the coal pores due to their immiscibility with water. The empty pores were then subsequently filled with the organic liquid, although it was possible that the empty pores could remain full of air if the sample was not wetted and hence affect separation. The use of aqueous salt solutions, such as zinc chloride, meant that the media was partially diffused in to the surface pores of the coal meaning that the sample could be analysed without drying the sample.

Alternative solutions that have been used as a dense medium include cesium chloride (CsCl), which can be prepared to a maximum relative density of 1.9. This solution was used as dense media to separate coal macerals by Dyrkacz and Horwitz (1982). A non-ionic surfactant Brij –35[®] (polyoxyethylene-23-lauryl ether) was added to the solutions to further improve wetting and dispersion of the fine coal particles. The centrifuge method was found to separate the macerals effectively with three key elements identified for successful separation:

- Effective grinding to free macerals
- Demineralisation
- Complete dispersion of fine coal samples.

An alternative inorganic dense media, which has previously been used for the laboratory separation of coal, is sodium polytungstate (known as SPT), where solutions can be prepared up to a maximum relative density of 3.1 (Rhodes, 1991). Static float-sink test work using SPT has been described in Cloke et al. (1994). A surfactant was used in the experiment to improve the dispersion of a 38-20 μm coal fraction. A disadvantage of solutions of salts such as CsCl and SPT is that they are expensive so after use it is normal to recover and reuse the salt in subsequent experiments.

The effect of various process variables used within centrifugal float-sink testing was assessed in an inter-laboratory study (Killmeyer et al. 1992). In the study eight laboratories conducted analysis on identical fine coal samples using existing in-house techniques. The test variables that varied between laboratories included sample preparation regimes, centrifuge speeds, solids concentrations and the choice of dense media. It was concluded that for the centrifugal float-sink testing of ultra-fine material ($<14 \mu\text{m}$) the use of a proper combination of medium and surfactants were significant experimental parameters. For coarser material these factors were less pronounced and the results acceptable. The choice of dense media and centrifuge speed were noted as being particularly significant parameters in the final results.

After centrifuging of the sample has been carried out the float and sinks fractions must be recovered from the centrifuge tube prior to analysis. A number of techniques exist to remove the samples from the tube although in practice it is difficult to remove the fractions without disturbing the remainder of the tube contents which may then introduce major sources of error through mixing of the fractions (Franzidis and Harris, 1986). Traditional fraction removal methods include the recovery of the sink fraction with a fine copper or glass tube connected to a vacuum pump and scooping of the float fraction with a spatula. More advanced methods were investigated by Franzidis

and Harris (1986) including the use of fine gauze placed in the tube to enable the float fraction to be lifted out after the test. However, it was thought that the gauze could trap sink material. The use of a novel separating device, which was able to fit inside a standard 100 ml centrifuge tube, was also investigated in an attempt to limit the mixing of the float and sink fractions during sample recovery. The sample was initially loaded into the inside of the device, which was then lowered in to the centrifuge tube containing the dense media. Once loaded into the centrifuge the centrifugal force released a conical plug on the base of the device and the sample mixed with the dense media and was separated as normal. At the end of the test the plug automatically resealed as the centrifuge slowed trapping the floats inside the device and the sinks in the centrifuge tube.

Clearly the selection of a suitable combination of technique, separation medium, sample handling and preparation methods are all important factors in the accuracy of float-sink experiments. A procedure was then developed where the process parameters were selected based upon their suitability to the application of the carbon ash.

9.3 Development of float-sink testing method

The main parts of the experiment that might affect the final outcome of the experiment were the separation technique, sample preparation, the choice of dense medium and fraction recovery method. The selection of the test parameters has been described and the precision and accuracy of the final procedure is discussed prior to the reporting of results.

9.3.1 Selection of separation technique

Since, after routine handling, the majority of the carbon ash, even prior to grinding, was fine (<1 mm) a centrifugal float-sink test method was applied to the material to reduce the time required for separation.

In centrifugal separation the amount of sample used in each test must be limited to ensure that the entrapment of floats in the sinks and *vice versa* was minimised in the confined space of the centrifuge tube. On the contrary the samples produced by the

separation must be large enough for subsequent chemical analysis. Therefore a parallel approach to the float-sink analysis was adopted where identical sub-samples were tested at each separation density as opposed to a serial approach where the floats and sinks would be recycled and used as the feed material in the next separation. This might result in the generation of insufficient quantities of analytical samples, since the volume of the centrifuge tube limited the mass of the initial feed sample

The sequence of events in the process is outlined in Figure 9.1. A representative sub-sample of the carbon ash used as the feed for the experiment was characterised to provide information on the initial distribution and concentration of elements in the sample. The carbon ash was then ground in a batch laboratory ball mill to enhance liberation prior to size separation using wet sieving to produce a series of samples with a relatively small particle size range. The preparation of the fractions is described in detail in Section 9.3.3. These size fractions were then tested individually at a range of densities to minimise the effect of entrainment. The resulting floats and sinks were then recovered and prepared for chemical and physical analysis.

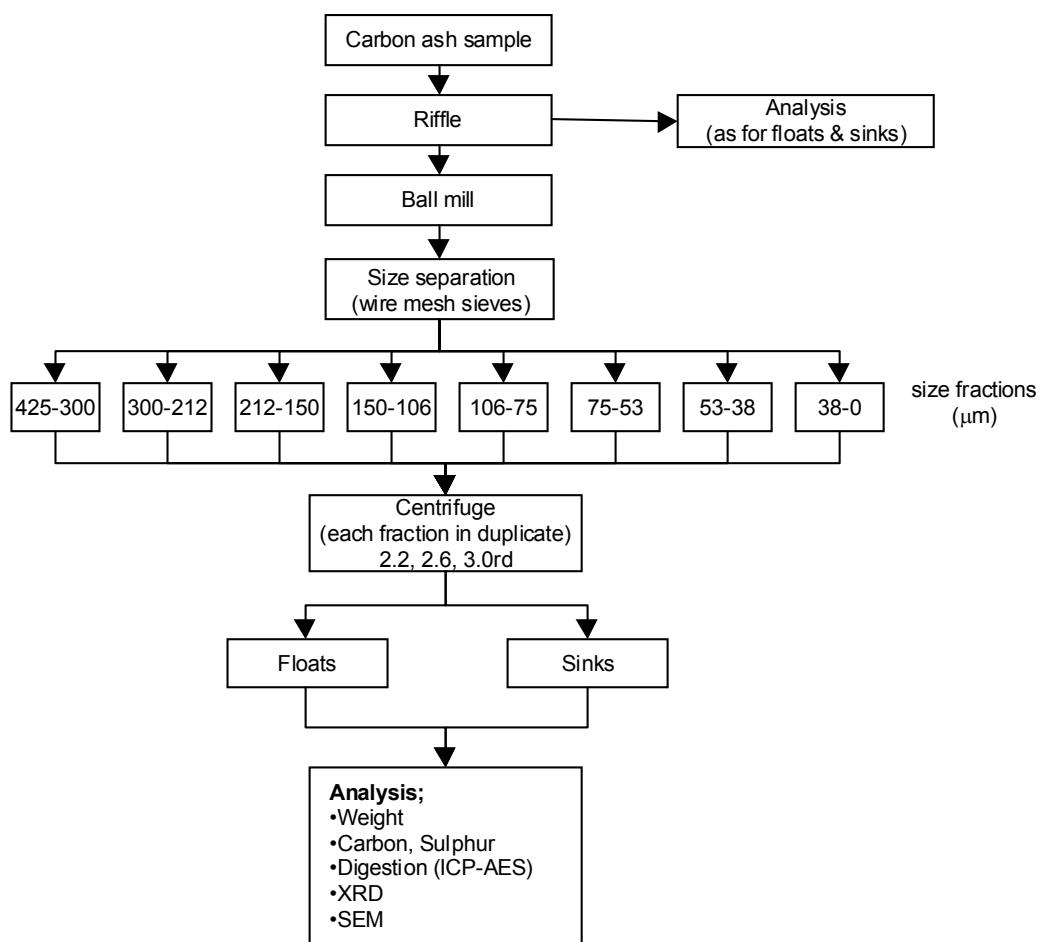


Figure 9.1 Flow chart of float-sink separation procedure

Separation was carried out using a Baird & Tatlock Auto Bench Mk. IV centrifuge. The rotor fitted to the centrifuge was equipped with four swinging buckets, which re-orientate themselves from vertical to horizontal as the speed of the rotor increased. Round bottomed 100 ml polypropylene tubes rested on rubber seats inside the swing buckets. With the specific rotor and full centrifuge tubes in place the speed was limited to 4000 rpm. At this rotor speed a G force of 2737 was generated, reducing the settling time of the particles contained in the dense medium in comparison with a static test where they solely under the influence of gravity. Some approximate settling times were calculated assuming a scenario where the density difference between the medium and the particle is 120 kgm^{-3} (0.12rd to water) and the settling distance was 0.1 m. The calculations were carried out using Stokes' law for the terminal settling velocity of a spherical particle, which can be found in Appendix 3 together with more details of the calculation. The settling times for a number of particle sizes have been presented in Table 9.1.

Particle size (microns)	G force	Settling time
300	1	152 secs
300	2737	0.5 secs
10	1	38.2 hours
10	2737	8.2 mins
5	1	152.9 hours
5	2737	32.9 mins

Table 9.1 Calculated settling times in centrifuge and static float-sink tests

It can be seen that the settling time of the particles in the centrifuge is reduced in comparison with a static separation. For example a 10 μm particle would take 38.2 hours to settle 0.1 m under gravity but this can be reduced to 8.2 minutes in the centrifuge.

9.3.2 Selection of appropriate separation medium

The choice of dense medium for the centrifugal separation was influenced by a number of factors including the ability to achieve the desired densities and the subsequent treatment of the separated samples. The relative densities of the medium for the test were selected so that the more dense mineral phases would sink whilst the less dense carbon (as carbon black) would float (see Table 9.2). The minimum relative density that was required would therefore be in excess of 1.9, immediately ruling out the use of CsCl and ZnCl. Although SPT had the capability of achieving the required densities previous work carried out at the University of Nottingham revealed that the tungsten element of the salt solution made subsequent ICP-AES analysis of the samples impossible (Laban and Atkin, 1999). Tungsten was found to be a major interfering ion in the analytical method due to the number of emission lines that are produced. Excessive water washing did not remove enough of the SPT in the sample to make analysis possible.

Mineral	Specific gravity
Zincite (ZnO)	5.6
Goethite (FeO(OH))	4.3
Lepidocrocite (FeO)	4.26
Wurtzite (ZnS)	4.09
Sphalerite (ZnS)	4.04
Calcite (CaO)	2.71
Silicon (Si)	2.32
Carbon (Carbon black)	1.8-2.1

**Table 9.2 Specific gravity of selected minerals present in carbon ash
(adapted from (Carmichael, 1984))**

The use of an organic heavy liquid was chosen to allow the preparation of a wide range of liquid densities as well as causing minimum interference to subsequent analytical techniques. 1,1,2,2 Tetrabromoethane (TBE) in its pure form has a relative density of 2.95 and lower densities were prepared by mixing TBE with Triethyl Phosphate (TEP) which has a relative density of 1.07. TBE is very toxic by inhalation so all work was carried out inside a fume cupboard, including the centrifuging. Prior to chemical analysis the TBE/TEP was washed from the sample with the solvent, acetone. The use of organic dense media also necessitated that the sample be thoroughly dried prior to testing to improve wetting of the sample.

9.3.2.1 Dense liquid preparation

The separation mediums at each RD were prepared in advance of the float-sink test work and stored in glass vessels prior to use. A 500 ml volume of each density was prepared by mixing appropriate volumes of TBE and TEP. The highest density liquid was formed using TBE only. During preparation it was noticed that the two organic liquids did not mix very quickly and often formed distinct layers in the sample container when initially combined and stirred. This was thought to be due to differing temperatures of the two liquids, as after a period of time the liquids were well mixed. After a float sink test had been conducted the filtered separation medium was returned to the storage container and the density checked prior to reuse in a subsequent test.

The density of the prepared media was measured by weighing a known volume at room temperature. A 10 ml volume of the liquid was decanted from the storage container into a clean, dry measuring cylinder and weighed. The density of the liquid was checked before and after each use to detect potential contamination and to ensure a uniform density from one test to the next.

9.3.3 Sample preparation

The sample of carbon ash selected for the float-sink testing was that generated from the pilot scale magnetic separation trial. In addition to the magnetic separation any remaining visible wire was removed manually. The sample was then similar to the carbon ash that might be produced by the primary separation of carbon ash from the ash/wire. The whole sample was then riffled, with one half being retained for grinding whilst the other was physically and chemically characterised to provide information on the starting concentration and distribution of contaminants. Wet sieving was used to size separate the fractions, which were then dried at 85°C and weighed prior to chemical analysis. A bulk sample (all size fractions) was also prepared for chemical analysis.

The sample set aside for grinding was oven dried at 85°C to stabilise the sample prior to use.

9.3.3.1 Comminution

Grinding of the carbon ash was carried out in a laboratory-scale ceramic ball mill with steel balls as the charge. The sample of dry carbon ash was weighed and combined with water to form a 32% (by weight) slurry and added to the mill along with the ball charge. The mill conditions are summarised in Table 9.3.

Grind duration (minutes)	20
Weight - carbon ash (g)	950
Weight - water (g)	2000
Total weight of ball charge (g)	3700
Ball charge distribution:	
Large	34
Medium	35
Small	75

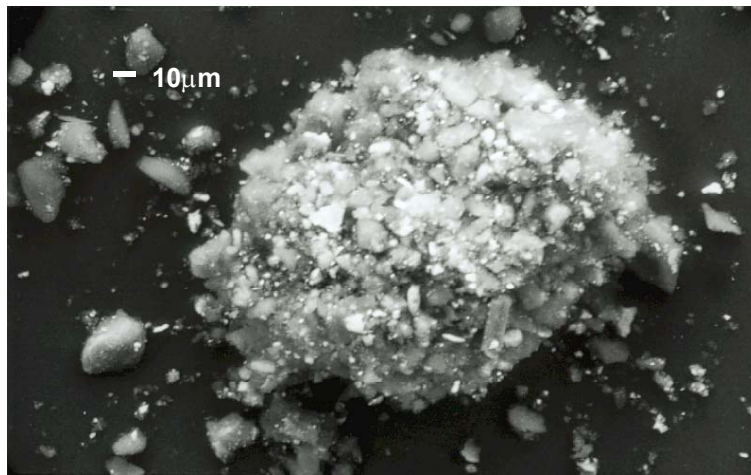
Table 9.3 Ball milling conditions of carbon ash sample

After grinding the slurry was passed through a set of sieves, to provide a size classification to be compared with the feed material as well as preparing samples for float-sink testing. The contents of each sieve, as well as the sub sieve (38-0 μm) material was dried by pressure filtering the fraction onto a filter paper and then oven drying at 85°C. Individual size fractions were then analysed to determine the concentration and distribution of elements in comparison to the original pre-grinding material.

After oven drying it was noticed that the finest size fraction, (38-0 μm), was found to have re-agglomerated into a single solid cake, which was unsuitable for float-sink separation. The coarser size fractions contained only discrete particles. In an attempt to maintain the original discrete particles in the 38-0 μm sample a different approach to drying the individual fraction was investigated.

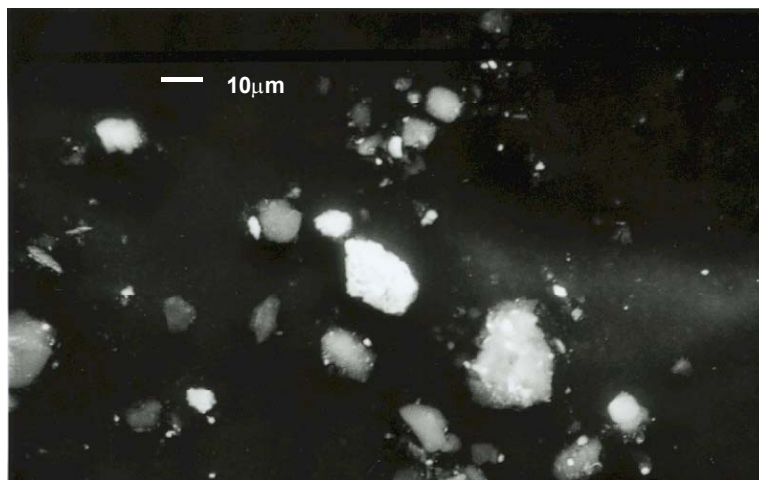
The 38-0 μm fraction was re-ground in the ball mill using similar conditions to the original grind. The slurry was then passed through a 38 μm wire mesh sieve. The majority of the water associated with the sample was then removed using a pressure filter. Acetone was then added, in a number of stages, and the sample filtered to near dryness until it was considered that all of the water had been replaced with acetone. The sample was then allowed to dry at ambient temperature in a fume cupboard. After the acetone had evaporated from the solid sample the majority of the material was found to consist of discrete particles but also some oversize re-agglomerated material which had formed during drying. SEM analysis of the individual size fraction

confirmed that the oversized ($>38\ \mu\text{m}$) material within the sample was the result of the re-agglomeration of fine particles, see Figure 9.2 and Figure 9.3.



A re-agglomerated particle in the sample. It is approximately $160\ \mu\text{m}$ in diameter.

Figure 9.2 Re-agglomerated particle in 38-0 μm size fraction



Some discrete metallic and carbon phases in the same sample

Figure 9.3 Dispersed particles in 38-0 μm size fraction

Since the agglomeration of the fine particles only occurred once the material had been dried then a method was developed that would allow the float-sink testing to be conducted on the 38-0 μm fraction without drying the material.

9.3.3.2 Special treatment of 38-0 μm fraction

The 38-0 μm fraction was re-ground in the ball mill and the previous operation repeated until the final air drying of acetone. At this stage the acetone was allowed to

evaporate until a high solids concentration slurry remained. A sub sample of the slurry was taken that was estimated to contain 5-6 g of dry solid material and placed into a glass beaker. Approximately 100 ml of the appropriate dense medium was then added to the beaker, which was then moved to the fume cupboard. The contents of the beaker were then stirred, using a magnetic stirrer, until the sample was required for separation. During this time the acetone evaporated from the mixture leaving a slurry consisting solely of the dense medium and the sample, which was assumed to consist of discreet particles. It was not possible check that any particle agglomeration had occurred during the sample preparation due to the presence of the heavy liquid which made the handling and treatment outside of the fume cupboard unsafe. The slurry was then thoroughly mixed and split between two centrifuge tubes and made up to equal mass with additional dense media. The samples were then treated in accordance with the standard procedure (described in Section 9.3.4) except that after the recovery of the floats and sinks from each centrifuge tube the samples were combined to produce a single floats and a single sinks sample. This was to eliminate variations in the feed sample that may have occurred when the contents of the beaker were split. The 38-0 μm fraction is the only sample for which duplicate results are not available for each separation density. It would have been preferable to conduct the test on the sample a number of times but this was not possible due to the excessive time taken to process each sample from preparation to test work and analysis.

9.3.4 Experimental procedure

Each size fraction (425-300, 300-212, 212-150, 150-106, 106-75, 75-53, 53-38 and 38-0 μm) generated by grinding was subjected to a single float-sink test at three densities, these were 3.0, 2.6 and 2.2rd. Oversize (>425 μm) material was not tested since it represented less than 5% of the total sample and contained mainly fine wire pieces. All samples were centrifuged in duplicate pairs, two tubes of the same sample were spun in the centrifuge at the same time. This ensured that the rotor remained balanced during the experiment and also provided information on the precision of the experiment.

9.3.5 Centrifugal separation

Early samples in the experiment were used to determine suitable sample masses and to develop a suitable fraction separation strategy. An accurately weighed sample for separation was placed in to the bottom of a clean, dry centrifuge tube. It would have been preferable to riffle a series of identical sub-samples from the main sample, however this was not possible as a consistent, precise, feed mass was required. The test conditions were initially set at 3.4 g of sample in 80 ml of dense medium (42.5 g/ml) although this was reduced to 2.5 g (31.25 g/ml) after early tests generated sufficient quantity of floats and sinks samples for analysis. Using a lower sample mass also reduced problems associated with the physical entrapment of particles during separation by allowing more space for particles to float or sink unhindered.

After the sample was added to the tube approximately 40 ml of the relevant dense liquid was added. Particles were observed to remain on top the liquid surface and did not appear to be readily wetted. To properly wet the sample and also to improve dispersion of the particles the tubes were placed in to a sonic water bath for 30 minutes which was found to be sufficient time to fully incorporate the particles into the liquid. Whilst in the sonic bath the volume of the dense media was made up through the addition of a further 40 ml of dense liquid, the contents of the tubes were then stirred. The precise volume added was determined by the requirement to balance the total weight of the two tubes and contents to ensure the centrifuge would operate without imbalance. The total volume of dense liquid in the tubes was always within the range of 80-82 ml. The tubes containing the sample and appropriate volume of dense liquid were then left in the sonic bath for a further 30 minutes, after which the tubes were placed into the centrifuge on opposite sides of the rotor.

The centrifuge was then switched on and the speed set at 4000 rpm for an initial period of 10 minutes. After this time the rotor was allowed to stop naturally i.e. no external braking force applied. The tube contents were then stirred *en situ* with a glass rod to ensure that the sample was well dispersed with the particular aim of re-distributing any plug of floats that may have formed. The centrifuge was then set to run for a further 30 minutes at 4000 rpm. At the end of this period the rotor was allowed to stop naturally and the tubes were removed gently to avoid disturbing the

contents to a rack for recovery of the floats and sinks. After centrifuging it was found that the tubes and contents had slightly increased in temperature. The feed liquid was usually within the temperature range 12-15°C whilst immediately after centrifuging the liquid was found to be in the range of 15-20°C. The increase in temperature was not sufficient to cause a measurable change in the density compared to the feed liquid. It should be noted that the volume used to measure the density was small (10 ml) so it would have been difficult to measure relatively minor changes in density. This was due to the difference in weight between 10 ml of feed liquid and 10 ml of the used liquid being smaller than the accuracy of the balance. Room temperature liquid was used as the feed for each test to limit the potential for the temperature to steadily rise throughout a test series.

9.3.5.1 Recovery of floats and sinks fractions

The floats and sinks were recovered immediately following the stopping of the centrifuge. It would have been preferable to use the sort of device described in Franzidis and Harris (1986) as discussed earlier to recover the fractions, but since the device was not available an alternative recovery method was developed. It was found that it was very difficult to identify boundaries between the floats and sinks phases due to the translucence of the polypropylene tubes and the presence of near density material (material occupying the middle portion of the tube). The floats fraction was therefore arbitrarily defined as the top 50% of the slurry volume, the sinks fraction was defined as the remaining material. If the sample was initially assumed to be dispersed throughout the volume of heavy liquid then the 'worst case scenario' was that a particle that should report to the sinks was located at the slurry surface prior to centrifuging. By identifying the top and bottom 50% volumes of the slurry as the floats and the sinks, particles present at the extremes of the tube can report to the correct fraction by settling only half the depth of the slurry. The same reasoning applies for a particle that should report to the floats being present at the base of the slurry.

The removal of exactly 50% of the volume was found to be difficult due to the fine suspension of black coloured particles covering graduations in volumetric equipment. A line was therefore marked on the outside of each centrifuge tube that represented

50% of the slurry volume, slurry was then removed to that point for each test. The floats fraction was removed from the tube using a combination of a stainless steel spatula and a modified pipette. The teat of a 25 ml pipette was ground to produce a larger aperture allowing easy passage of material up to the largest particle size, i.e. 425 μm . Any plug of material that had formed at the top of the tube was carefully removed with a spatula taking care to minimise the disturbance of the underlying material. The remainder of the floats was drawn into the pipette and deposited into a glass beaker along with the material removed by the spatula. The pipette was lowered inside the tube as the slurry surface fell, ensuring that the slurry was drawn from just below the surface. Any solids that were deposited on the side of the tubes during the withdrawal of floats fraction was scraped out using the spatula and included in the floats fraction. The slurry that remained in the tube was included in the sinks sample, acetone was used to rinse material from the base of the tube into the filtration equipment.

The solid sample was separated from the dense medium, recovered as a part of the floats and sinks, by vacuum filtration through a Whatman[®] 543 hardened ash-less filter paper. This operation often took considerable time due to the fine material blinding the filter paper and the relatively high viscosity of the organic liquid in comparison with water. By the end of all of the test work, when the technique was well practised, the entire procedure from centrifuging to filtration took one day for each pair of duplicate samples at a single separation density. When the organic liquid had been separated from the solid phase it was returned to the storage container ready for reuse in the next test. Acetone was then used to rinse any remaining organic liquid from the solid sample, approximately 100 ml of acetone was used in several stages for each sample. The separated sample was then removed from the filter paper and placed in a labelled glass jar with the top removed to air dry in the fume cupboard. Waste acetone, contaminated with traces of organic liquid, was disposed of in accordance with Nottingham University waste disposal regulations.

Mass balancing was carried out on a selection of early samples to determine the losses of material during the test. However it was found that a significant quantity of dense media remained associated with the sample after the acetone washing as the total

weight of the recovered material was found to be greater than the feed weight. It was considered that this was due to the entrapment of dense media inside the pores of the carbon ash. The small sample masses of the float-sink fractions made the effect of the entrapped dense media particularly significant. The removal of the remaining dense media was improved by drying the sample at a temperature in excess of the boiling point of both the TBE (244°C) (BDH, 1994) and the TEP (210°C) (BDH, 2000). This drying stage was carried out in a single batch after all of the float-sink samples had been generated. The samples, in open-top glass jars, were placed in a vented furnace and heated to 250°C for a period of at least 12 hours. After furnace drying and cooling each sample was weighed on a clean polystyrene sample boat to provide information on the mass split of material between the floats and sinks before being returned to a sealed glass jar prior to chemical analysis.

Control samples (run alongside the experimental samples) were used to monitor the effectiveness of the drying process. The sample weights recorded before and after drying of the control samples in the furnace revealed that as much as 23% of the air dried sample mass was due to the presence of organic liquid, see Table 9.4.

Sample	After air drying (g)	After 12 hours @ 250°C (g)
Control (all)	3.07	2.35
Control (floats)	1.90	1.68
Control (sinks)	0.66	0.66

Table 9.4 Mass of control samples before and after furnace drying

The results also indicated that less organic liquid was associated with the sinks fraction. It is thought that this may have been due to a lower concentration of the porous carbon phase being associated with this fraction.

9.3.6 Chemical analysis of test samples

A standard suite of chemical analyses was carried out on all samples. The samples for analysis were the duplicate floats and sinks generated by float-sink testing, the

original feed material size fractions, the post grinding size fractions and a bulk feed sample (all size fractions).

9.3.6.1 Elemental analysis

Carbon and sulphur concentrations were determined in the sample using the techniques described in Chapter 4. Samples were prepared for analysis by hand grinding in an agate pestle and mortar as the sample mass was not sufficient to utilise the Tema[®] mill as described in previous experiments.

The quantitative determination of other elements in the samples was determined using a wet digestion technique. Due to the large number of samples requiring analysis an alternative to the time consuming total digestion method was used. An Aqua Regia digestion was used to draw elements into solution before measurement using ICP-AES, the method has been described in detail in Chapter 4.

9.3.6.2 Mineral phase identification

XRD analysis was carried out on selected floats and sinks samples to identify mineral phases reporting to the floats and sinks. Analysis was carried out on the material that remained after all other chemical analysis was complete. The sample was then low temperature ashed to remove the carbon. Pairs of duplicate samples were combined to ensure that a sufficient sample mass remained after ashing although it was found that this still did not provide sufficient material to fill a slide. The slides were therefore half packed with blue-tac[®] to reduce the volume of sample required for the analysis without altering the results.

9.4 Float-sink test results

9.4.1 Size characterisation of feed and grind material

The size characterisation of the original carbon ash and the same sample after grinding is presented in Figure 9.4.

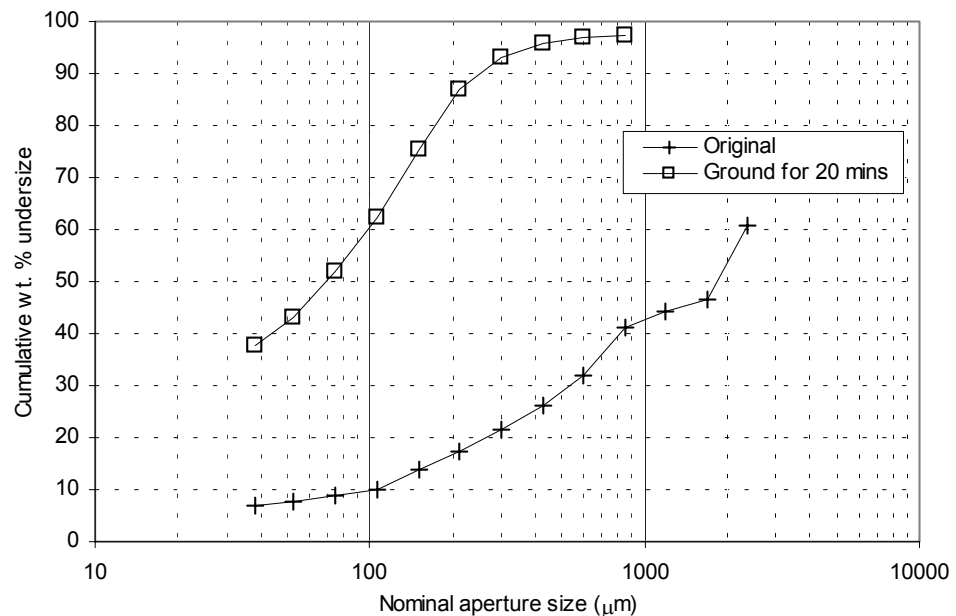


Figure 9.4 Carbon Ash - size classification before and after grinding

It can be seen that grinding the carbon ash resulted in the production of a significantly finer material. Approximately 40% of the post grind material reported to the 38-0 μm size fraction, in the feed material less than 10% of the feed material reported to the same size fraction. The float-sink test work will then determine if the increased presence of finer material enhanced the liberation of non-carbon phases. The full results of the size characterisation have been presented in Appendix 3.

9.4.2 Precision of float-sink test work

The float-sink testing of sample in duplicate enabled the precision of the experiment to be monitored and also provided a means of detecting gross experimental errors. However, the detection of errors is limited as the duplicates were run at the same time meaning that both could contain the same gross or systematic errors. A more accurate

determination of precision of the experiment would have required the testing of a larger number of replicate samples over a longer time period, which was not possible in this study.

The floats and sinks fractions were weighed on a two decimal place (1/100 g) analytical balance. The combined mass of the floats and sinks fractions were then compared to the original mass of the feed sample and the percentage recovery calculated. The results are presented in Figure 9.5.

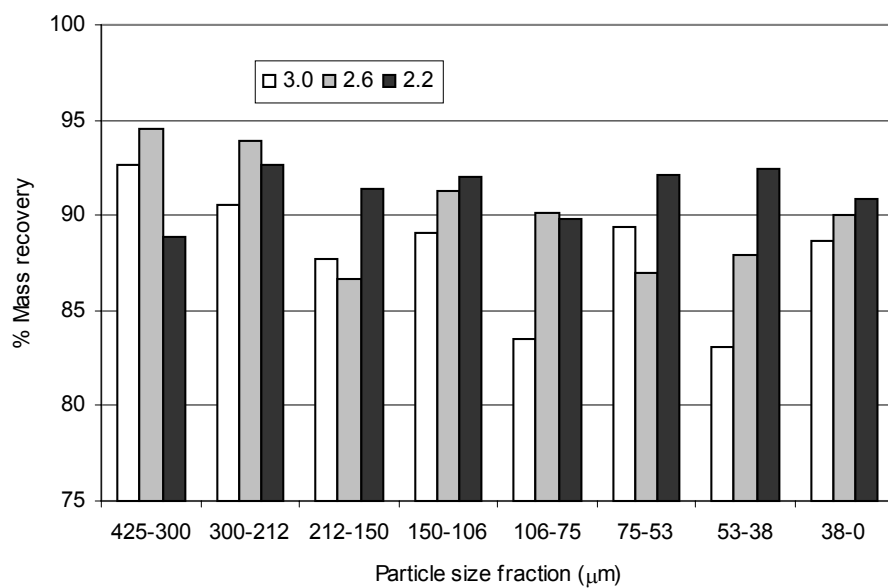


Figure 9.5 Mass recovery at three separation densities

The overall average recovery of the feed sample was 90%. The average recovery from each media density (all size fractions) was found to improve as the density decreased with recoveries of 88%, 90% and 91% respectively from the 3.0, 2.6 and 2.2rd. It was thought that loss of material was likely to have been caused by two main procedures within the experiment. Firstly, as a result of material not being recovered from the centrifuge tube as part of either the floats or the sinks fraction and secondly due to losses during the filtration stage. The main material losses were suspected to be associated with the filtration stage as fine material blocked pores in the filter paper and this could not be recovered as part of the solid sample. This effect can be seen in Figure 9.5 as the percentage of the sample recovered is generally greater for the larger

particle sizes. It was possible that the preferential loss of finer material may have introduced a systematic error into the experiment and this is discussed later.

The distribution of material between the floats and sinks fractions was investigated for the each of duplicate samples to determine the precision of the float-sink test. The percentage of material reporting to the floats and sinks fractions was calculated by comparing the mass of the separated fraction to the total mass of the two fractions combined. The coefficient of variation (CV), expressed as a percentage, provides a measure of the closeness of two results and has been calculated for the mass of floats material in each feed sample, see Figure 9.6. The CV was not calculated for the finest size fraction since no replicates were carried out due to the different methodology used. A gross experimental error occurred during the treatment of the 53-38 μm sample at 2.6rd requiring that one of the replicates was discarded, therefore the CV was not calculated.

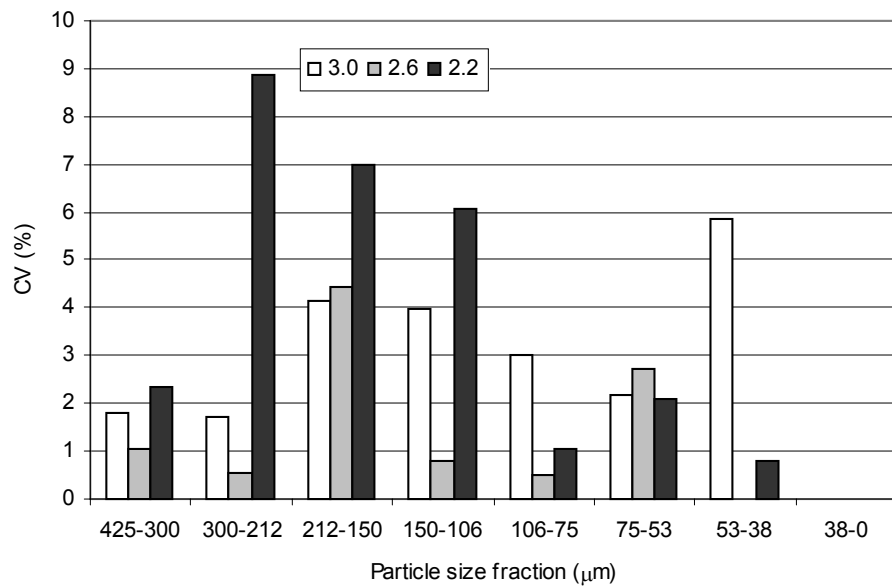


Figure 9.6 Coefficient of variation in mass of floats fraction at three separation densities

From Figure 9.6 it can be seen that the precision of the sample mass was always <10% and <5% in the majority of the samples. It should be noted that a maximum of one replicate was carried out for each sample so the CV only provides an approximation of precision.

The relatively good agreement between the mass of samples and their duplicates indicated that the method adopted for the float-sink centrifuge analysis was capable of generating reproducible, reliable results. Although the true accuracy of the experiment cannot be determined the repeatability of the results indicated that the experiment is capable of allowing comparisons to be made between samples generated by the same methodology. Due to the good precision measured in the mass data all of the results of the float-sink test work have been expressed as an average of that data generated by the duplicate samples.

9.4.3 Mass distribution

The percentage of the feed material reporting to the floats fraction at the three separation densities is presented in Figure 9.7.

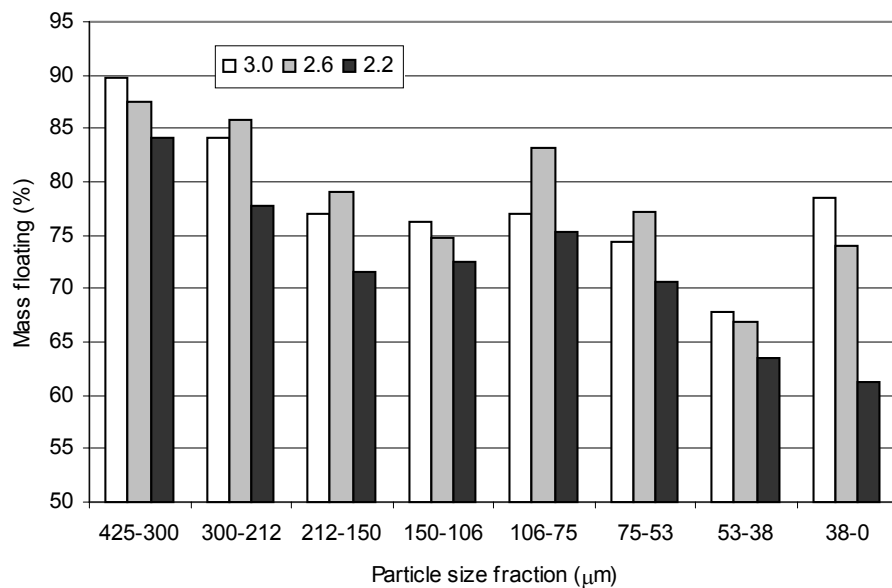


Figure 9.7 Percentage of material reporting to floats fraction at three separation densities

In all samples the majority of the feed material can be seen to report to the floats fraction. The highest degree of separation (i.e. most material reporting to the sinks fraction) was achieved in the finer size fractions and in the 2.2rd media. In general it can be seen that more material reported to the sinks fraction as the separation density

was decreased, although many of the mid density separations (2.6rd) exhibit higher masses in the float compared to the higher and lower densities. It was thought that this may be due to the difficulties associated with filtering the 3.0rd (made with TBE only) as the liquid would have a higher viscosity than the lower density liquids. The material recovery from the separations at this density was often inferior and this may have introduced a bias in the data.

9.4.4 Characterisation of feed and ground material

As previously shown in Table 4.5 the use of an AR digestion reduces the recovery of many elements from a sample in comparison with a total microwave digestion technique. However, in this experiment the generation of accurate data (true values) was not as important as being able to make comparisons between samples so the technique was fit for the purpose.

9.4.4.1 Bulk chemistry of feed sample

A representative sample of the feed material (all size fractions) used for the float-sinks experiment was subject to chemical analysis. The results have been presented in Table 9.5.

Element	Concentration ($\times 10^5$ ppm)
C	6.54
Fe	1.4
Zn	0.22
S	0.12
Ca	0.086
Mn	0.0079
Al	0.0079
Mg	0.0071
Cu	0.0032
Ti	0.00062
Ni	0.0004
Cr	0.0003
Ba	0.00004
Cd	<LOD
Pb	<LOD

Table 9.5 Chemical analysis of bulk feed sample [LOD - limit of detection]

The carbon content of the feed material was 65% with an associated iron concentration of 14%. Cadmium and lead were not measurable in the solutions.

9.4.4.2 Distribution of elements before and after grinding

The size fractions generated by the size characterisation of the feed were analysed to determine the concentration and distribution of elements in the original carbon ash. Similarly the size fractions of the ground material were analysed to determine the effect of grinding on the distribution of the elements. The distribution of the major elements in the sample before and after grinding is presented in Figure 9.8.

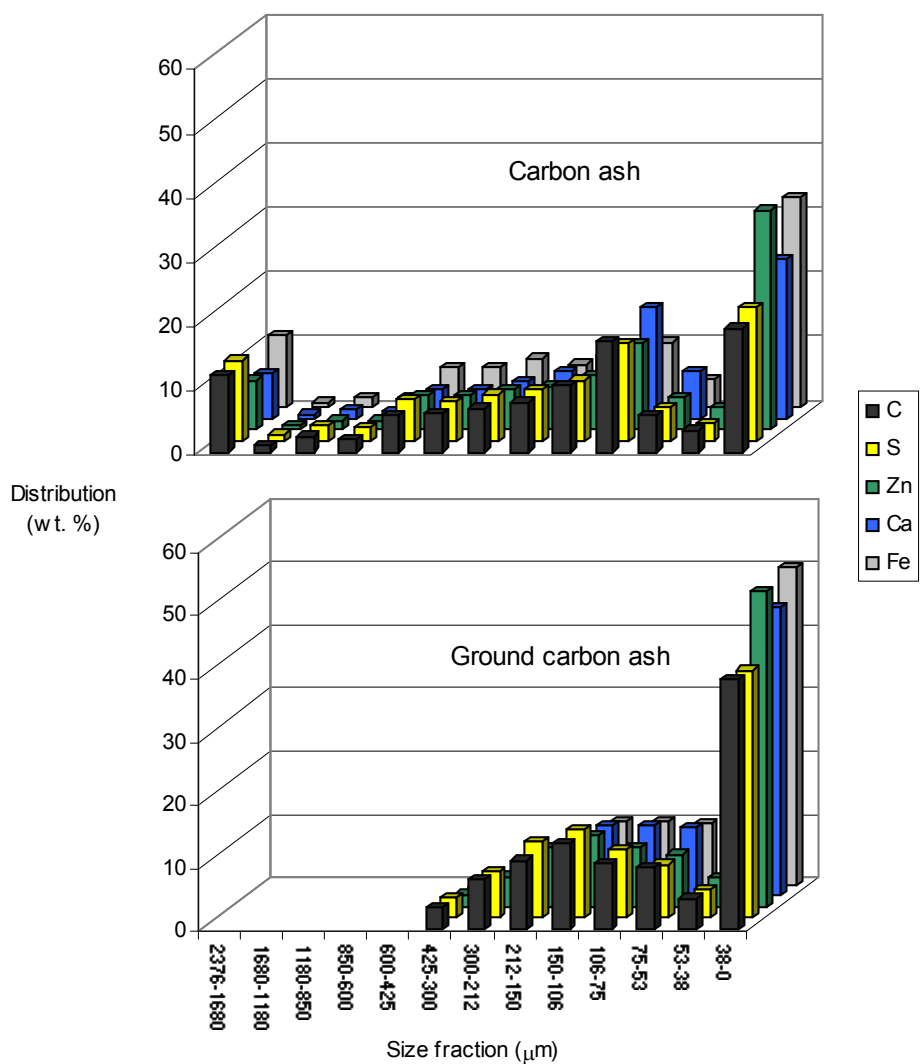


Figure 9.8 Distribution of major elements before and after grinding

In the original material the major elements are distributed mainly in the finest size fraction. Grinding the material had the effect of moving more of the elements in to the finest fraction. For example it can be seen that originally 20% of the carbon was present in the 38-0 μm fraction and after grinding this was increased to approximately 40%. The distribution of minor elements is presented in Figure 9.9.

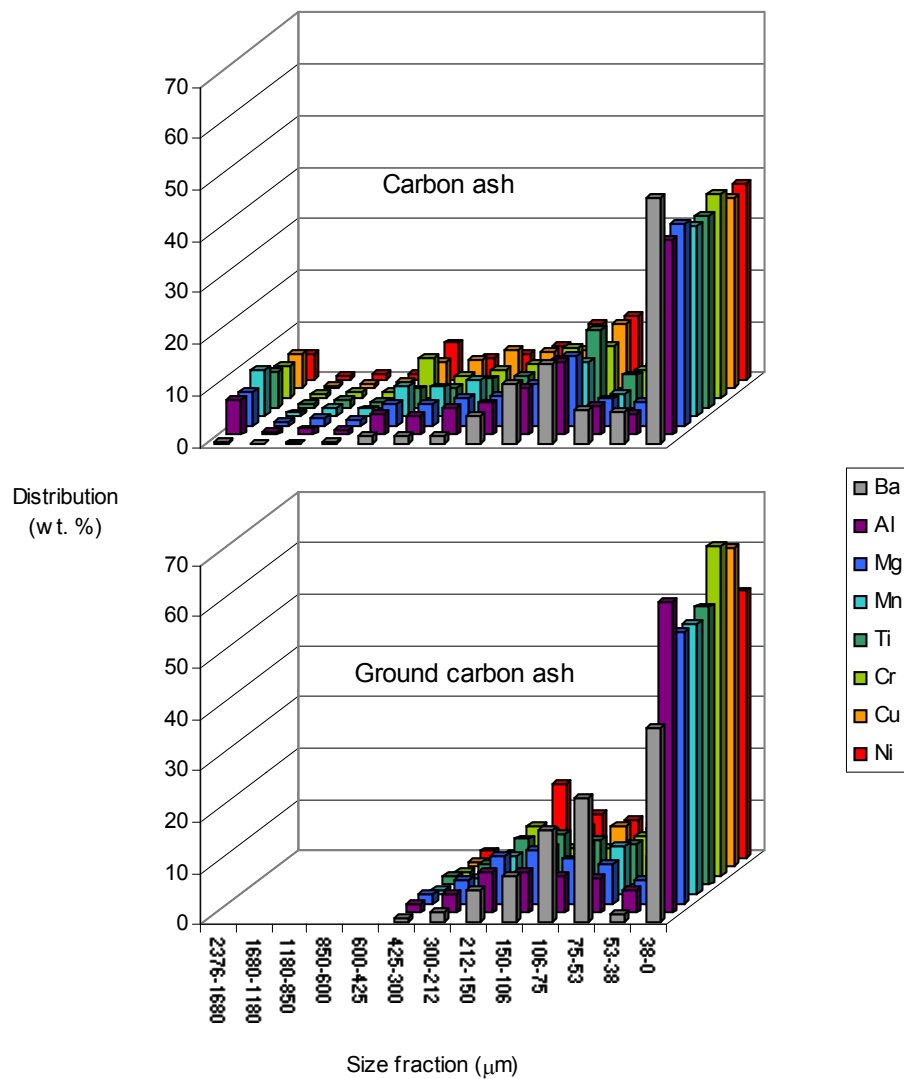


Figure 9.9 Distribution of minor elements before and after grinding

From Figure 9.9 it can be seen that in a similar manner to that observed with the major elements the grinding has moved the distribution of the minor elements into the 38-0 μm fraction. The results of the float-sink test would therefore determine if the movement of element distribution, through grinding, into the finer particles size range was effective in liberating the carbon from the non-carbon phases. The full characterisation results of the original and ground samples have been presented in Appendix 3.

9.4.5 Characterisation of float-sink samples

Samples of float and sinks fractions for the three separation densities were initially analysed to determine the carbon concentration only as this was the major element of interest. The concentrations of carbon in the floats are presented in Figure 9.10 and the sinks in Figure 9.11.

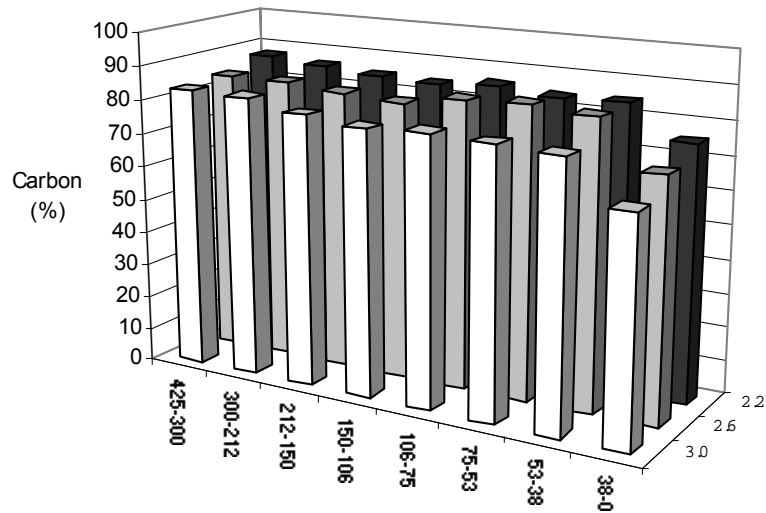


Figure 9.10 Carbon concentration in floats at three separation densities

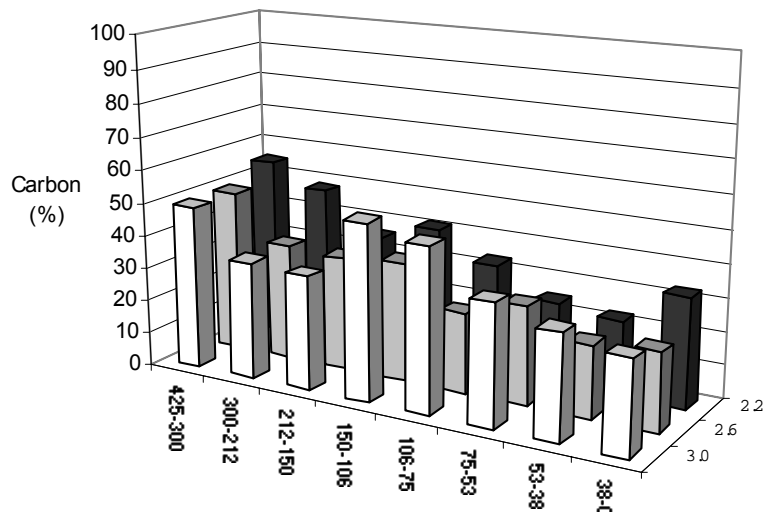


Figure 9.11 Carbon concentration in sinks at three separation densities

Carbon concentrations in the floats fractions were measured at levels between 65% and 89%. The results show that generally the carbon concentration of the floats fraction increased as the separation density decreased. The carbon concentration of the floats fraction in the 38-0 μm size fraction was significantly lower compared to the coarser sizes indicating the increased presence of non-carbon material in the samples. The agglomeration of particles in the finest size fraction observed during sample preparation, which was reduced using the new method, meant that particles might not have been well dispersed in the centrifuge. Entrapment of contaminants in the agglomerated material might then account for a reduced carbon concentration in the floats fraction and an increased carry over of carbon into the sinks sample. However, the reduced carbon concentration may also be as a result of the increased settling times required by the smaller particles. The carbon concentrations of the sinks fractions generally reduced as the particle size decreased indicating improved liberation of contaminant phases in the finer size fractions.

The distribution of carbon and other elements during the density separations was determined by incorporating the size distribution (to determine the contribution of each size fraction to the whole sample) and float-sink mass split with the element concentration data. The overall distribution of each element for the whole sample (all size fractions) was then reconstituted by summing the data from all of the size fractions for each separation density. The distribution of carbon in the floats fraction for each separation density is presented in Figure 9.12. The carbon distribution in the sinks is presented in Figure 9.13.

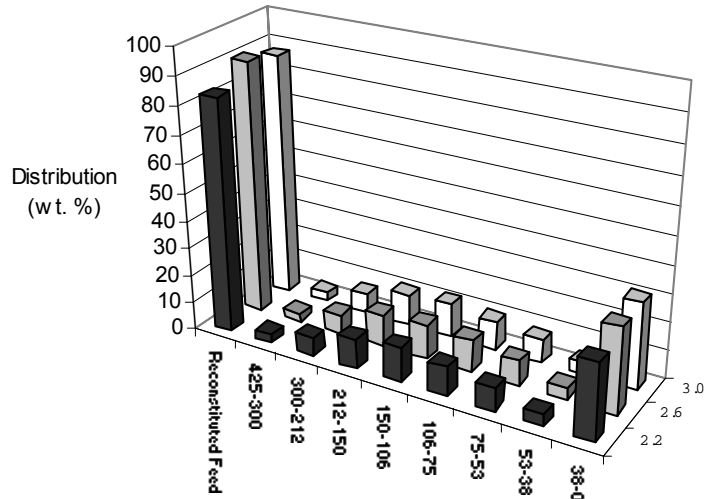


Figure 9.12 Distribution of carbon in floats fractions

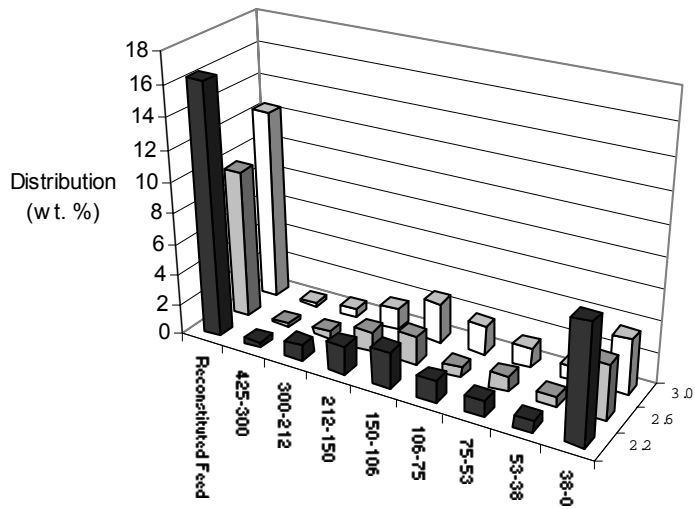


Figure 9.13 Distribution of carbon in sinks fractions

From the reconstituted data it can be seen that the majority of the carbon present in the samples reports to the floats fraction at all three densities. The highest degree of separation, i.e. more carbon reported to the sinks fraction, occurred at 2.2rd. This indicates that mixed carbon/non-carbon phases with an overall density in excess of 2.2rd were reporting to the sinks fraction. The carbon concentration of the floats

fraction generated at 2.2rd varied between 84% and 88% with the exception of the 38-0 μm fraction where the concentration was lower at 75%. To reduce the number of samples requiring further investigation only the fractions generated by the 2.2rd separation were subject to further chemical analysis.

9.4.6 Characterisation of 2.2rd samples

Sulphur and other contaminating elements were measured in the 30 samples generated by the 2.2rd separation. The results from each duplicate analyses were averaged to provide a single data point for each fraction. The results have been split into groups (major and trace) based upon the concentration of the element determined in the samples. The concentration and distribution of each individual major element has been presented whilst the trace elements have been summarised.

9.4.6.1 Major elements in float-sink fractions

The concentration and distribution of carbon in the samples generated at the 2.2rd separation only is presented in Figure 9.14 and Figure 9.15. The data has previously been presented in Figure 9.10 through Figure 9.13 but is included here for clarity.

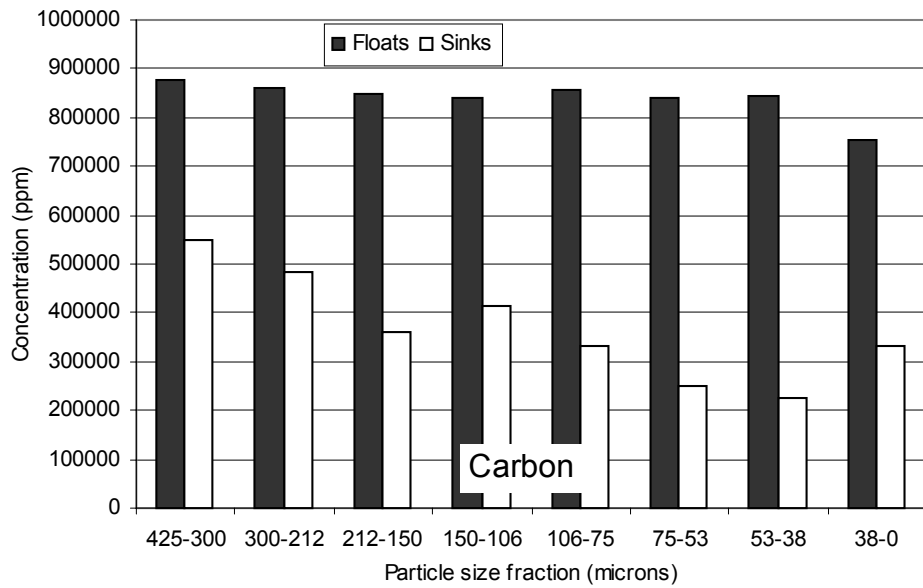


Figure 9.14 Carbon concentration in 2.2rd float-sink fractions

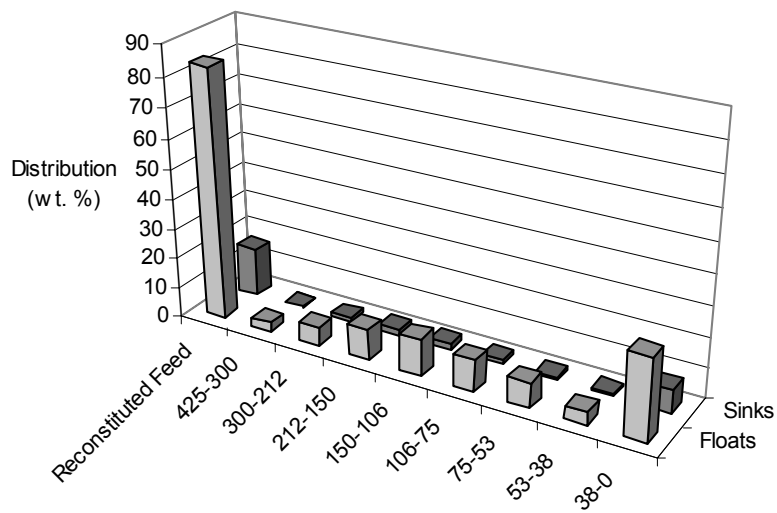


Figure 9.15 Carbon distribution in 2.2rd float-sink fractions

The results show that carbon concentrates in the floats for all size fractions although it was slightly less concentrated in the 38-0 μm fraction. The concentration of carbon in the sinks fraction reduced as the particle size decreased. The bulk of the carbon in the original sample reported to the floats, the majority of which was associated with the 38-0 μm fraction. The carbon reporting to the sinks was associated with the same size

sulphur reported to the floats fraction whilst the sulphur reporting to the sinks was mainly associated with the finest material. The concentration and distribution of iron in the samples is presented in Figure 9.18 and Figure 9.19.

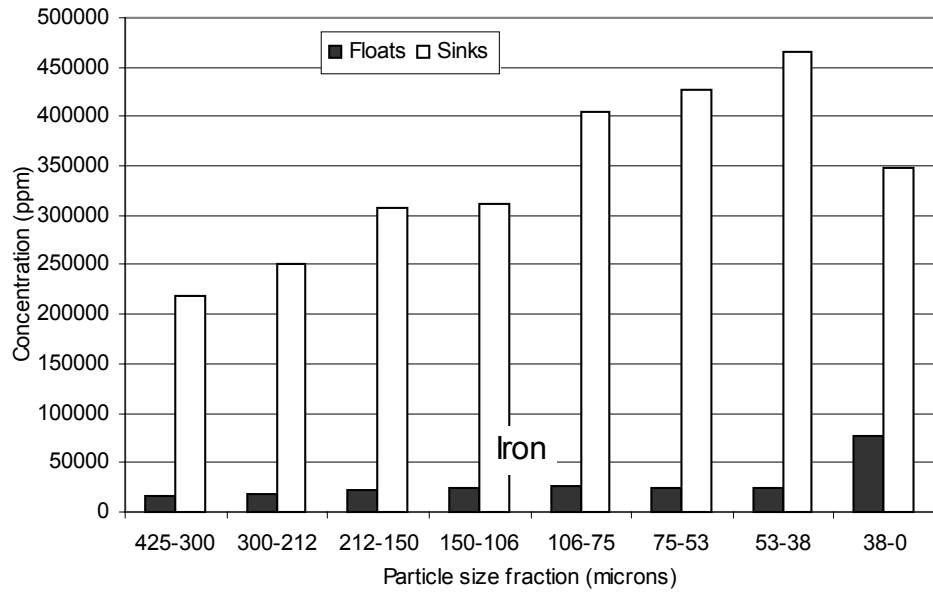


Figure 9.18 Iron concentration in 2.2rd float-sink fractions

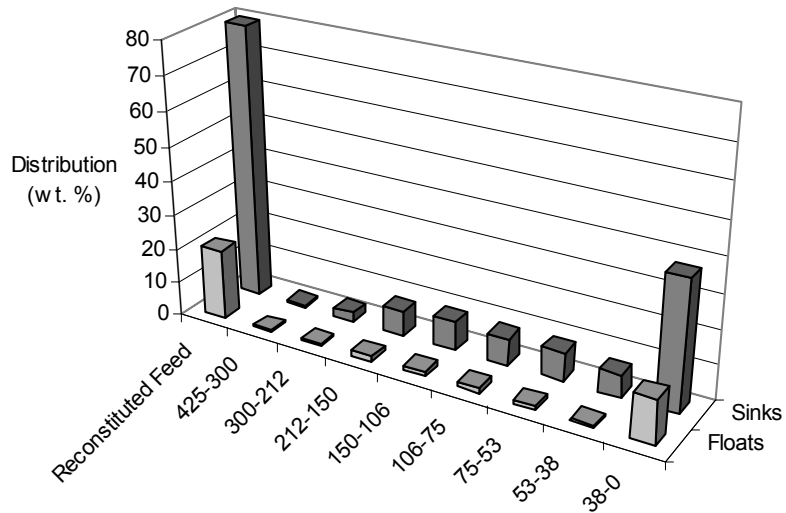


Figure 9.19 Iron distribution in 2.2rd float-sink fractions

Figure 9.18 shows that iron concentrates strongly in the sinks, the concentration increases as the particle size decreases, with the exception of the finest material. The concentration in the floats was comparatively low although it was slightly higher in the 38-0 μm fraction. This fraction accounted for the majority of the iron reporting to the floats. Zinc concentration and distribution is presented in Figure 9.20 and Figure 9.21.

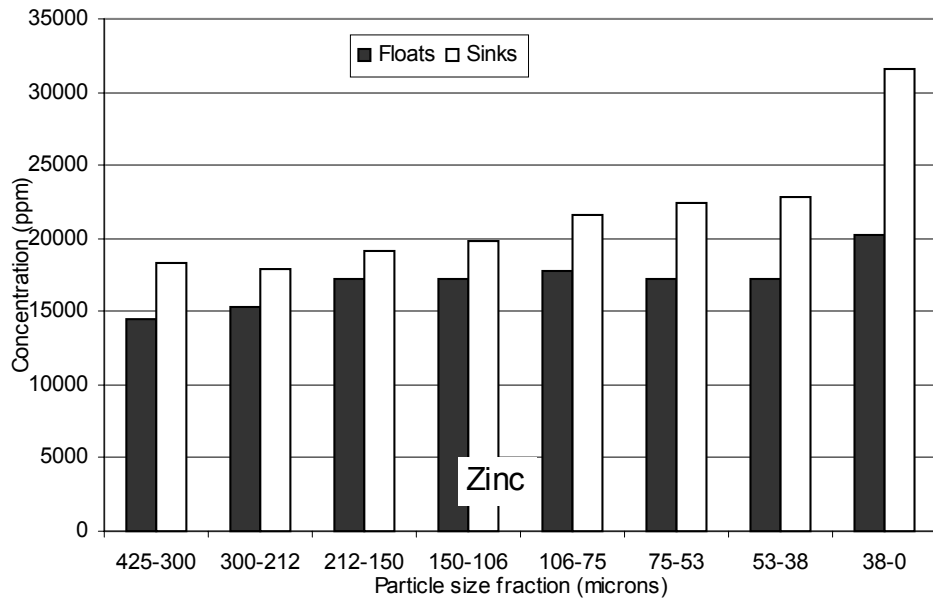


Figure 9.20 Zinc concentration in 2.2rd float-sink fractions

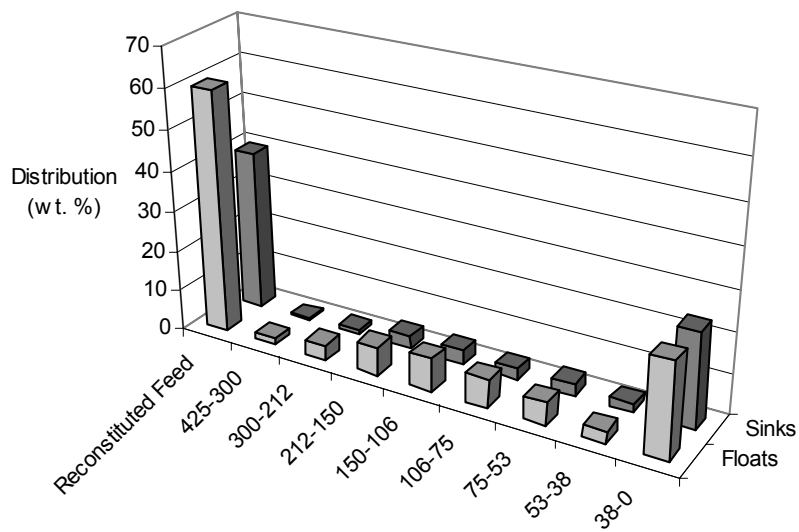


Figure 9.21 Zinc distribution in 2.2rd float-sink fractions

The results show that zinc concentrations were relatively uniform in all of the float-sink fractions although the concentration was slightly higher in the sinks for all sizes. It can be seen that the majority (60%) of the zinc reported to the floats. The concentration and distribution of calcium is presented in Figure 9.22 and Figure 9.23.

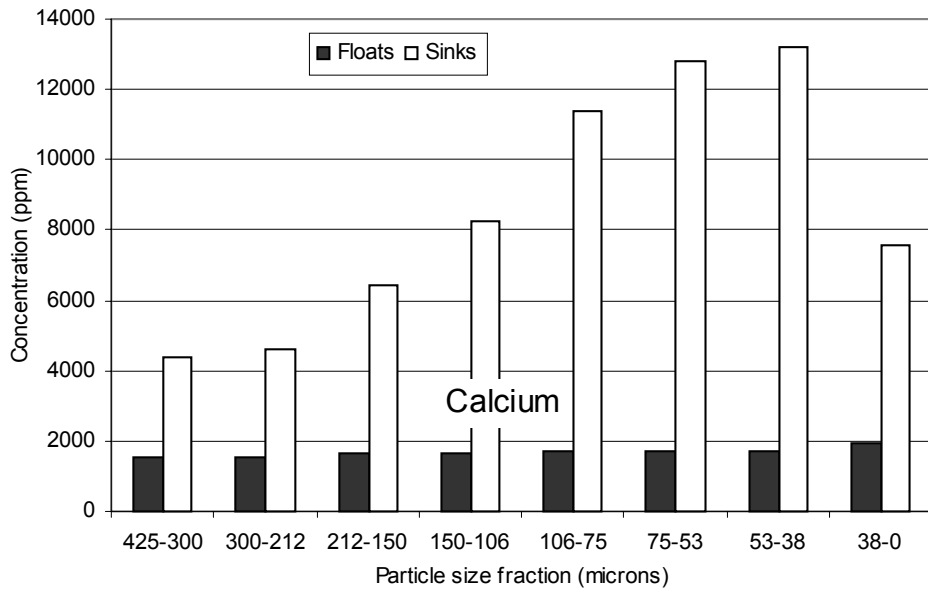


Figure 9.22 Calcium concentration in 2.2rd float-sink fractions

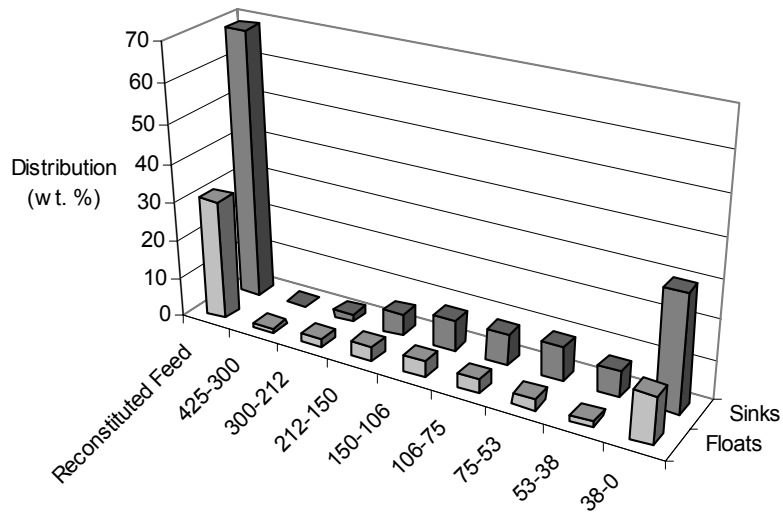


Figure 9.23 Calcium distribution in 2.2rd float-sink fractions

Calcium exhibited a similar behaviour to the iron in the samples. The element concentrated in the sinks, the concentration increased as the particle size decreases, with the 38-0 μm fraction being the exception. The majority of the calcium reported

to the sinks. The concentration and distribution of aluminium is presented in Figure 9.24 and Figure 9.25.

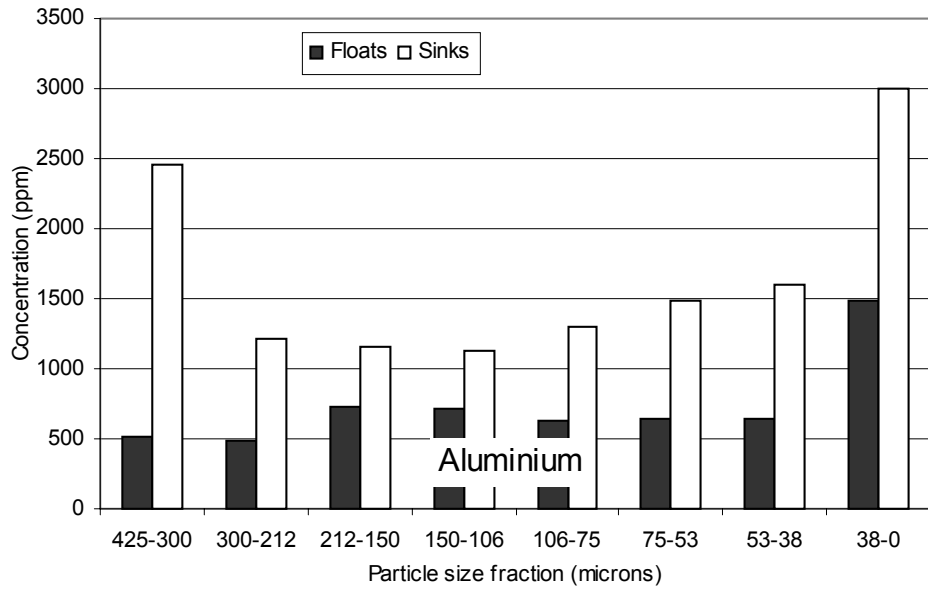


Figure 9.24 Aluminium concentration in 2.2rd float-sink fractions

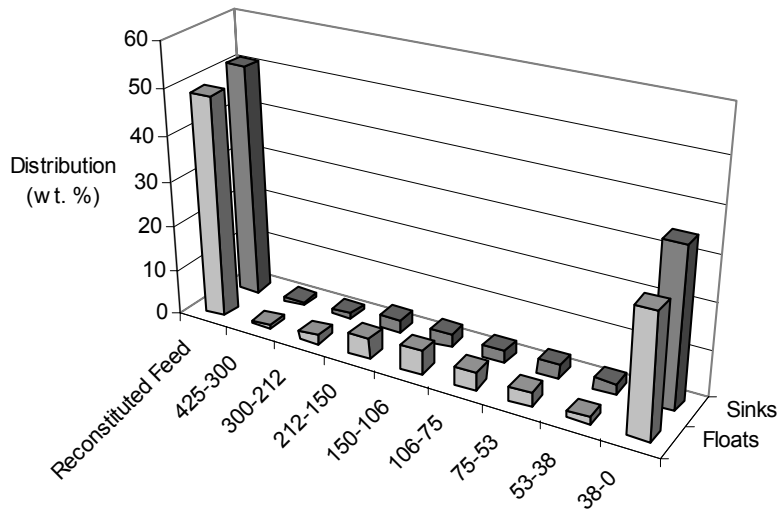


Figure 9.25 Aluminium distribution in 2.2rd float-sink fractions

From Figure 9.24 it can be seen that aluminium concentrated in the sinks. The element can also be seen to report equally to the floats and sinks. The concentration and distribution of manganese is presented in Figure 9.26 and Figure 9.27.

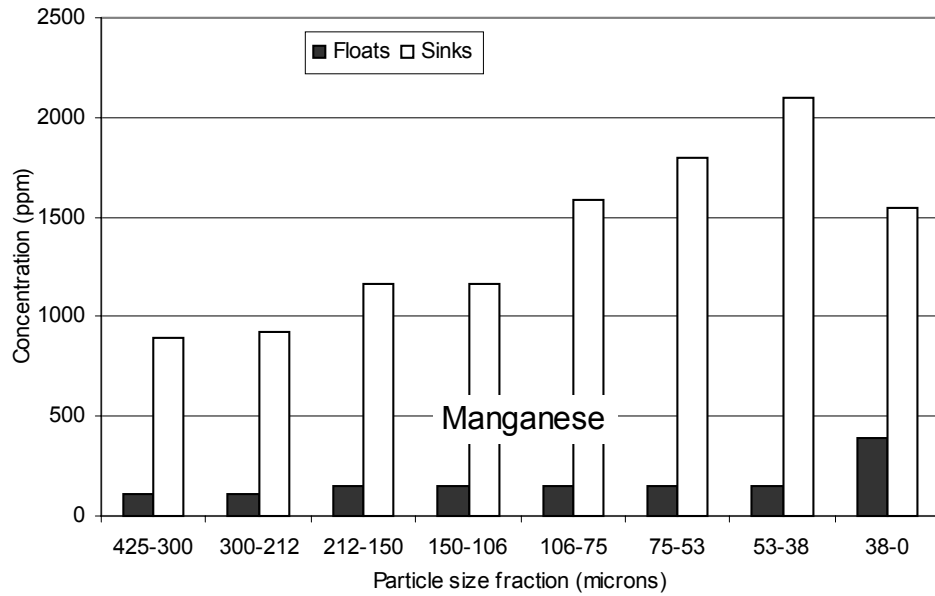


Figure 9.26 Manganese concentration in 2.2rd float-sink fractions

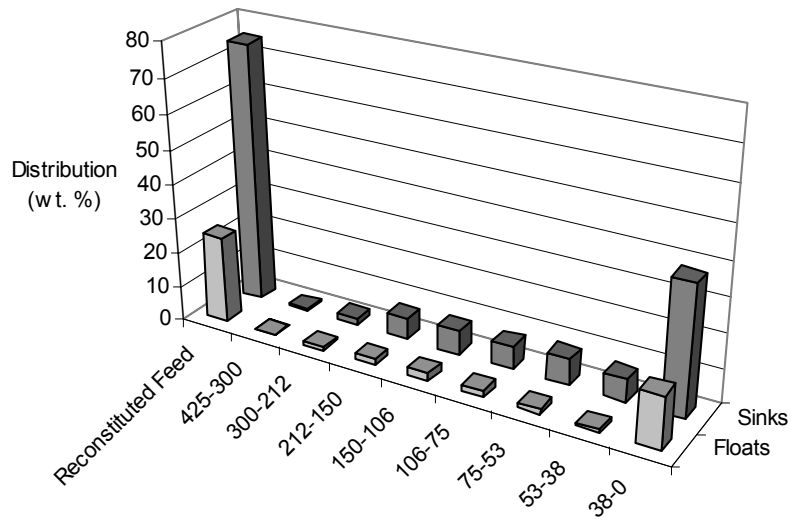


Figure 9.27 Manganese distribution in 2.2rd float-sink fractions

The results show that the manganese concentration pattern, although lower in magnitude, is similar to that of iron, also resulting in a similar distribution of the element. The concentration and distribution of magnesium is presented in Figure 9.28 and Figure 9.29.

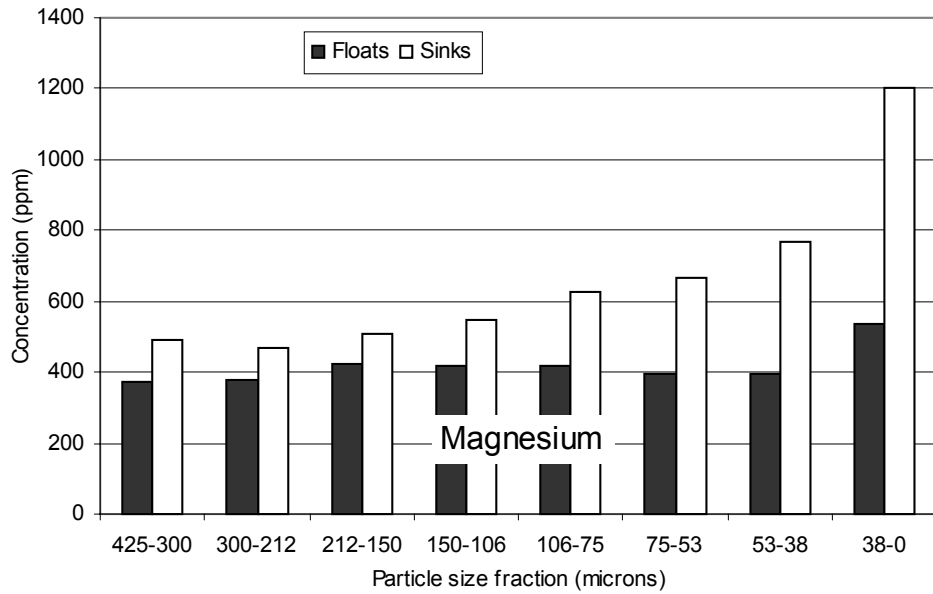


Figure 9.28 Magnesium concentrations in float-sinks fractions at 2.2rd

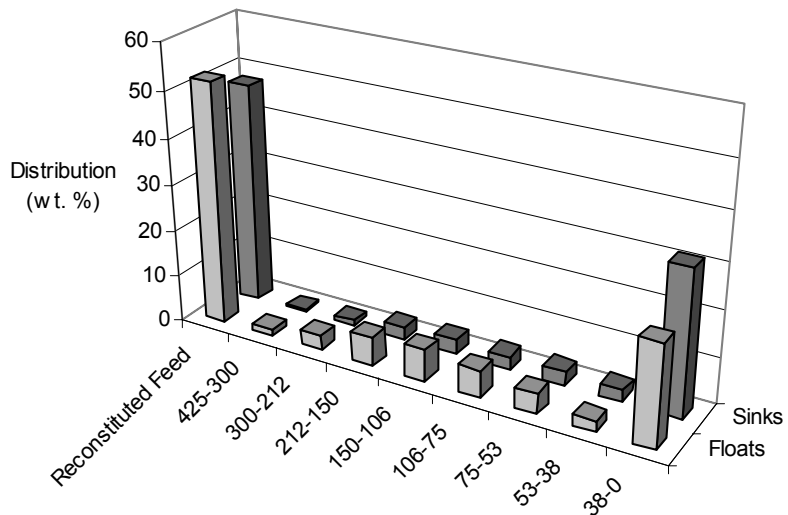


Figure 9.29 Magnesium distribution in 2.2rd float-sink fractions

The results show that magnesium was slightly concentrated in the sinks and was similarly distributed in the floats and sinks. The concentration and distribution of copper is presented in Figure 9.30 and Figure 9.31.

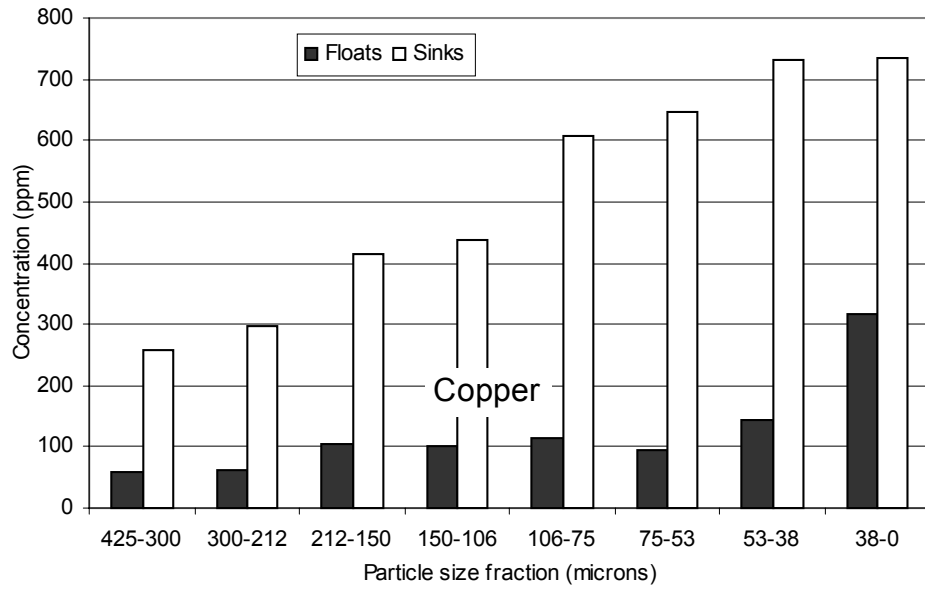


Figure 9.30 Copper concentration in 2.2rd float-sink fractions

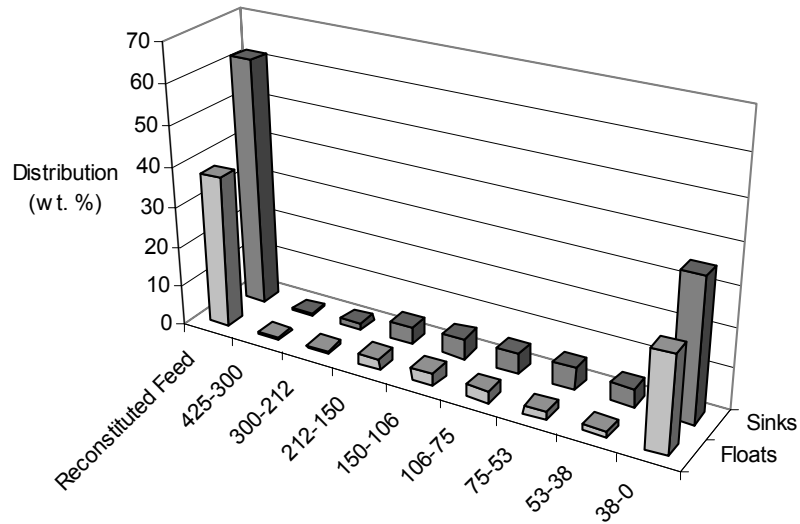


Figure 9.31 Copper distribution in 2.2rd float-sink fractions

Copper can be seen to concentrate in the sinks, the concentration increased as the particle size reduced. The majority of the copper reported to the sinks.

9.4.6.2 Distribution of trace elements in float-sink fractions

The distribution of trace elements in the float-sink fractions has been summarised in Figure 9.32 and Figure 9.33. The full concentration data can be found in Appendix 3.

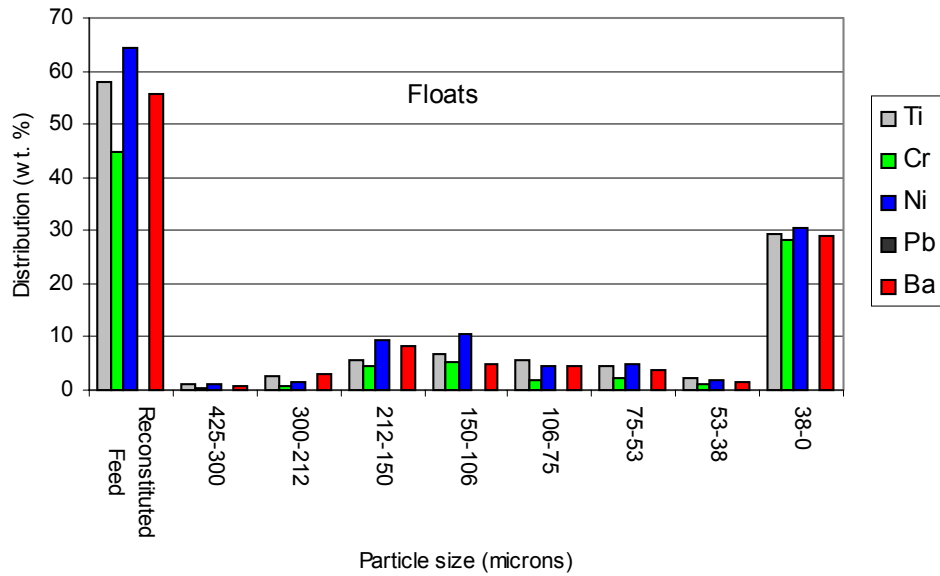


Figure 9.32 Trace element distribution in 2.2rd floats fractions

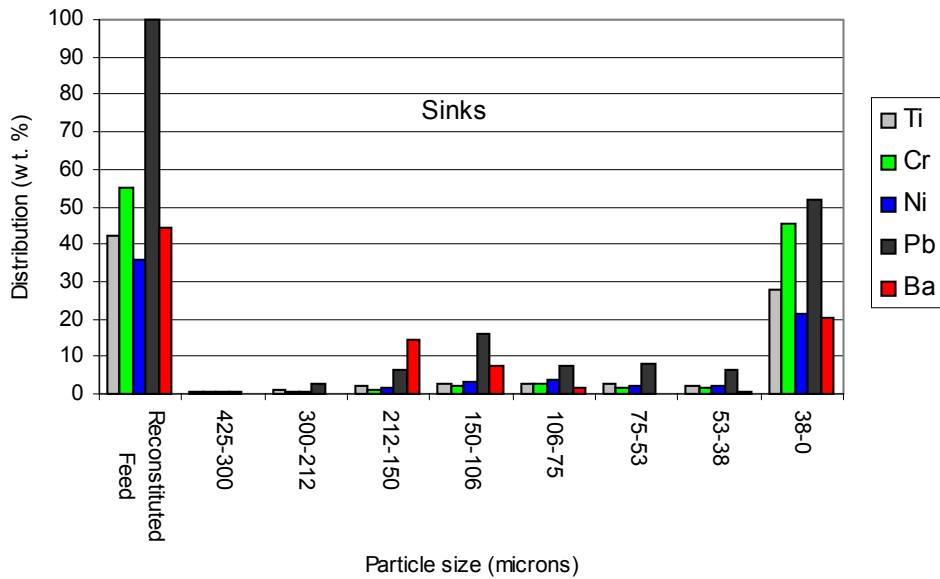


Figure 9.33 Trace element distribution in 2.2rd sinks fractions

The results show that all the trace elements exhibited a similar behaviour in the experiment. The distribution of each element between the floats and sinks was relatively balanced although the majority of nickel (64%) reported to the floats. It should be noted that although lead appears to report entirely to the sinks this is due to the element being present at levels below the detection limit in the floats. The use of

an Aqua-Regia digestion meant that silica could not be quantitatively analysed in the samples, although it was detected qualitatively during XRD analysis.

9.4.6.3 Mineral phase identification in float-sink fractions

Two pairs of floats and sinks were analysed, using XRD, to identify the mineral phases reporting to the fractions. Specific samples were chosen that appeared to indicate a good degree of separation, therefore reducing the chance of the same minerals being identified in both the floats and sinks. This ruled out the analysis of the 38-0 μm fraction since many elements were detected at similar concentrations in the floats and sinks. The samples selected were the 53-38 μm and the 106-75 μm floats and sinks. The results have been summarised in Table 9.6.

Sample	Floats	Sinks
53-38 μm	Wurtzite (ZnS)	Wustite (FeO)
	Sphalerite (ZnS)	CaO ₂
	Silicon (Si)	
106-75 μm	Wurtzite (ZnS)	Wustite (FeO)
	Sphalerite (ZnS)	CaO ₂
	Silicon (Si)	

Table 9.6 Mineral phases identified in 53-38 μm and 106-75 μm float-sink fractions

A limited number of minerals were detected with an acceptable level of certainty in the samples. Zinc sulphide, in two mineral forms, was detected in each floats fraction, but not in the corresponding sinks fraction. The relative density of both zinc sulphide minerals is in excess of 4 (see Table 9.2) so these minerals would normally be expected to report to the sinks. The XRD results therefore indicate that the mineral bearing phase was not fully liberated from the carbon causing it to report to the floats in mixed carbon phases where the overall particle density was less than the media density (2.2). As mentioned previously in Chapter 5 the presence of silicon (as silicon) in the carbon ash is unlikely. The result might be indicative of silica in the floats fraction although the standard XRD peaks are different. Calcium and iron minerals were detected in the sinks while silicon was detected only in the floats.

9.5 Interpretation of float-sink test

The ultimate aim of the float-sink experiment was to determine the potential for the concentration of carbon through the physical separation of the contaminant elements. The carbon concentrates (floats) generated during the experiment consisted of 80-90% carbon in all but the finest fraction. The 38-0 μm floats comprised of only 75% carbon, whilst the carbon measured in the sinks fraction was higher in comparison to the other sizes. This concentration difference was significant since the grinding process resulted in 40% of the ball mill feed material reporting to the 38-0 μm fraction. The reduced carbon concentrations measured in the floats generated from this fraction indicated that contaminant elements remained associated with the carbon at fine particle sizes. However observations made during sample preparation and separation suggested that the experimental method was not as effective for application to the finest material in comparison with the coarser fractions. The 38-0 μm feed material might still have contained agglomerated particles even after extra precautions were taken which might result in the physical entrapment of previously liberated phases and hence incorrect reporting to the floats or sinks. An increased loss of fine material was also experienced during recovery of the floats and sinks from the centrifuge tube after the test.

Individual analysis of each contaminant element in the floats and sinks samples showed that although some elements were effectively separated from the carbon phase during the test, others were not. Elements that were effectively separated from the carbon phase reported to the sinks fraction resulting in a higher concentration in the sinks compared to the corresponding floats. Such elements were found to include iron, copper, calcium and manganese, which concentrated strongly in the sinks although in each case a relatively low concentration of the element remained associated with the floats. The residual concentration in the floats might be an indication of physical entrapment during the separation or a result of incomplete liberation of the contaminating element during grinding.

Other than carbon, the only element observed to concentrate significantly in the floats was sulphur. Relatively uniform levels of sulphur were measured in all floats fractions and were all found to be approximately 1.2-1.3% sulphur, with the exception of the

38-0 μm fraction where the concentration in the floats and sinks was similar and also lower (0.7% in Floats, 0.9% in Sinks). Zinc was slightly more concentrated in the sinks fraction, although it was still present in the floats at similar levels. The zinc distribution showed that, overall, more of the element reported to the floats fraction. Mineral phase identification revealed that zinc sulphides were present in a selection of floats but were not detected in the corresponding sinks. This suggests that zinc sulphide was not separated from the carbon product whilst the zinc that reported to the sinks was in an alternative form, for example as a component of brass. Iron and calcium minerals were detected in the sinks, which may be expected due to the high concentration of these elements in the fraction. Using XRD silicon was detected in the floats fraction, but not in the sinks indicating an association of the element with the carbon phase. However, since the element was not quantitatively analysed it cannot be assumed that the element did not also report to the sinks. If silicon was perfectly liberated in the feed samples it might prove difficult to separate since its specific gravity (2.32) was relatively close to the separation density (2.2) in comparison with the other mineral phases present in the carbon ash (see Table).

The distribution of elements between the floats and sinks and also across the particle size range demonstrated the massive contribution of the 38-0 μm fraction to the overall elemental distribution. The separation of all elements was inferior for this particular fraction which was due to a number of factors which have been summarised below:

- Agglomeration of particles after grinding
- Systematic errors in experiment (particularly in floats and sinks recovery) which were more significant for the finer material
- Poor liberation of contaminant phases due to high dispersion of elements within carbon matrix

The poor separation of carbon from contaminants measured in the 38-0 μm fraction might have been due to a combination of all these factors. To further investigate the liberation and dispersion of contaminant phases present in the ground carbon ash material a sample was prepared for SEM analysis.

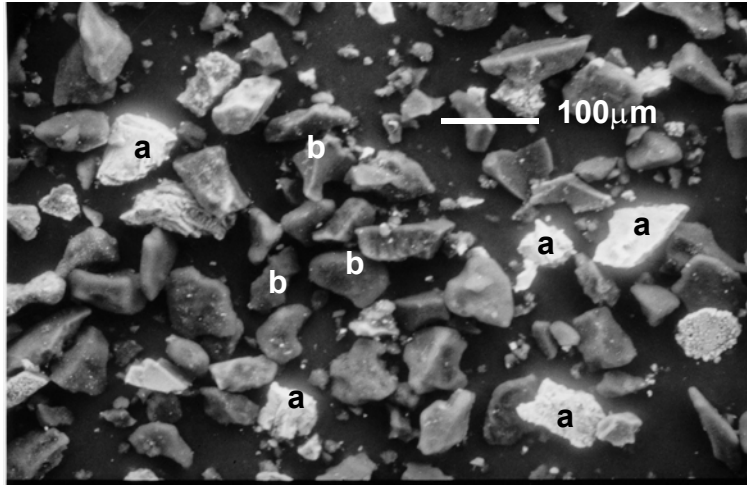
9.5.1 SEM investigation of float-sink feed samples

The extent to which mineral phases were liberated during grinding was investigated with a SEM. Two samples were prepared for analysis, the first consisted of a feed sample as input into the separation and the second consisted of an identical sample but after LTA. The sample was low temperature ashed for a period of 6 hours with the objective to remove as much of the carbon as possible whilst leaving all other phases intact. Theoretically the approximate particle sizes of the material remaining 'carbon-free' sample could then be compared to the original sample to determine the extent of contaminant dispersion.

The sample selected for analysis was the finest size possible that was thought to be free of agglomerated material, i.e. the 53-38 μm fraction. Images of the non-ashed sample have been presented first. Qualitative EDX analysis was used to identify elements present in areas of interest within the samples.

9.5.1.1 Non-ashed sample

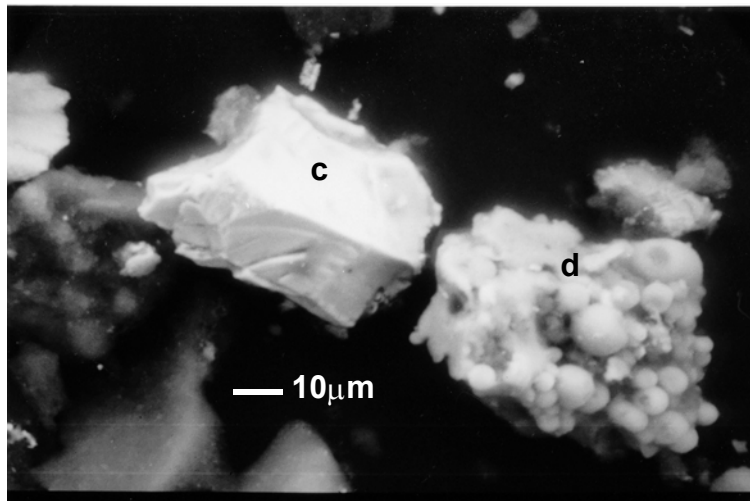
A series of three images of the 53-38 μm fraction have been presented. One image shows a general, lower magnification, view of the sample (Figure 9.34) whilst the remaining two images were collected at a higher magnification and show some typical particles present in the sample (Figure 9.35 and Figure 9.36).



A mixture of metallic phases (shown brighter) (a) and (darker) carbon based phases (b).

Material <38 μm can be seen in the sample.

Figure 9.34 SEM micrograph of ground 53-38 μm fraction



Higher magnification image of two metallic phases with carbon phase below left. The sample consisted of:

- A particle (c) comprising of iron with a trace of zinc.
- A particle with melted appearance (d) comprising mainly of aluminium, magnesium, iron, phosphorus and silicon. Also traces of zinc and sulphur.

Figure 9.35 High magnification SEM image of ground 53-38 μm fraction - Image 1

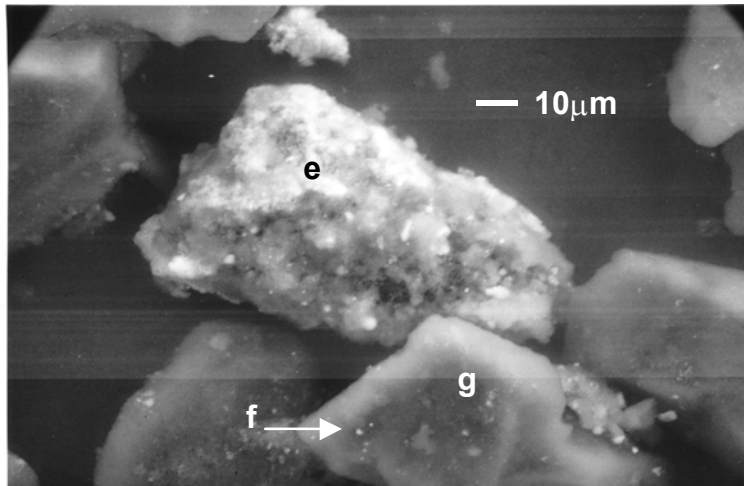


Figure 9.36 High magnification SEM micrograph of ground 53-38 μm fraction - Image 2

A metallic mixed particle **(e)** consisting of iron, zinc and sulphur.

Sub-micron metallic particle associated with surface of carbon phase **(f)** consisting of iron, zinc and sulphur.

Multiple analysis in carbon phase **(g)** zinc and sulphur.

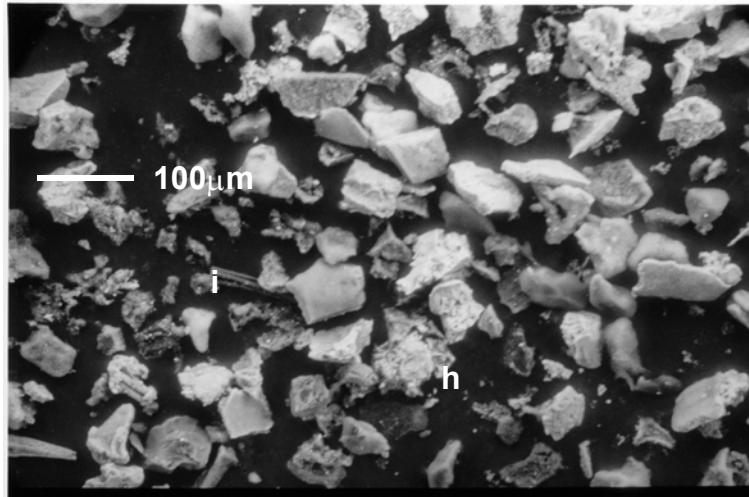
From Figure 9.34 it can be seen that the sample consisted of separate metallic and carbon based phases. The sample was also found to contain a significant amount of material that was $<38 \mu\text{m}$, which should have reported to the next finest size fraction during wet sieving. Although it was also thought to be possible that the fine material may have formed as a result of particle-particle attrition during sample handling. The presence of the fine material also makes the determination of the extent of contaminant dispersion in the sample more difficult to identify. This is discussed during analysis of the ashed sample.

Closer inspection of typical particles in the sample revealed the presence of sub-micron metallic contaminants associated with the surface of carbon particles, which would account for a portion of the non-carbon elements reporting to the floats. Particles in the sample that appeared to be well liberated included the iron and mixed phase particles present in Figure 9.35 which are likely to have reported to the sinks as both particles would have an overall density in excess of the medium (2.2rd). The type of particle labelled (e) in Figure 9.36 was common in the sample and was found to consist of a mixture of iron, zinc and sulphur. Similar particles were also found which had no iron content, but were much rarer. This particle type was generally separate from any carbon phases and is likely to be responsible for a part of the zinc and sulphur elements reporting to the sinks. The portion of zinc and sulphur that

reported to the floats were likely to be as a result of particles such as that labelled (g) in the same image. Sub-micron zinc-sulphur phases were found on the particle surface and were also detected within the carbon. When EDX analysis was conducted at various points within this and other similar particles, zinc and sulphur was often detected, although it was rarely visible. This may indicate that the zinc-sulphur phase was highly dispersed in the carbon. The level of dispersion was investigated by examining an ashed sample with the SEM.

9.5.1.2 Ashed sample

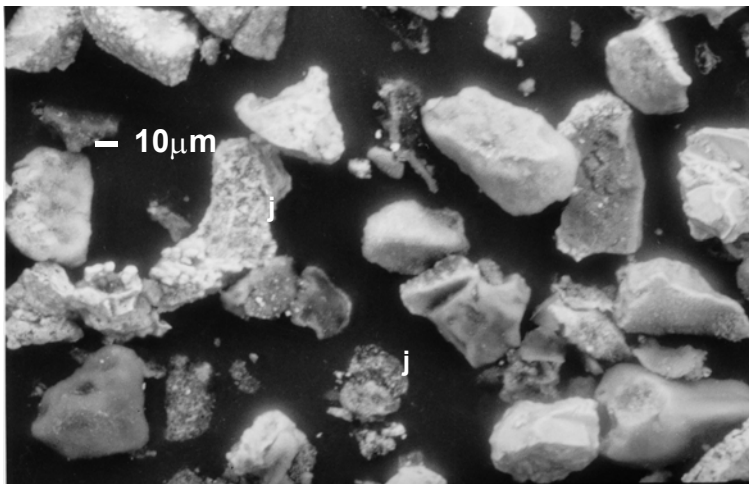
A lower magnification image of the ashed sample is has been presented in Figure 9.37 and a higher magnification image in Figure 9.38.



The increased presence of particles (**h**) with a rough surface was identified.

A splinter of multiple core steel wire (**l**).

Figure 9.37 SEM image of ashed 53-38 μm fraction



Close up of particles in Figure 9.37.

Residual carbon was still present after ashing.

Evidence of former metallic/carbon mixed phases (**j**)

Figure 9.38 High magnification SEM image of ashed 53-38 μm fraction

Theoretically the approximate particle size distribution of the ashed sample could be compared to the original sample to determine the liberation of carbon from contaminant phases in the 53-38 μm size range. The presence of undersize material in the original sample complicated the analysis since the fine material present in the ashed sample could not confidently be determined to have originated from a mixed carbon phase. The ashed sample was also found to contain carbon, which had not been completely removed during ashing.

A small wire splinter, see Figure 9.37, not associated with any carbon phases and would readily report to the sinks was found in the sample. This was not a common occurrence as the majority of the wire was present in the coarser size fractions. A rough surface texture, not observed in the original sample, was found in the ashed material. The texture was thought to become visible as a result of the carbon in a mixed phase particle being removed, exposing the former phase interface. Examples of the previously mixed phase particles have been labelled (j) in Figure 9.38. The two particles, when liberated from the carbon phase, would report to the next smallest size fraction (38-0 μm), indicating that the carbon ash would need to be ground finer to improve liberation.

9.5.2 Elemental relationships in float-sink samples

The SEM analysis carried out in this chapter and also during the initial characterisation study found that contaminants were usually present in mixed phases. The only exception to this was found to be iron, which was present both as individual particles and in the form of wire. The association of various elements in the float-sink samples generated at 2.2rd was analysed by comparing the concentrations of different elements directly to each other. The data from the 38-0 μm floats and sinks has not been included due to the experimental difficulties associated with preparing and separating the sample.

When the concentration of carbon and sulphur in float-sink samples were compared a linear relationship was produced, see Figure 9.39.

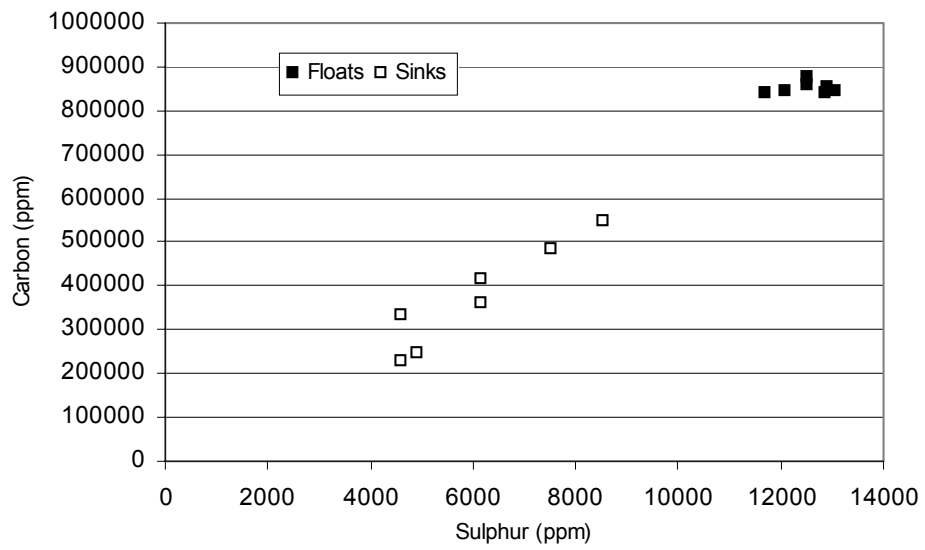


Figure 9.39 Relationship between carbon and sulphur concentrations in float-sink samples

The linear relationship between the sulphur and carbon concentrations across both the floats and sinks samples indicated the association of the two elements in the carbon ash. The sulphur bearing minerals detected previously with XRD included sphalerite and wurtzite, both zinc sulphide minerals. To determine if the sulphur content was related to zinc the relationship was plotted and has been presented in Figure 9.40.

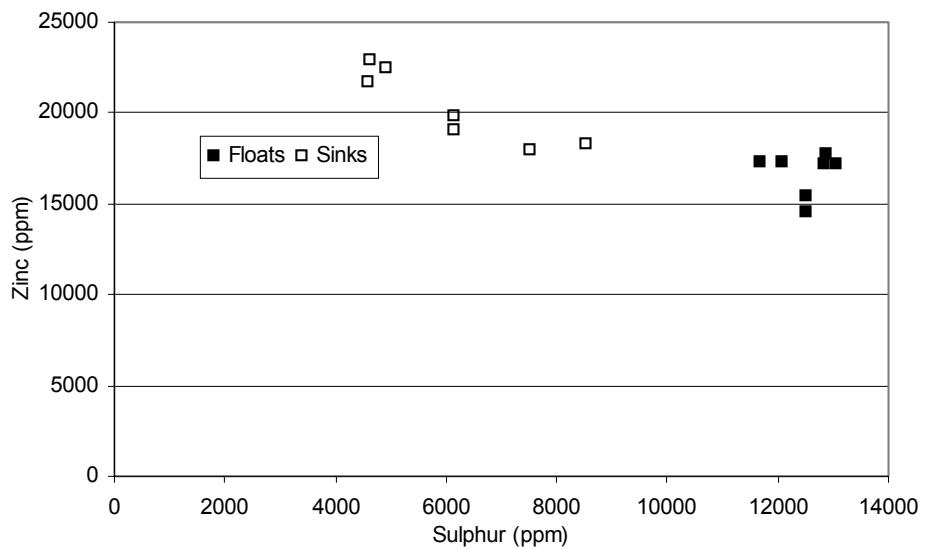


Figure 9.40 Relationship between zinc and sulphur concentrations in float-sink samples

The relationship between zinc and sulphur concentrations is not as clear, indicating that zinc is present in a number of phases in the float-sink fractions. During this research zinc had been detected in the carbon ash samples in the form of sulphur minerals and also as zinc oxide, the original feed chemical into the rubber compound. Zinc sulphides were detected both inside, and on the surface of, <math> < 53 \mu\text{m}</math> carbon particles, it was thought that these occurrences would be responsible for the majority of the zinc reporting to the floats. Zinc sulphide was also found as discrete particles and also in mixed metallic phases, which are likely to have an overall relative density of >2.2 and therefore would report to the sinks. The float-sink experiment demonstrated that a large proportion of the zinc phases were not liberated from the carbon by grinding, indicating that the element was highly dispersed in the carbon ash.

Major elements that appeared to be well liberated from the carbon ash included iron. The iron originates in the carbon ash mainly from the beads and also from the reinforcing mesh material. Prior to inclusion in the tyre the wire is coated in brass to promote adhesion between the rubber and the bead. The relationship between iron and copper, a part of the brass alloy, in the floats and sinks has been presented in Figure 9.41.

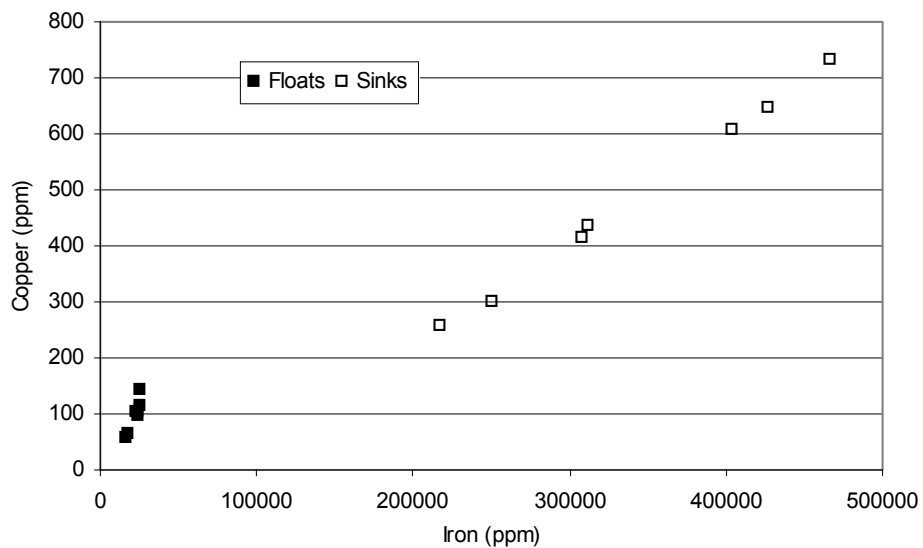


Figure 9.41 Relationship between copper and iron concentrations in float-sink samples

From Figure 9.41 it can be seen that the copper concentration in the floats and sinks related to the iron concentration, indicating that the brass coating on the wire remains associated with the post-combustion steel. The validity of this type of correlation was checked by comparing the concentrations of manganese, used in the production of the steel forming the bead wire and this yielded a similar relationship as presented in Figure 9.42.

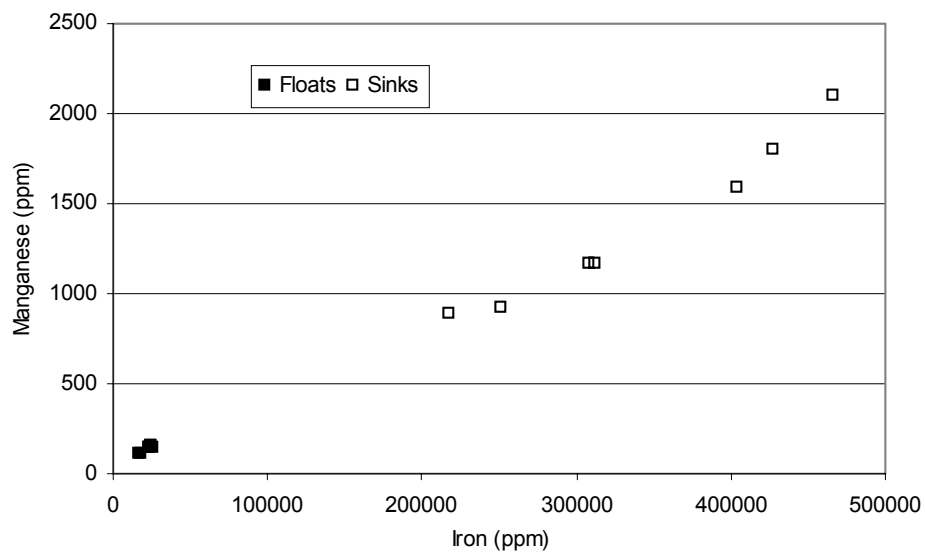


Figure 9.42 Relationship between manganese and iron concentrations in float-sink samples

The linear relationship in Figure 9.42 indicates that the manganese content of the samples was associated with the iron phase.

9.6 Interim summary and conclusions

The potential for the physical separation of contaminant phases from the carbon product was investigated with the use of a centrifugal float-sink test. A sample of carbon ash that had been generated during the pilot scale magnetic separation trial was subject to wet grinding in a ball mill to enhance liberation. Grinding of the carbon was shown to re-distribute both the carbon and contaminant elements mainly into the finest particle size, 38-0 μm . During the preparation of samples for float-sink testing the re-agglomeration of particles within the finest size separated fraction was observed. By altering the experiment methodology specifically for the single fraction

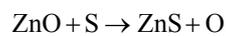
the formation of agglomerates was minimised although the results indicated that it was not completely successful. The separation of carbon from non-carbon elements in the 38-0 μm fraction was generally inferior to that measured in the coarser fractions although experimental factors might also have been responsible for the poorer separation. The precision of the experiment, measured by comparing the recovered masses of duplicate samples was found to be acceptable which indicated that the experimental method was capable of producing reliable results.

The most highly concentrated carbon product was generated at the lowest separation density used in the experiment. At a separation of 2.2rd carbon concentrates in the region of 85% were generated from all but the 38-0 μm feed fraction (see figure 9.14). The results indicated that of the major carbon ash components, certain elements were well separated from the carbon whilst others were not. Iron, calcium, manganese and copper concentrated in the sinks which indicated that the phases containing these elements were dense and liberated from the carbon. Conversely, zinc and sulphur were present in similar concentrations in both the floats and sinks indicating poor liberation. Comparing the concentrations of carbon and sulphur in float-sink samples indicated that the two elements were linked, although it was not determined if this was a chemical or physical relationship. SEM analysis of individual feed fractions confirmed that zinc and sulphur bearing phases were highly dispersed in the carbon material suggesting that a physical separation would be difficult.

9.6.1 Sulphur phases in float-sink samples

XRD analysis of the 53-38 μm floats fraction revealed the presence of zinc sulphide mineral phases. This compound forms due to the reaction of the zinc oxide with sulphur during the incineration process. In the original tyre, the sulphur added during the vulcanisation process is bound to carbon in organic compounds, which decompose during tyre pyrolysis and the sulphur formed reacts with zinc oxide (Darmstadt *et al* 1994). The presence of sulphide minerals in the carbon ash suggests the same is true for the incineration process at STR. It should also be noted that a small proportion of sulphur in the feed tyre originates in the carbon black filler material. The float-sink experiment demonstrated a direct relationship between the concentration of carbon and sulphur in fractions suggesting a physical association in the carbon ash. The

sulphur association is likely to take two main forms; as surface deposits of zinc sulphide, which have also been identified with a SEM, and also as organic sulphur compounds. By assuming all of the zinc in the sample to be converted to zinc sulphide an estimation can be made of the concentration of sulphur associated with the organic phase. The balance of zinc and sulphur vary slightly between the two mineral forms of zinc sulphide. Wurtzite is slightly richer in sulphur (S/Zn = 1.001) than sphalerite (S/Zn = 0.995) (Scott and Barnes, 1972) but since the proportion of either mineral form is unknown in the carbon ash the calculation assumes that the reaction and stoichiometry is assumed to be as shown in Equation 9.1.



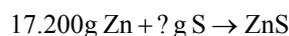
RMM

Zn = 65.38g

S = 32.06g

Equation 9.1 Reaction of zinc oxide with sulphur during pyrolysis/incineration process

The concentration of zinc in the 53-38 μm fraction was measured as 17,200 ppm and sulphur as 13,000 ppm. Assuming complete conversion of zinc to zinc sulphide, as shown in Equation 9.1, the excess sulphur present in the sample can be calculated. The calculation is simplified by assuming a sample quantity of 1 kg. The concentration of sulphur in the sample not present in the form of zinc sulphide is calculated as shown in Equation 9.2.



$$0.26309 \text{ moles S} = 8.434\text{g} = 8435\text{ppm}$$

Therefore the sulphur not associated with zinc is :

$$13,000 - 8435 = 4565\text{ppm}$$

Equation 9.2 Calculation of excess sulphur in zinc oxide reaction

The sulphur in the material not associated with zinc was estimated to be 4565 ppm, which is in the order of that normally associated with virgin carbon blacks (0.2-1.2%); see Table 2.4.

The simple hydrochloric acid leach process described previously demonstrated the potential of such a process to produce a carbon concentrate by generating a 92% carbon product. However, employing an acid leach process consisting of a combination of strong acids (such as hydrochloric and nitric acids), as well as hydrofluoric acid to aid removal of silica phases, could remove virtually all mineral and metallic elements associated with the carbon ash. This assumes that they are physically available to the leachant, since the hydrochloric leach was found to perform similarly not only on carbon ash in the original size distribution, but also with powdered material, which suggests good availability. This may then lead to the development of a product with a similar bulk chemistry to the carbon black input into the tyres typified by a very high carbon concentration and very low ash content (<0.2%). An estimation can be made of the carbon content of the potential product if the complete removal of the ash forming content of the carbon ash is assumed. The balance of the material can then be assumed to consist of carbon, sulphur oxygen and hydrogen. If the oxygen and hydrogen content are considered to be similar to that of commercial grade carbon black (0.4 wt.% each, see Table 6.6) then carbon content of the acid leached product could be as high as 98.7%. In practice the actual carbon concentration is likely to be less as 100% removal of the mineral content is unlikely. Standard physical and chemical characterisation techniques applied to carbon blacks would then be required to assess properties such as the reinforcing ability prior to reuse.

The application of this type of acid leaching process would be dependent to a large extent on the market value of the product that was generated. The market demand for the product would also have to be considered, since a recycled carbon black might be viewed as inferior to virgin carbon blacks in much the same way as retreaded tyres are compared to newly manufactured tyres.

9.6.2 Origins of elements in float-sink samples

Elements that were well separated from the carbon generally originated from the bead wire of the original tyres. Iron and manganese originate in the steel whilst copper originates from the brass coating. The destination of the zinc content of the brass coating cannot be specified due to the zinc that was originally associated with the rubber compound (as zinc oxide). However, it is likely that zinc in the brass mainly reported to the sinks whilst zinc in the carbon ash reported to the floats or sinks depending on the overall density of the mixed phase particle. An element that originated in the rubber compound but was still effectively separated was calcium. Calcium carbonate originates in the rubber compound as filler in the pre-vulcanised tyre to enhance characteristics such as stiffness and reinforcement. Other elements that initially formed a part of the rubber compound such as zinc and sulphur were found to be present as highly dispersed mixed phases, which were not liberated from the carbon and therefore remained associated with the carbon concentrates.

The float-sink experiment indicated that the high dispersion of contaminants in the carbon would make a high quality separation based on density difficult to achieve without further size reduction. The batch grinding process carried out on the carbon ash to enhance liberation did not result in a sample consisting solely of dispersed carbon and contaminant phases and this was confirmed by the analysis of the floats and sinks. Further grinding to finer particle sizes followed by float-sink testing would be required to quantify the liberation of contaminants from the carbon ash. However, further grinding would also result in an increase of material reporting to the 38-0 µm particle size range, making the accurate analysis of the sample difficult due to the problems encountered with the treatment of the finest material.

Characterisation of a Tyre Pyrolysis Char

10.1 Introduction

SITA Tyre Recycling initially closed down in June 2000 for a 10 month, £4 million refurbishment primarily aimed at improving plant reliability (SITA, 2000). At the time of writing this Thesis (2002) the plant has not reopened and is currently mothballed awaiting a buyer (Hall, 2000). Due to the uncertain future of STR it was clear that, at least in the short to medium term, the incineration of scrap tyres would cease in the UK. In order to determine the applicability of this research in application to alternative tyre derived waste streams a sample of pyrolysis char was obtained to allow a general comparison to be made. The pyrolysis process represents a growing area of research into the treatment of scrap tyres. The sample of pyrolysis char was obtained from the Coalite[®] process described previously in Chapter 2. The sample characterisation and comparison to the STR waste stream is now described.

10.2 Sample description

The sample was produced through the pyrolysis of shredded tyres in the Coalite retorts for a period of 8-10 hours at a temperature of 640°C. The process is generally operated under a slight suction which removes the oil and gas fractions for separate treatment. The resultant char phase is dry and wire is removed by passing the material over a rotary drum magnet. No mixed phases are removed during the separation, the magnetic phase consists entirely of wire (Bell, 2002). The resulting char phase is therefore suitable for comparison with the carbon ash produced by STR and not the original ash/wire stream.

10.3 Characterisation

An initial visual inspection of the sample (see Figure 10.1) in the form as received revealed the material to be similar in appearance to a dried sample of carbon ash. Very little wire was associated with the sample although small amounts were visible in the sample and some evidence of iron corrosion was visible on the surface of carbon particles. The material was black in colour and the larger particles could easily be broken down into a fine powder by rubbing between two fingers. The maximum

particle size in the sample was approximately 70 mm in diameter. A slight 'oily' odour was evident when the seal of the sample bag was first broken although this soon faded.



Figure 10.1 Coalite[®] pyrolysis char after magnetic separation

The sample was characterised using the techniques, where appropriate, developed for the characterisation of carbon ash. Chemical characterisation was carried out using the techniques described in Chapter 4. The type of sample digestion technique used is discussed later. The large sample of as received material was first riffled to obtain a bulk sample and a sample for particle size characterisation. Any visible pieces of wire, see Figure 10.1, were manually removed from the sample.

10.3.1 Particle size analysis

The sample was supplied in a dry state so a dry sizing technique was used as opposed to the wet sieving carried out on the carbon ash. A series of 200 mm wire mesh sieves were used to separate the material with the same aperture sizes as used for the carbon ash except for the addition of a larger top size to account for the increased abundance of coarse particles in the sample. The sieve sizes used were [μm]: 6300, 3350, 2000, 1000, 500 and 75. The nest of sieves were then loaded onto a Pascal Inclino[®] sieve shaker with a pan at the base to collect the $<75 \mu\text{m}$ material. The integrated timer was then set to shake the sieves for a period of 2 minutes, after which time the contents of

each sieve were examined to determine the extent of the sorting. As had previously been encountered with the carbon ash samples the pyrolysis char particles were brittle and the action of the sieve shaker appeared to enhance particle breakage. For this reason shaking was stopped after 2 minutes at which point the majority of the material had reported to the appropriate sieve. The contents of each sieve, and the pan, were then weighed and the material stored in separate sealed glass jars. The fraction of the sample reporting to each sieve is presented in Figure 10.2. The individual size fractions were retained for chemical analysis.

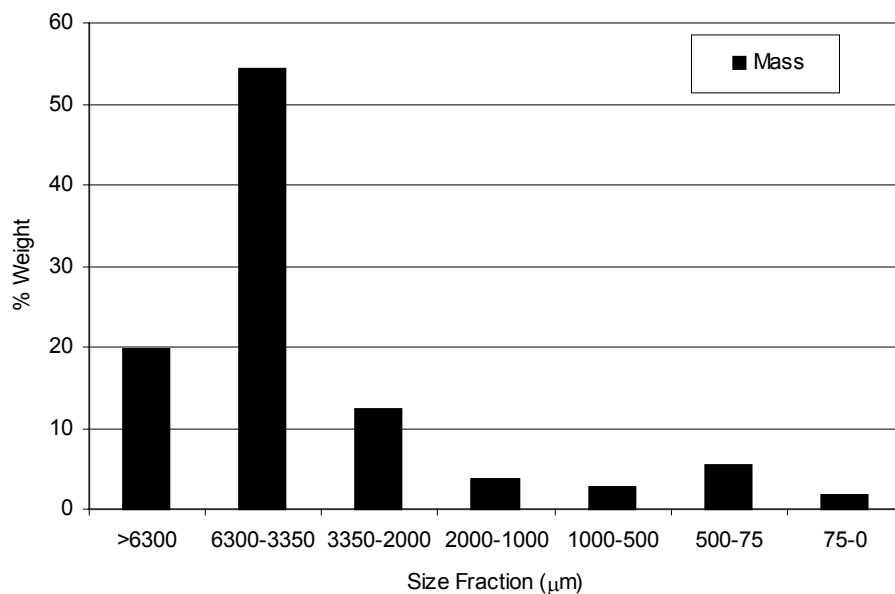


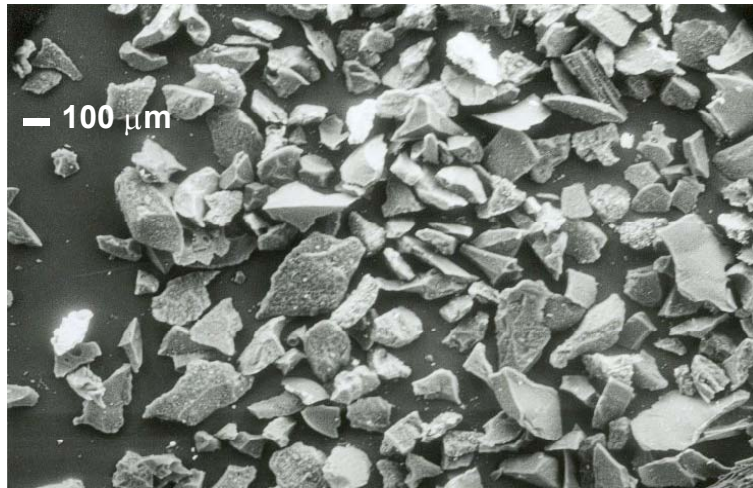
Figure 10.2 Pyrolysis char - fractional size distribution

The sample of pyrolysis char was coarser than the carbon ash although the problems identified in effectively sizing both materials make a detailed comparison difficult. The pyrolysis char contained a greater proportion of larger particles (>3350 μm). This might simply reflect the different handling regimes employed for the post pyrolysis/combustion material at STR and in the Coalite process.

A sub-sample of the 500-75 μm fraction was taken for SEM analysis to establish the association and distribution of char components in the material.

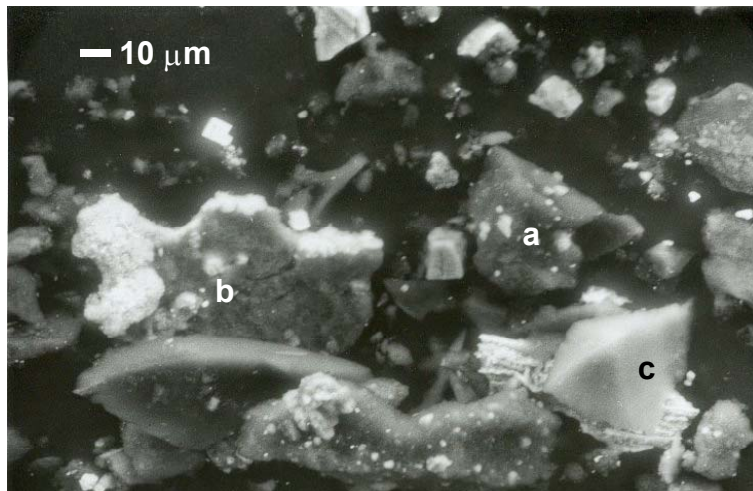
10.3.2 SEM analysis

A small amount of the 500-75 μm fraction was mounted onto a 30 mm diameter stub using a double sided sticky tab, the stub was then sputter coated in gold. At the time of analysis the EDX system was not available so component elements of sample phases could not be identified. The images collected from the sample are shown in Figures 10.3 to 10.5.



General view of sample showing particle shapes. Many appear to have a smooth, clean surface. Some porous looking particles are also visible.

Figure 10.3 Low magnification SEM image of Coalite® pyrolysis char



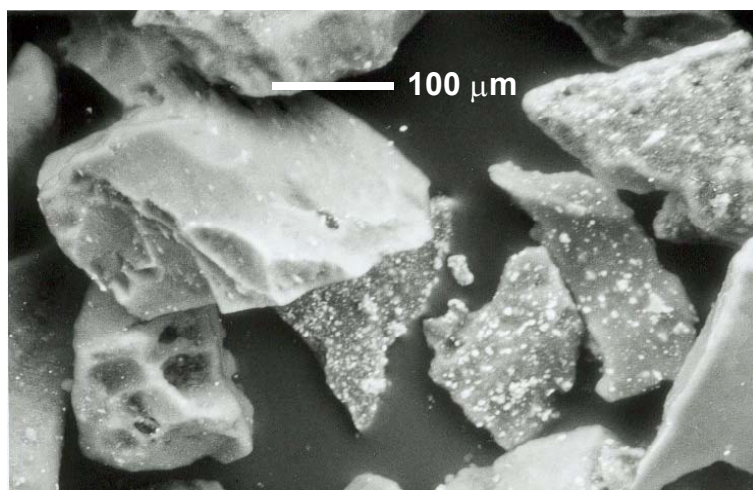
High magnification backscatter image of particles showing:

Some metallic associations with surface of carbon particles (a).

A semi-coated carbon particle (b)

A separate metallic particle (c)

Figure 10.4 High magnification SEM image of Coalite® pyrolysis char - Image 1



High magnification backscatter image showing extent of metallic surface associations with the surface of some carbon particles.

Figure 10.5 High magnification SEM image of Coalite® pyrolysis char - Image 2

The partial coating of the carbon particle observed in Figure 10.4 is similar to that seen previously in a carbon ash particle pictured in Figure 5.11. In carbon ash it was thought that the coating was caused by the corrosion of steel wire in the material and this might also be true for the pyrolysis char. Although without EDX analysis of the metallic phase it could not be confirmed. The metallic elements in the pyrolysis char appear to be both highly dispersed on the surface of particles and also very fine ($<5 \mu\text{m}$) which indicates that, as with the carbon ash, physical carbon separation processes might be ineffective.

The individual size fractions together with the bulk sample were then chemically analysed to quantitatively determine the concentration of elements in the material.

10.3.3 Chemical characterisation

The methods for used for the preparation and analysis of sample for carbon and sulphur have previously been described in Chapter 4. An Aqua-Regia digestion followed by analysis of the resulting solutions with ICP-AES was used to determine the concentration of elements in the samples. This method has also been described in Chapter 4. The results of the analysis of the size fractions are summarised in Figure 10.6 to Figure 10.9. Analysis of the bulk sample is summarised in Table 10.1. The full results can be found in Appendix 5.

10.3.3.1 Carbon and sulphur concentration in size fractions

The results of carbon analysis conducted on the individual size fractions are shown in Figure 10.6, sulphur analysis is shown in Figure 10.7. Each result represents an average of two separate analyses.

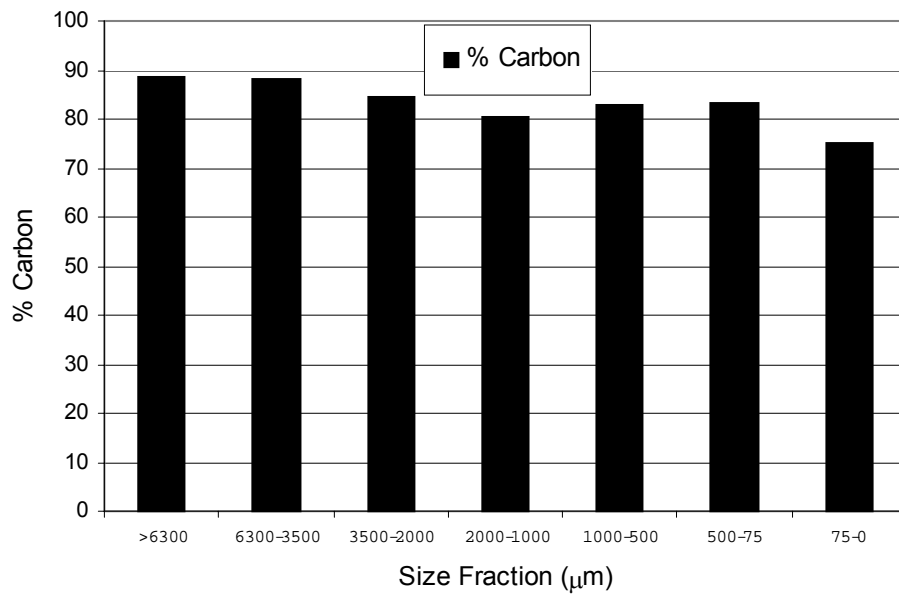


Figure 10.6 Pyrolysis char - fractional size versus % carbon

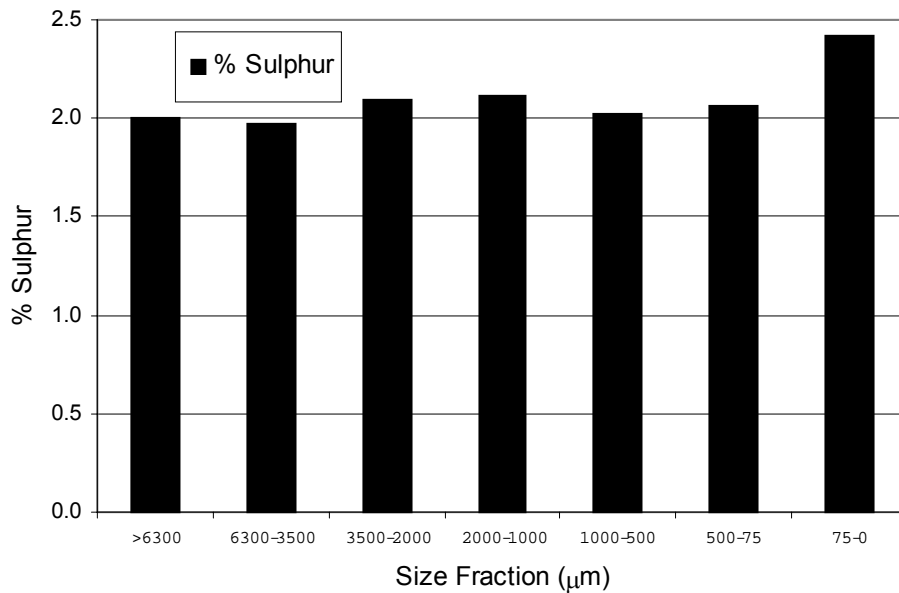


Figure 10.7 Pyrolysis char - fractional size versus % sulphur

Carbon and sulphur concentrations measured in the pyrolysis char size fractions were relatively uniform across the entire particle size range with the exception of the 75-0 μm fraction. In this fraction the carbon concentration was slightly lower and the sulphur content slightly higher in comparison with the remainder of the sample.

10.3.3.2 Concentration of major and minor elements in size fractions

Each sample was digested in duplicate and the results averaged. The data has been split into two groups of minor and major concentrations for clarity. The major elements are presented in Figure 10.8 and the minor elements are presented in Figure 10.9. During the digestion stage the samples initially effervesced violently, probably due to the presence of a heavy oil fraction. In some samples the reaction resulted in material escaping from the liquor and coating the inside of the digestion vessel. This then caused an unknown proportion of the sample mass not to be fully digested and hence introduced errors in the analysis of the solution. The results generated by these samples were discarded.

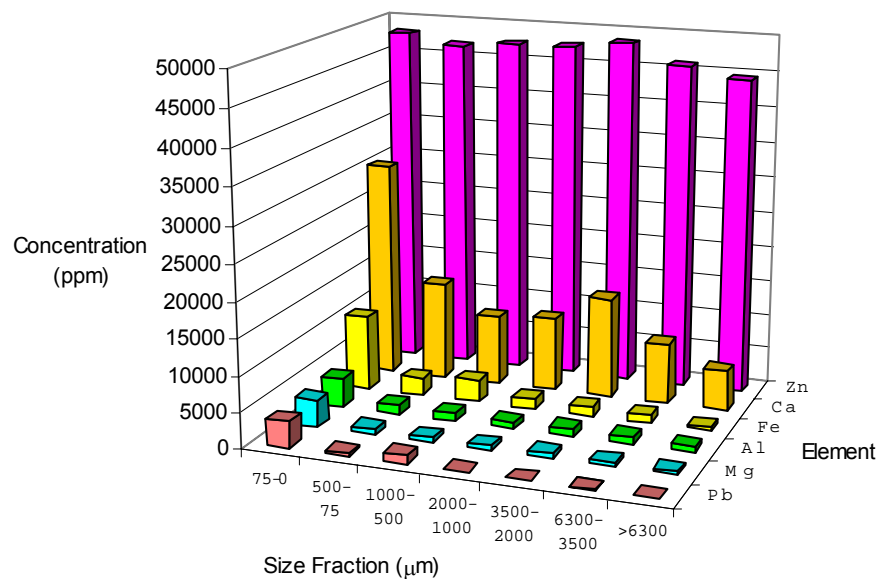


Figure 10.8 Concentration of major elements in pyrolysis char fractions

From Figure 10.8 it can be seen that zinc was present at concentrations of approximately 45,000 to 50,000 ppm (4.5-5.0%) and that the concentration is relatively uniform across the particle size range. Other elements such as calcium, iron,

aluminium, magnesium and lead were more concentrated in the 75-0 μm fraction. This is also evident for the minor elements shown in Figure 10.9.

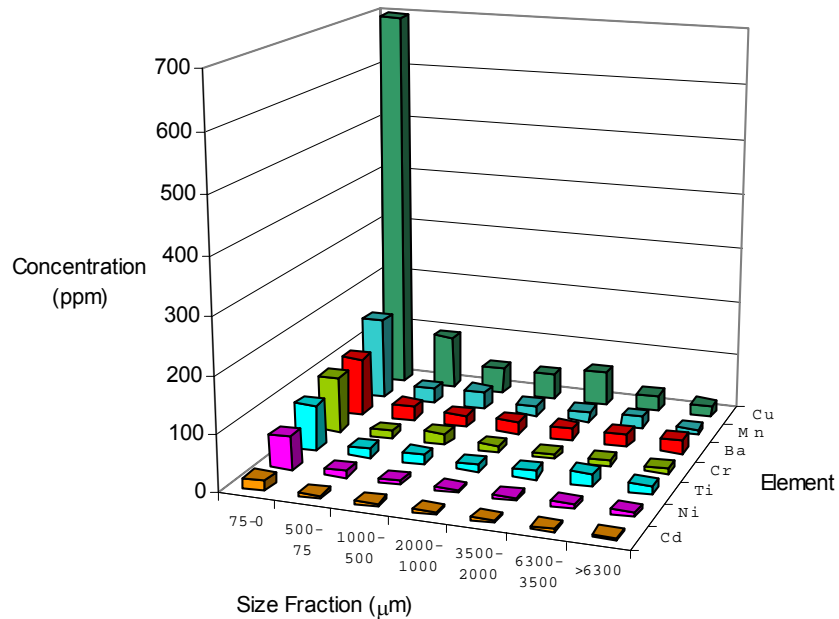


Figure 10.9 Concentration of minor elements in pyrolysis char fractions

From Figure 10.9 it can be seen that copper is significantly more concentrated in the 75-0 μm fraction.

10.3.3.3 Characterisation of bulk sample

The bulk sample was analysed within the analytical run containing the size fractions. The sample was analysed in triplicate for each element and the results have been expressed as an average in Table 10.1. The sulphur and carbon data has been combined with the digestion results to provide a more complete analysis.

Element	Concentration ($\times 10^5$ ppm)
C	8.38
Zn	0.47
S	0.21
Ca	0.11
Al	0.013
Fe	0.0093
Mg	0.0055
Pb	0.001
Cu	0.00032
Ba	0.0002
Mn	0.00016
Ti	0.00015
Cr	0.0001
Ni	0.00008
Cd	0.00004

Table 10.1 Combined analysis results of pyrolysis char bulk sample

The principal components in the sample are carbon (84%), zinc (4.7%) and sulphur (2.1%). Calcium was present at a concentration of 1.1% and all other elements were present at concentrations below 0.2%.

10.4 Discussion

In general the physical and chemical properties of the pyrolysis char appear to be similar to that of the carbon ash produced by incineration. The main point to note is that the carbon concentration is very high in the Coalite material as it was in the STR carbon ash. The results of the chemical analysis of bulk samples of each material are compared in Table 10.2. It is important to note that different methods were used in the acid digestion stage of each analysis. Carbon and sulphur were analysed using an identical technique for each sample. For the STR material a total microwave digestion was used whilst the Coalite material was analysed using an Aqua-Regia method. The differences between the two methods have previously been discussed in Chapter 4, typically the recovery of elements from the sample is lower using the Aqua-Regia method. It is therefore difficult to make direct comparisons between the two samples but the results may still be used to provide an indication of similar properties. Differing feedstock between the two processes might also influence the characteristics

of the char and ash fractions due to some tyres containing differing quantities of components such as carbon black.

Element	STR ($\times 10^5$ ppm)	Coalite ($\times 10^5$ ppm)
Al	0.2	0.13
Ba	0.0002	0.0002
C	8.09	8.38
Ca	0.098	0.10
Cd	<LOD	0.00004
Cr	<LOD	0.0001
Cu	0.0020	0.00032
Fe	0.34	0.0093
Mg	0.011	0.0055
Mn	0.0019	0.00016
Ni	<LOD	0.00008
Pb	0.0008	0.001
S	0.18	0.21
Ti	0.0021	0.00015
Zn	0.37	0.47

**Table 10.2 Comparison between carbon STR and Coalite bulk carbon phases
[LOD - limit of detection]**

From Table 10.2 the main difference between the two materials can be identified as the iron concentration, which is significantly higher in the STR material. This is a reflection of the reduced amount of wire associated with the pyrolysis char sample. The reason for the low iron content in the char in comparison with the carbon ash might be the differing separation and handling methods used in each process. In pyrolysis a shredded tyres are used as a feed and the char fraction is produced dry and is relatively easy to handle. Dry magnetic separation was then effective in removing the majority of the wire from the char and only a small amount remains in the char fraction, this was then manually removed prior to characterisation. In the incineration process at STR whole tyres are used as a feed and the resulting ash/wire process stream is wet which results in a material that is less easily handled and more difficult to process using dry magnetic separation as described in Chapter 8. During characterisation of the carbon ash it was observed that the rapid corrosion of the steel wire in the wet carbon ash increased the dispersion of the iron throughout the material making separation from the carbon phase more difficult.

The association of manganese and copper with the steel as identified in the STR material during Chapter 9 appears to be similar in the pyrolysis char. The concentrations of copper and manganese are an order of magnitude less in the char than in the carbon ash sample that also contained a significant iron content. Although this could only be confirmed with the analysis of the pyrolysis char with the steel wire left in.

Carbon and sulphur concentrations can be seen to be slightly higher in the pyrolysis char and is likely to be as a result of the lower concentration of iron in the material. The concentration of zinc in the pyrolysis char is approximately 10% greater than that measured in the carbon ash, even with the potentially lower element recovery expected from the Aqua-Regia digestion. This can probably be explained due to the fact that in the STR incineration process not all of the zinc reported to the ash/wire phase as a portion was collected in the form of a zinc oxide dust in the baghouse filters.

10.5 Summary

The main chemical properties of pyrolysis char produced by the Coalite[®] process were found to be similar in terms of element concentrations when compared to the STR carbon ash. The shredded tyre feed of the pyrolysis process and the dry nature of the char process stream resulted in a superior separation of the wire fraction from the material compared to removal from ash/wire. Physically the pyrolysis char was found to contain a greater proportion of larger particles although, as with the carbon ash, they were relatively weakly formed and quickly broke down during handling.

On the basis of this initial characterisation it is possible that the pyrolysis char might be chemically and physically suitable for use as a secondary fuel as generated from the carbon ash for use in a zinc smelter. Further work would be required since other parameters such as burnout and suitability for tuyere injection have not been considered. The SEM images indicate that the non-carbon elements in the char are highly dispersed which would make it difficult to use physically process the material with the aim on increasing the carbon concentration. The level of dispersion of the

elements could be confirmed by performing an experiment based upon that described in Chapter 9. The results could be compared directly to those generated by the carbon ash.

This chapter has concentrated solely on the characterisation of the char fraction from pyrolysis. The characteristics of the wire phase was not investigated although the lower concentration of copper measured in the char phase might be an indication that the element remains associated with the steel wire during pyrolysis. The sulphur content of the post pyrolysis steel was not determined so it is not clear if an attrition process would be required to treat the phase.

11 Conclusion

11.1 Discussion

The objective of this research was to determine the potential for recycling all or a part of, the main waste residue resulting from the incineration of scrap tyres at SITA Tyre Recycling. The waste stream had been disposed to landfill since the plant began operation. This was achieved through the physical and chemical characterisation of material sampled from the 'ash/wire' waste stream. Analytical methods routinely applied to the analysis of coals and other geological materials were used to quantitatively and qualitatively determine properties of the material that might indicate potential for recovery and reuse.

A method was developed to retrieve representative sub-samples of ash/wire from the most appropriate point in the STR process and these samples were then characterised. Three main phases were identified in the ash/wire which were referred to as 'carbon ash' (material derived from the combustion of the rubber portion of the tyre), 'bushy wire' (intact tyre beads) and water. The poor handleability characteristics of the material made taking representative samples difficult, it was also a major factor in the poor reliability of the STR process. The nature of the two solid phases meant that different techniques had to be employed to characterise them so they were treated separately. The two phases initially being hand separated at the sample collection stage. The water associated with the ash/wire was ignored as a potential product

stream in its own right although it was associated with the carbon ash and to a lesser extent the bushy wire. To recover the most value from the waste stream it was decided that the two solid phases would most likely be sold into separate markets

The primary property identified for successful recycling of the bushy wire was the sulphur content of the post-combustion steel. An experiment was devised to determine the association of sulphur with the wire. The results showed that the sulphur was associated with surface coatings of the carbon ash phase of the ash/wire. Removing virtually all of the surface coatings resulted in a low-sulphur steel product with suitable chemical properties for reuse in a variety of industries.

Initial characterisation of the carbon ash revealed that the dominant element in the material was carbon. Finer pieces of wire that were not collected with the bushy wire phase complicated the characterisation of the carbon phase so a dry magnetic separation process was used to remove the wire. This also resulted in the removal of a magnetic carbon ash phase which was returned the sample for characterisation. Along with carbon other elements such as zinc, iron, sulphur and calcium were measured in significant concentrations (>1%) reflecting the initial feed components used in the manufacture of the tyre. Magnetic carbon ash phases were dominated by mixed carbon-iron particles formed as the bead wires corrode in the wet carbon ash. A bulk sample of carbon ash generated by the dry magnetic separation of a dry sample of carbon ash contained in excess of 80% carbon. This indicated that products derived from this phase would be based around the recovery of carbon. Potential markets such as reuse as a fuel or possibly higher value applications after further reprocessing were identified.

A series of separation studies attempted to generate separate phases of wire and high concentration carbon products. Physical processes were relatively unsuccessful due to the apparent high dispersion of non-carbon phases in the carbon matrix, which made the further concentration of the carbon product difficult. An acid leach process showed potential for generating a high carbon concentrate although it required further investigation to generate a product with similar characteristics to the highest value potential carbon product, carbon black. A suitable market for the carbon product generated by the laboratory dry magnetic separation of carbon-ash was identified as a

secondary fuel in a zinc smelter. An initial sample supplied to the user passed a number of specifications. The production of a larger sample for assessment using pilot-scale equipment was then investigated.

The mechanism of removing the surface coatings of carbon ash from the wire was developed into a process by adapting the mineral processing technique of attrition scrubbing. After size reduction and attrition scrubbing of the bushy wire a low sulphur concentration product was generated that had numerous applications in areas of the steel manufacturing and reprocessing industries. The process was optimised and scaled-up to pilot scale with success. The recovery of bushy wire, which would form the feed to the attrition process, from the ash/wire was also investigated in a pilot-scale trial.

The direct separation of carbon ash and bushy wire from the ash/wire using pilot scale dry magnetic separation was found to be unsuitable mainly due to the poor handleability of the material. By shredding the entire ash/wire process stream using a whole tyre shredder the handleability of the material was vastly improved which made the dry magnetic separation of carbon ash and bushy wire more effective. However, the properties of the non-magnetic product stream were inferior to that generated during the laboratory scale separation. The increased abundance of mixed carbon-iron particles and the physical entrainment of wire in the carbon ash were identified as the main reasons for the inferior separation and both were related to the high moisture content of the feed material compared to the dry samples separated in the laboratory. The bushy-wire recovered through pilot scale dry magnetic separation was used as a feed material for the optimisation and scale-up of the attrition process after further size reduction.

Ready markets and end users were identified for the products developed from the main phases present in the SITA Tyre Recycling ash/wire waste stream. Some technical hurdles remained to be solved concerning the primary separation of bushy wire and carbon ash from the ash/wire although initial tests with an alternative method using a spiral classifier showed promise.

In the case of the carbon ash derived product the product generated represented the lower value end of the market. Further information on the dispersion and association of the non-carbon phases was required to enable the carbon concentration to be increased and hence increase the product value. This was investigated through the development of a centrifugal float-sink test using an organic dense medium. Particles of carbon ash were separated based on their density being greater or less than the dense medium. The centrifuge reduced the time required for the separation to occur. It was found that, in general, elements originally associated with the tyre bead wire and other reinforcing structures (e.g. iron, copper, manganese) were effectively separated from the carbon whilst those associated with the rubber compound (e.g. zinc, sulphur) were not separated and remained associated with the carbon phase. The high dispersion of these elements meant that liberation and separation was difficult therefore limiting the likely success of any physical separation process. Further concentration of the carbon product might therefore be based on a chemical process such as the acid leach discussed previously.

The incineration of scrap tyres has a number of benefits such as volume reduction, power generation and diversion of waste from landfill. The generation of valuable products from the main waste stream further increases the desirability of the process. The technical problems encountered at the sole UK tyre incineration plant, which have led to the long term closure of the plant, limit the direct application of this research. However, the initial characterisation carried out on the tyre pyrolysis char material indicated a number of similarities to the carbon ash without many of the material handleability issues which complicated work on the ash/wire. As the scale-up of tyre pyrolysis processes continue and their contribution to the UK scrap tyre management increases, the char (carbon) and steel-based products might find industrial application which would further enhance the economics of the process.

11.2 Contributions to knowledge

- The primary waste stream generated by the incineration of scrap tyres was found to contain two distinct solid phases. 'Carbon ash' was derived from the combustion of the rubber portion of the tyre whilst the bushy wire was derived mainly from the intact beads of the tyre.

- The carbon concentration of the carbon ash was very high, approximately 70-80% on a 'steel free' basis.
- The sulphur content of the post-combustion steel was found to be in excess of that required for recycling. Experiments determined that sulphur was associated with surface coatings of carbon ash. By removing the entire surface coating of carbon ash with sandpaper a reduced sulphur concentration steel was generated.
- Attrition scrubbing of shredded (<4 mm) bushy wire recreated the sanding action and generated a high bulk density product suitable for reuse in a number of industrial applications.
- Laboratory scale dry magnetic separation of the carbon ash phase generated a carbon product with a concentration slightly in excess of 80%. After size reduction the material was suitable for use as a secondary fuel in a zinc smelter where it would be added to the smelter through tuyere injection.
- Physical processing techniques were not successful in further concentrating the carbon and thereby forming a product of increased value. This was thought to be due to the high dispersion of non-carbon elements within the carbon matrix, which was confirmed with the development of a centrifugal float-sink test. The experiment showed that many contaminants remained associated with carbon particles at very fine particle sizes.
- A simple acid leach experiment demonstrated the potential of a chemical treatment process and produced a high carbon (>90%) concentrate.
- The pilot-scale dry magnetic separation of carbon ash and bushy wire directly from the as produced waste stream was found to be difficult due to the poor handleability of the ash/wire.
- Shredding the ash/wire in a whole tyre shredder vastly improved handleability and improved the performance of dry magnetic separation but not sufficiently to match the product generated at laboratory scale.
- An initial characterisation of a pyrolysis char demonstrated that it had many similar properties to the carbon ash.

11.3 Recommendations for future work

The study was carried out on a process that was the only one of its kind in the UK, further research on the process stream is impossible whilst the plant is not operating. For continuation of the area of this research, a number of recommendations are suggested.

- Pyrolysis chars generated from processes such as at Coalite should be characterised in detail with a view to generating high value saleable products.
- The steel wire phase from tyre pyrolysis processes should also be characterised with a view to product generation.
- Suitable analytical standards should be sought or developed to allow effective monitoring of accuracy during chemical characterisation studies of high carbon and high ash content materials.
- Develop the centrifuge float-sink method further to improve the results for fine materials to allow the theoretical potential for physical separation from similar materials to be assessed.
- Investigate the possibility of landfill mining to recover and recycle the ash/wire already discarded during the operation of the SITA Tyre Recycling plant.

Publications

The following paper was written during the course of this study:

G.E. Rice, N.J. Miles and B.P. Atkin. (2001) Generating products from tyre incineration residues. *Proc. Waste 2000 – Waste Management at the Dawn of the Third Millennium*, pp 290-338

References

- Adhikari, B. and S Maiti, D. (2000) Reclamation and recycling of waste rubber. *Progress in Polymer Science* **25**, 909-948.
- Allen, R.M., Carling, R.W. and VanderSande, J.B. (1986) Microstructural changes in coal during low temperature ashing. *FUEL* **65**, 321-326.
- Allred, R.E., Coons, N.C., Finley, D.J., Shoemaker, J.M., Wilder, R.L. and Wilder, J.D. (2000) Large-scale Recycling Process for Scrap Tyres and Rubber Products. *Proceedings of 32nd International SAMPE Technical Conference* 398-408.
- Anon (2000) Oil from old tyres. *Environment Business Magazine* 10-10.
- Atkin, B.P. and Somerfield, C. (1994) The determination of total sulphur in geological materials by coulometric titration. *Chemical Geology* **111**, 131-134.
- Austin, L.G., Kalligeris-Skentzos, A. and Woodburn, E.T. (1994) Ash liberation in fine grinding of a British Coal. *Powder Technology* **80**, 147-158.
- BDH (1994) Tetrabromoethane (TBE) Safety Data Sheet.
- BDH (2000) Triethyl phosphate (TEP) Safety Data Sheet.
- Bell, P. Personal Communication, 2002. Development Engineer. Coalite Smokeless Fuels Ltd.
- Bird, B.M. and Messmore, H.E. (1924) The float and sink test for fine coal. 2586, United States Bureau Of Mines.
- Boxmag-Rapid Ltd (2002) Boxmag-Rapid Lab Scale electromagnetic ore separator. Installation, operation and maintenance instructions.
- Bruce, S. Personal Communication, 1999. Britannia Zinc Ltd. Raw Materials Manager.

- CADDET (1994) Power from Scrap Tyres at Wolverhampton. Technical Brochure number 7. Download from <http://www.caddet-re.org> Last accessed September 2002.
- Carmichael, R.S. (1984) *Handbook of physical properties of rocks*,
- Chaalal, A., Darmstadt, H. and Roy, C. (1996) Acid-base method for the demineralization of pyrolytic carbon black. *Fuel Processing Technology* **46**, 1-15.
- Chanel, S. and Pebere, N. (2001) An investigation on the corrosion of brass-coated steel cords for tyres by electrochemical techniques. *Corrosion Science* **43**, 413-427.
- Cloke, M., Clift, D., Gillfillan, A.J., Miles, N.J. and Rhodes, D. (1994) Liquefaction of density separated coal fractions. *Fuel Processing Technology* **38**, 153-163.
- Coran, A.Y. (1994) Vulcanization. In: Mark, J.E., Erman, B. and Eirich, F.R., (Eds.) *Science and Technology of Rubber*, 2 edn. pp. 339-385. San Diego: Academic Press]
- Darmstadt, H., Roy, C. and Kaliaguine, S. (1994) Inorganic Components and Sulphur Compounds in Carbon Blacks from Vacuum Pyrolysis of used Tires. *Gummi und Kunststoffe* **47**,
- Department of the Environment, T.a.t.R. (1997) *National road traffic forecasts*, London: The Stationary Office.
- Department of Trade and Industry (1997) Digest of United Kingdom energy statistics. London: The Stationary Office.
- Donnet, J.-B. and Voet, A. (1993) *Carbon Black* , 2 edn. New York: Marcell Dekker.
- Dyrkacz, G.R. and Horwitz, P.E. (1982) Separation of coal macerals. *Fuel* **61**, 3-13.
- ENDS Report (2000) Agency eases path for tyre burning in cement kilns. *ENDS Report* **309**, 18-19.

- ERJ (1999) Cement kilns start burining tyres in the UK. *European Rubber Journal* **181**, 40-41.
- 1999/31/EC. European Council (Apr 26, 1999) European Council Landfill Directive on the Landfill of Waste.
- 2000/53/EC. European Council (Oct 21, 2000) End of Life Vehicles (ELV) Directive.
- Feng, D., Lorenzen, L., Aldrich, C. and Mare, C.W. (2001) Ex situ diesel contaminated soil washing with mechanical methods. *Minerals Engineering* **14**, 1093-1100.
- Ferrer, G. (1997) The economics of tyre remanufacturing. *Resources, Conservation and Recycling* **19**, 221-255.
- Franzidis, J.-P. and Harris, M.C. (1986) A new method for the rapid float-sink analysis of coal fines. *Journal of the South African Insitute of Mining and Metallurgy* **86**, 409-414.
- Greenwood, N.N. and Earnshaw, A. (1997) *Chemistry of the Elements*, 2 edn. Oxford: Butterworth-Heinemann.
- Hall, P. Personal Communication, 2000. SITA Tyre Recycling Plant Manager 1999-2000.
- Hassan, M.S. and Abdel-Khalek, N.A. (1998) Benefication and applications of egyptian bentonite. *Applied Clay Science* **13**, 99-115.
- Helleur, R., Popovic, N., Ikura, M., Stanciulescu, M. and Liu, D. (2001) Characterization and potential applications of pyrolytic char from ablative pyrolysis of used tyres. *Journal of Analytical and Applied Pyrolysis* **58-59**, 813-824.
- Helmich, T. Personal Communication, 2000. Eriez Magnetics Europe Limited.
- Hurditch, P. Anonymous, 1999. London & Scandinavian Metallurgical Company Limited.

- Ji-Won Yang, Taek-Soo Yoo, Jae-Hyun Oh and Iwao Iwasaki (1998) Discarded tire recycling practices in the United States, Japan and Korea. *Resources, Conservation and Recycling* **22**, 1-14.
- Killmeyer, R.P., Hucko, R.E. and Jacobsen, P.S. (1992) Centrifugal Float-Sink Testing of Fine Coal: An Interlaboratory Test Program. *Coal Preparation* **10**, 107-118.
- Kovac, F.J. and Rodgers, M.B. (1994) Tire Engineering. In: Mark, J.E., Erman, B. and Eirich, F.R., (Eds.) *Science and Technology of Rubber*, 2 edn. pp. 675-717. San Diego]
- Laban, K.L. and Atkin, B.P. (1999) The determination of minor and trace element associations in coal using a sequential microwave digestion procedure. *International Journal of Coal Geology* **41**, 351-369.
- Lee, W.H., Kim, J.Y., Ko, Y.K., Reucroft, P.J. and Zondlo, J.W. (1999) Surface analysis of carbon black waste materials from tire residues. *Applied Surface Science* **141**, 107-113.
- Lynch, A.J., Johnson, N.W., Manlapig, E.V. and Thorne, C.G. (1981) *Mineral and Coal flotation circuits. Their simulation and control.*, Elsevier Scientific Publishing Company.
- Mukherjee, S. and Borthakur, P.C. (2001) Chemical demineralization/desulphurization of high sulphur coal using sodium hydroxide and acid solutions. *Fuel* **80**, 2037-2040.
- Orjela, G. (1994) A new wire/rubber adhesion system for pneumatic tires. *Tire Technology International* 70-76.
- Othmer, K. (1992) *Encyclopedia of Chemical Technology*, 4th edn. New York: Wiley & Sons.
- Palowitch, E.R. and Nasiatka, T.M. (1961) Using a centrifuge for float-and-sink testing fine coal. 5741, United States Bureau Of Mines.

- Perry, D. and Thompson, J. (1998) Collecting and analysing data for waste sampling and monitoring. *Institute of Waste Management Proceedings* 4-7.
- Piskorz, J., Majerski, P., Radlein, D., Torsten Wik and Scott, D.S. (1999) Recovery of Carbon Black from Scrap Rubber. *Energy & Fuels* **13**, 544-551.
- Rapra Technology Limited (1995) Scrap tyres - disposal and recycling options. Shrewsbury, Shropshire: RAPRA Technology Ltd.
- Rhodes, D. (1991) The characterization of fine coal particles. University of Nottingham. PhD.
- Robinson, S. (1989) Wave goodbye to scrap tyres. *European Rubber Journal* **171**, 32-33.
- Rodriguez, I.d.M., Laresgoiti, M.A., Torres, A., Chomon, M.J. and Caballero, B. (2001) Pyrolysis of scrap tyres. *Fuel Processing Technology* **72**, 9-22.
- Roy, C., Chaala, A. and Darmstadt, H. (1999) The vacuum pyrolysis of used tires. End-uses for oil and carbon black products. *Journal of Analytical and Applied Pyrolysis* **51**, 201-221.
- Roy, C., Labrecque, B. and Caumia, B.d. (1990) Recycling of scrap tyres to oil and carbon black by vacuum pyrolysis. *Resources, Conservation and Recycling* **4**, 203-213.
- Scrap Tyre Working Group (1997) Second annual report to ministers. London: STWG.
- Sharma, V.K., Fortuna, F., Mincarini, M., Berillo, M. and Cornacchia, G. (2000) Disposal of waste tyres for energy recovery and safe environment. *Applied Energy* **65**, 381-394.
- SITA (2000) Major investment boost planned for S.I.T.A Tyre Recycling. *S.I.T.A News Release* (In Press)
- Scott, S.D. & Barnes, H.L. (1972) *Geochim. Cosmochim. Acta.* **36**, 1275 in Darmstadt *et al.* (1994)

- Somerfield, C. Personal Communication, 1998. Sulphur analysis of coal by coulometric titration.
- Steel, K.M. and Patrick, J.W. (2001) The production of ultra clean coal by chemical demineralisation. *Fuel* **80**, 2019-2023.
- Svoboda, J. (1987) *Magnetic methods for the treatment of minerals*, 1st edn. Elsevier Science Publishers.
- The Environment Agency (1999) Tyres in the Environment.
- Tsai, C.I. (1985) Effects of surface chemistry and particle size and density on froth flotation of fine coal. *Colloids and Surfaces* **16**, 323-336.
- Tyson, J. (1994) *Analysis - What analytical chemists do*, 1st edn. The Royal Society of Chemistry.
- Walters, D. Personal Communication, 2002. Cabot Corporation, UK.
- Williams, P.T., Besler, S. and Taylor, D.T. (1990) The pyrolysis of scrap automotive tyres - The influence of temperature and heating rate on product composition. *FUEL* **69**, 1474-1482.
- Williams, P.T., Besler, S., Taylor, D.T. and Bottrill, R.P. (1995) The pyrolysis of automotive tyre waste. *Journal of the Institute of Energy* **68**, 11-21.
- Wills, B.A. (1997) *Mineral Processing Technology*, 6th edn. Oxford: Butterworth-Heinemann.

Appendix 1

Results of Carbon Ash Characterisation

Contents

Characterisation results for magnetic and non-magnetic size fractions

Concentration ($\times 10^5$ ppm)	Particle size (μm)					
	75-0	500-75	1000-500	2000-1000	3350-2000	>3350
C	6.98	8.00	8.40	8.06	6.20	8.22
S	0.18	0.18	0.18	0.17	0.14	0.20
Al	0.04	0.02	0.02	0.01	0.01	0.02
Ba	0.001	0.0003	0.0002	0.0003	0.0001	0.0001
Ca	0.26	0.10	0.063	0.065	0.055	0.082
Cd	< LOD	< LOD	< LOD	< LOD	< LOD	< LOD
Cr	< LOD	< LOD	< LOD	< LOD	< LOD	< LOD
Cu	0.0028	0.0011	0.00087	0.0010	0.00080	0.00048
Fe	0.21	0.050	0.028	0.047	0.066	0.15
Mg	0.032	0.013	0.0090	0.0086	0.0073	0.0083
Mn	0.0015	0.00033	0.00020	0.00032	0.00040	0.00088
Ni	< LOD	< LOD	< LOD	< LOD	< LOD	< LOD
Pb	0.0008	0.0006	0.0006	0.0007	0.0007	0.0004
Si	0.06	0.07	0.07	0.05	< LOD	< LOD
Ti	0.0039	0.0030	0.0019	0.0017	0.0015	0.0014
Zn	0.55	0.39	0.34	0.35	0.25	0.38

Carbon Ash – non-magnetic size separated fractions

Concentration ($\times 10^5$ ppm)	Particle size (μm)					
	75-0	500-75	1000-500	2000-1000	3350-2000	>3350
C	7.12	3.06	4.57	3.70	2.45	All wire in this size fraction
S	0.18	0.22	0.19	0.17	0.13	
Al	0.04	0.03	0.02	0.02	0.02	
Ba	0.001	0.0003	< LOD	< LOD	< LOD	
Ca	0.27	0.085	0.064	0.062	0.056	
Cd	< LOD	< LOD	< LOD	< LOD	< LOD	
Cr	0.00025	0.0010	0.0013	0.0014	0.0014	
Cu	0.0056	0.038	0.014	0.011	0.015	
Fe	0.36	4.23	3.44	3.71	4.90	
Mg	0.032	0.015	0.010	0.009	0.007	
Mn	0.002	0.023	0.018	0.021	0.027	
Ni	< LOD	0.0006	0.0009	0.0009	0.0009	
Pb	0.0008	0.001	0.0009	0.001	0.002	
Si	0.07	0.06	0.07	0.08	0.07	
Ti	0.0039	0.0030	0.0036	0.0024	0.0042	
Zn	0.62	0.61	0.45	0.41	0.38	

Carbon Ash – magnetic size separated fractions

Appendix 2

Separation Studies Results

Contents

Acid leach test results

Attrition optimisation test results

Acid leach test results

($\times 10^5$ ppm)	S	C
Feed carbon ash	0.16	7.45

Properties of carbon ash sample used as feed for leach test

($\times 10^5$ ppm)	S	C
Feed	0.13	6.47
1M Cold	0.12	6.43
5M Hot	0.11	6.57

Properties of coal control sample used in leach test

Element ($\times 10^5$ ppm)	Powdered		Non-powdered	
	Cold	Hot	Cold	Hot
C	8.19	9.19	8.27	9.01
S	0.16	0.17	0.17	0.15
Mn	0.00089	0.0013	0.00080	0.0012
Fe	0.00063	0.0012	0.00054	0.0012
Mg	0.00053	0.00059	0.00046	0.00054
Ca	0.0014	0.0011	0.0013	0.0012
Ti	0.000060	0.00022	0.000050	0.00019
Al	0.0004	0.0006	0.0003	0.0004
Zn	0.00052	0.00082	0.00049	0.00080
Pb	0.0006	0.0006	<LOD	0.0006
Cd	<LOD	<LOD	<LOD	<LOD
Ni	<LOD	<LOD	<LOD	<LOD
Ba	0.001	0.001	0.0006	0.0009
Cr	<LOD	<LOD	<LOD	<LOD
Cu	0.00014	0.00026	0.00018	0.00031

Analysis of post-leach carbon ash material

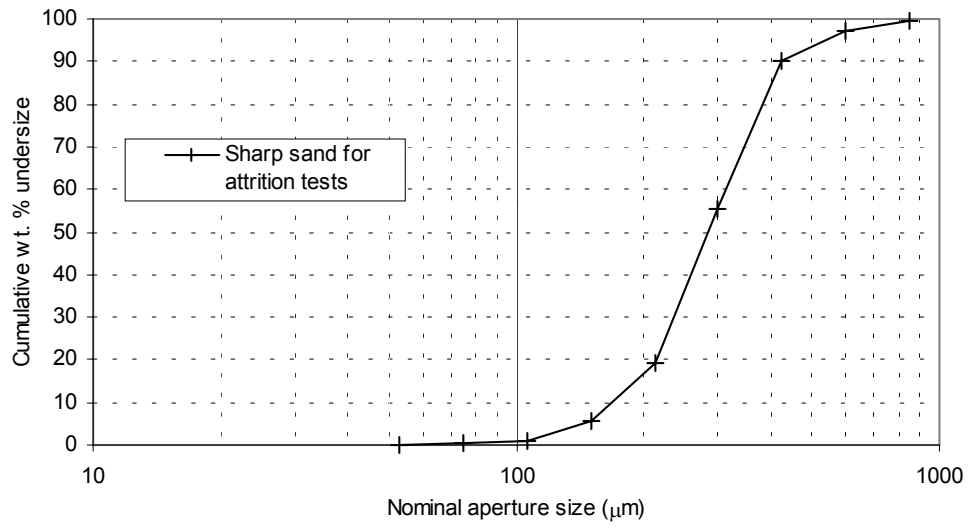
Attrition optimisation test results

Overall solids (%)	Feed components			Sulphur in attrited wire (%)				
	Sand (g)	Water (ml)	Wire (g)	2 mins	4 mins	6 mins	8 mins	10 mins
70	500	257	100			0.037		
	400	257	200			0.034 ¹		
	300	257	300	0.044	0.027	0.045	0.048	0.025
	200	257	400			0.032		
	100	257	500			0.032 ²		
60	416	330	84			0.045		
	333	330	167			0.037		
	250	330	250	0.055	0.042	0.033	0.044 ³	0.044
	167	330	333			0.051		
	83	330	417			0.036		

Attrition optimisation test process parameters and sulphur concentration of attrited product

Size fraction (μm)	Cumulative passing size %
>850	99.6
850-600	97.1
600-425	89.9
425-300	55.4
300-212	19.3
212-150	5.8
150-106	1.2
106-75	0.5
75-53	0.2
53-0	0.0

Size characterisation of sharp sand used in attrition scrubbing



Sharp sand size characterisation

Appendix 3

Float-sink Test Results

Contents

Feed analysis results

Float-sink test results matrix

Description of method used for the calculation of settling time of particles in dense media

Feed analysis results

Size fraction ($<\mu\text{m}$)	($\times 10^5$ ppm)				
	C	Fe	Zn	S	Ca
38-0	5.35	1.64	0.38	0.10	0.063
53-38	6.38	1.28	0.27	0.095	0.12
75-53	6.95	0.961	0.25	0.11	0.083
106-75	7.57	0.807	0.24	0.12	0.070
150-106	7.22	0.823	0.24	0.12	0.064
212-150	6.79	1.08	0.24	0.13	0.059
300-212	6.40	1.31	0.24	0.12	0.051
425-300	6.63	1.23	0.24	0.12	0.047
600-425	5.98	1.21	0.23	0.12	0.045
850-600	6.98	1.01	0.21	0.13	0.040
1180-850	7.43	0.942	0.19	0.13	0.039
1680-1180	7.09	0.969	0.19	0.12	0.041
2376-1680	6.93	1.17	0.18	0.13	0.037

Major elements in feed size fractions

Size fraction ($<\mu\text{m}$)	($\times 10^4$ ppm)									
	Al	Mn	Mg	Cu	Ti	Ni	Cr	Pb	Ba	Cd
38-0	0.16	0.12	0.12	0.061	0.010	0.009	0.007	0.007	0.004	<LOD
53-38	0.12	0.083	0.092	0.046	0.0070	0.004	0.003	<LOD	0.003	0.0004
75-53	0.11	0.065	0.070	0.035	0.0070	0.006	0.004	<LOD	0.002	<LOD
106-75	0.10	0.055	0.065	0.033	0.0060	0.005	0.003	<LOD	0.002	<LOD
150-106	0.10	0.055	0.062	0.031	0.0059	0.006	0.004	<LOD	0.002	<LOD
212-150	0.085	0.066	0.056	0.037	0.0050	0.005	0.004	<LOD	0.001	<LOD
300-212	0.077	0.079	0.055	0.042	0.0047	0.004	0.003	<LOD	0.0004	<LOD
425-300	0.066	0.075	0.051	0.036	0.0038	0.004	0.003	<LOD	0.0005	<LOD
600-425	0.068	0.073	0.050	0.032	0.0034	0.006	0.005	<LOD	0.0004	<LOD
850-600	0.061	0.060	0.046	0.024	0.0031	0.003	0.002	<LOD	0.0004	<LOD
1180-850	0.057	0.054	0.047	0.016	0.0035	0.003	0.002	<LOD	0.0002	<LOD
1680-1180	0.045	0.051	0.044	0.015	0.0030	0.003	0.003	<LOD	0.0002	<LOD
2376-1680	0.060	0.062	0.043	0.023	0.0035	0.003	0.002	<LOD	0.0001	<LOD

Minor elements in feed size fractions

Float-sink test results matrix (next page)

		Particle size (µm) / Concentration (×10 ⁵ ppm unless stated)															
		425-300		300-212		212-150		150-106		106-75		75-53		53-38		38-0	
Density	Parameter	Floats	Sinks	Floats	Sinks	Floats	Sinks	Floats	Sinks	Floats	Sinks	Floats	Sinks	Floats	Sinks	Floats	Sinks
Feed	C (%)	86.4		87.0		65.8		71.8		67.8		75.4		64.8		72.3	
	S (%)	1.4		1.3		1.2		1.2		1.2		1.1		1.0		1.2	
	Al	0.0069		0.0063		0.0078		0.0066		0.0073		0.0085		0.0093		0.018	
	Ca	0.019		0.022		0.027		0.032		0.039		0.045		0.054		0.045	
	Fe	0.431		0.731		0.859		0.976		1.19		1.38		1.71		1.65	
	Mg	0.0039		0.0040		0.0044		0.0043		0.0045		0.0046		0.0049		0.0076	
	Mn	0.0021		0.0030		0.0038		0.0041		0.0053		0.0063		0.0083		0.0082	
	Ti	0.00033		0.00032		0.00039		0.00037		0.00041		0.00044		0.00042		0.00071	
	Ba	0.00005		0.00004		0.00008		0.0001		0.0003		0.0004		0.00005		0.0002	
	Cd	0.00001		0.00001		0.00001		0.00001		0.00002		0.00001		0.00002		0.00002	
	Cr	0.0001		0.0001		0.0003		0.0002		0.0002		0.0003		0.0004		0.0007	
	Cu	0.00089		0.0013		0.0020		0.0019		0.0024		0.0027		0.0034		0.0053	
	Ni	0.0002		0.0002		0.00047		0.00024		0.00026		0.00039		0.00031		0.00052	
	Pb	0.0001		0.0002		0.0002		0.0002		0.0002		0.0003		0.0003		0.0005	
Zn	0.15		0.15		0.16		0.17		0.17		0.18		0.18		0.26		
3	Mass (%)	89.79	10.21	84.05	15.95	77.08	22.92	76.28	23.72	77.07	22.93	74.30	25.70	67.83	32.17	78.42	21.58
	C (%)	83.1	49.3	82.9	35.1	80.1	34.2	78.2	52.8	79.2	49.1	78.5	36.3	77.7	31.5	65.7	27.9
2.6	Mass (%)	87.5	12.5	85.77	14.23	79	21	74.8	25.2	83.18	16.82	77.24	22.76	66.82	33.18	73.97	26.03
	C (%)	84.5	49.1	84.1	35.3	82.9	34.4	81.9	36.0	84.8	24.3	85.6	29.6	84.2	21.7	70.9	23.4
2.2	Mass (%)	84.1	15.9	77.83	22.17	71.58	28.42	72.45	27.55	75.25	24.75	70.72	29.28	63.55	36.45	61.2	38.8
	C	8.76	5.50	8.59	4.83	8.46	3.60	8.40	4.13	8.56	3.32	8.39	2.48	8.46	2.27	7.52	3.31
	S	0.13	0.085	0.13	0.075	0.12	0.062	0.12	0.062	0.13	0.046	0.13	0.049	0.13	0.046	0.074	0.087
	Al	0.0051	0.025	0.0049	0.012	0.0072	0.012	0.0072	0.011	0.0063	0.013	0.0064	0.015	0.0065	0.016	0.015	0.030
	Ca	0.016	0.044	0.016	0.046	0.017	0.064	0.017	0.082	0.017	0.11	0.017	0.13	0.017	0.13	0.020	0.076
	Fe	0.170	2.18	0.18	2.51	0.23	3.08	0.239	3.12	0.253	4.04	0.247	4.28	0.252	4.67	0.760	3.49
	Mg	0.0037	0.0049	0.0038	0.0047	0.0042	0.0051	0.0042	0.0055	0.0042	0.0062	0.0040	0.0067	0.0039	0.0077	0.0054	0.012
	Mn	0.0011	0.0089	0.0011	0.0093	0.0015	0.012	0.0015	0.012	0.0015	0.016	0.0015	0.018	0.0015	0.021	0.0039	0.015
	T	0.00028	0.00059	0.00029	0.00050	0.00038	0.00042	0.00039	0.00044	0.00040	0.00056	0.00040	0.00062	0.00041	0.00062	0.00071	0.0011
	Ba	0.00008	0.00006	0.0001	<LOD	0.0002	0.0009	0.0001	0.0004	0.0001	0.0001	0.0001	0.00002	0.0001	0.00005	0.0003	0.0003
	Cd	<LOD	0.00005	<LOD	0.00003	<LOD	<LOD	<LOD	<LOD	<LOD	<LOD						
	Cr	0.0003	0.0007	0.0002	0.0003	0.0006	0.0004	0.0007	0.0007	0.0003	0.001	0.0004	0.0007	0.0004	0.001	0.001	0.004
	Cu	0.00058	0.0026	0.00064	0.0030	0.0011	0.0042	0.0010	0.0044	0.0011	0.0061	0.00096	0.0065	0.0014	0.0073	0.0032	0.0073
	Ni	0.0004	0.0008	0.0002	0.0004	0.0009	0.0004	0.0009	0.0008	0.0005	0.001	0.0006	0.0006	0.0005	0.0009	0.001	0.001
Pb	<LOD	0.0004	<LOD	0.0005	<LOD	0.0005	<LOD	0.001	<LOD	0.0007	<LOD	0.0007	<LOD	0.0008	<LOD	0.0008	
Zn	0.15	0.18	0.15	0.18	0.17	0.19	0.17	0.20	0.18	0.22	0.17	0.22	0.17	0.23	0.20	0.32	

Description of method for the calculation of settling time of particles in dense media

Particles are assumed to be spherical to allow an estimation of the settling time to be calculated under the influence of gravity only and also under the g-force generated by the centrifuge. The g-force is first calculated (assumed to be 9.81 for gravity separation). The terminal settling velocity can be calculated with Stokes' law when the difference in density between the particle and the fluid is known. The fluid is assumed to have a viscosity of tetrabromoethane (TBE) although a fluid density of 2.2 was formed from a mixture of TBE and triethyl-phosphate. The calculated terminal velocity is then used to determine the time taken for a particle to settle a specific distance.

$$G = \frac{r\omega^2}{g}$$

Calculation of g-force G generated by centrifuge rotor

$$v = \frac{gd^2(\rho_p - \rho_f)}{18\mu}$$

Stokes' law for the terminal settling velocity of a spherical particle

$$t = \frac{s}{v}$$

Calculation of settling time for particle travelling at terminal velocity

Parameter	Value
Rotor radius (r)	0.155 m
Angular velocity (ω)	$\frac{4000 \times 2\pi}{60} \text{ rads}^{-1}$
Particle diameter (d)	5, 10, 300_{10}^{-6} m
Particle density (ρ^p)	2.32
Fluid density (ρ^f)	2.20
TBE viscosity (μ)	0.009 Nsm ⁻²
Settling distance	0.1 m

Parameters used in calculation of particle settling time

Appendix 4

Analytical Method Development Results

Contents

Sulphur analysis - determination of analysis time and sample mass

Sulphur analysis - determination of analysis time and sample mass

Sample	Analysis time (mins)	Sample mass (g)	Oxidiser mass (g)	Endpoint (mA)	S (mg)	S (ppm)	Comments
POA	10	0.0916		5.9	1154	12598	
POA	10	0.0962		5.9	1294	13451	
POA	10	0.0974		5.9	1329	13645	
POA	10	0.0971		5.9	1345	13852	
POA	10	0.0974		5.9	1336	13717	
Carbon ash	10	0.0978		5.9	1393	14243	
	15				1476	15092	
	20				1510	15440	Non-combusted material in boat
Carbon ash	10	0.0408		5.9	557	13652	
	15				605	14828	
	20				635	15564	Non-combusted material in boat
POA	10	0.0946		5.9	1387	14662	
	15				1414	14947	
	20				1431	15127	
Carbon ash	10	0.0427	0.9951	5.9	818	19157	
	15				841	19696	
	20				853	19977	
POA	20	0.047	0.9543	5.9	619	13170	
POA	10	0.042	1.0389	5.9	550	13095	
	20				564	13429	
Oxidiser	20		0.9636	5.9	49.06	51	

Appendix 5

Results of Pyrolysis Char Characterisation

Contents

Pyrolysis char size characterisation data

Elemental concentration in bulk sample and size fractions of char

Pyrolysis char size characterisation data

Size	Mass (%)
>6300	19.74
6300-3350	54.29
3350-2000	12.25
2000-1000	3.61
1000-500	2.83
500-75	5.45
75-0	1.84

Size characterisation of pyrolysis char

Elemental concentration in bulk sample and size fractions of char

Element ($\times 10^5$ ppm)	Bulk	>6300	6300-3500	3500-2000	2000-1000	1000-500	500-75	75-0
C	8.38	8.84	8.83	8.45	8.05	8.29	8.34	7.49
S	0.21	0.20	0.20	0.21	0.21	0.20	0.21	0.24
Al	0.013	0.0076	0.0098	0.011	0.0097	0.012	0.013	0.041
Ba	0.0002	0.0002	0.0002	0.0002	0.0002	0.0002	0.0003	0.0010
Ca	0.11	0.056	0.086	0.14	0.11	0.10	0.14	0.30
Cd	0.00004	0.00005	0.00004	0.00005	0.00004	0.00005	0.00005	0.0002
Cr	0.0001	0.00009	0.0001	0.00008	0.0001	0.0002	0.0001	0.001
Cu	0.00032	0.00020	0.00029	0.00063	0.00047	0.00048	0.00097	0.0070
Fe	0.0093	0.0046	0.011	0.013	0.013	0.031	0.024	0.11
Mg	0.0055	0.0045	0.0050	0.0070	0.0062	0.0063	0.0078	0.038
Mn	0.00016	0.00010	0.00021	0.00019	0.00018	0.00033	0.00028	0.0015
Ni	0.00008	0.00007	0.00008	0.00006	0.00005	0.00008	0.0001	0.0006
Pb	0.001	0.0006	0.0007	0.001	0.001	0.01	0.004	0.04
Ti	0.00015	0.00015	0.00023	0.00016	0.00013	0.00017	0.00016	0.00082
Zn	0.47	0.45	0.46	0.49	0.48	0.48	0.47	0.48

